

Analysis of Synthetic and Natural Cannabinoids in the Forensic Field Applying High-Resolution Mass Spectrometry

Inaugural dissertation

to

be awarded the degree of Dr. sc. med.

presented at

the Faculty of Medicine
of the University of Basel

by

Manuela Carla

Monti

From Rüti (ZH)

Zürich

Basel, 2022

Approved by the Faculty of Medicine

On application of

Prof. Dr. med. Dipl. Phys. Eva Scheurer

Prof. Dr. med. Matthias Liechi

PD Dr. rer. nat. Cornelius Hess

Basel, 21.03.2022

Dean

Prof. Dr. Primo Schär

Acknowledgments

To begin with, I show my gratitude to my primary advisor Prof. Eva Scheurer for letting me conduct my PhD studies in the exciting field of forensic chemistry and toxicology at the Institute of Forensic Medicine Basel. I would furthermore like to thank Dr. Katja Mercer-Chalmers-Bender, for her guidance and valuable support throughout this work.

I thank all members of the IRM Basel, particularly of the forensic chemistry and toxicology department, for scientific input and support, but also for providing a positive work environment. Special thanks go to Priska Frei and Konrad Koch, for not only helping me during brainstorming and writing – making them valuable scientific colleagues – but also for always having an open ear and providing motivational speeches – as friends.

This work highly profited from collaborations with drug checking services (DIBS, DILU, and Suchthilfe Ost). I therefore want to thank all involved persons, with special thanks to Jill Zeugin (Suchthilfe Region Basel) and Natasa Milenkovic (Abteilung Sucht).

Sincere thanks go to my family and friends for their valuable support throughout this work. I want to thank my brothers Sandro Monti and Remo Monti who helped me in preparation of this thesis. Inarguably, conducting a PhD during a pandemic is a challenging task on multiple levels. In order to tackle these troubling times, I show my utmost gratitude to Saira Zavahir and Stig Solbach for always being there for me as well as their positive thinking.

Lastly, I want to thank Masashi Kishimoto. Not only did his art help me maintain a reasonable work life balance, but as seen with Naruto who finally became Hokage, he showed me that consistent effort pays off.

Table of contents

Zusammenfassung.....	V
Abstract	VI
List of abbreviations	VII
1 Background.....	1
1.1 Chemical analysis in the forensic field	1
1.1.1 High-resolution mass spectrometry	1
1.2 Endocannabinoid system.....	3
1.2 <i>Cannabis sativa</i>	4
1.3.1 History and political landscape.....	4
1.3.2 Cannabis and cannabis based products – non-medical use	4
1.3.3 Cannabis and cannabis based products – medical use	5
1.3.4 Beyond Δ^9 -tetrahydrocannabinol and cannabidiol.....	6
1.3.5 Forensic implications	8
1.4 Synthetic cannabinoids	9
1.4.1 Emergence	9
1.4.2 Products.....	11
1.4.3 Pharmacology and toxicology	11
1.4.4 Forensic implications	12
2 Motivation and Aims.....	13
3 Methodology	14
4 Results	15
4.1 Publication: <i>Study I</i>	16
4.2 Publication: <i>Study II</i>	31
4.3 Publication: <i>Study III</i>	50
5 Discussion	85
5.1 <i>In vitro</i> metabolism studies in forensic toxicology	85
5.2 Unraveling a novel trend surrounding synthetic cannabinoids	85
5.2.1 What can we learn for the rapid detection and monitoring of emerging NPS? ..	87
5.2.2 Future role of high-resolution mass spectrometry	88
5.3 Advances in phytocannabinoid characterization.....	89
5.3.1 Minor cannabinoids in the forensic field – where do we go from here?	90
6 Conclusion	92
7 Curriculum Vitae	93
8 Presentations and Posters	94
9 References	95

Zusammenfassung

Die fortlaufende Verbreitung synthetischer Cannabinoide (SC) sowie die zunehmende Legalisierung und der vermehrte medizinische Gebrauch von *Cannabis sativa* (*C. sativa*) stellen forensische Chemiker und Toxikologen vor multidimensionale Herausforderungen. Diese Arbeit nimmt sich diesen Herausforderungen an, unter Anwendung modernster Massenspektrometrie.

Studie I untersuchte den *in vitro* Metabolismus der beiden SC CUMYL-THPINACA und ADAMANTYL-THPINACA. Da das Wissen über den Metabolismus neuer SC in der Regel stark limitiert ist, sind *in vitro*-Metabolismus Studien für die Identifizierung geeigneter Screening-Targets erforderlich. *Studie I* beinhaltete die Implementierung eines *in silico*-gestützten Arbeitsverfahrens für die Identifizierung und Strukturaufklärung von Metaboliten. Es wurde gezeigt, dass beide SC in hohem Masse metabolisiert werden. Zudem wurden geeignete Screening-Targets präsentiert. Darüber hinaus lieferte die Untersuchung der beteiligten Cytochrom P450 (CYP) Isoenzyme Informationen über mögliche metabolische Arzneimittelinteraktionen und den möglichen Einfluss von CYP-Polymorphismen.

Studie II befasste sich mit Cannabisprodukten, die mit SC versetzt sind. Solche Produkte wurden seit dem Jahr 2020 vermehrt in der Schweiz und in verschiedenen europäischen Ländern festgestellt. Die Unkenntnis der Drogenkonsumenten über das Vorhandensein von SC zusammen mit der typischerweise höheren Potenz von SC im Vergleich zu Δ^9 -Tetrahydrocannabinol (THC) wurde als Bedrohung der Öffentlichen Gesundheit eingestuft. Für *Studie II* wurden Proben und Erfahrungsberichte, die in drei Drug Checking Einrichtungen gesammelt wurden, untersucht. Dafür wurde eine umfassende Screening-Methode für SC unter Anwendung hochauflösender Massenspektrometrie (*high-resolution mass spectrometry*; HRMS) entwickelt und validiert. Zusätzlich wurde das Trägermaterial hinsichtlich seines THC- und Cannabidiol (CBD)-Gehalts charakterisiert. Die erhaltenen Daten umfassten Erfahrungsberichte der Konsumenten über unerwünschte Wirkungen nach dem Konsum der jeweiligen behandelten und regulären Cannabisprodukte. Es wurde festgestellt, dass Produkte, die SC enthalten, im Vergleich zu unbehandelten (regulären) Cannabisprodukten ein erhöhtes Risiko für unerwünschte Wirkungen, insbesondere für kardiovaskuläre und psychologische Nebenwirkungen, aufweisen. Die Rolle von Drug Checking Einrichtungen als Marktüberwachungsinstrument und als Informationsquelle für Wirkungen neuer psychoaktiver Substanzen (NPS) wurde aufgezeigt.

Studie III präsentiert die Entwicklung und Validierung einer umfassenden Analyseverfahren zur Bestimmung von Haupt- und Nebencannabinoiden (sogenannte *minor cannabinoids*) in Cannabisblüten. Nebencannabinoide gewinnen für unterschiedliche Anwendungen an Interesse, z. B. für eine verbesserte Produktcharakterisierung, Differenzierung von Cannabis-Varietäten und bioanalytischen Fragestellungen im rechtsmedizinischen Bereich. Proben von 18 Cannabis-Varietäten, die unter standardisierten Bedingungen angebaut und gelagert wurden, wurden unter Anwendung von *targeted* und *untargeted* Analyseverfahren mittels HRMS charakterisiert. Multivariate Statistiken, z. B. Hauptkomponentenanalysen, wurden durchgeführt, um Ähnlichkeiten und Unterschiede zwischen den Varietäten hervorzuheben. Die vorgestellten Methoden ermöglichten eine verfeinerte Darstellung der chemischen Zusammensetzung der untersuchten Varietäten. Dies erlaubte eine Subklassifizierung, welche Klassifizierungssysteme basierend auf THC und CBD erweiterte.

Abstract

Multidimensional challenges arise in the field of forensic chemistry and toxicology from the ongoing emergence of synthetic cannabinoids (SCs) as well as the increasing legalization and medicalization of *Cannabis sativa* (*C. sativa*). This work addresses these challenges from different angles under the application of state-of-the-art mass spectrometry.

“Phase I In vitro Metabolic Profiling of the Synthetic Cannabinoid Receptor Agonists CUMYL-THPINACA and ADAMANTYL-THPINACA” (study I) investigated the *in vitro* metabolic fate of two SCs. As data on the metabolism of newly emerging SCs is typically scarce, *in vitro* metabolism studies are required for the identification of suitable screening targets. The implementation of an *in silico* assisted workflow aided identification and structure elucidation of metabolites. It was observed that both SCs are vastly metabolized. Suitable screening targets were proposed. Additionally, investigation of the involved cytochrome P450 (CYP) isoenzymes gave valuable information on potential metabolic drug-drug adverse reactions and the potential influence of CYP polymorphisms.

“Adulteration of low-delta-9-tetrahydrocannabinol products with synthetic cannabinoids: Results from drug checking services” (study II) presents data gained on the phenomenon of low-THC cannabis products adulterated with SCs. Since 2020, such products have been increasingly detected in Switzerland and various European countries. The drug user’s unawareness about the presence of SCs combined with the typically higher potencies of SCs when compared to Δ^9 -tetrahydrocannabinol (THC) raised public health concerns. Cannabis samples and data on the drugs’ effects obtained from three drug checking services were investigated. A comprehensive screening method for SCs applying high-resolution mass spectrometry (HRMS) was developed and validated. The carrier material was characterized regarding its THC and cannabidiol (CBD) contents. Data obtained from drug checking services included user self-reports on adverse effects after consumption of the respective adulterated and non-adulterated cannabis products. Increased risks for adverse effects, in particular cardiovascular and psychologic adverse effects, were found for products containing SCs when compared to regular cannabis products. The role of drug checking services as market monitoring tool and as source on effects of newly emerging new psychoactive substances (NPS) was highlighted.

“Beyond Δ^9 -tetrahydrocannabinol and cannabidiol: Chemical differentiation of cannabis varieties applying targeted and untargeted analysis” (study III) presents the development and validation of a comprehensive analytical method for the determination of major and minor cannabinoids in cannabis inflorescences. Minor cannabinoids are gaining interest for various applications, ranging from improved product characterization and differentiation of cannabis varieties to bioanalytical questions in the medico-legal field. Samples derived from 18 cannabis varieties grown and stored under standardized conditions were characterized, applying the targeted and untargeted analyses using HRMS. Multivariate statistics, e.g., principal component analysis, were conducted to investigate similarities and differences between varieties. The presented methods allowed for a refined representation of chemical differences, i.e., chemical fingerprints, between varieties, expanding traditionally applied classification systems based on THC and CBD alone.

List of abbreviations

CB1	Cannabinoid receptor 1
CB2	Cannabinoid receptor 2
CBC	Cannabichromene
CBD	Cannabidiol
CBDV	Cannabidivarin
CBE	Cannabielsoin
CBG	Cannabigerol
CBL	Cannabicyclol
CBN	Cannabinol
CBT	Cannabitriol
CNS	Central nervous system
CYP	Cytochrome P450 enzymes
dd-MS ²	Data dependent MS ²
DUID	Driving under the influence of drugs
ECS	Endocannabinoid system
EMCDDA	European Monitoring Centre for Drugs and Drug Addiction
FID	Flame ionization detector
GC	Gas chromatography
GMP	Good manufacturing practice
GPCR	G protein-coupled receptor
GTFCh	Gesellschaft für Toxikologische und Forensische Chemie
HLM	Human liver microsomes
HPLC	High performance liquid chromatography
HRMS	High-resolution mass spectrometry
ISTD	Internal standard
LOD	Limit of detection
LOQ	Limit of quantification
MS	Mass spectrometry
NPS	New psychoactive substances
PCA	Principal component analysis
pHLM	Pooled human liver microsomes
ppm	Parts per million
QQQ	Triple quadrupole mass analyzer
rCYP	Recombinant cytochrome P450 enzymes
SC	Synthetic cannabinoid
SPE	Solid phase extraction
THC	Δ^9 -tetrahydrocannabinol
THCA	Δ^9 -tetrahydrocannabinolic acid
THCV	Tetrahydrocannabivarin
TOF	Time of flight mass analyzer
UNODC	United Nations Office on Drugs and Crime
Δ^8 -THC	Δ^8 -tetrahydrocannabinol

1 Background

1.1 Chemical analysis in the forensic field

Chemical analysis of biological samples, e.g., blood, urine, and hair, to confirm the presence or absence of a xenobiotic, as well as the characterization of seized materials, e.g., powders, liquids, and tablets, are essential tasks conducted in forensic toxicology and chemistry.^{1,2} However, the applied analytical techniques are by far not unique to this field, as analytical chemistry is widely used in numerous areas of research,³ for instance in environmental,^{4,5} food,^{6,7} and pharmaceutical sciences.⁸ The gold-standards in clinical and forensic toxicology are gas chromatography (GC) and high performance liquid chromatography (HPLC) hyphenated to a diversity of detectors.^{9, 10} Chromatographic separation achieved via GC and LC is typically required to separate unwanted constituents, i.e., matrix, from the compounds of interest, i.e. analytes.^{9, 11} A vast variety of detectors exist, ranging from rather simple to highly complex instruments. The detector is ideally chosen based on specific needs and requirements of the analysis. For instance, for quantification of an analyte (e.g., a controlled substance) at low concentrations with high precision, the detector should be highly sensitive and robust. In contrast, for screening procedures, different detectors might be advantageous as they for example allow identification of a wider range of substances. Due to the vast number of detectors, even within the mass spectrometry family, a comprehensive comparison highlighting benefits and drawbacks of different detectors in analytical chemistry is beyond the scope of this thesis. Since this work mainly used high-resolution mass spectrometry (HRMS), this type of detector will be discussed in more detail in the following paragraph. Comprehensive information on different MS types used in the forensic field can be found in the reviews by Meyer *et al.*⁹, Remane *et al.*¹, and Maurer *et al.*¹⁰

1.1.1 High-resolution mass spectrometry

In the forensic field, two types of high-resolution mass analyzers are most commonly found: time of flight (TOF)^{1, 2} and Orbitrap mass analyzers.¹ The term *high-resolution* stands for the mass accuracy, which is considerably higher compared to low-resolution mass analyzers, such as triple quadrupole (QQQ) or conventional ion trap instruments. Low-resolution mass analyzers achieve selectivity and specificity via fragmentation, meaning that during a QQQ measurement specific mass transitions are monitored. The first quadrupole will detect a range of m/z (e.g., theoretical $[M+H]^+ \pm 0.5$ Da) of a set of previously defined analytes. The molecules presenting an m/z within the mass range covered by the first quadrupole are then fragmented in the second quadrupole. The generated fragments are detected in the third quadrupole. Yet

the first quadrupole alone would not be able to distinguish cocaine ($C_{17}H_{21}NO_4$) and chlorphenoxamine ($C_{18}H_{22}ClNO$), both presenting at $[M+H]^+$ 304 m/z . Only the subsequent fragmentation achieved via the second quadrupole, which is generally specific to the different molecules, renders these compounds distinguishable. When using HRMS, cocaine and chlorphenoxamine present at different exact masses, with $[M+H]^+$ at 304.1543 m/z for cocaine and 304.1463 m/z for chlorphenoxamine. Thus, these compounds are already distinguishable even without fragmentation. The difference at the second decimal place gives these signals a mass difference of 26 parts per million (ppm), which is far beyond commonly applied accepted mass error of ± 5 ppm. Nevertheless, differentiation of isobaric compounds with identical chemical formulas still requires further information obtained via chromatographic separation or fragmentation.⁹

The possibility to conduct full scan measurements with high mass accuracy make TOF and Orbitrap instruments particularly interesting for screening procedures. During a full scan measurement, a mass range (e.g., 200 – 1000 m/z) is constantly screened, thus any signal presenting within this mass range is detected. Therefore, full scan measurements are also typically referred as untargeted analyses. This largely differs from targeted methods (e.g., conducted using QQQ instruments), which only allow the detection of a set of previously defined ions, i.e., via defined mass transitions. In contrast, full scan measurements allow the screening of a vast diversity of compounds (e.g., >1000 compounds) using only one scan mode. When conducting a full scan measurement applying HRMS, additional compounds might be retrospectively detected. The need to retrospectively search for compounds, even under the absence of reference standard material, is commonly encountered in forensic work, arising from newly emerging drugs of abuse. Additionally, the chemical formula of a signal belonging to a unknown compound may be derived from an exact mass signal of the parent and/or fragments, giving valuable hints on structure and identity.^{2, 10} The easy incorporation of new analytes into a screening method is considered a further advantage of HRMS.⁹

HRMS is considered an advanced *omics* technology with diverse applications ranging from proteomics,¹² lipidomics,¹³ foodomics,^{14, 15} and metabolomics.^{16, 17} Metabolomics research aims at the comprehensive representation of the metabolome achieved via the detection and identification of a broad range of metabolites, typically focused on small molecules.¹⁷ Recent metabolomics studies in forensic toxicology comprise postmortem interval determination¹⁸ and biomarker identification for drug consumption and sample manipulation.^{19, 20} The identification of metabolites of newly emerging drugs using *in vitro* and *in vivo* metabolism models, is increasingly conducted with the aid of metabolomic methodologies.²¹⁻²⁴ These studies typically focus on the metabolic fate of one compound, i.e., a newly emerging drug, and not the complete metabolome, thus differing from classic metabolomic approaches.¹⁶

1.2 Endocannabinoid system

The endocannabinoid system (ECS) describes a neuromodulatory system found in humans and many animal species.^{25, 26} The ECS is comprised of cannabinoid receptors, endogenous cannabinoids (endocannabinoids), and enzymes controlling the biosynthesis and degradation of these endocannabinoids. The best-known endocannabinoids are anandamide (arachidonoyl ethanolamide) and 2-arachidonoyl glycerol (2-AG; Figure 1). Endocannabinoids, and exogenous cannabinoids (e.g., Δ^9 -tetrahydrocannabinol; THC),²⁷ mainly act through binding at the cannabinoid receptors 1 and 2 (CB1 and CB2). CB1 and CB2 are G protein-coupled receptors (GPCRs). CB1 is predominantly expressed by neurons in the central nervous system (CNS). CB2 is primarily found on immune cells and, thus, is expressed to a much lower extent in the CNS compared to CB1. Additional to CB1 and CB2 endocannabinoids were shown to target various additional receptors, for instance, GPR55, GPR18, GPR119, transient receptor potential ankyrin 1 (TRPA1), transient receptor potential channel type V1 (TRPV1), and peroxisome proliferator-activated receptors (PPARs).²⁸

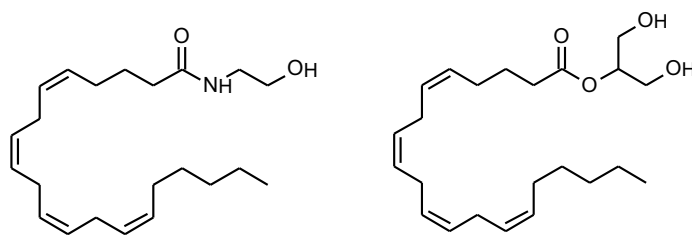


Figure 1. Chemical structures of anandamide (left) and 2-arachidonoyl-glycerol

The complexity of the ECS is reflected in the diverse biological functions in which it is involved, including the regulation of the sleep wake cycle, memory, stress response,²⁸ appetite,²⁹ mood,³⁰ and nociception.³¹ Ever since its discovery in the 1990s, the ECS has been investigated as therapeutic target for various implications.^{27, 28, 31, 32} For instance, CB1 agonists were developed and tested for the treatment of neuropathic and inflammatory pain, multiple sclerosis, anxiety, and depression, whereas CB1 antagonists were considered in the field of diabetes and Alzheimer's disease. Clinical outcomes of CB1 agonists and antagonists were mixed, which was attributed to the diversity of cell types expressing CB1 and associated increased risk of adverse effects. For example, severe psychiatric side effects were the reason for the withdrawal of rimonabant, a CB1 inverse agonist that has been licensed for the treatment of obesity. Strong activation at CB1 resulting from high-affinity agonists have also been shown to cause unwanted side effects. However, some of these potent CB1 agonists appeared on the recreational drug market decades later as constituents of so-called "Spice".³³

1.2 *Cannabis sativa*

1.3.1 History and political landscape

Cannabis cultivation dates back 5000 to 6000 years, making *Cannabis sativa* (*C. sativa*) one of the oldest plants used for fiber and food. First reports on the medicinal use of *C. sativa* originated from the Middle East and Asia around 500 B.C.³⁴ The mechanisms of action of *C. sativa* remained undiscovered until the 1960s, when the main active ingredient of cannabis, THC, was identified.^{34,35} THC is best known for its psychotropic effects, which are the basis for the plant's long and controversial history of abuse.³⁰ As of today, *C. sativa* is the most widely used recreational drug worldwide.³⁶ The United Nations Office on Drugs and Crime (UNODC)³⁶ estimated that roughly 200 million people (approximately 4% of population aged 14-64 years) used cannabis at least once in 2019. The past-year prevalence (year 2019) for cannabis use for central Europe was estimated at 8% (population aged 14-64 years), and even 15% for people aged 15-34 years.³⁶

Political changes resulted in the legalization of cannabis for recreational use in some regions, with Canada and some US states being prominent examples. Legalization of cannabis currently is also subject to discussion in several European countries, including Luxembourg, Portugal, and Czechia.³⁷ In Switzerland, an amendment to the Federal Narcotics Act introduced spring 2021 has opened the way for pilot trials allowing the dispense of recreational cannabis in pharmacies.³⁸ The political landscape is also changing regarding cannabis for medical use, which is increasingly becoming available.³⁹ In 2021, Europe counted 23 countries in which cannabis medicines can be prescribed. Yet there are considerable differences in the type of products, as some countries (e.g., Germany) allow the prescription of medical-grade herbal products,⁴⁰ while other countries (e.g., Spain) only allow the use of cannabinoid-based preparations.³⁷

1.3.2 Cannabis and cannabis based products – non-medical use

THC, well-known for its psychotropic effects, is found at highest concentrations in the female flowers of the cannabis plant.³⁰ Dried cannabis flowers (cannabis inflorescences, marijuana) and derived products (e.g. cannabis resin, hashish) are widely found on the recreational drug market.^{36, 41} In recent years, high-potency cannabis products, e.g., cannabis concentrates and edibles, were increasingly observed.^{36, 42, 43} The rising diversity and potency of cannabis products, especially in regions that have legalized cannabis, has been associated with increased acute harms, reflected in increasing numbers of emergency visits.⁴³ Even though cannabis regulations are loosening, the majority of European countries (including Switzerland) still schedule

cannabis and cannabis products as a narcotic, based on defined THC-thresholds. Most European countries apply a THC-threshold of 0.2% (w/w). Switzerland applies a slightly higher threshold with 1% THC.

In recent years, a growing industry around low-THC preparations, often promoted as life-style products, is further complicating the legal landscape surrounding cannabis. Low-THC products are defined by the European Monitoring Centre for Drugs and Crime (EMCDDA) as “products being or containing cannabis herb, resin, extracts or oils that claim or appear to have a very low percentage of THC and which would be unlikely to cause intoxication”.⁴⁴ Low-THC products typically present elevated cannabidiol (CBD) levels and THC levels below legal thresholds (<1% for Switzerland, <0.2% most of Europe). CBD is the second best-known cannabinoid of *C. sativa* and is regarded as non-intoxicating.⁴⁵ Low-THC products started to appear in 2016 in Switzerland, followed by Austria and Italy in 2017 and Germany, Belgium, and France in 2018.⁴⁴ A wide range of these so-called CBD products, ranging from dried herbal products to oils, are currently found on the Swiss and European market. The market surrounding CBD products is characterized by a variety of different manufacturers and retailers.^{44, 45} The popularity of CBD products is believed to result from health claims. Despite limited evidence in the scientific literature, CBD is often promoted to improve well-being and as potential treatment for various conditions including, but not limited to, migraines, anxiety, and insomnia.⁴⁴

1.3.3 Cannabis and cannabis based products – medical use

For decades *C. sativa* was highly restricted, hampering research on its potential medical uses. However, the loosening of laws and restrictions led to various cannabis based products entering the drug market in recent years.^{33, 46, 47} THC and CBD are the main ingredients of cannabis based products for medical use, but preparations containing synthetically produced cannabinoids (synthetic cannabinoids) can also be prescribed, depending on local legal frameworks. Popular examples are: i) Sativex®, containing cannabis extracts resulting in equal amounts of THC and CBD, used for the treatment of spasticity in multiple sclerosis; ii) Epidyolex® (also: Epidiolex®), containing pure CBD, licensed for the treatment of rare forms of childhood epilepsy; iii) dronabinol (e.g., contained in Marinol®), containing synthetically produced THC; and iv) nabilone (e.g., contained in Cesamet®), a synthetic cannabinoid closely related to THC. The aforementioned synthetically produced compounds are authorized for the treatment of weight loss in patients with acquired immunodeficiency syndrome (AIDS) and nausea and vomiting during chemotherapy in some countries.³⁹ Additionally, several countries, e.g., the Netherlands,⁴⁸ Germany, and the United Kingdom (UK),³⁷ have authorized the prescription of herbal cannabis, e.g., Bedrocan®. The cannabis inflorescence contained in Bedrocan® are produced following the quality standards of good manufacturing practice (GMP), providing a high degree of product standardization.³⁹

1.3.4 Beyond Δ 9-tetrahydrocannabinol and cannabidiol

Although THC and CBD are the best-studied cannabinoids of the cannabis plant, nearly 150 additional cannabinoids are known today.⁴⁹ These cannabinoids are typically referred to as minor cannabinoids, due to their typically lower contents in *C. sativa*.⁵⁰ Based on their chemical structure, the cannabinoids of *C. sativa* are classified into eleven types, with the following representative cannabinoids: cannabichromene (CBC), cannabidiol (CBD), cannabielsoin (CBE), cannabigerol (CBG), cannabicyclol (CBL), cannabinol (CBN), cannabinodiol (CBND), cannabitrinol (CBT), Δ 9-tetrahydrocannabinol (THC), Δ 8-tetrahydrocannabinol (Δ 8-THC). A further subclass is comprised of miscellaneous cannabinoids.³⁰ While the representative cannabinoids all have pentyl (C5) side chains, analogues with varying lengths of the alkyl side chain are also expressed in *C. sativa*, for instance, tetrahydrocannabivarin (THCV) and cannabidivarin (CBDV), which both have propyl (C3) side chains. Moreover, cannabinoids are biosynthesized as acidic cannabinoids in the cannabis plant, meaning that these acidic forms (also named pre-cannabinoids) are predominantly found in the plant and native extracts, e.g., THC as THC-acid (THCA) and THCV as THCV-acid (THCVA).³⁰ Decarboxylation resulting in neutral cannabinoids is influenced via various non-enzymatic processes, e.g., heating (including smoking),³⁰ but also occurs spontaneously.⁴⁹ An overview of the cannabinoid types are shown in Figure 2.

Ultimately, *C. sativa* contains a diversity of bioactive cannabinoids beyond the “big two”. This raises the question of their pharmacologic relevance. Moreover, studies have detected clinical differences between the effects of purified cannabinoids compared to cannabis preparations, ultimately highlighting the complex polypharmaceutical nature of cannabis.^{33, 51} Apparent synergistic benefits of cannabinoids taken together instead of individually are termed *entourage effect*. Possible explanations lie within the interaction of cannabinoids with different receptors belonging to or associated with the ECS, as well as differences in the modulating mechanisms at specific receptors, such as CB1. This interplay is believed to partly counterbalance, and thus regulate, the effects of single cannabinoids. For instance, the interplay between THC and CBD is partly explained by both of them binding at CB1: THC is a partial agonist at CB1, while CBD, a low-affinity ligand at a different binding site, is a negative allosteric modulator.³³ A recent review by Freeman *et al.*⁵² investigated influence of CBD on THC’s acute effects. Although several clinical studies reported on the synergistic contributions of CBD, the overall literature remains inconsistent. It is suggested that CBD may alter acute effects of THC, but further research is required.⁵² Regarding the biological activity of minor cannabinoids data is more limited. Only for a few minor cannabinoids pharmacologic parameters have been assessed.^{30, 33} Whilst THCV, CBC, and CBG are considered non-psychotropic, due to lacking or neutral antagonistic action at CB1,³⁰ all three cannabinoids exerted effects via interaction with other targets than CB1, as shown in various *in vitro* and *in vivo* systems.

The binding at receptors associated to the ECS, i.e., TRPV1 and TRPA1, as observed respectively for CBG and CBC, highlights the potential therapeutic relevance of minor cannabinoids.^{30, 33, 51}

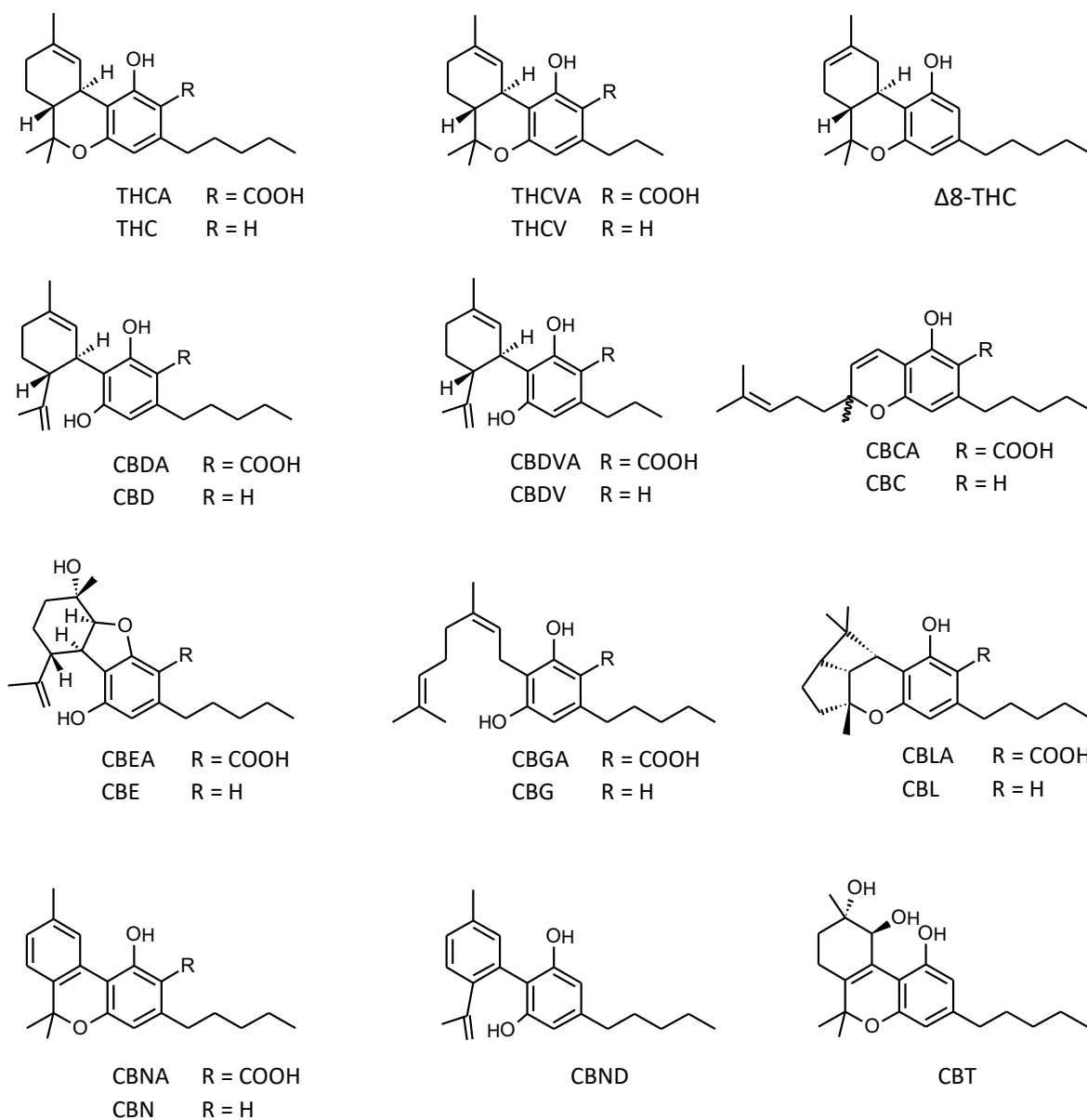


Figure 2. Chemical structures of representative cannabinoids.

1.3.5 Forensic implications

THC is a key compound in forensic chemistry and toxicology.^{36, 53} Seized cannabis products undergo THC quantification for the assessment of THC levels that are used to classify a plant or product as a narcotic – a task with increasing complexity due to the growing industry surrounding low-THC cannabis products.^{44, 54} In forensic toxicology, THC and its major metabolites are detected to assess overall uptake and impairment, for instance in driving under the influence of drugs (DUID) investigations.⁵⁵⁻⁵⁹ The complex pharmacokinetics of THC, resulting from extensive metabolism and prolonged release from lipid storage departments, renders the interpretation of THC levels a highly difficult task.⁶⁰ For instance, in frequent consumers, residual THC and THC-metabolites can be found in blood and urine even after periods of abstinence.^{61, 62} Despite the general use of THC thresholds with regard to DUID investigations,⁶³ clear concentration activity profiles of THC enabling a relationship between performance and impairment are subject to ongoing discussions.⁵⁵ The introduction of cannabis based products for medical use and the growing industry surrounding low-THC cannabis products is further complicating toxicological data interpretation, posing various challenges for forensic institutions.^{64, 65} Unsurprisingly, considerable efforts to overcome the described challenges have been made.^{45, 56-58, 63, 64, 66, 67} In this context, comprehensive bioanalytical methods including CBD and minor cannabinoids, enabling more profound data interpretation, are of growing interest.^{64, 65, 68-73} CBD and minor cannabinoids have been investigated as possible distinguishing markers between medical and recreational cannabis intake.^{40, 64, 71} Furthermore, minor cannabinoids have been discussed as tools to discriminate occasional from frequent cannabis consumption,⁶⁴ as well as markers for recent cannabis exposure.^{54, 65, 72, 74} In a recent review, Drummer *et al.*⁷⁵ discussed THC's potential to contribute to sudden death. The aforementioned author encouraged the incorporation of CBD into post-mortem analyses, as CBD has been discussed to alter the effects of THC.^{52, 75} A recent study published by Cliburn *et al.*⁷⁶ presents a comprehensive method for the quantification of post-mortem fluids for THC, CBD, CBN, CBG, and THCV, including selected metabolites of these major and minor cannabinoids.

1.4 Synthetic cannabinoids

1.4.1 Emergence

In the mid-2000s products called “Spice”, comprising herbal mixtures and promoted as legal alternatives to cannabis, appeared on the European market. In 2008, increasing popularity of “Spice” and similar smoking mixtures (e.g., labelled “K2”, “Black Mamba”, and “Bonsai”), typically sold via internet shops, was observed. During the same time, poisonings associated with these “legal-highs” raised questions on their chemical composition and underlying mechanisms. Comprehensive chemical analyses conducted in 2008 revealed that the cannabis-like effects were not resulting from natural constituents of the herbal material, but were explained by the admixture of pharmacologically highly active compounds.^{77,78} The identified compounds were shown to be synthetic cannabinoids (SCs) some of which were first developed during research of the ECS decades ago.⁷⁸ Auwärter *et al.*⁷⁷ were quick in foreseeing the future challenges arising from these newly appearing cannabinoid-like designer drugs in their letter published in late 2008:

“So far nothing is known about the metabolism of these compounds. Some of the metabolites may be toxic and/or pharmacologically active. Furthermore, differences from batch to batch in the kind and amount of applied drugs result in the risk of accidental overdosing, which in the last weeks occurred several times in our region with hospitalization of the patients. There are hundreds of further compounds with cannabinoid receptor activity and it can be assumed that further substances will appear on the market soon, which will be an ongoing challenge for toxicologists as well as for law enforcement.”⁷⁷

The year 2008 marked what is indeed considered the starting point of the emergence of SCs on the recreational drug market.⁷⁸ As predicted,⁷⁷ SCs quickly took over a prominent role in the world of new psychoactive substances (NPS), with new SCs appearing every year. With currently 209 compounds, SCs are the largest family within the class of NPS monitored by the EMCDDA.⁵³ The family of SCs is comprised of a wide diversity of compounds that are further categorized into chemical subfamilies. Regarding their emergence on the recreational drug market, first generation SCs were cyclohexylphenols (CP-47,497-C8) and naphthoylindoles (e.g., JWH-018), followed by the broader class of aminoalkylindoles (e.g., XLR-11). Afterwards, the emergence of the prominent indole-carboxamides (e.g., 5F-MDMB-PICA) and indazole-carboxamides (e.g., 5F-MDMB-PINACA) was observed. More recently cumyl derivatives (e.g., 5F-CUMYL-PINACA), 7-azaindoles (e.g., 5F-MDMB-P7AICA), carbazoles (e.g., EG-018), and γ -carbolinones (e.g., CUMYL-PeGACLONE) have been identified.⁷⁸

Structures of all aforementioned SCs are depicted in Figure 3. The emergence of new SCs is largely driven by legislative changes. Scheduling of a compound or compound class was usually associated with the emergence of new SCs with altered chemical structures circumventing these legal frameworks.^{78, 79} Especially the legal framework in China, believed to be the main production site of SCs, is considered highly relevant.^{78, 80, 81}

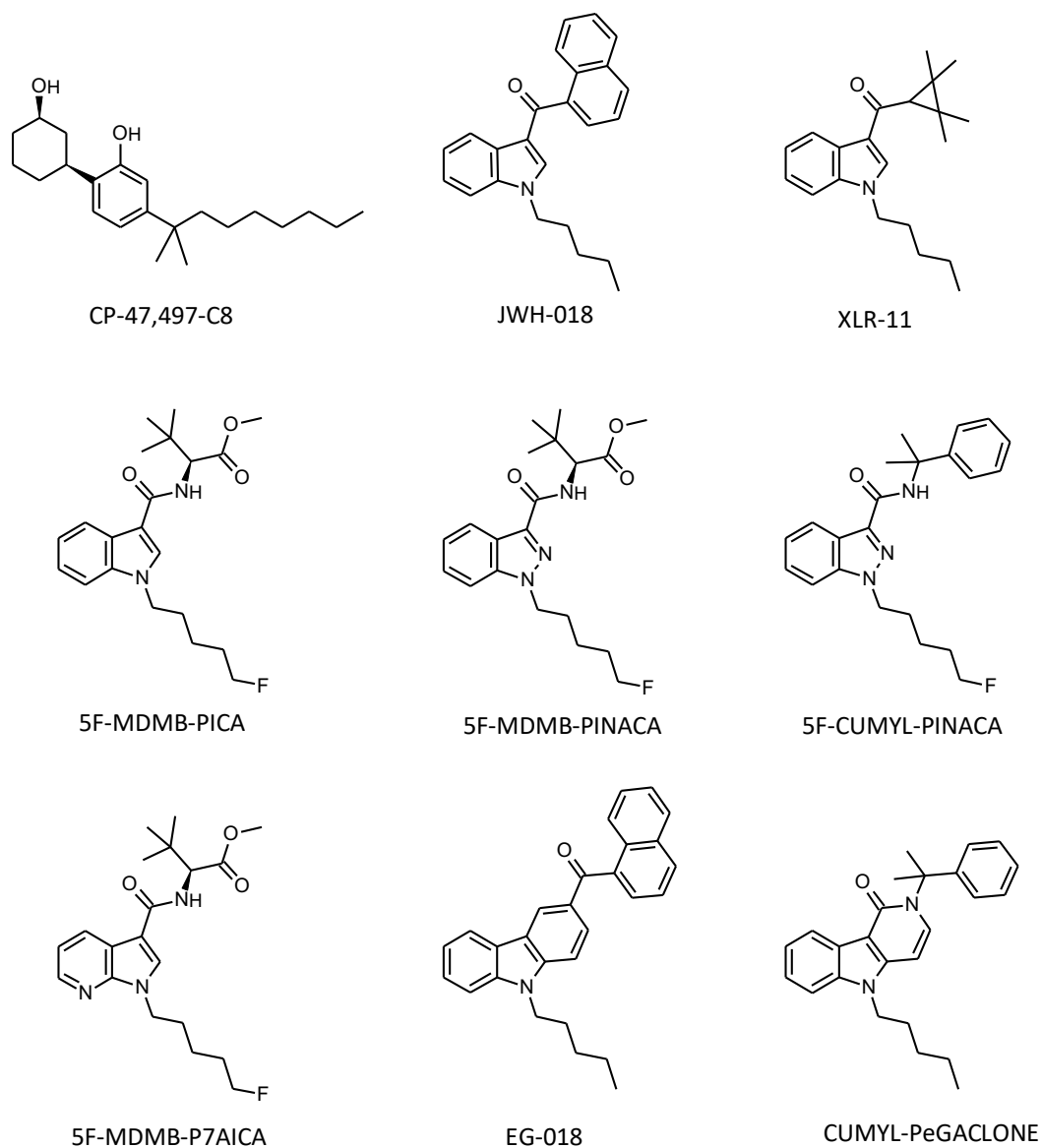


Figure 3. Structures of various SCs belonging to different subfamilies.

1.4.2 Products

The types of products containing SCs typically comprise smoking mixtures, e-liquids, and SC impregnated papers. Smoking mixtures are the most popular form and are typically produced by spraying SCs onto inert herbal material.^{78, 81} These herbal incenses are then either rolled into a cigarette and smoked or inhaled from a vaporizer or bong. SC containing e-liquids used for electronic cigarettes are increasingly observed.⁷⁸ Papers infused with SCs are typically found in prison settings, as these preparations are used to smuggle SCs into prison.^{80, 81} SCs are associated with unknown and potentially serious health risks, arising from limited knowledge on pharmacologic and toxicologic effects of newly emerging SCs.⁷⁸ Health risks are further exacerbated, as the production of SC infused products, i.e., smoking mixtures and papers, were seen to result in inhomogenous distribution of SCs, consequently increasing the risk of accidental overdosing.^{80, 82, 83}

1.4.3 Pharmacology and toxicology

Many SCs have shown to bind CB1 and CB2 with little subtype selectivity.⁷⁹ However, the THC-like effects of SCs, such as mood elevation, relaxation, and euphoria,⁸⁴ are largely attributed to the often proven high binding affinities and potencies at CB1.^{78, 79, 85-90} Many SCs are considered more potent than THC, reflected in enhanced psychotropic effects, but also associated with higher toxicity.^{84, 91-93} Systematic clinical data on pharmacologic or toxicologic effects of SCs, however, are scarce.^{42, 94-96} This is further aggravated by the ever changing market surrounding SCs, with new compounds readily entering the market.^{53, 95} The lack of systematic studies in humans makes case reports and case series the main source of information on clinical effects of SCs.^{42, 95}

Ever since their emergence on the drug market over a decade ago, various intoxications including fatal outcomes have been associated with SCs.^{94, 97-102} Adverse effects linked to SCs include nausea, vomiting,⁹¹ agitation,⁹² psychotic symptoms and psychosis,^{101, 103} hallucinations,^{100, 101} seizures,⁸⁴ as well as various cardiologic adverse effects e.g., dysrhythmia⁹², tachycardia,^{98, 100} and chest pain.^{96, 100} Potential life-threatening effects of SCs include myocardial infarction and acute kidney injury.⁸⁴ In addition, behavioral changes leading to injuries⁸⁴ and violence towards self and others have been associated with SCs.⁴² Considerable morbidity and mortality of SCs renders this substance class a serious public health threat.⁵³

1.4.4 Forensic implications

Even though a slight reduction in the number of newly identified SCs per year has been observed since 2014, SCs remain present on the drug market, with approximately ten newly identified compounds per year.⁵³ SCs are generally not detected by routine drug tests, e.g., rapid-reagent tests for common drugs of abuse. This is believed to be one reason why certain users prefer SCs over common recreational drugs, for instance, prisoners and people under abstinence control. However, even specialized laboratories applying elaborated techniques for the analysis of seized products and biological samples are facing difficulties in keeping pace with the ever-changing drug market surrounding SCs.⁸¹ Moreover, the interpretation of blood levels to assess impairment or contribution to death is hampered by limited reference values in literature.⁸⁴ A further challenge arises from the limited knowledge on the metabolism of SCs. It has been observed that several SCs produce metabolites that remain active at CB1, potentially adding to the often-observed toxicity.¹⁰⁴⁻¹⁰⁷ Regarding analysis of biological specimens in clinical or forensic toxicology, knowledge on suitable screening targets is essential. Many SCs were shown to be mostly metabolized, with the unchanged parent compound excreted in small quantities. It is therefore advisable, especially when analyzing urine samples, to additionally screen for metabolites. The metabolism of newly emerging SCs is often unknown, posing the need for studies applying metabolic models, such as human hepatocytes and human liver microsomes (HLM).^{108, 109} Various studies deciphering the metabolism of SCs, applying varying metabolism models, have therefore been published in recent years.^{23, 110-119} Even with major metabolites identified, the lack of reference standards is often an additional hurdle faced by forensic laboratories.¹⁰⁸ In summary, SCs pose different challenges in the forensic field, largely attributable to the general lack of pharmacologic and toxicologic data paired with technical challenges requiring highly specialized analytical methodologies.

2 Motivation and Aims

The ongoing emergence of SCs and the changing legal situation and market surrounding *C. sativa* result in an array of challenges for juridical, public health, and forensic institutions. The overarching motivation of this work is, to address the challenges of particular concern in the forensic field, while approaching them from different angles. Advances arising from the use of HRMS are hereby highlighted.

As data on the metabolism of newly emerging SCs is typically scarce, *in vitro* metabolism studies are a means to identify suitable screening targets. *Study I*'s aim was the *in vitro* metabolic profiling of two SCs, resulting in recommended screening targets and initial data on involved cytochrome P450 isoenzymes.

Beginning in 2020, low-THC cannabis products adulterated with SCs have been increasingly observed in Switzerland and other European countries. The user's unawareness of the presence of SCs, paired with the often-observed higher potency and toxicity of SCs when compared to THC, raised considerable public health concerns. The aim of *Study II*, therefore, was to gain insights into this new trend by means of collaboration with three drug checking services. The products were thoroughly characterized, including detection of SCs and natural cannabinoids (THC and CBD). User self-reports were investigated to evaluate risks of adverse effects of adulterated compared to non-adulterated (regular) cannabis products.

With growing interest in minor cannabinoids in the medico-legal field, e.g., for improved bioanalytical data interpretation, comprehensive analytical techniques enabling deeper understanding of cannabinoid contents of cannabis products beyond THC and CBD are urgently required. The main goal of *Study III* was to develop a comprehensive analytical method for major and minor cannabinoids of *C. sativa*, allowing the extensive phytocannabinoid characterization of cannabis varieties. The method was applied to characterize a set of THC-rich plants cultivated under controlled conditions and belonging to 18 varieties.

3 Methodology

Brief summaries of the methodologies applied in *studies I-III* are presented below. Detailed information on chemicals, reagents, instruments, and experiments are contained within the respective presented publications and manuscripts.

Study I comprises the *in vitro* metabolic profiling of the two SCs CUMYL-THPINACA and ADAMANTYL-THPINACA. Both SCs were incubated using pooled human liver microsomes (pHLM). To evaluate the potential of metabolic drug-drug interactions and the influence of CYP polymorphisms, primarily involved CYPs were additionally determined using recombinant CYP enzymes (rCYP). For sample clean-up, a protocol employing solid phase extraction (SPE), initially developed for urine samples by Gaunitz *et al.*¹²⁰, was adapted. For the subsequent analysis a HPLC-HRMS method was implemented. The obtained high-resolution full scan data was thoroughly screened for signals of potential metabolites. The data-mining software Compound Discoverer™ (by Thermo Fisher Scientific™) aided data evaluation, by the means of an *expected workflow* (workflow defined within the software) during which common biotransformation products are predicted and automatically searched for. In a second step, MS² spectra of the tentatively identified metabolites were obtained and investigated to elaborate type and sites of biotransformation. A derivatization experiment using iodomethane was used to narrow down the location of selected hydroxyl-groups. The comparison of the peak area of the metabolites divided by the area of an internal standard (ISTD) led to the identification of the most abundant metabolites and was used to compare the involvement of the investigated rCYP.

Study II comprises the characterization of 94 cannabis samples obtained from three collaborating drug checking services between January 2020 to July 2021. A comprehensive screening method using HPLC-HRMS was developed. The method was validated regarding selectivity, specificity, and limits of detection (LODs) for 63 SCs. HRMS enabled retrospective data analysis and rapid identification and implementation of newly emerging SCs. The extraction and sample dilution procedure were evaluated employing spiking experiments. At a later stage, the method was expanded allowing semi-quantification of commonly detected SCs. The samples, where sufficient material was available, were additionally characterized based on their THC and CBD levels using gas chromatography coupled with flame ionization detection (GC-FID). Data obtained from the drug checking services included user self-reports on the drug's effects after consumption. As the obtained samples comprised adulterated as well as non-adulterated (regular; high-THC) cannabis material, these reports were statistically evaluated to detect differences in the likelihood of adverse effects.

Study III encompasses the development and validation of a comprehensive analytical method for the quantification of phytocannabinoids of *C. sativa* using HPLC-HRMS. The method was validated for selectivity, specificity, LODs, limits of quantification (LOQs), linearity, and accuracy for 15 cannabinoids. The applied HRMS technique and scan mode enabled the complementation of the targeted method with an untargeted metabolomics workflow. Cannabis inflorescence derived from 45 plants belonging to 18 cannabis varieties were analysed. Quantitative results for the 15 targeted cannabinoids were obtained. Additionally, initially untargeted compounds were detected and in a second step fragmented employing a data dependent MS² measurement (dd-MS²). Principal component analysis (PCA) was conducted to investigate differences and similarities between varieties.

4 Results

The subsequent pages contain Studies I-III:

❖ **4.1 Study I: Publication**

“Phase I In vitro Metabolic Profiling of the Synthetic Cannabinoid Receptor Agonists CUMYL-THPINACA and ADAMANTYL-THPINACA”

DOI: 10.3390/metabo11080470

p. 16 – 30 (25 numbered pages; *p. 1-25*)

❖ **4.2 Study II: Publication**

“Adulteration of low-delta-9-tetrahydrocannabinol products with synthetic cannabinoids: Results from drug checking services”

DOI: 10.1002/dta.3220

p. 31 – 44 (main article: 14 numbered pages; *p. 1-14*)

p. 45 – 49 (supplementary material: 5 numbered pages; *p. 1-5*)

❖ **4.3 Study III: Publication**

“Beyond Δ 9-tetrahydrocannabinol and cannabidiol: Chemical differentiation of cannabis varieties applying targeted and untargeted analysis”



DOI: 10.1007/s00216-022-04026-2

p. 50 – 65 (main article: 16 unnumbered pages)

p. 66 – 84 (supplementary material: 19 numbered pages; *p. 1-19*)

Article

Phase I In Vitro Metabolic Profiling of the Synthetic Cannabinoid Receptor Agonists CUMYL-THPINACA and ADAMANTYL-THPINACA

Manuela Carla Monti , Eva Scheurer and Katja Mercer-Chalmers-Bender * 

Institute of Forensic Medicine, Department of Biomedical Engineering, University of Basel, 4056 Basel, Switzerland; manuela.monti@unibas.ch (M.C.M.); eva.scheurer@unibas.ch (E.S.)

* Correspondence: katja.mercer-chalmers-bender@unibas.ch

Abstract: Synthetic cannabinoid receptor agonists (SCRAs) remain popular drugs of abuse. As many SCRAs are known to be mostly metabolized, in vitro phase I metabolic profiling was conducted of the two indazole-3-carboxamide SCRAs: CUMYL-THPINACA and ADAMANTYL-THPINACA. Both compounds were incubated using pooled human liver microsomes. The sample clean-up consisted of solid phase extraction, followed by analysis using liquid chromatography coupled to a high resolution mass spectrometer. In silico-assisted metabolite identification and structure elucidation with the data-mining software Compound Discoverer was applied. Overall, 28 metabolites were detected for CUMYL-THPINACA and 13 metabolites for ADAMANTYL-THPINACA. Various mono-, di-, and tri-hydroxylated metabolites were detected. For each SCRA, an abundant and characteristic di-hydroxylated metabolite was identified as a possible in vivo biomarker for screening methods. Metabolizing cytochrome P450 isoenzymes were investigated via incubation of relevant recombinant liver enzymes. The involvement of mainly CYP3A4 and CYP3A5 in the metabolism of both substances were noted, and for CUMYL-THPINACA the additional involvement (to a lesser extent) of CYP2C8, CYP2C9, and CYP2C19 was observed. The results suggest that ADAMANTYL-THPINACA might be more prone to metabolic drug–drug interactions than CUMYL-THPINACA, when co-administrated with strong CYP3A4 inhibitors.

Keywords: synthetic cannabinoid receptor agonists; in vitro metabolism; high resolution mass spectrometry; Compound Discoverer



Citation: Monti, M.C.; Scheurer, E.; Mercer-Chalmers-Bender, K. Phase I In Vitro Metabolic Profiling of the Synthetic Cannabinoid Receptor Agonists CUMYL-THPINACA and ADAMANTYL-THPINACA.

Metabolites **2021**, *11*, 470. <https://doi.org/10.3390/metabo11080470>

Academic Editor: Cornelius Hess

Received: 18 June 2021

Accepted: 16 July 2021

Published: 21 July 2021

Publisher's Note: MDPI stays neutral with regard to jurisdictional claims in published maps and institutional affiliations.



Copyright: © 2021 by the authors. Licensee MDPI, Basel, Switzerland. This article is an open access article distributed under the terms and conditions of the Creative Commons Attribution (CC BY) license (<https://creativecommons.org/licenses/by/4.0/>).

1. Introduction

Synthetic cannabinoid receptor agonists (SCRAs) are a prominent class within the world of new psychoactive substances (NPS). In recent years, SCRAs, together with synthetic cathinones, were the predominantly seized classes of NPS in Europe [1]. SCRAs encompass a large variety of structurally diverse compounds with binding affinities to the cannabinoid receptors 1 and 2 (CB1 and CB2). Particularly via interaction with CB1, most SCRAs present cannabimimetic effects similar to Δ^9 -tetrahydrocannabinol (THC), the major psychoactive compound in cannabis [2–4]. The typically higher binding affinities of SCRAs as full agonists at CB1 and CB2, when compared to THC, are attributed to the often-observed increased potency, but also toxicity, of these compounds. Nevertheless, data on the pharmacology and toxicity of SCRAs is still limited [2,5,6]. Several cases of severe intoxication, including lethal outcomes, have been associated with the intake of SCRAs, thus underlining the public health threat posed by these compounds [7–12].

SCRAs are classified based on their chemical structure [2]. In recent years, many indazole- and indole-carboxamide-derived SCRAs have been reported, with 5F-MDMB-PINACA (5F-ADB), 5F-MDMB-PICA, and MDMB-4en-PINACA being frequently reported after detection in diverse formulations, ranging from shredded herbs that have been sprayed with SCRAs (“spice”), infused papers, e-liquids, and bulk powders [13–15]. Since

the end of 2019, drug checking services in Switzerland have increasingly reported SCRA fortified THC-low cannabis [16]. As these illicit products are generally sold as the non-altered natural drug hemp, consumers unknowingly consuming SCRA are clearly posed with an increased health threat. As the emergence of SCRA on the drug market is constantly changing, as well as showing regional differences (for instance due to varying legal frameworks), it is important that analytical laboratories are constantly developing their analytical approach to SCRA. Urine is a matrix that is often used for screening procedures in clinical and forensic toxicology due to favorable accessibility, higher concentrations of the substance of interest, and often longer detection windows when compared to blood. However, many SCRA are known to be extensively metabolized, leading to a significant decrease or even lack of the parent compound in urine. As a consequence, metabolism studies identifying suitable target metabolites of NPS are inevitable [17–20].

CUMYL-THPINACA is classified as an indazole-3-carboxamide SCRA. A patent for CUMYL-THPINACA was issued in 2014 [21]. The cumyl-moiety is part of several SCRA, as in, for example, CUMYL-BICA, 5F-CUMYL-PINACA, 5F-CUMYL-PICA, and CUMYL-4CN-BINACA [22]. The metabolism of several cumyl-bearing SCRA has been investigated before [23–26], therefore the obtained results for CUMYL-THPINACA expand the current knowledge on the metabolism of members of this diverse subgroup. Considering its activity, Asada et al. synthesized CUMYL-THPINACA, finding strong activity at CB1 and CB2 [27]. This was confirmed via radioligand binding studies conducted by Schoeder et al. that showed high binding affinities of CUMYL-THPINACA at both CB1 ($K_i = 1.23 \pm 0.20$ nM) and CB2 ($K_i = 1.38 \pm 0.86$ nM) [28]. Even though these data on the affinity and activity of CUMYL-THPINACA exist, metabolic profiling, resulting in suggested biomarkers for the detection of the consumption of CUMYL-THPINACA, has, to the best of our knowledge, not been conducted yet.

ADAMANTYL-THPINACA, also referred to as ATHPINACA, is structurally related to CUMYL-THPINACA and AKB48 (APINACA). The adamantyl-moiety can be connected to the rest of the molecule, yielding two positional isomers of ADAMANTYL-THPINACA, which are referred to as isomer 1 [N-(1-adamantyl)] and isomer 2 [(N-(2-adamantyl))]. This study focusses on isomer 1, if not further specified. ADAMANTYL-THPINACA was first reported by EMCDDA's Early Warning System after it appeared in Slovenia in 2015 [29], followed by Hungary in 2016 [30]. Recently, a study was published focusing on the metabolism of adamantyl-positional isomers of SCRA, including first data on both isomers of ADAMANTYL-THPINACA. Metabolites were produced via incubation of pooled human liver microsomes (pHLM) and nine metabolites resulting from mono-, di-, and tri-hydroxylation were identified for isomer 1 of ADAMANTYL-THPINACA. Additionally, two glucuronidated metabolites were identified [31].

In this study, we present the phase I in vitro metabolic profiling of CUMYL-THPINACA and ADAMANTYL-THPINACA, applying two experimental set-ups. First, both SCRA were incubated using pHLM, resulting in structural elucidation and identification of potential in vivo biomarkers of the detected metabolites. The incubation of active pharmaceutical ingredients with pHLM, amongst other in vitro models (such as human hepatocytes), is an established procedure for initial characterization of human metabolism [18,20,32] and therefore highly valuable for the study of SCRA, for which information on the metabolism and suitable biomarkers is often lacking [20]. Metabolites as certified reference standards are often not available. Therefore, in vitro metabolism studies are a good alternative to incorporating metabolites into screening methods. Second, the cytochrome P450 enzymes (CYP) responsible for the phase I metabolism of the studied SCRA were identified via incubation of a panel of recombinant CYP isoforms (rCYP), thus expanding the present knowledge on the metabolism of ADAMANTYL-THPINACA as reported by Kadomura et al. [31]. Information on the metabolizing CYP isoforms gives the opportunity to predict the likelihood of metabolic drug–drug interactions or adverse events due to CYP polymorphisms [33–37]. A study conducted by Holm et al. showed that CYP3A4 was mainly responsible for the biotransformation of AKB48, an SCRA structurally related to ADAMANTYL-

THPINACA. Nevertheless, specific CYP isoforms involved in the metabolism of SCRAAs are often understudied and have, so far, not been investigated for CUMYL-THPINACA or ADAMANTYL-THPINACA.

Due to the diversity and large numbers of NPS emerging on the drug market, the rapid identification of target metabolites for screening procedures is urgently needed. High-resolution mass spectrometry (HR-MS) data analysis software is gaining importance, as *in silico*-assisted workflows enable higher throughput and are able to markedly facilitate metabolite identification [38,39]. In this study, data analysis was assisted by the Compound Discoverer (Thermo Fisher Scientific, Reinach, Switzerland) software, which has already been proven helpful for metabolite identification and structure elucidation in previously published studies [38,40–43].

2. Results and Discussion

2.1. Metabolite Identification for CUMYL-THPINACA and ADAMANTYL-THPINACA after Incubation with pHLM and rCYP

Functionality of the pHLM assay was assured by incubations of UR-144 (positive control) and subsequent detection of its N-(5-hydroxypentyl) and N-pentanoic acid metabolites. Negative controls did not result in any metabolite signals.

CUMYL-THPINACA and ADAMANTYL-THPINACA were extensively metabolized, resulting in a substantial decrease of the parent compound in the incubation mixture. Several metabolites resulting from mono-, di-, tri-hydroxylation, desaturation (most likely via hydroxylation followed by dehydration), and carbonylation, as well as combinations thereof, were identified. A summary of all detected metabolites and artefacts, and the results obtained via rCYP incubation, are shown in Tables 1 and 2 (for CUMYL-THPINACA) and Tables 3 and 4 (for ADAMANTYL-THPINACA).

2.2. In-Source Water Loss of Metabolites

As a consequence of using electrospray ionization (ESI), in-source-fragmentation processes may occur [39–42]. For example, the observed alleged metabolites, presenting a mass shift of +13.9838 Da in comparison to the parent compound, may result from either hydroxylation in combination with desaturation (e.g., di-hydroxylation followed by dehydration) or carbonylation. However, the corresponding signals may also arise from in-source water loss, resulting from the cleavage of aliphatic hydroxyl-groups (e.g., at the 4-methyl-tetrahydropyran- and adamantyl-moiety). In-source water loss was considered as likely, where (i) a hydroxylated metabolite was detected, exhibiting a hydroxyl group at a position predestined for in-source water loss, (ii) a co-eluting signal was identified, presenting a dehydration-specific mass shift of -18.0153 Da ($-H_2O$), and (iii) after fragmentation, when the type and position of biotransformation were identical for the hydroxylated metabolite and the alleged artefact. For example MC21, a metabolite produced by mono-hydroxylation at the 4-methyl-tetrahydropyran-moiety (i) was detected, but additionally a signal at the corresponding retention time (Rt) with mass shift of $[M + H]^+ - 18.0153$ Da was found (ii), which exhibits dehydration at the 4-methyl-tetrahydropyran-moiety (iii). Therefore, this signal was classified as an artefact (MCArt4).

The diversity in the hydroxylation patterns of metabolites, especially in cases of two or three concurrent hydroxylations, makes the evaluation of in-source processes highly complex. The observed results suggest that the susceptibility for in-source water loss considerably varies between aliphatic structures (e.g., adamantyl versus 4-methyl-tetrahydropyran). This becomes obvious when comparing the peak areas of genuine metabolites and the corresponding in-source artefacts. In the case of MA2 (hydroxylated at the adamantyl-moiety) the corresponding artefact (MAArt1) showed a 6.8 times higher signal than observed for MA2 itself. In comparison, MC21 (hydroxylated at the 4-methyl-tetrahydropyran-moiety) exhibited an in-source dehydration signal of roughly the same intensity as that observed for MC21. Additionally, positional isomers of hydroxylations within a moiety led to varying levels of observed water loss. For instance, when investigating the metabolite cluster

MC8a–e (consisting of several co-eluting di-hydroxylated metabolites, bearing a hydroxyl-group at the 4-methyl-tetrahydropyran-moiety), in-source water loss varied from excessive (artefact signal [MCart2a–b] > metabolite signal) to not detectable.

In this study, several hydroxylated metabolites of CUMYL-THPINACA and one of ADAMANTYL-THPINACA were prone to in-source dehydration, in most cases attributable to the instability of the hydroxylated 4-methyl-tetrahydropyran-moiety. This most likely resulted in the identification of several artefacts that are discussed in the corresponding chapters referring to the genuine metabolites. In addition, several signals were detected lacking a hydroxylated counterpart, therefore not meeting the above-stated criteria for in-source water loss—they were thus classified as genuine metabolites produced by hydroxylation and desaturation (MC3, MC6, MC12, MC17, MA3, MA8, MA11) or carbonylation (MC13, MC15, MC18, MC20, MC22, MA13, MA10). However, the possibility remains, that the hydroxylated original metabolite was prone to complete in-source water loss, i.e., the original parent ion was no longer detectable. In the context of analytics and the herein presented aims, the focus of this study lies in the identification of suitable biomarkers, which may include highly abundant artefacts resulting from true metabolites. As in-source fragmentation is often seen as an unwanted ESI byproduct, it has also been proposed that in-source-fragment information can improve metabolite identification [44]. However, it must be kept in mind, that the occurrence of in-source-fragmentation processes may also depend on the instrument used, instrument configurations, and ESI conditions.

2.3. Metabolic Profiling of CUMYL-THPINACA

The fragmentation of CUMYL-THPINACA resulted in three diagnostic fragments at m/z 119.0855, representing the cumyl-moiety, m/z 260.1394, referring to the unaltered 1-(tetrahydropyranyl-4-methyl)-indazole-3-carboxamide structure, and m/z 243.1128, representing the 1-(tetrahydropyranyl-4-methyl)-indazole-3-acylium-ion. A total of three mono-hydroxylated (MC19a–b, MC21), eight di-hydroxylated (MC1, MC8a–e, MC14, MC16), and eight tri-hydroxylated (MC2a–b, MC4, MC5, MC7, MC9, MC10, MC11) metabolites were detected (see Table 1). The di-hydroxylated metabolite MC16, presenting with highest peak areas in the conducted experiments, is suggested as a suitable target in screening procedures. Additional minor metabolites were produced via either hydroxylation with concurrent dehydration, referred to as mono-/di-hydroxylated and desaturated metabolites, or carbonylation. In this context, two mono-hydroxylated and desaturated metabolites (MC12, MC17) and two di-hydroxylated and desaturated metabolites (MC3, MC6) were identified. Finally, carbonylation led to the production of one metabolite (MC22) and mono-hydroxylation in combination with carbonylation resulted in four metabolites (MC13, MC15, MC18, MC20). In-source water loss could not be ruled out for some metabolites; thus, these signals were classified as artefacts (MCart1, MCart2a–b, MCart4, MCart5). Through conduction of a derivatization experiment, employing iodomethane as the methylating agent, the location of the hydroxyl-groups could be narrowed down to the indazole-core. The main site for biotransformation in regard to number of individual metabolites as well as when considering the most abundant metabolites was the 4-methyl-tetrahydropyran-moiety, while oxidation of the cumyl-moiety was less often observed. There are several other studies investigating the metabolism of SCRA containing a cumyl-moiety [22,23,26]. These aforementioned studies also concluded that the cumyl-moiety was not the main site of metabolism. A chromatogram showing the mass traces of all metabolites is depicted in Figure 1 and the proposed metabolic pathway of CUMYL-THPINACA is visualized in Figure 2. MS^2 spectra of CUMYL-THPINACA and the three most abundant metabolites, including proposed fragments, are shown in Figure 3.

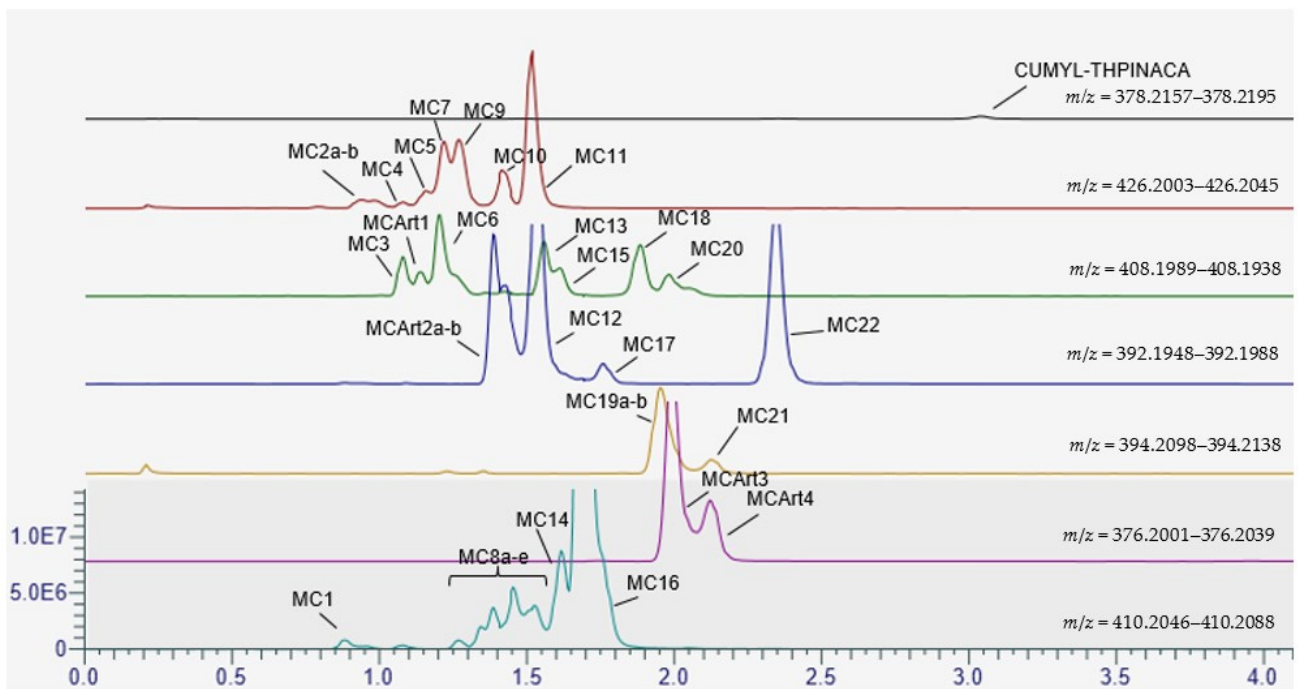


Figure 1. Chromatogram showing the mass traces of the detected metabolites (and artefacts) of CUMYL-THPINACA after 2 h of incubation. The traces are normalized globally, with a maximum at 12% of the base peak (MC16).

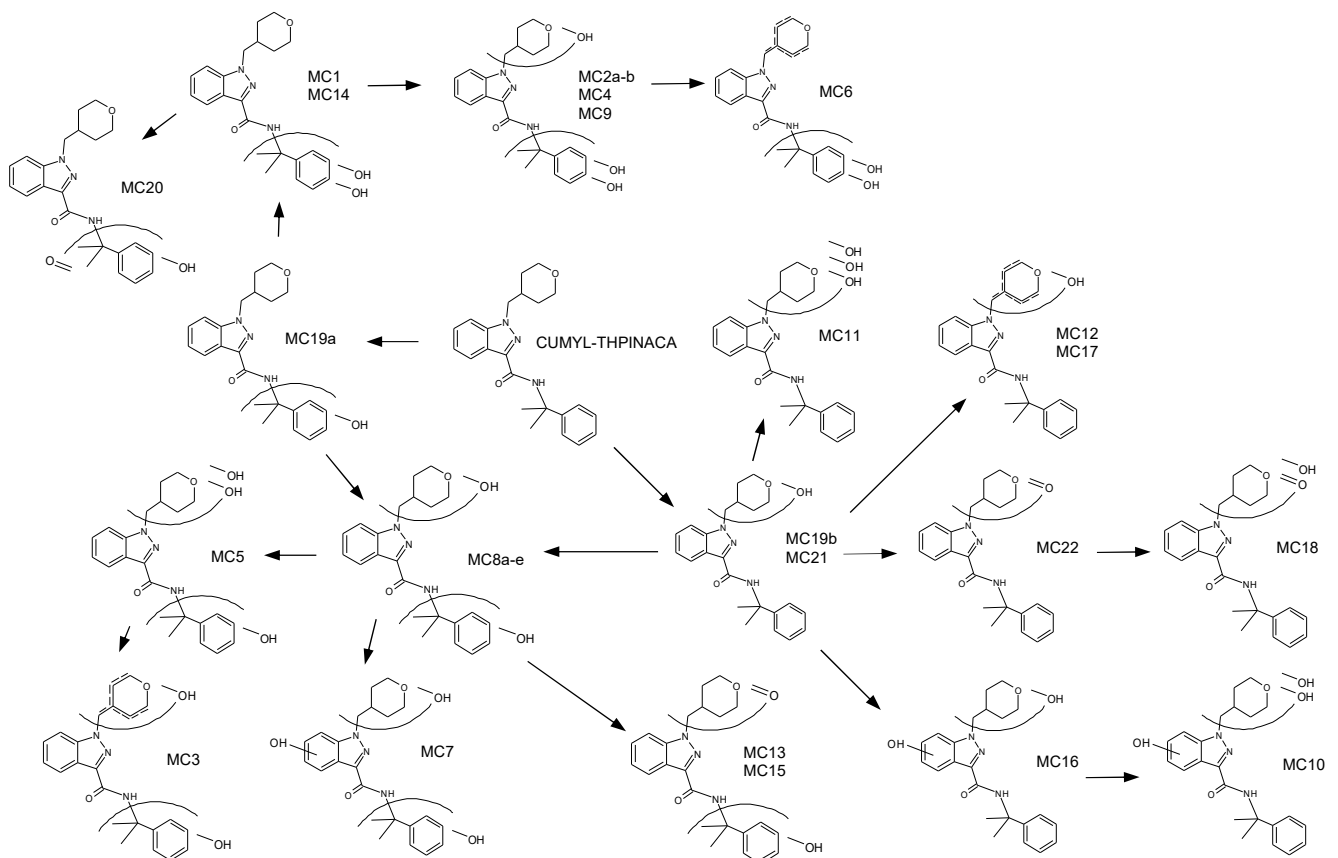


Figure 2. Proposed metabolic pathway for CUMYL-THPINACA.

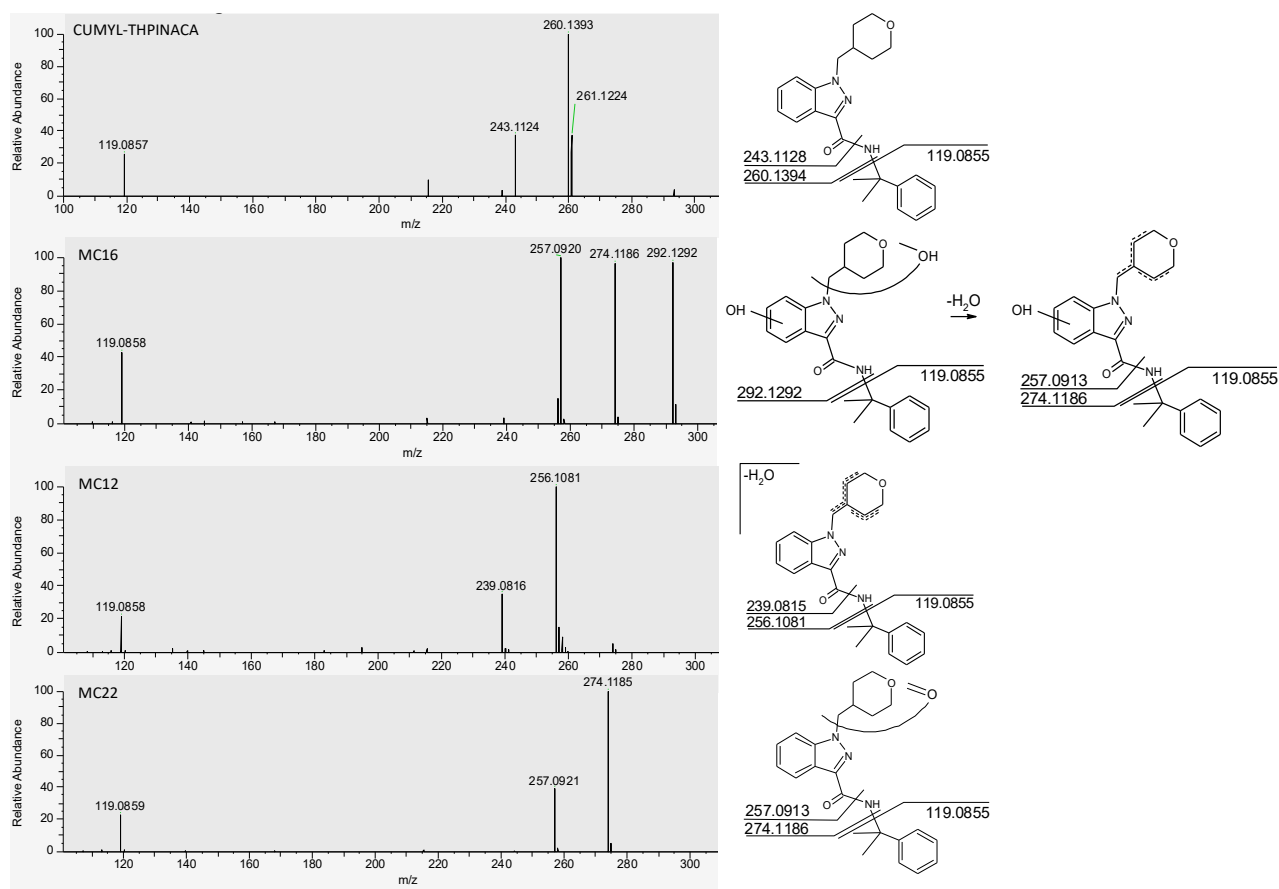


Figure 3. MS² spectra of CUMYL-THPINACA and its three most abundant metabolites (MC12, MC16, and MC22, shown in order of decreasing intensity). The proposed fragments leading to the respective signals are shown on the right.

Table 1. Summary of all detected metabolites and the two detected artefacts of CUMYL-THPINACA (listed in the order of the observed retention times) with suggested biotransformations, chemical formulas, calculated [M + H]⁺ of the parent ions with associated product ions (*m/z*), mass error (ppm), retention times (Rt), areas after 2 h of incubation using pHLM and ranking (highest to lowest abundance).

ID	Biotransformation	Formula	[M + H] ⁺ Productions (<i>m/z</i>)	Mass Error (ppm)	Rt (min)	Area (<i>n</i> = 2)	Rank
MC1	di-hydroxylation at cumyl	C ₂₃ H ₂₈ N ₃ O ₄	410.2074 259.1077 151.0754	0.4	0.89	3.0 × 10 ⁶	21
MC2a–b	di-hydroxylation at cumyl, mono-hydroxylation at 4-methyl-tetrahydropyran	C ₂₃ H ₂₈ N ₃ O ₅	426.2023 408.1918 259.1077 151.0754	0.4	a: 0.90 b: 0.99	3.9 × 10 ⁶	19
MC3	mono-hydroxylation at cumyl, mono-hydroxylation and desaturation at 4-methyl-tetrahydropyran	C ₂₃ H ₂₈ N ₃ O ₅	408.1918 256.1081 135.0804	−0.1	1.08	8.00 × 10 ⁶	14
MC4	di-hydroxylation at cumyl, mono-hydroxylation at 4-methyl-tetrahydropyran	C ₂₃ H ₂₈ N ₃ O ₅	426.2023 408.1918 259.1077 151.0754	−0.2	1.08	1.1 × 10 ⁶	22

Table 1. Cont.

ID	Biotransformation	Formula	[M + H] ⁺ Productions (<i>m/z</i>)	Mass Error (ppm)	Rt (min)	Area (<i>n</i> = 2)	Rank
MCArt1	In-source water loss of MC5	C ₂₃ H ₂₈ N ₃ O ₅	408.1918 256.1081 135.0804	0.4	1.16	4.5 × 10 ⁶	-
MC5	mono-hydroxylation at cumyl, di-hydroxylation at 4-methyl-tetrahydropyran	C ₂₃ H ₂₈ N ₃ O ₅	426.2023 274.1186 256.1081 135.0804	0.8	1.19	3.7 × 10 ⁶	20
MC6	di-hydroxylation at cumyl, desaturation at 4-methyl-tetrahydropyran	C ₂₃ H ₂₈ N ₃ O ₅	408.1918 258.1237 151.0754	-0.3	1.20	2.3 × 10 ⁷	7
MC7	mono-hydroxylation at cumyl, mono-hydroxylation at indazole, mono-hydroxylation at 4-methyl-tetrahydropyran	C ₂₃ H ₂₈ N ₃ O ₅	426.2023 292.1292 274.1186 257.0913 135.0804	-0.6	1.23	1.6 × 10 ⁷	10
MC8a-e	mono-hydroxylation at cumyl and mono-hydroxylation at 4-methyl-tetrahydropyran	C ₂₃ H ₂₈ N ₃ O ₄	410.2074 258.1237 241.0972 135.0804	-1.3	a: 1.28 b: 1.35 c: 1.39 d: 1.46 e: 1.53	4.4 × 10 ⁷	4
MC9	di-hydroxylation at cumyl, mono-hydroxylation at 4-methyl-tetrahydropyran	C ₂₃ H ₂₈ N ₃ O ₅	426.2023 258.1237 151.0754	-0.6	1.27	1.9 × 10 ⁷	9
MCArt2a-b	In-source water loss MC8a-e	C ₂₃ H ₂₆ N ₃ O ₃	392.1969 258.1237 241.0972 135.0804	-1.7	a: 1.39 b: 1.44	5.5 × 10 ⁷	-
MC10	di-hydroxylation at 4-methyl-tetrahydropyran, mono-hydroxylation at indazole	C ₂₃ H ₂₈ N ₃ O ₅	426.2023 308.1241 290.1135 272.103 119.0855	-0.7	1.42	9.1 × 10 ⁶	13
MC11	tri-hydroxylation at 4-methyl-tetrahydropyran	C ₂₃ H ₂₈ N ₃ O ₅	426.2023 308.1241 290.1135 272.103 254.0924 119.0855	-0.5	1.51	3.8 × 10 ⁷	5
MC12	mono-hydroxylation and desaturation at 4-methyl-tetrahydropyran	C ₂₃ H ₂₆ N ₃ O ₃	392.1969 256.1081 239.0815	-1.6	1.54	7.8 × 10 ⁷	2
MC13	mono-hydroxylation at cumyl, carbonylation at 4-methyl-tetrahydropyran	C ₂₃ H ₂₈ N ₃ O ₅	408.1918 274.1186 257.0913 135.0804	-1.2	1.56	1.1 × 10 ⁷	12
MC14	di-hydroxylation at cumyl	C ₂₃ H ₂₈ N ₃ O ₄	410.2074 260.1394 151.0754	-1.1	1.62	2.3 × 10 ⁷	8

Table 1. Cont.

ID	Biotransformation	Formula	[M + H] ⁺ Productions (<i>m/z</i>)	Mass Error (ppm)	Rt (min)	Area (<i>n</i> = 2)	Rank
MC15	mono-hydroxylation at cumyl, carbonylation at 4-methyl-tetrahydropyran	C ₂₃ H ₂₈ N ₃ O ₅	408.1918 274.1186 257.0913 135.0804	−0.1	1.62	6.3 × 10 ⁶	16
MC16	mono-hydroxylation at 4-methyl-tetrahydropyran, mono-hydroxylation at indazole	C ₂₃ H ₂₈ N ₃ O ₄	410.2074 292.1292 274.1186 257.0913 119.0855	−1.3	1.69	3.4 × 10 ⁸	1
MC17	mono-hydroxylation and desaturation at 4-methyl-tetrahydropyran	C ₂₃ H ₂₆ N ₃ O ₃	392.1969 256.1081 239.0815 119.0855	−0.9	1.81	5.6 × 10 ⁶	17
MC18	mono-hydroxylation and carbonylation at 4-methyl-tetrahydropyran	C ₂₃ H ₂₈ N ₃ O ₅	408.1918 290.1135 273.087 272.103 119.0855	−0.2	1.88	1.3 × 10 ⁷	11
MC19a–b	a: mono-hydroxylation at cumyl	C ₂₃ H ₂₈ N ₃ O ₃ a:	394.2118 135.0804 260.1394 243.1128	1.4	1.99	3.0 × 10 ⁷	6
	b: mono-hydroxylation at 4-methyl-tetrahydropyran	b:	276.1343 119.0855				
MCArt3	In-source water loss MC19b	C ₂₃ H ₂₅ N ₃ O ₂	376.2020 258.1237 119.0855	−0.7	2.03	1.5 × 10 ⁷	-
MC20	mono-hydroxylation and carbonylation at cumyl	C ₂₃ H ₂₈ N ₃ O ₅	408.1918 260.1394 243.1128 149.1660	−0.1	1.98	7.0 × 10 ⁶	15
MC21	mono-hydroxylation at 4-methyl-tetrahydropyran	C ₂₃ H ₂₈ N ₃ O ₃	394.2118 258.1237 119.0855	1.4	2.15	4.4 × 10 ⁶	18
MCArt4	In-source water loss MC21	C ₂₃ H ₂₅ N ₃ O ₂	376.2020 258.1237 119.0855	−0.5	2.17	4.7 × 10 ⁶	-
MC22	carbonylation at 4-methyl-tetrahydropyran	C ₂₃ H ₂₆ N ₃ O ₃	392.1969 274.1186 257.0913 119.0855	−1.3	2.39	5.0 × 10 ⁷	3
CUMYL-THPINACA		C ₂₃ H ₂₇ N ₃ O ₂	378.2176 260.1394 243.1128 119.0855	0.1	3.07	8.9 × 10 ⁵	-

2.3.1. Mono-Hydroxylation

MC19a is mono-hydroxylated at the cumyl-moiety, as a fragment at *m/z* 135.0804 was detected. For M19b and MC21, mono-hydroxylation at the 1-(tetrahydropyranyl-4-methyl)-indazole-3-carboxamide structure was detected instead (*m/z* 276.1343). Due to the observation of in-source dehydration (MCArt3 and MCArt4), and as derivatization did not

alter the signals of MC19b and MC21, the location of the hydroxyl groups are suggested to be located at the unsaturated 4-methyl-tetrahydropyran-moiety. MCArt3 and MCArt4 are signals matching the criteria defined in chapter 2.2, and thus are classified as artefacts resulting from in-source dehydration of MC19b and MC21. Fragmentation of MCArt3 and MCArt4 showed desaturation at the 4-methyl-tetrahydropyran-moiety (m/z 258.1237), which corresponds to the location of mono-hydroxylation of the co-eluting metabolites MC19b and MC21.

2.3.2. Di-Hydroxylation

The most abundant metabolite after 2 h of incubation was the di-hydroxylated metabolite MC16. For MC16, the unaltered cumyl-moiety was detected. As a dehydration reaction was identified during fragmentation, resulting in a fragment at m/z 274.1186, it was concluded that the second hydroxyl-group is located at the 4-methyl-tetrahydropyran-moiety. The location of the second hydroxyl-group at the indazole-core was verified after derivatization. When fragmenting the proposed product of methylation of MC16 at m/z 424.2231 (mass shift of 14.0157 Da), a specific fragment corresponding to the 1-(tetrahydropyranyl-4-methyl)-indazole-3-carboxamide-moiety which had been di-hydroxylated and methylated, was detected at m/z 306.1448.

MC1, MC8a–e, and MC16 are additional metabolites resulting from di-hydroxylation. MC1 is produced via di-hydroxylation at the cumyl-moiety, indicated by a fragment at m/z 151.0754. Several isomers were detected arising from concurrent mono-hydroxylation at the cumyl-moiety and the 1-(tetrahydropyranyl-4-methyl)-indazole-3-carboxamide-moiety, resulting in the metabolite cluster MC8a–e. As the fragment at m/z 258.1237 was found throughout (produced via water loss from the 4-methyl-tetrahydropyran-moiety), the hydroxyl-group of the metabolites MC8a–e were concluded to be located at the 4-methyl-tetrahydropyran-moiety. Co-eluted with the metabolite cluster MC8a–e, MCArt2a–b (consisting of two fused peaks), was detected. After fragmentation of MCArt2a–b, the location of one hydroxyl-group was identified at the cumyl-moiety and desaturation was found at the 4-methyl-tetrahydropyran-moiety. Due to the matching type and location of the biotransformation between the original metabolites MC8a–e and MCArt2a–b, the origin of the signal leading to MCArt2a–b was defined as in-source water loss. Finally, MC14 is di-hydroxylated at the di-hydroxylated cumyl-moiety, as the diagnostic fragment at m/z 151.0754 was identified.

2.3.3. Mono-Hydroxylation and Additional Desaturation and Carbonylation

MC12, MC17, and MC22 are all metabolites sharing the parent ion at m/z 392.1969. As no co-eluting di-hydroxylated metabolites exhibiting the same patterns were detectable (considering the type and location of biotransformation), in-source water loss as the origin of the corresponding signals was ruled out for these metabolites. MC12 and MC17 presented a fragment at m/z 256.1081 that resulted from the dehydration of the already desaturated 1-(tetrahydropyranyl-4-methyl)-indazole-3-carboxamide-moiety. Due to the observed desaturation, MC14 and MC19 were classified as mono-hydroxylated and desaturated at the 4-methyl-tetrahydropyran-moiety. The absence of phenolic hydroxyl groups was confirmed via derivatization experiments, as no signal decline of the parent ion was observed. MC22 did not present a dehydration reaction during fragmentation as only the fragments with m/z 274.1186 (desaturated 1-(tetrahydropyranyl-4-methyl)-indazole-3-carboxamide structure) and m/z 257.09134 (acylium-ion after cleavage of the C–N bond) were detected. Therefore, M22 was concluded to be carbonylated at the 4-methyl-tetrahydropyran-moiety.

2.3.4. Tri-Hydroxylation

MC2a–b and MC4 are di-hydroxylated at the cumyl-moiety, as verified by detection of the fragment at m/z 151.0754. MC2a–b and MC4 also present a fragment at m/z 408.1918 as a result of water loss during fragmentation of the otherwise intact structure. Due to the

observed water loss, the location of the one hydroxyl group is situated at the 4-methyl-tetrahydropyran-moiety. MC5 was observed to be mono-hydroxylated at the cumyl-moiety, showing the diagnostic fragment at m/z 135.0804. The additional fragment at m/z 256.1081, resulting from two dehydration reactions of the di-hydroxylated 1-(tetrahydropyranyl-4-methyl)-indazole-3-carboxamide structure, verifies the positions of the two other hydroxyl groups at the 4-methyl-tetrahydropyran-moiety. In-source water loss of MC5, leading to the signal of MCArt1, could not be ruled out, due to the proximity of MC5 and the observed signal of MCArt1, which also has one hydroxyl-group at the cumyl-moiety (m/z 135.0804) but is hydroxylated and additionally desaturated at the tetrahydropyran-moiety. Thus, MCArt1 was defined as a possible artefact.

Mono-hydroxylation at the cumyl-moiety was also observed for MC7. As for MC7, only one dehydration reaction was detected, indicated by the fragment at m/z 274.1186. Observed fragments for MC7 indicated mono-hydroxylation at the cumyl-moiety, the indazole-core, and at the 4-methyl-tetrahydropyran-moiety. This was also confirmed via the derivatization experiment, as the methylated product of MC7 was detected, presenting a diagnostic fragment at m/z 306.1448, which represents the di-hydroxylated and methylated 1-(tetrahydropyranyl-4-methyl)-indazole-3-carboxamide-moiety. MC9 is di-hydroxylated at the cumyl-moiety, as shown by the fragment at m/z 151.0754. Additionally, a fragment at m/z 258.1237 was detected, which was the dehydration product of the 1-(tetrahydropyranyl-4-methyl)-indazole-3-acylium-ion, thus indicating the location of the third hydroxyl group at the 4-methyl-tetrahydropyran-moiety. MC10 is suggested to be di-hydroxylated at the 4-methyl-tetrahydropyran-moiety, but additionally mono-hydroxylated at the indazole-core. Further, an ion corresponding to the product of tri-hydroxylation and methylation of MC10 at m/z 440.2180 was detected after derivatization. Fragmentation of this methylated metabolite produced a diagnostic ion at m/z 322.1397, referring to the methylated tri-hydroxylated 1-(tetrahydropyranyl-4-methyl)-indazole-3-acylium-ion, and thus verifying the location of one hydroxyl group at the unsaturated indazole-region. MC11 is tri-hydroxylated at the 1-(tetrahydropyranyl-4-methyl)-indazole-3-carboxamide structure, as the fragment standing for the tri-hydroxylated 1-(tetrahydropyranyl-4-methyl)-indazole-3-carboxamide-moiety (m/z 308.1241) was detected. Additionally, this moiety produced further fragments, after one (m/z 290.1135), two (m/z 272.1030), and three dehydrations (m/z 254.0924). Derivatization did not result in a decline of the MC11 signal, thus confirming the location of all three hydroxyl-groups at the unsaturated 4-methyl-tetrahydropyran-moiety.

2.3.5. Mono-Hydroxylation and Additional Desaturation and Carbonylation

MC3 is most likely formed via metabolic tri-hydroxylation (MC5) and concurrent dehydration, resulting in a di-hydroxylated and desaturated molecule. MC3 presented a fragment at m/z 135.0804, which represents the mono-hydroxylated cumyl-moiety. The desaturation reaction and the second hydroxyl group are located at the 4-methyl-tetrahydropyran-moiety, as the fragment at m/z 256.1081 was detected—resulting from additional dehydration of this moiety. For MC6, the location of both hydroxyl-groups was found to be at the cumyl-moiety, as a fragment at m/z 151.0754 was detected. An additionally observed fragment at m/z 258.1237 was attributed to the desaturated 1-(tetrahydropyranyl-4-methyl)-indazole-3-acylium-ion.

MC13 and MC15 are classified as mono-hydroxylated and carbonylated metabolites. With the diagnostic ion at m/z 135.0804, both are identified as to be mono-hydroxylated at the cumyl-moiety. Due to the lack of the dehydration reaction during occurring fragmentation, it is suggested that MC13 and MC15 are therefore carbonylated at the 4-methyl-tetrahydropyran-moiety. Mono-hydroxylation in combination with carbonylation was also observed for MC18. Due to the presence of the fragment at m/z 119.0855, and as MC18 was not methylated during derivatization, proving the absence of phenolic hydroxyl groups, it is assumed that hydroxylation and carbonylation must be located at the 4-methyl-tetrahydropyran-moiety. The fragment at m/z 290.1135 represents the mono-hydroxylated and carbonylated 1-(tetrahydropyranyl-4-methyl)-indazole-3-carboxamide

structure. The fragment at m/z 272.1030 is produced by additional dehydration and a fragment at m/z 273.087 results from nitrogen cleavage. MC20 presented two diagnostic ions at m/z 260.1394 and m/z 243.1128, representing the unaltered 1-(tetrahydropyranyl-4-methyl)-indazole-3-carboxamide-moiety. The fragment at m/z 149.0597 represents the cumyl-moiety that has been mono-hydroxylated and carbonylated. With the methylated product of MC21, the location of the hydroxyl was assigned at the phenyl-ring of the cumyl-moiety. In-source water loss, resulting in an additional signal associated with MC3, MC6, MC13, MC17, MC18, and MC20, was not further considered, due to the lack of corresponding tri-hydroxylated metabolites in the respective elution windows. The observed later elution of metabolites MC18 and MC20 was in concordance with the suggested carbonylation, as this biotransformation would result in less polar metabolites compared to the product of di-hydroxylation and desaturation.

2.3.6. Identification of the Primarily Involved CYP Isoenzymes

The results obtained showed that CYP3A4 and CYP3A5 are primarily involved in the metabolism of CUMYL-THPINACA, followed by CYP2D6, CYP2C8, and, to a much lesser extent, by CYP2C19. The involvement of CYP2C9, CYP1A2, and CYP2B6 was also observed. Signals at the retention times of MCArt3 and MCArt4, presenting an area ratio (peak area/internal standard (ISTD) area) of <0.1 , were detected in the negative control as well as in the incubation mixture of CYP2E1 and CYP2A6. As these were the only signals detected for CYP2E1 and CYP2A6, it suggests that CYP2E1 and CYP2A6 did not show any metabolic activity for CUMYL-THPINACA. Two metabolites (MC4 and MC5), which were observed after incubation using pHLM, could not be detected after incubation with rCYP (tested with different incubation times), most likely due to these metabolites being produced via a more complex pathway; the involvement of a combination of different CYP; or at concentration levels below the limit of detection. These results are summarized in Table 2.

CYP3A4 is an important CYP isoform with regard to abundance in the human liver as well as the majority of drugs being known to be substrates of CYP3A4. Overall, due to the primary involvement of CYP3A4, drug–drug interactions may be observable in combination with strong CYP3A4 inhibitors (e.g.,azole-antifungals) [45]. Nevertheless, due to the involvement of further CYP isoforms (e.g., CYP2D6, CYP2C8, and CYP2C19), this risk is most likely reduced.

Table 2. Results of the incubation of CUMYL-THPINACA with rCYP. Listed area ratios (absolute peak area (metabolite)/absolute peak area (ISTD)) are classified as follows: (+): <0.1 , +: ≥ 0.1 – ≤ 1 , ++: >1 – ≤ 5 , +++: $>$. Where the negative control contained trace amounts of metabolites in a comparable amount, as in the samples after incubation, the result is marked as: (+) *.

ID	3A4	3A5	2D6	2C8	2C9	2C19	2B6	1A2	2E1	2A6	Negative Control
	<i>n</i> = 2	<i>n</i> = 2	<i>n</i> = 2	<i>n</i> = 2	<i>n</i> = 2	<i>n</i> = 2	<i>n</i> = 2	<i>n</i> = 2	<i>n</i> = 2	<i>n</i> = 2	<i>n</i> = 2
MC1	(+)	(+)	-	-	-	-	-	-	-	-	-
MC2a–b	+	(+)	-	-	-	-	-	-	-	-	-
MC3	(+)		-	-	-	-	-	-	-	-	-
MC4	-	-	-	-	-	-	-	-	-	-	-
MCArt1	(+)	(+)	-	-	-	-	-	-	-	-	-
MC5	-	-	-	-	-	-	-	-	-	-	-
MC6	(+)	(+)	-	-	-	-	-	-	-	-	-
MC7	(+)	(+)	-	-	-	-	-	-	-	-	-
MC8a–e	+	+	(+)	(+)	(+)	(+)	-	-	-	-	-
MC9	(+)				-		-	-	-	-	-

Table 2. Cont.

ID	3A4	3A5	2D6	2C8	2C9	2C19	2B6	1A2	2E1	2A6	Negative Control
	<i>n</i> = 2	<i>n</i> = 2	<i>n</i> = 2	<i>n</i> = 2	<i>n</i> = 2	<i>n</i> = 2	<i>n</i> = 2	<i>n</i> = 2	<i>n</i> = 2	<i>n</i> = 2	<i>n</i> = 2
MCArt2a–b	+	+	(+)	(+)	-	(+)	-	-	-	-	-
MC10	+	+	-	-	-	-	-	-	-	-	-
MC11	+	(+)	-	-	-	-	-	-	-	-	-
MC12	++	+	-	-	-	-	-	-	-	-	-
MC13	(+)	-	-	-	-	-	-	-	-	-	-
MC14	+	+	(+)	(+)	-	(+)	-	-	-	-	-
MC15	(+)	-	-	-	-	-	-	-	-	-	-
MC16	++	++	+	(+)	-	(+)	-	-	-	-	-
MC17	+	(+)	-	-	-	-	-	-	-	-	-
MC18	+	(+)	-	-	-	-	-	-	-	-	-
MC19a–b	+++	++	++	+	(+)	+	(+)	(+)	-	-	-
MCArt3	+++	+++	+++	++	+	++	+	+	(+)*	(+)*	(+)*
MC20	+	(+)	-	-	-	-	-	-	-	-	-
MC21	+++	+++	++	++	+	++	(+)	(+)	-	-	-
MCArt4	+++	+++	+++	+++	+	+++	(+)*	(+)*	(+)*	(+)*	(+)*
MC22	++	+	(+)	(+)	-	(+)	-	-	-	-	-

2.4. Metabolite Identification for ADAMANTYL-THPINACA

ADAMANTYL-THPINACA was prone to hydroxylation at the adamantyl-moiety and, to a lesser extent, at the 1-(tetrahydropyranyl-4-methyl)-indazole-3-carboxamide-moiety. Extensive hydroxylation at the adamantyl-moiety has also been observed for other adamantyl-bearing SCRAAs [31,46,47]. Overall, one mono-hydroxylated (M12), three di-hydroxylated (MA5, MA7, MA9), and four tri-hydroxylated (MA1, MA2, MA4, MA6) were detected. During analysis, two artefacts were detected (MAArt1 and MAArt2), resulting from in-source water loss of di- and a tri-hydroxylated metabolites. In-source water loss was ruled out for three additional metabolites produced via hydroxylation with concurrent desaturation (MA3, MA8, MA11) and mono-hydroxylation in combination with carbonylation (MA10 and MA13). In this study, a total of 13 metabolites were detected for ADAMANTYL-THPINACA (see Table 3). Kadomura et al. reported nine metabolites resulting from phase I metabolism and two glucuronidated metabolites resulting from phase II metabolism [31]. Regarding the previously reported phase I metabolites produced via mono-, di-, and tri-hydroxylation, the results of our study are in good agreement with theirs, with the exception of one additional tri-hydroxylated metabolite that was not detected in our study. This was most probably due to insufficient chromatographic resolution. However, Kadomura et al. did not present the herein observed metabolites produced from hydroxylation in combination with desaturation (MA3, MA8, MA11) and the two mono-hydroxylated and carbonylated metabolites (MA10 and MA13). In the presented study, MA3 and MA8 were ranked as the third and fourth most abundant metabolites, while the rest could be considered as minor metabolites, and thus more likely of limited importance as biomarkers in the in vivo setting. In contrast to Kadomura et al. we did not study the phase II metabolism.

A chromatogram showing the mass traces of all the above-mentioned metabolites and signals in this study is given in Figure 4. Due to the high abundance of the di-hydroxylated metabolite MA9, this metabolite is suggested as a suitable biomarker for urine screenings. Nevertheless, due to limitations of in vitro models, verification in vivo by

ana-lysis of positive human urine samples is needed. The proposed metabolic pathway is presented in Figure 5. Fragmentation of the parent compound ADAMANTYL-THPINACA resulted in only one fragment at m/z 135.1168. Variation of the collision energies did not result in more diagnostic ions for the parent compound (data not shown). Additional diagnostic fragments were detected for the metabolites of ADAMANTYL-THPINACA. The respective MS² spectra of ADAMANTYL-THPINACA, incorporating the three most abundant metabolites with their suggested fragments, are shown in Figure 6.

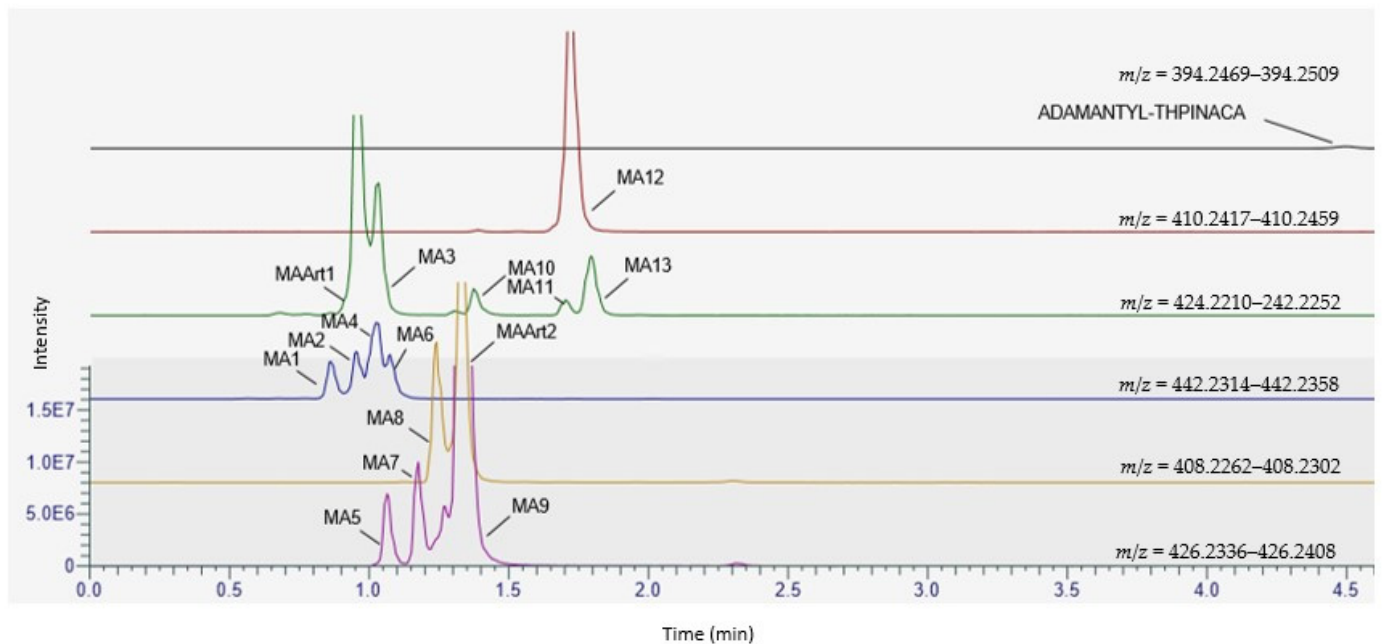


Figure 4. Chromatogram showing the mass traces of the detected metabolites (and artefacts) of ADAMANTYL-THPINACA after 2 h of incubation. The traces are normalized globally, with a maximum at 12% of the base peak (MA9).

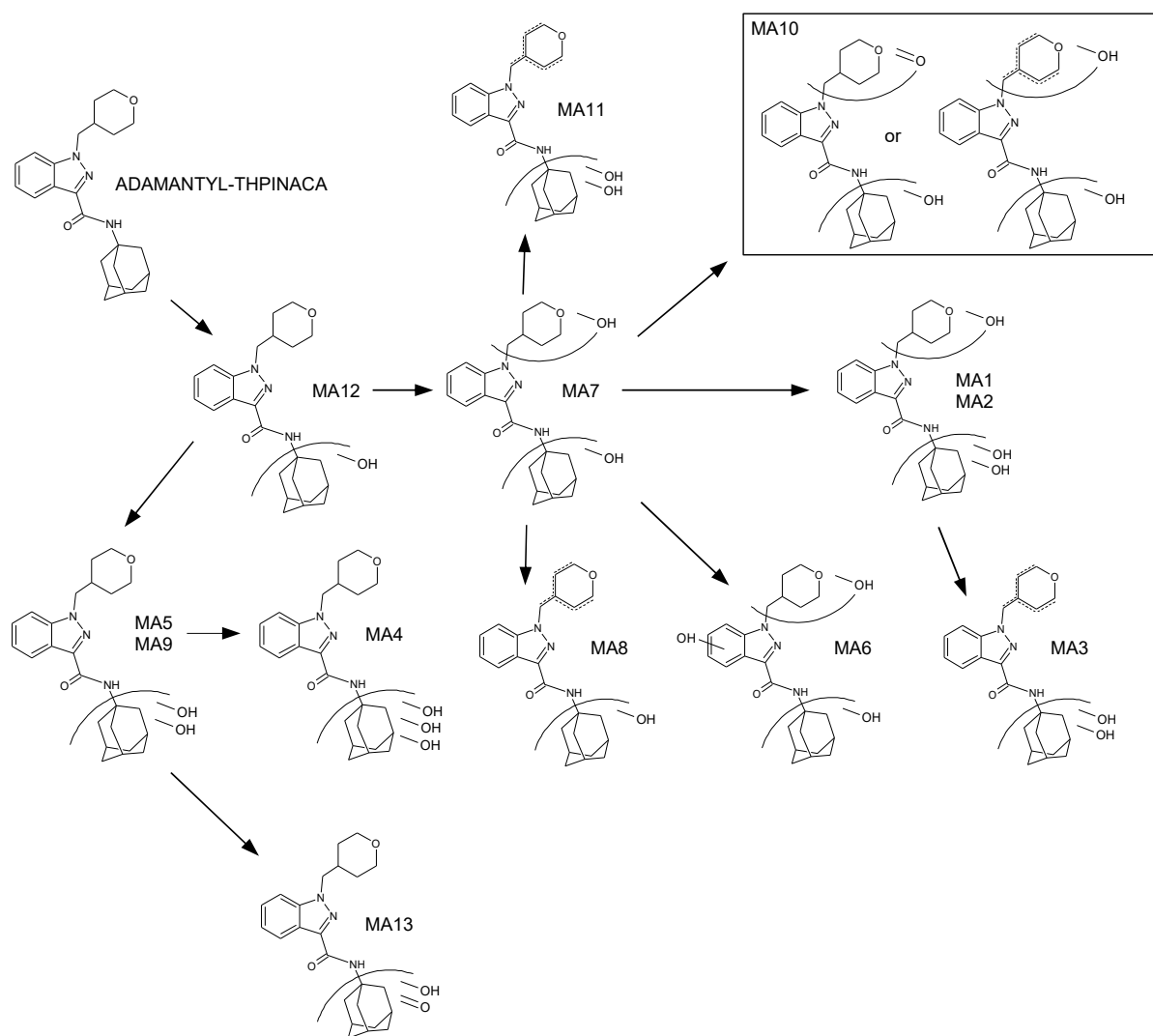


Figure 5. Proposed metabolic pathway of ADAMANTYL-THPINACA.

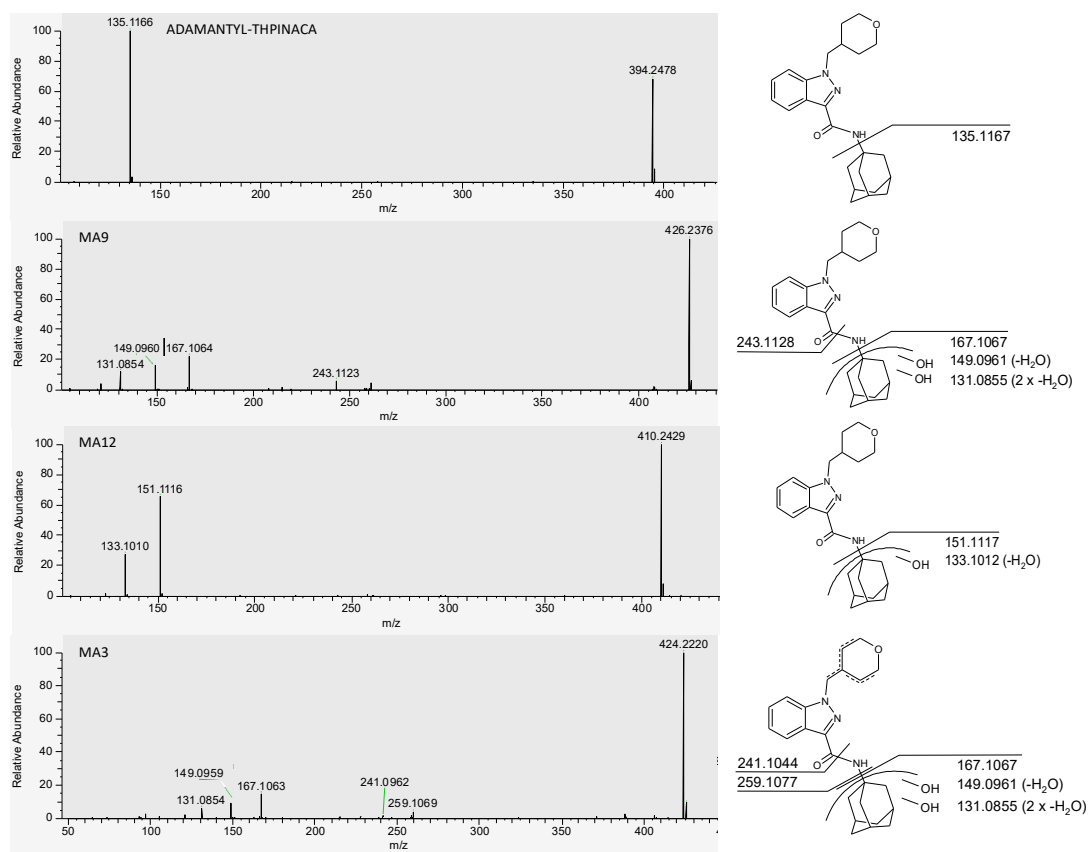


Figure 6. MS2 spectra of ADAMANTYL-THPINACA and its three most abundant metabolites. The proposed fragments leading to the respective signals are shown on the right.

Table 3. Summary of all detected metabolites, and observed artefacts thereof, of ADAMANTY-THPINACA (listed in the order of the observed retention times). Shown are the suggested biotransformations, chemical formulas, calculated [M + H] of the parent ions and the corresponding product ions, as well as retention times, area after 2 h of incubation, and rank.

ID	Biotransformation	Formula	[M + H] ⁺ Product ions (<i>m/z</i>)	Mass error (ppm)	Rt (min)	Area (<i>n</i> = 2)	Rank
MA1	di-hydroxylation at adamantyl, mono-hydroxylation at 4-methyl-tetrahydropyran	C ₂₄ H ₃₁ N ₃ O ₅	442.2336 424.2221 259.1077 167.1067 149.0961 131.0855	1.4	0.87	9.2 × 10 ⁶	11
MA2	di-hydroxylation at adamantyl, mono-hydroxylation at 4-methyl-tetrahydropyran	C ₂₄ H ₃₁ N ₃ O ₅	442.2336 424.2221 259.1077 167.1067 149.0961 131.0855	−0.7	0.97	1.1 × 10 ⁷	10
MAArt1	in-source water loss of MA2	C ₂₄ H ₂₉ N ₃ O ₄	424.2231 259.1077 241.1044 167.1067 149.0961 131.0855	−0.7	0.98	7.5 × 10 ⁷	
MA3	di-hydroxylation at adamantyl, desaturation at 4-methyl-tetrahydropyran	C ₂₄ H ₂₉ N ₃ O ₄	424.2231 259.1077 241.1044 167.1067 149.0961 131.0855	−0.5	1.03	3.8 × 10 ⁷	3
MA4	tri-hydroxylation at adamantyl	C ₂₄ H ₃₁ N ₃ O ₅	442.2336 424.2231 260.1393 243.1128	−0.5			
MA5	di-hydroxylation at adamantyl	C ₂₄ H ₃₁ N ₃ O ₃	426.2387 260.1394 243.1128 167.1067 149.0961 131.0855	1.2	1.09	1.7 × 10 ⁷	8
MA6	mono-hydroxylation at adamantyl, mono-hydroxylation at indazole, mono-hydroxylation at 4-methyl-tetrahydropyran	C ₂₄ H ₃₁ N ₃ O ₅	442.2336 424.2221 406.2114 151.1117 133.1012 274.1186 257.0921	0	1.1	1.3 × 10 ⁷	9
MA7	mono-hydroxylation at adamantyl, mono-hydroxylation at 4-methyl-tetrahydropyran	C ₂₄ H ₃₁ N ₃ O ₃	426.2387 151.1117 133.1012	0.5	1.2	2.4 × 10 ⁷	6
MA8	Mono-hydroxylation at adamantyl, desaturation at 4-methyl-tetrahydropyran	C ₂₄ H ₂₉ N ₃ O ₃	408.2282 151.1117 133.10118	−0.2	1.27	3.2 × 10 ⁷	4

Table 3. Cont.

ID	Biotransformation	Formula	[M + H] ⁺ Product ions (<i>m/z</i>)	Mass error (ppm)	Rt (min)	Area (<i>n</i> = 2)	Rank
MA9	di-hydroxylation at adamantyl	C ₂₄ H ₃₁ N ₃ O ₃	426.2387 243.1128 167.1067 149.0961 131.0855	−1.2	1.36	4.2 × 10 ⁸	1
MAArt2	in-source water loss of MA9	C ₂₄ H ₂₉ N ₃ O ₃	408.2282 260.1394 243.1128 149.0961 131.0855	−0.7	1.36	7.9 × 10 ⁷	
MA10	Mono-hydroxylation at adamantyl, and carbonylation or mono-hydroxylation and desaturation at 4-methyl-tetrahydropyran	C ₂₄ H ₂₉ N ₃ O ₄	424.2231 151.1117 133.1012	0	1.39	6.9 × 10 ⁶	12
MA11	Di-hydroxylation at adamantyl, desaturation at 4-methyl-tetrahydropyran	C ₂₄ H ₂₉ N ₃ O ₄	424.2231 259.1077 167.1067 149.0961 131.0855	−0.9	1.73	4.1 × 10 ⁶	13
MA12	mono-hydroxylation at adamantyl	C ₂₄ H ₃₁ N ₃ O ₃	410.2438 151.1117 133.1012	−0.5	1.75	7.6 × 10 ⁷	2
MA13	carbonylation and mono-hydroxylation at adamantyl	C ₂₄ H ₂₉ N ₃ O ₄	424.2231 406.2125 260.1394 243.1128 165.091 119.0855	0.2	1.8	1.8 × 10 ⁷	7
MA1	ADAMANTYL-THPINACA	C ₂₄ H ₃₁ N ₃ O ₃	394.2489 135.1167	0.6	4.56	1.0 × 10 ⁶	-

2.4.1. Mono-Hydroxylation

MA12 is produced via mono-hydroxylation at the adamantyl-moiety, as shown by the diagnostic fragment at *m/z* 151.1117.

2.4.2. Di-Hydroxylation

For MA7, the observed fragment of *m/z* 151.1117 indicated mono-hydroxylation at the adamantyl-moiety. Therefore, the second hydroxyl group is located at the rest of the molecule. Because derivatization did not change the signal intensity of the MA7 metabolites, this suggests that the second hydroxyl-group is located at the 4-methyl-tetrahydropyran-moiety. The di-hydroxylated metabolite MA9 was the most abundant metabolite. Due to the fragment observed at *m/z* 167.1067, the location of both hydroxyl groups was assigned to the adamantyl-moiety. Additional fragments consisted of two dehydration reactions of the di-hydroxylated adamantyl moiety (*m/z* 149.0961 and *m/z* 131.0855) and the unaltered 1-(tetrahydropyranyl-4-methyl)-indazole-3-acylium-ion (*m/z* 243.1128). Two additional, but less abundant, di-hydroxylated metabolites were detected, of which MA5 showed a similar fragmentation pattern to MA9, thus being di-hydroxylated at the adamantyl-moiety. As MAArt2, presenting fragments at *m/z* 149.0961 and *m/z* 131.0855 indicating dehydration reactions at the hydroxylated adamantyl-moiety, co-eluted with the metabolite MA9, MAArt2 was classified as an in-source artefact produced by dehydration of MA9.

2.4.3. Mono-Hydroxylation and Additional Desaturation

The metabolite MA8 is produced via mono-hydroxylation at the adamantyl-moiety, indicated by fragment m/z 151.1117. The observed desaturation was assigned to the rest of the molecule (4-methyl-tetrahydropyran-moiety), even though the corresponding fragment was not detected due to neutral loss. As MA8 did not co-elute with a di-hydroxylated metabolite, which is mono-hydroxylated at the adamantyl-moiety as well as at the 4-methyl-tetrahydropyran-moiety, this signal was classified as a genuine metabolite.

2.4.4. Tri-Hydroxylation

The two early-eluting metabolites, MA1 and MA2, were identified to be di-hydroxylated at the adamantyl-moiety and mono-hydroxylated at the 1-(tetrahydropyranyl-4-methyl)-indazole-3-carboxamide structure. For these two metabolites, the observed fragment at m/z 167.2066 represents the di-hydroxylated adamantyl-moiety and the fragment at m/z 259.1077 denotes the mono-hydroxylated 1-(tetrahydropyranyl-4-methyl)-indazole-3-acylium-ion. As derivatization did not result in methylation of MA1 and MA2, it was concluded that both metabolites are produced via hydroxylation at the 4-methyl-tetrahydropyran-moiety. MAArt1 was detected via the parent ion at m/z 424.2231 and is denoted as an in-source dehydration artefact. MAArt1 was identified to be di-hydroxylated at the adamantyl-moiety (m/z 167.1067) and desaturated at the 4-methyl-tetrahydropyran-moiety (m/z 259.1077). Due to the presence of the coeluting tri-hydroxylated metabolite MA2, showing the same alterations, a potential contribution from MAArt1 to the observed MA2 signal could not be ruled out. MA4 presented MS² spectra with two fragments at m/z 260.1393 and m/z 243.1128, both indicating an unaltered 1-(tetrahydropyranyl-4-methyl)-indazole-3-carboxamide moiety. It was consequently concluded that the adamantyl-moiety was hydroxylated three times, despite the fragment representing this moiety not being detected, due to neutral loss. The latest eluting tri-hydroxylated metabolite MA6 is produced via mono-hydroxylation at the adamantyl-moiety, shown by the diagnostic fragment at m/z 151.1117, and di-hydroxylation of the remaining molecule. One observed fragment of MA6 at m/z 274.1184 is produced via dehydration of the 1-(tetrahydropyranyl-4-methyl)-indazole-3-carboxamide-moiety. Therefore, one hydroxyl group must be located at the 4-methyl-tetrahydropyran-moiety. As no second dehydration reaction of this moiety was detected, the third hydroxy group was proposed to be located at the indazole-core. The location of the hydroxyl group at the indazole-moiety was verified via derivatization, as the corresponding methylated metabolite MA6 was detected at m/z 456.2493. Additionally, fragmentation of this product resulted in a fragment with m/z 288.1343, indicative of the methylated and desaturated 1-(tetrahydropyranyl-4-methyl)-indazole-3-carboxamide-moiety.

2.4.5. Di-Hydroxylation and Additional Desaturation, Mono-Hydroxylation and Additional Carbonylation

Fragmentation of MA3 with $[M + H]^+$ 424.2231 (m/z), resulted in a fragment at m/z 167.1067, indicating di-hydroxylation at the adamantyl-moiety. Additionally, the desaturated 4-methyl-tetrahydropyran-moiety was identified with the detected m/z 259.1077, a fragment indicative of the desaturated 1-(tetrahydropyranyl-4-methyl)-indazole-3-carboxylic acid-moiety after amide hydrolysis. Due to the lack of a tri-hydroxylated counterpart, in-source dehydration was not considered for MA3. The metabolite MA10 resulted in a fragment at m/z 151.1117, representing the mono-hydroxylated adamantyl-moiety. A fragment produced from subsequent water loss at the adamantyl-moiety was also detected at m/z 133.1012. Due to a lack of further fragments, as a result of neutral loss, it was concluded that further sites of biotransformation are located elsewhere on the molecule. Potential biotransformations resulting in the signal at m/z 424.2231 include di-hydroxylation and desaturation (likely derived from dehydration of a tri-hydroxylated metabolite, which was not detected) or mono-hydroxylation in combination with carbonylation. As derivatization did not result in a decrease of the MA10-signal, hydroxylation at the indazole-region

was ruled out. In conclusion, MA10 was defined as the product of mono-hydroxylation at the adamantyl-region with concurrent mono-hydroxylation and desaturation or carbonylation at the 4-methyl-tetrahydropyran-moiety. Due to the later elution of MA10, when compared to the detected tri-hydroxylated metabolites, in-source dehydration was not considered. MA11 is a further metabolite with a parent ion at m/z 424.2231, in this case as a result of di-hydroxylation and desaturation, as indicated by the detection of the di-hydroxylated adamantyl-moiety at m/z 167.1067. As this fragment was observed, the location of desaturation was concluded to be at the 4-methyl-tetrahydropyran-moiety. As no corresponding tri-hydroxylated metabolites were detected within the MA11 elution window, in-source dehydration of this metabolite is unlikely. MA13 is classified as a product of mono-hydroxylation and carbonylation. This was concluded from the presence of m/z 260.1393 (unaltered 1-(tetrahydropyranyl-4-methyl)-indazole-3-carboxamide structure) and m/z 165.0910 (mono-hydroxylation and carbonylation of the adamantyl-moiety). An additional fragment (m/z 119.0855) was detected, assigned to the cleavage of CO and dehydration of the mono-hydroxylated and carbonylated adamantyl-moiety. The longer retention time of this metabolite when compared to hydroxylated and desaturated metabolites is also in accordance with carbonylation, due to the expected lower polarity of a carbonyl group in comparison to a hydroxyl group.

2.4.6. Identification of the Primarily Involved CYP Isoenzymes

As for CUMYL-THPINACA, CYP3A4 and CYP3A5 were found to mainly contribute to the metabolism of ADAMANTYL-THPINACA (Table 4). In contrast to CUMYL-THPINACA, limited metabolic activity of CYP2D6, and CYP2C8 was observed. CYP2C9 and CYP2C19 mediated the production of M12, but no other metabolites, thus leading to the conclusion that these isoforms play a minor role in the metabolism of ADAMANTYL-THPINACA. For CYP2B6, CYP1A2, CYP2E1 und CYP2A6, no metabolic activity could be observed.

Experiments revealed CYP3A4 also to be the major metabolizing CYP for ADAMANTYL-THPINACA. In comparison to CUMYL-THPINACA, far fewer CYP isoforms were involved in ADAMANTYL-THPINACA metabolism. The intake of strong CYP3A4 inhibitors together with ADAMANTYL-THPINACA is more likely to pose a higher risk of metabolic drug–drug interactions than CYP3A4 in combination with CUMYL-THPINACA.

Table 4. Summary of the incubation results of ADAMANTYL-THPINACA with rCYP. Area ratios (absolute peak area (metabolite)/absolute peak area (ISTD)) are expressed as follows: (+): <0.1 , +: ≥ 0.1 – ≤ 1 , ++: >1 – ≤ 5 , +++: >5 . Where the negative control contained trace amounts of metabolites in a comparable amount, as in the samples after incubation, the result is marked as: (+) *.

ID	3A4	3A5	2D6	2C8	2C9	2C19	2B6	1A2	2E1	2A6	Negative Control
	<i>n</i> = 2	<i>n</i> = 2	<i>n</i> = 2	<i>n</i> = 2	<i>n</i> = 2	<i>n</i> = 2	<i>n</i> = 2	<i>n</i> = 2	<i>n</i> = 2	<i>n</i> = 2	<i>n</i> = 2
MA1	+	(+)	-	-	-	-	-	-	-	-	-
MA2	+	(+)	-	-	-	-	-	-	-	-	-
MAArt1	++	(+)	-	-	-	-	-	-	-	-	-
MA3	++	(+)	-	-	-	-	-	-	-	-	-
MA4	+	(+)	-	-	-	-	-	-	-	-	-
MA5	+	(+)	(+)	(+)	-	-	-	-	-	-	-
MA6	(+)	(+)	-	-	-	-	-	-	-	-	-
MA7	+	(+)	(+)	(+)	-	-	-	-	-	-	-
MA8	+	++	+	(+)	-	-	-	-	-	-	-
MA9	+++	++	(+)	(+)	-	-	-	-	-	-	-

Table 4. Cont.

ID	3A4	3A5	2D6	2C8	2C9	2C19	2B6	1A2	2E1	2A6	Negative Control
	<i>n</i> = 2	<i>n</i> = 2	<i>n</i> = 2	<i>n</i> = 2	<i>n</i> = 2	<i>n</i> = 2	<i>n</i> = 2	<i>n</i> = 2	<i>n</i> = 2	<i>n</i> = 2	<i>n</i> = 2
MAArt2	++	+	(+)	(+)	-	-	-	-	-	-	-
MA10	(+)	(+)	-	-	-	-	-	-	-	-	-
MA11	(+)	(+)	-	-	-	-	-	-	-	-	-
MA12	+	+++	++	+++	+	+	(+)*	(+)*	(+)*	(+)*	(+)*
MA13	+	(+)	-	-	-	-	-	-	-	-	-

3. Materials and Methods

3.1. Chemicals and Reagents

LC-MS grade acetonitrile (ACN), methanol (MeOH), and water, and HPLC grade acetone and 2-isopropanol (IPA) were obtained from Macherey-Nagel AG (Oensingen, Switzerland). Ammonium formate (>99.0%), ethyl acetate (EtOAc, HPLC grade), iodomethane (stabilized with silver), and formic acid (98–100%) were purchased from Merck (Zug, Switzerland). Potassium carbonate (Ph. Eur.) was purchased from Carl Roth AG (Arllesheim, Switzerland). Certified reference standards of UR-144, UR-144 N-(5-hydroxypentyl) metabolite, UR-144 N-pentanoic acid metabolite, and d,l-11-Hydroxy-THC-D₃ were purchased from Lipomed AG (Arllesheim, Switzerland). CUMYL-THPINACA (N-(1-methyl-1-phenylethyl)-1-(tetrahydropyran-4-ylmethyl)-1H-indazole-3-carboxamide; purity >97%) and ADAMANTYL-THPINACA (N-(1-adamantyl)-1-(tetrahydropyran-4-ylmethyl)-1H-indazole-3-carboxamide; purity >93%) were kindly provided by the Zurich Forensic Science Institute (Switzerland) in solid form (as certified reference substances were not available at the time of this work). Stock solutions were prepared at 1 mg/mL in MeOH for both compounds and stored at −20 °C until use. Pooled human liver microsomes (donor pool > 20, 20 mg/mL protein content in 250 mM sucrose, specified total P450 enzyme content of 360 pmol/mg protein) and Gentest NADPH regenerating system solutions: A (containing 26 mM β-nicotinamide adenine dinucleotide phosphate [NADP⁺], 66mM MD-glucose-6-phosphate [Glc-6-P], 66mMmagnesium chloride [MgCl₂] in water), and B (containing 40 U/mL Glc-6-P dehydrogenase [Glc-6-P-DH; EC 1.1.1.49] in sodium citrate) were purchased from Corning (Amsterdam, The Netherlands). Human CYP3A4 (100 pmol/mg protein), CYP2C9 (100 pmol/mg protein), CYP2E1 (100 pmol/mg protein), CYP3A5 (100 pmol/mg protein), CYP2C8 (100 pmol/mg protein), CYP2B6 (100 pmol/mg protein), CYP2A6 (with purified human cytochrome b5, 100 pmol/mg protein), CYP1A2 (770 pmol/mg protein), CYP2D6 (142 pmol/mg protein), CYP2C19 (202 pmol/mg protein), CYP3A5, and CYP2B6 EasyCYP Bactosomes co-expressed with human CYP-reductase in *Escherichia coli*, and membrane protein isolated from *Escherichia coli* host strain (EasyCYP control, 10 mg/mL protein), were ordered from tebu-bio (Offenbach, Germany).

3.2. Microsomal Incubation with pHLM

CUMYL-THPINACA, ADAMANTYL-THPINACA were incubated in duplicate at final concentrations of 10 μM in a total reaction volume of 1000 μL. Following the vendors instructions (Corning), the incubation mixture consisted of 100 mM potassium phosphate buffer (pH 7), 50 μL NADPH Regenerating System Solution A, and 10 μL NADPH Regenerating System Solution B. The percentage of organic solvent (MeOH) was limited to 0.4% in the incubation mixture, thus no inhibition due to organic solvents was to be expected (limit for MeOH defined by Corning: 1%). The reaction was started by the addition of 0.5 mg liver microsomes per assay to the reaction mixture that was then tempered to 37 °C. Negative controls were prepared by replacing the pHLMs with an equivalent volume of water and by incubating enzymes without the addition of SCRA, while parallel incubation of the SCRA UR-144 served as a positive control for the functionality of the incubation. The

samples were then incubated at 37 °C in an Eppendorf ThermoStat C heating block. In a preliminary experiment (data not shown) samples were drawn after 0.5 h, 1 h, 1.5 h and 2 h after incubation with pHLM. For the presented data, the samples were incubated for 2 h, as this incubation time gave the best outcome with respect to number and concentration of metabolites. The reaction was terminated by the addition of an equal volume of ice-cold ACN to 400 µL of drawn sample. The samples were then centrifuged at room temperature for five minutes at 13,400 rpm (approximately 9000× *g*) using an Eppendorf MiniSpin centrifuge (Eppendorf, Schönenbuch, Switzerland). The supernatant was stored in glass vials at −20 °C until sample cleanup.

3.3. Microsomal Incubation with rCYP

Substrate solutions (final concentration 10 µM) were incubated in 100 mM potassium phosphate buffer (pH 7), containing a final reaction volume of 500 µL, containing 38 µL NADPH regenerating solution A and 13 µL NADPH Regenerating Solution B. The reaction was started by the addition 25 µL of the CYP-solutions (or negative control EasyCYP), resulting in 0.5 mg protein per assay. Following the vendors instructions (tebu-bio), the reaction was quenched—after incubating for 20 min at 37 °C—by addition of 400 µL ice-cold ACN to 400 µL of drawn sample. Subsequently, the samples were centrifuged at 13,400 rpm (approximately 9000× *g*) for five minutes. The supernatant was stored in glass vials at −20 °C until further processing.

3.4. Sample Preparation

For sample clean-up, a protocol was adapted from one developed for the analysis of metabolites of SCRAs in urine, published by Gaunitz et al. [35]. In brief, 600 µL of the supernatants of the precipitated samples were diluted 1:1 with 100 mM ammonium formate buffer (pH 4). At this point the internal standard (ISTD) d,l-11-Hydroxy-THC-D₃ was added, resulting in a concentration of 100 ng/mL (final concentration at time of analysis, with presumed 100% recovery, 300 ng/mL). Strata phenyl SPE cartridges obtained from Phenomenex (Basel, Switzerland) were conditioned with 2 mL MeOH, 2 mL water, and 2 mL ammonium formate buffer (pH 4), prior to being loaded with the diluted samples. After loading the samples, the cartridges were washed with 2 mL of 5:95 MeOH:water (*v/v*) and dried for 15 min. Elution of the analytes was achieved with twice 2 mL of 85:15 EtOAc:IPA (*v/v*). Extracts were collected in glass tubes and the solvent was evaporated until dryness at 40 °C under a gentle stream of nitrogen. Finally, the dried residues were resolved in 200 µL of 1:1 ACN:water (*v/v*), centrifuged (2465× *g*, 15 min) and transferred to HPLC-vials, thus resulting in a concentration by a factor of 3.

3.5. Derivatization Using Iodomethane

SPE extracts obtained from pHLM incubation experiments were solved in 200 µL acetone and then transferred into glass-vials, which were pre-filled with a spatula tip (approximately 500 mg) of potassium carbonate. At this point 100 µL iodomethane was added, the vials were closed, and the mixtures were incubated for 1 h at 60 °C. The samples were transferred into a new vial using a glass Pasteur pipet omitting the insoluble potassium carbonate. The samples were evaporated to dryness under a gentle nitrogen stream at 60 °C, and reconstituted in 200 µL 1:1 ACN:water. A negative control was conducted for both SCRAs, where the addition of iodomethane was omitted while the rest of the experiment was kept as above.

3.6. Analysis

Chromatographic separation of the metabolites was achieved using a Dionex UltiMate 3000 ultra UHPLC system equipped with a Hypersil Gold (50 × 2.1 mm 1.9 µM) analytical column, thermostatted at 40 °C using a MutliSLEEVE column heater, all obtained from Thermo Fisher Scientific (Reinach, Switzerland). Mobile phase A consisted of water with 0.1% (*v/v*) formic acid and mobile phase B of ACN with 0.1% (*v/v*) formic acid. After

injection of 5 μL of the prepared sample the gradient commenced at 20% mobile phase B, which then increased to 40% within 0.9 min and to 71% within the following 6 min, after which the mobile phase B was increased to 100% during a time interval of 0.25 min and held for 1 min. The system was then returned to the initial settings and held for 1.25 min, prior to the injection of the next sample. The mobile phase flow was 0.6 mL/min throughout. The mobile phase flow during the first 0.1 min and after 7 min was directed to the waste and not to the mass spectrometer by means of a bypass valve connected after the column.

Subsequent analysis was undertaken with a Thermo Scientific Q Exactive HF Hybrid Quadrupole-Orbitrap mass spectrometer equipped with a heated electrospray ionization (HESI-II) source, obtained from Thermo Fisher Scientific (Reinach, Switzerland), operated with a sheath gas flow rate of 50 arbitrary units (AU) and an auxiliary gas flow rate of 5 AU. The capillary temperature and auxiliary gas heater temperature were 200 °C and 350 °C, respectively, and the spray voltage was set to 3.5 kV. Parent ions of metabolites were screened using a full MS acquisition in positive ion mode and at a resolution of 120,000 full width at half-maximum (FWHM) at m/z 200, within a scan range from m/z 150 to m/z 1000. Metabolite identification was conducted by manual investigation of the raw data in FreeStyle (version 1.7, SP1, Thermo Fisher Scientific, Reinach, Switzerland), assisted by the Compound Discoverer (version 3.1, Thermo Fisher Scientific, Reinach, Switzerland) software, by running an expected workflow (Forensics Expected w FiSh scoring), that enables the screening for software predicted products generated by biotransformation of a predefined compound. The software thus calculates the expected masses of common phase I metabolites and searches for corresponding signals in the data. The program additionally identifies background signals by comparison of blank samples and negative control samples, which are then filtered out and, therefore, not considered.

In a subsequent analysis, the software-proposed metabolites were transferred into an inclusion list for a full MS—data-dependent MS² (dd-MS²) analysis. The resolution for this measurement was set to 60,000 FWHM for the full MS analysis and 15,000 FWHM for the dd-MS² analysis. Normalized stepped collision energies of 10, 17.5, and 35 (normalized to m/z 500 [$z = 1$]) were applied. In order to ensure fragmentation of low abundance and close eluting isobaric compounds, the minimum automated gain control (AGC) target to trigger an MS² measurement was set to zero and dynamic exclusion was set to one second. The generated MS² spectra were investigated with the aid of Compound Discoverer, which enables comparison of the obtained MS² spectra to the theoretical in silico generated MS²-spectra [38].

The criterion for metabolite identification was a mass accuracy <5 ppm for the proposed parent ions and diagnostic fragments along with the plausibility of observed fragments and observed retention times of metabolites in relation to each other. The biotransformations were identified by mass shifts of the detected fragments, indicative of hydroxylation (+15.9994 Da per hydroxylation), desaturation (−2.01565 Da), carbonylation (+13.9838 Da), dehydration (−18.0153 Da), and combinations thereof. The position of hydroxylation was narrowed down by a derivatization experiment employing iodomethane, which selectively methylates aromatic hydroxyl-groups (i.e., cumyl- and indazole-moiety).

4. Conclusions

Incubation with pHLM yielded 28 metabolites for CUMYL-THPINACA and 13 metabolites for ADAMANTYL-THPINACA. The observed extensive metabolism of the studied SCRA again highlights, as previously observed for many other SCRA, the need to include the metabolites in screening procedures—particularly in urine. Both compounds presented a highly abundant di-hydroxylated metabolite, which is recommended as a suitable target for screening procedures. For both compounds, in-source dehydration artefact formation was observed for a few hydroxylated metabolites, supporting the need for in vitro studies prior to moving on to in vivo measurements. However, several metabolites, sharing the same mass as the described dehydration artefacts, were identified. This

emphasizes the requirement to thoroughly investigate all signals of potential metabolites in order not to miss potential biomarkers. Furthermore, as some dehydration products presented higher abundancies than the underlying metabolite, their detection may improve investigations of substance use and they should, therefore, be included into screening protocols. However, such recommendations would need to be verified by means of analysis of human urine samples.

The reported protocols, along with the instrumentation and software used, proved to be beneficial for the investigation of SCRA metabolite profiles. The *in silico* tools were invaluable in speeding up the elucidation of the metabolic profile of the studied SCRA. Concerning the metabolism, the involvement of mainly CYP3A4 along with CYP3A5, was observed for both compounds. For CUMYL-THPINACA the additional involvement of 2D6, 2C8, and 2C19 was found (all to a lesser extent than for CYP3A4), making CUMYL-THPINACA less susceptible for metabolism-based drug–drug interactions or the effects of CYP-polymorphism. Due to the main involvement of CYP3A4 in the metabolism of ADAMANTYL-THPINACA, metabolic drug–drug interactions in combination with a strong CYP3A4 inhibitor are considered more likely with ADAMANTYL-THPINACA than with CUMYL-THPINACA.

Author Contributions: M.C.M.: data curation, formal analysis, visualization, writing—original draft preparation; M.C.M., K.M.-C.-B., E.S.: conceptualization; M.C.M., K.M.-C.-B.: methodology, investigation; K.M.-C.-B. and E.S.: writing—review and editing; K.M.-C.-B. and E.S.: supervision. All authors have read and agreed to the published version of the manuscript.

Funding: This research received no external funding.

Institutional Review Board Statement: Not applicable.

Informed Consent Statement: Not applicable.

Data Availability Statement: Data is available in the article.

Acknowledgments: The authors thank June Mercer-Chalmers-Bender for English language editing. Special thanks go to Christian Bissig from the Zurich Forensic Science Institute for providing reference material. Further thanks go to Priska Frei for valuable discussions and input during manuscript preparation.

Conflicts of Interest: The authors declare no conflict of interest.

References

1. European Monitoring Centre for Drugs and Drug Addiction. *European Drug Report 2020: Trends and Developments*; Publications Office of the EU: Luxembourg, 2020.
2. Castaneto, M.S.; Gorelick, D.A.; Desrosiers, N.A.; Hartman, R.L.; Pirard, S.; Huestis, M.A. Synthetic cannabinoids: Epidemiology, pharmacodynamics, and clinical implications. *Drug Alcohol Depend.* **2014**, *144*, 12–41. [[CrossRef](#)] [[PubMed](#)]
3. Wiley, J.L.; Marusich, J.A.; Huffman, J.W. Moving around the molecule: Relationship between chemical structure and *in vivo* activity of synthetic cannabinoids. *Life Sci.* **2014**, *97*, 55–63. [[CrossRef](#)] [[PubMed](#)]
4. Gatch, M.B.; Forster, M. Cannabinoid-like effects of five novel carboxamide synthetic cannabinoids. *NeuroToxicology* **2019**, *70*, 72–79. [[CrossRef](#)] [[PubMed](#)]
5. Fantegrossi, W.E.; Moran, J.H.; Radominska-Pandya, A.; Prather, P.L. Distinct pharmacology and metabolism of K2 synthetic cannabinoids compared to $\Delta(9)$ -THC: Mechanism underlying greater toxicity? *Life Sci.* **2014**, *97*, 45–54. [[CrossRef](#)]
6. Hutchison, R.D.; Ford, B.M.; Franks, L.N.; Wilson, C.D.; Yarbrough, A.L.; Fujiwara, R.; Su, M.K.; Fernandez, D.; James, L.P.; Moran, J.H.; et al. Atypical Pharmacodynamic Properties and Metabolic Profile of the Abused Synthetic Cannabinoid AB-PINACA: Potential Contribution to Pronounced Adverse Effects Relative to $\Delta(9)$ -THC. *Front. Pharmacol.* **2018**, *9*, 1084. [[CrossRef](#)] [[PubMed](#)]
7. Angerer, V.; Jacobi, S.; Franz, F.; Auwärter, V.; Pietsch, J. Three fatalities associated with the synthetic cannabinoids 5F-ADB, 5F-PB-22, and AB-CHMINACA. *Forensic Sci. Int.* **2017**, *281*, e9–e15. [[CrossRef](#)] [[PubMed](#)]
8. Harris, C.R.; Brown, A. Synthetic Cannabinoid Intoxication: A Case Series and Review. *J. Emerg. Med.* **2013**, *44*, 360–366. [[CrossRef](#)]
9. Westin, A.A.; Frost, J.; Brede, W.R.; Gundersen, P.O.; Einvik, S.; Aarset, H.; Slørdal, L. Sudden Cardiac Death Following Use of the Synthetic Cannabinoid MDMB-CHMICA. *J. Anal. Toxicol.* **2016**, *40*, 86–87. [[CrossRef](#)]
10. Hermanns-Clausen, M.; Kneisel, S.; Szabo, B.; Auwärter, V. Acute toxicity due to the confirmed consumption of synthetic cannabinoids: Clinical and laboratory findings. *Addiction* **2013**, *108*, 534–544. [[CrossRef](#)]

11. Trecki, J.; Gerona, R.R.; Schwartz, M.D. Synthetic Cannabinoid-Related Illnesses and Deaths. *N. Engl. J. Med.* **2015**, *373*, 103–107. [[CrossRef](#)]
12. Kleis, J.; Germerott, T.; Halter, S.; Héroux, V.; Roehrich, J.; Schwarz, C.S.; Hess, C. The synthetic cannabinoid 5F-MDMB-PICA: A case series. *Forensic Sci. Int.* **2020**, *314*, 110410. [[CrossRef](#)]
13. Norman, C.; Walker, G.; McKirdy, B.; McDonald, C.; Fletcher, D.; Antonides, L.H.; Sutcliffe, O.B.; Nic Daéid, N.; McKenzie, C. Detection and quantitation of synthetic cannabinoid receptor agonists in infused papers from prisons in a constantly evolving illicit market. *Drug Test. Anal.* **2020**, *12*, 538–554. [[CrossRef](#)]
14. Mogler, L.; Franz, F.; Rentsch, D.; Angerer, V.; Weinfurter, G.; Longworth, M.; Banister, S.D.; Kassiou, M.; Moosmann, B.; Auwärter, V. Detection of the recently emerged synthetic cannabinoid 5F-MDMB-PICA in ‘legal high’ products and human urine samples. *Drug Test. Anal.* **2018**, *10*, 196–205. [[CrossRef](#)] [[PubMed](#)]
15. Norman, C.; Halter, S.; Haschimi, B.; Acreman, D.; Smith, J.; Krotulski, A.J.; Mohr, A.L.A.; Logan, B.K.; NicDaéid, N.; Auwärter, V.; et al. A transnational perspective on the evolution of the synthetic cannabinoid receptor agonists market: Comparing prison and general populations. *Drug Test. Anal.* **2021**, *13*, 841–852. [[CrossRef](#)] [[PubMed](#)]
16. European Monitoring Centre for Drugs and Drug Addiction. EMCDDA Initial Report on the New Psychoactive Substance Methyl 3,3-Dimethyl-2-(1-(Pent-4-En-1-yl)-1H-Indazole-3-Carboxamido)Butanoate (MDMB-4en-PINACA), Initial Reports; Publications Office of the European Union: Luxembourg, 2020. Available online: https://www.emcdda.europa.eu/publications/initial-reports/mdmb-4en-pinaca_en (accessed on 1 December 2020).
17. Scheidweiler, K.B.; Jarvis, M.J.Y.; Huestis, M.A. Nontargeted SWATH acquisition for identifying 47 synthetic cannabinoid metabolites in human urine by liquid chromatography-high-resolution tandem mass spectrometry. *Anal. Bioanal. Chem.* **2015**, *407*, 883–897. [[CrossRef](#)]
18. Diao, X.; Huestis, M.A. Approaches, Challenges, and Advances in Metabolism of New Synthetic Cannabinoids and Identification of Optimal Urinary Marker Metabolites. *Clin. Pharmacol. Ther.* **2017**, *101*, 239–253. [[CrossRef](#)]
19. Franz, F.; Angerer, V.; Moosmann, B.; Auwärter, V. Phase I metabolism of the highly potent synthetic cannabinoid MDMB-CHMICA and detection in human urine samples. *Drug Test. Anal.* **2017**, *9*, 744–753. [[CrossRef](#)]
20. Diao, X.; Huestis, M.A. New Synthetic Cannabinoids Metabolism and Strategies to Best Identify Optimal Marker Metabolites. *Front. Chem.* **2019**, *7*, 109. [[CrossRef](#)] [[PubMed](#)]
21. Bowden, M.; Williamson, J. Cannabinoid Compounds. WO2014/167530/A1, 11 April 2014.
22. Åstrand, A.; Vikingsson, S.; Lindstedt, D.; Thelander, G.; Gréen, H.; Kronstrand, R.; Wohlfarth, A. Metabolism study for CUMYL-4CN-BINACA in human hepatocytes and authentic urine specimens: Free cyanide is formed during the main metabolic pathway. *Drug Test. Anal.* **2018**, *10*, 1270–1279. [[CrossRef](#)] [[PubMed](#)]
23. Staeheli, S.N.; Poetzsch, M.; Veloso, V.P.; Bovens, M.; Bissig, C.; Steuer, A.E.; Kraemer, T. In vitro metabolism of the synthetic cannabinoids CUMYL-PINACA, 5F-CUMYL-PINACA, CUMYL-4CN-BINACA, 5F-CUMYL-P7AICA and CUMYL-4CN-B7AICA. *Drug Test. Anal.* **2018**, *10*, 148–157. [[CrossRef](#)] [[PubMed](#)]
24. Staeheli, S.N.; Steuer, A.E.; Kraemer, T. Identification of urinary metabolites of the synthetic cannabinoid 5F-CUMYL-P7AICA in human casework. *Forensic Sci. Int.* **2019**, *294*, 76–79. [[CrossRef](#)] [[PubMed](#)]
25. Mogler, L.; Wilde, M.; Huppertz, L.M.; Weinfurter, G.; Franz, F.; Auwärter, V. Phase I metabolism of the recently emerged synthetic cannabinoid CUMYL-PEGACLONE and detection in human urine samples. *Drug Test. Anal.* **2018**, *10*, 886–891. [[CrossRef](#)] [[PubMed](#)]
26. Mogler, L.; Halter, S.; Wilde, M.; Franz, F.; Auwärter, V. Human phase I metabolism of the novel synthetic cannabinoid 5F-CUMYL-PEGACLONE. *Forensic Toxicol.* **2019**, *37*, 154–163. [[CrossRef](#)] [[PubMed](#)]
27. Asada, A.; Doi, T.; Tagami, T.; Takeda, A.; Satsuki, Y.; Kawaguchi, M.; Nakamura, A.; Sawabe, Y. Cannabimimetic activities of cumyl carboxamide-type synthetic cannabinoids. *Forensic Toxicol.* **2018**, *36*, 170–177. [[CrossRef](#)]
28. Schoeder, C.T.; Hess, C.; Madea, B.; Meiler, J.; Müller, C.E.J.F.T. Pharmacological evaluation of new constituents of “Spice”: Synthetic cannabinoids based on indole, indazole, benzimidazole and carbazole scaffolds. *Forensic Toxicol.* **2018**, *36*, 385–403. [[CrossRef](#)]
29. EMCDDA-Europol. Annual Report on the Implementation of Council Decision 2005/387/JHA. 2015. Available online: <https://www.emcdda.europa.eu/system/files/publications/2880/TDAS16001ENN.pdf> (accessed on 26 March 2021).
30. Kovács, K.; Kereszty, É.; Berkecz, R.; Tizslavicz, L.; Sija, É.; Körmöczi, T.; Jenei, N.; Révész-Schmehl, H.; Institoris, L. Fatal intoxication of a regular drug user following N-ethyl-hexedrone and ADB-FUBINACA consumption. *J. Forensic Leg. Med.* **2019**, *65*, 92–100. [[CrossRef](#)]
31. Kadomura, N.; Ito, T.; Kawashima, H.; Matsuhisa, T.; Kinoshita, T.; Soda, M.; Kohyama, E.; Iwaki, T.; Nagai, H.; Kitaichi, K. In vitro metabolic profiles of adamantyl positional isomers of synthetic cannabinoids. *Forensic Toxicol.* **2021**, *39*, 26–44. [[CrossRef](#)]
32. Broberg, M.N.; Knych, H.; Bondesson, U.; Pettersson, C.; Stanley, S.; Thevis, M.; Hedeland, M. Investigation of Equine In Vivo and In Vitro Derived Metabolites of the Selective Androgen Receptor Modulator (SARM) ACP-105 for Improved Doping Control. *Metabolites* **2021**, *11*, 85. [[CrossRef](#)]
33. Holm, N.B.; Nielsen, L.M.; Linnet, K. CYP3A4 Mediates Oxidative Metabolism of the Synthetic Cannabinoid AKB-48. *AAPS J.* **2015**, *17*, 1237–1245. [[CrossRef](#)]
34. Nielsen, L.M.; Holm, N.B.; Olsen, L.; Linnet, K. Cytochrome P450-mediated metabolism of the synthetic cannabinoids UR-144 and XLR-11. *Drug Test. Anal.* **2016**, *8*, 792–800. [[CrossRef](#)]

35. Zanger, U.M.; Schwab, M. Cytochrome P450 enzymes in drug metabolism: Regulation of gene expression, enzyme activities, and impact of genetic variation. *Pharmacol. Ther.* **2013**, *138*, 103–141. [[CrossRef](#)]
36. Gaunitz, F.; Thomas, A.; Fietzke, M.; Franz, F.; Auwärter, V.; Thevis, M.; Mercer-Chalmers-Bender, K. Phase I metabolic profiling of the synthetic cannabinoids THJ-018 and THJ-2201 in human urine in comparison to human liver microsome and cytochrome P450 isoenzyme incubation. *Int. J. Leg. Med.* **2019**, *133*, 1049–1064. [[CrossRef](#)]
37. Gaunitz, F.; Dahm, P.; Mogler, L.; Thomas, A.; Thevis, M.; Mercer-Chalmers-Bender, K.J.A.; Chemistry, B. In vitro metabolic profiling of synthetic cannabinoids by pooled human liver microsomes, cytochrome P450 isoenzymes, and *Cunninghamella elegans* and their detection in urine samples. *Anal. Bioanal. Chem.* **2019**, *411*, 3561–3579. [[CrossRef](#)]
38. Swortwood, M.J.; Carlier, J.; Ellefsen, K.N.; Wohlfarth, A.; Diao, X.; Concheiro-Guisan, M.; Kronstrand, R.; Huestis, M.A. In vitro, in vivo and in silico metabolic profiling of α -pyrrolidinopentiothiophenone, a novel thiophene stimulant. *Bioanalysis* **2016**, *8*, 65–82. [[CrossRef](#)] [[PubMed](#)]
39. Mardal, M.; Dalsgaard, P.W.; Qi, B.; Mollerup, C.B.; Annaert, P.; Linnet, K. Metabolism of the synthetic cannabinoids AMB-CHMICA and 5C-AKB48 in pooled human hepatocytes and rat hepatocytes analyzed by UHPLC-(IMS)-HR-MSE. *J. Chromatogr. B Analyt. Biomed. Life Sci.* **2018**, *1083*, 189–197. [[CrossRef](#)]
40. Carlier, J.; Diao, X.; Huestis, M.A. Synthetic cannabinoid BB-22 (QUCHIC): Human hepatocytes metabolism with liquid chromatography-high resolution mass spectrometry detection. *J. Pharm. Biomed. Anal.* **2018**, *157*, 27–35. [[CrossRef](#)] [[PubMed](#)]
41. Fabregat-Safont, D.; Mardal, M.; Noble, C.; Cannaert, A.; Stove, C.P.; Sancho, J.V.; Linnet, K.; Hernández, F.; Ibáñez, M. Comprehensive investigation on synthetic cannabinoids: Metabolic behavior and potency testing, using 5F-APP-PICA and AMB-FUBINACA as model compounds. *Drug Test. Anal.* **2019**, *11*, 1358–1368. [[CrossRef](#)] [[PubMed](#)]
42. Kevin, R.C.; Lefever, T.W.; Snyder, R.W.; Patel, P.R.; Fennell, T.R.; Wiley, J.L.; McGregor, I.S.; Thomas, B.F.J.F.T. In vitro and in vivo pharmacokinetics and metabolism of synthetic cannabinoids CUMYL-PICA and 5F-CUMYL-PICA. *Forensic Toxicol.* **2017**, *35*, 333–347. [[CrossRef](#)]
43. Montesano, C.; Vincenti, F.; Fanti, F.; Marti, M.; Bilel, S.; Togna, A.R.; Gregori, A.; Di Rosa, F.; Sergi, M. Untargeted Metabolic Profiling of 4-Fluoro-Furanylfentanyl and Isobutyrylfentanyl in Mouse Hepatocytes and Urine by Means of LC-HRMS. *Metabolites* **2021**, *11*, 97. [[CrossRef](#)]
44. Seitzer, P.M.; Searle, B.C. Incorporating In-Source Fragment Information Improves Metabolite Identification Accuracy in Untargeted LC-MS Data Sets. *J. Proteome Res.* **2019**, *18*, 791–796. [[CrossRef](#)]
45. Anzenbacher, P.; Anzenbacherová, E. Cytochromes P450 and metabolism of xenobiotics. *Cell. Mol. Life Sci.* **2001**, *58*, 737–747. [[CrossRef](#)] [[PubMed](#)]
46. Hemmer, S.; Manier, S.K.; Fischmann, S.; Westphal, F.; Wagmann, L.; Meyer, M.R. Comparison of Three Untargeted Data Processing Workflows for Evaluating LC-HRMS Metabolomics Data. *Metabolites* **2020**, *10*, 378. [[CrossRef](#)] [[PubMed](#)]
47. Gandhi, A.S.; Zhu, M.; Pang, S.; Wohlfarth, A.; Scheidweiler, K.B.; Liu, H.F.; Huestis, M.A. First characterization of AKB-48 metabolism, a novel synthetic cannabinoid, using human hepatocytes and high-resolution mass spectrometry. *AAPS J.* **2013**, *15*, 1091–1098. [[CrossRef](#)] [[PubMed](#)]

RESEARCH ARTICLE

WILEY

Adulteration of low-delta-9-tetrahydrocannabinol products with synthetic cannabinoids: Results from drug checking services

Manuela Carla Monti¹  | Jill Zeugin² | Konrad Koch¹ | Natasa Milenkovic³ | Eva Scheurer¹ | Katja Mercer-Chalmers-Bender¹ 

¹Institute of Forensic Medicine, Department of Biomedical Engineering, University of Basel, Basel, Switzerland

²Addiction Support, Region Basel (Suchthilfe Region Basel), Basel, Switzerland

³Addiction Services (Abteilung Sucht), Health Department Kanton Basel-Stadt, Basel, Switzerland

Correspondence

Katja Mercer-Chalmers-Bender, Institute of Forensic Medicine, Department of Biomedical Engineering, University of Basel, Basel, Switzerland.

Email: katja.mercer-chalmers-bender@unibas.ch

Abstract

Since late 2019, low-delta-9-tetrahydrocannabinol (THC) preparations adulterated with synthetic cannabinoids (SCs) have been frequently observed in Switzerland. The unawareness of users concerning the presence of SCs and the typically higher potency and toxicity of SCs, when compared with THC, can result in increased health risks. In Switzerland, low-THC (<1%) cannabis products, except hashish, are legal. These products can act as carrier materials for SCs. In this study, cannabis samples and user self-reports received through three drug checking services were collected and analysed, to gain deeper insight into this new phenomenon. Samples were collected from January 2020 to July 2021. Liquid chromatography coupled with high-resolution mass spectrometry was used for the qualitative screening and semi-quantification of SCs, while gas chromatography with flame ionization detector was applied for the quantification of THC and cannabidiol levels. Reported adverse effects were compared between users who consumed adulterated (SC-group) and non-adulterated (THC-group) products. Of a total 94 samples, 50% contained up to three different SCs. MDMB-4en-PINACA was most often detected. All adulterated cannabis flowers contained $\leq 1\%$ THC. Adulterated hashish also typically presented low THC-levels (median: 0.8%). The SC-group was associated with higher numbers of adverse events ($p = 0.041$). Furthermore, psychologic ($p = 0.0007$) and cardiologic ($p = 0.020$) adverse effects were more profound in the SC-group than in the THC-group. Drug checking services enabled the timely detection and monitoring of new and potentially dangerous trends. Furthermore, due to user-reports, additional valuable information was gained on adverse events associated with the consumption of novel SCs.

KEYWORDS

adverse effects, drug checking, high-resolution mass spectrometry, market monitoring, synthetic cannabinoids

This is an open access article under the terms of the Creative Commons Attribution-NonCommercial-NoDerivs License, which permits use and distribution in any medium, provided the original work is properly cited, the use is non-commercial and no modifications or adaptations are made.

© 2022 The Authors. *Drug Testing and Analysis* published by John Wiley & Sons Ltd.

1 | INTRODUCTION

1.1 | Background and aims

Synthetic cannabinoids (SCs) currently comprise the largest substance class within the group of new psychoactive substances (NPS).¹ However, data on the pharmacology and toxicology of NPS, such as SCs,²⁻⁷ are generally scarce.^{8,9} Data on NPS are obtained through case reports and series,^{5,6,8,10-12} poisons information centres,⁸ online forums,¹³ and surveys.⁹ However, the lack of analytical confirmation of the consumed product is often a serious limitation.⁸ In order to monitor illegal markets and detect new trends, seized material from forensic casework or products obtained via online test purchase are investigated.¹⁴⁻²¹ In contrast to studies examining user reports, these instances will give no information on pharmacodynamics or toxicological effects. Drug checking services offer valuable insights into the drug market often including user self-reports describing the drug's effects. For instance, Oomen et al. recently highlighted the importance of drug checking services for the monitoring of new trends, demonstrated by the example of adulterated cannabis products.²²

This study presents data, gained through drug checking services, and elucidates the new phenomenon of low-THC cannabis preparations adulterated with synthetic cannabinoids (SCs). Study aims are to inform on present developments, with regard to identified compounds, applied carrier material, and reported adverse effects after consumption of adulterated cannabis products. As both adulterated as well untreated drug-type cannabis (high-THC) samples were handed-in, this offered the opportunity to compare reported adverse effects between drug-type cannabis (THC-group) and SCs (SC-group). This study underlines the potential of drug checking services to act as a market monitoring tool as well as source of information on effects of NPS.

1.2 | Synthetic cannabinoids

Since the emergence of SCs on the recreational drug market in 2008, 209 SCs are being monitored by the European Monitoring Centre on Drugs and Drug Addiction (EMCDDA), illustrating the considerable variety of compounds belonging to this class.¹ Most SCs show high binding affinities and demonstrated activities at the cannabinoid receptors 1 and 2 (CB1 and CB2).^{4,6,12,23-25} Therefore, many SCs have similar cannabimimetic effects as tetrahydrocannabinol (THC), the main psychoactive ingredient of THC-rich cannabis. The psychoactive effects of THC are mostly attributed to the binding and activation of CB1.^{6,26} SCs are often associated with much higher potency²⁷ and toxicity when compared with THC, resulting in increased health risks for individuals and escalated public health concerns.²⁸ Since their emergence on the drug market, numerous cases of severe intoxication, including lethal outcomes, have been associated with SC uptake.^{12,28,29} The EMCDDA issued a report in 2020, stating a total of 768 seizures of the SC MDMB-4en-PINACA in 20 member states.³⁰ This illustrates the extensive availability of MDMB-4en-

PINACA, which made its first appearance on the drug market in 2018.¹² A transnational study conducted by Norman et al.²⁰ found MDMB-4en-PINACA to be one of the most popular SCs by end of September 2020, while comparing SC prevalence in prisons and in the wider population in Germany, the United Kingdom, and the United States. However, the aforementioned authors also observed significant regional differences in the identified SCs, probably resulting from local supply networks and differences in legislation.²⁰ It is believed that the legal frameworks in China, thought to be the main production site of many SCs, influence the emergence and availability of SCs on the European market.³¹

1.3 | Drug checking services

Switzerland, as well as other European countries, has a long history of drug checking services, with the first of these services being introduced in the 1990s.^{32,33} Drug checking services are low threshold harm reduction services, which offer recreational drug users the possibility to subject their samples to chemical analysis without legal consequences. The drug test results obtained from drug checking services generally include identity and quantity of the main active ingredient as well as any pharmacologically relevant adulterants and, in cases of fixed dosage forms (i.e., tablets and trips), the respective dosages. Drug checking services offer an insight into the recreational drug market at consumer level and, thus, act as a market monitoring tool.^{22,33,34} Drug checking services range from onsite (mobile) testing at festivals or nightclubs to stationary premises.^{32,33,35} The analytical methods, and, therefore, the reliability of results, may vary considerably between these services.^{32,36} Mass spectrometric techniques are considered the gold standard in regards of specificity and sensitivity, however, due to the technical requirements of the instruments (i.e., gas supply, electricity, and ambient conditions), mass spectrometry is typically limited to stationary settings.^{32,37}

1.4 | Low-THC cannabis products: regulatory and clinical aspects

Low-THC cannabis products are defined by the EMCDDA as "products being or containing cannabis herb, resin, extracts or oils that claim or appear to have a very low percentage of THC and which would be unlikely to cause intoxication."³⁸ The regulatory limit for THC varies between national drug policies, with Switzerland applying a higher threshold than most European countries (e.g., 0.2%).³⁹ Swiss law allows the production, selling, and possession of cannabis products (including plants, dried cannabis flowers, oils, and tinctures) with a THC content of <1%, with the exception of hashish (cannabis resin)—the latter being considered illegal, regardless of its THC content.⁴⁰ In 2011, in order to facilitate industrial hemp production, the threshold for THC was increased from 0.3% to 1%, ultimately resulting in an emerging market for low-THC cannabis products, including dried cannabis flowers, regulated as tobacco substitutes.³⁸

In recent years, a growing industry around low-THC and high-cannabidiol (CBD) products, often referred to as “CBD-products” with the main focus on CBD-oils, has been observed globally.^{38,39,41,42} The selling of low-THC cannabis herbs has also been reported for some European countries.^{38,43} Information on legal frameworks and market trends surrounding low-THC cannabis products on a cross-national level has been extensively reviewed and reported by McGregor et al.³⁹

For low-THC cannabis products, fibre-type varieties of cannabis (industrial hemp) are often used, due to higher levels of CBD being present in these materials when compared with those found in drug-type cannabis.^{26,39,42} CBD and THC are the main and best-characterized phytocannabinoids of the cannabis plant.^{26,41,42,44} CBD is considered non-intoxicating and has been recommended for several therapeutic applications.⁴⁴ Nevertheless, clinical studies systematically investigating therapeutic effects of CBD are limited, resulting in little evidence of CBD's medical benefits and, therefore, requiring further research.^{41,42} Purified CBD is widely considered to be safe and well tolerated.^{39,44} In Switzerland, low-THC cannabis flowers are typically smoked with and without addition of tobacco³⁸; thus, the transferability of results obtained for medicinal CBD products is limited due to differences in the route of administration and dosage.⁴⁴ However, due to the lack of intoxicating effects of CBD and the low percentage of THC, no intoxicating effects as in drug-type cannabis are expected for low-THC cannabis products.^{39,45}

1.5 | Low-THC-cannabis products: challenges

The availability of legal low-THC cannabis flowers and derived products has resulted in several challenges, including concerns around the ability to distinguish between low- and high-THC cannabis plant material. The Swiss police addressed this by introducing a rapid reagent test, enabling the distinction between low- and high-THC products.^{38,46} Further questions arose concerning driving ability after intake of low-THC products.^{43,45–47} In parallel, an additional challenge has emerged: the adulteration of low-THC cannabis products with SCs.^{1,30} Since late 2019, increasing numbers of cannabis preparations adulterated with SCs have been reported in Switzerland, with both forensic institutions and drug checking services contributing to the detection and monitoring of this new trend.³⁰ These adulterated cannabis products, which are neither visually nor olfactorily distinguishable from regular cannabis products, are typically sold as regular high-THC cannabis flowers and hashish and thus leave recreational cannabis users uninformed of adulteration. The generally higher potency of SCs, when compared with THC, and the user's unawareness of the presence of SCs result in an increased potential for intoxications and health risks.^{1,6} This is further aggravated by the fact that little is known about the pharmacology and short- and long-term toxicity of most SCs.^{6,17} Regarding the SC adulterated products, consumer risk is further exacerbated by unknown SC content and potential inhomogeneity.¹⁷

In response to the emerging health risks, the public were informed and warned via several media releases.^{48–50} Oomen et al.²² recently presented data gained from different European drug checking services, including one Swiss drug checking service, on cannabis products adulterated with the SC MDMB-4en-PINACA. It was shown that even though first detected in Switzerland, adulterated cannabis products have been detected in other countries as well, for instance Italy, Germany, France, and Austria.

2 | MATERIAL AND METHODS

2.1 | Sample and data collection

Cannabis samples were collected between January 2020 and July 2021 at stationary drug checking services in three cities in Switzerland (Basel: DIBS, Lucerne: DILU, Olten: Suchthilfe Ost). Users of the drug checking services were obligated to undertake professional counselling in order to have their sample analysed. The entire drug checking process is fully anonymous, meaning that no personal information (e.g., name, date of birth, visual nature, address, and phone number) is collected. Therefore, all data received from the drug checking services were fully anonymised at the time point of data collection, leaving no possibility to trace back individuals. Consequently, according to Swiss national legal standards, this study did not require formal ethics approval.

During sample collection, the visitors were routinely questioned on sample-specific information, including the alleged identity and dosage of the product. The volunteers were further asked if they had already consumed the product and, if consumption was affirmed, they were asked for additional detail on their experience (e.g., adverse effects, effect duration, potency, and further observations). These self-reports were noted by means of free text by staff at the drug checking centre. After analysis, the users received their results anonymously via phone. For this, the user called the drug checking centre while hiding their phone number and mentioned a password that was defined during counselling. For cannabis material, results included presence and identity of detected SCs and estimation of cannabis type (high- versus low-THC). All remaining material was stored at room temperature in a dark storage area and preserved in individual pressure lock bags. To expand the scientific impact of this study, the samples (where sufficient material was available) were subjected to additional THC and CBD quantification and semi-quantification of selected SCs.

2.2 | Evaluation of reported adverse effects

Prior to the statistical evaluation of the reported adverse effects and further experiences (e.g., short effect duration), the self-reports were randomized. The reported side-effects and experiences were designated to applicable categories by a different scientific employee, while remaining uninformed about the analytical results,

that is, if a sample was adulterated or not. For the comparison of the occurrence of adverse events, the individual reports were classified into the categories “adverse event” or “no adverse event.” The latter was chosen in cases where the drug’s effects were described as “normal” or “potent,” therefore lacking in apparent unwanted effects. Adverse events were further evaluated by sorting them into pharmacologic subcategories. The subcategory “cardiovascular adverse effects” included palpitations, circulatory collapse, circulatory issues, and chest discomfort. For “neurologic adverse effects,” paraesthesia, seizure, muscular cramps, paralysis, agitation, dizziness, headache, unconsciousness, and vomiting were considered. The subcategory “psychologic adverse effects” comprised strong psychedelic effects (for example hallucination), anxiety and paranoia, panic attacks, general psychologic discomfort and stress, as well as disorientation. For each subcategory, one or more of the above-mentioned symptoms had to be met for an adverse effect subcategory to be considered as confirmed. Independency testing of the occurrence of adverse events, adverse effect subcategories, and other experiences, enabling the comparison between the THC- and SC-group, was performed using the Fisher’s exact test. Statistical testing and calculation of odds ratios (ORs) and 95% confidence intervals (95% CIs) were conducted in R (version 3.4.3) using the *fisher.test* function.

2.3 | Chemicals and analytical reference material

LC-MS grade methanol (MeOH), water, and acetonitrile (ACN) were purchased from Macherey-Nagel AG (Oensingen, Switzerland). Formic acid (98–100%), analytical grade ethylacetate (EtOAc) with purity $\geq 99.0\%$, docosane analytical standard with purity $>99.9\%$, and analytical grade warfarin (4-hydroxy-3-(3-oxo-1-phenylbutyl)-cumarin) with purity $\geq 98.0\%$ were obtained from Merck (Zug, Switzerland).

Certified reference standards of d,l-11-nor-delta-9-THC (THC), d,l-11-nor-delta-9-THC carboxylic acid (THCA), cannabidiol (CBD), and cannabidiolic acid (CBDA) were obtained from Lipomed AG (Arllesheim, Switzerland).

Reference material for SCs was obtained from Cayman Chemical Company (Michigan, USA), Lipomed AG (Arllesheim, Switzerland), or provided either by the Zurich Forensic Science Institute (Zurich, Switzerland) or the State Criminal Investigation Office Baden-Württemberg (Stuttgart, Germany)—for detailed information, see Table S1

2.4 | Homogenization and sampling

Prior to analysis, flower samples were homogenized using a grinder, after removal of larger branches. Hashish samples were finely cut using a scalpel. In order to achieve a mean value for the SC and phytocannabinoid contents, the whole sample was homogenized before weighing for the respective analyses.

2.5 | Qualitative screening for SCs

For screening of the SCs, 1 ml MeOH containing the internal standard (ISTD) warfarin at 0.25 mg/ml was added to 50 mg of homogenized sample. Warfarin was chosen as ISTD instead of a deuterated SC, due to the relatively large quantities required for this analytical method and associated costs. Samples were vortexed for 10 s and filtered using Simplepure™ syringe filters (13 mm, 0.45 μm) obtained from BGB Analytik AG (Boeckten, Switzerland). Finally, the extracts were diluted 1:10,000 in MeOH.

All instrumentation and the analytical column described in the following sections were obtained from Thermo Fisher Scientific™ (Reinach, Switzerland). For chromatographic separation, a Dionex Ultimate 3000 RS ultra UHPLC system was used equipped with a Hypersil™ Phenyl analytical column (1.9 μm , 100 \times 2.1 mm), kept at 30°C by a MutliSLEEVE™ column heater. The injection volume was 5 μl and the total flow rate 0.6 ml/min. The gradient started at 80% mobile phase A, consisting of 0.1% (v/v) formic acid in water, and 20% mobile phase B, comprised of 0.1% (v/v) formic acid in ACN. The percentage of mobile phase B was increased over 0.92 min to 40%, after which it was increased further to 71% over 6 min, and finally ramped to 100% over 0.25 min. This setting was held for 1 min, after which the system was allowed to re-equilibrate to the initial settings for 1.25 min, resulting in a total run time of less than 10 min per sample.

Subsequent analysis was conducted using a Thermo Scientific™ Q Exactive™ HF Hybrid Quadrupole-Orbitrap™ mass spectrometer operated with a heated electrospray ionization (H-ESI) source in positive ionization mode. A sheath gas flow rate of 50 arbitrary units (AU) and auxiliary gas flow rate of 5 AU were applied. The spray voltage was +3.5 kV, and the capillary temperature and auxiliary gas heater temperature were 200°C and 300°C, respectively. A full scan measurement from m/z 150 to m/z 1000 was conducted at a resolution of 120,000 full width at half-maximum (FWHM) at m/z 200. Automatic gain control (AGC) target was set to $3e6$, and maximum injection time (IT) was 200 ms. Data acquisition and evaluation was conducted using the Tracefinder™ (version 5.1, Thermo Scientific™) software. With a mass error 5 ppm and detection windows of 30 s, exact mass signal and retention times were used for qualitative identification. Besides SCs, the natural cannabinoids THCA, THC, CBDA, and CBD were additionally detected to compare the respective areas—enabling a rough estimation of the cannabis type. This estimation was based on comparison on the ratio of the total peak areas of THC and CBD, $\text{area}_{\text{THC} + \text{THCA}}/\text{area}_{\text{CBD} + \text{CBDA}}$. High-THC and low-CBD samples were defined for ratios >1 , high-CBD and low-THC for samples with ratios <1 , while a ratio of approximately 1 was estimated as intermediate type. Screened $[M + H]^+$ and retention times are listed in Table S2. Prior to every sequence, a quality control (QC) sample was injected containing a mixture (see Table S1) of all 63 SCs validated for the qualitative screening at 5 ng/ml to assure functionality and performance of the analysis.

In order to screen for novel SCs, for which no reference material was available at the time of analysis, and to retrospectively search for SCs which have only recently entered the drug market and were,

therefore, not known at the time of analysis, data were also manually screened using the software FreeStyle™ (version 1.7, SP1, Thermo Scientific™). This was conducted by investigating the data for corresponding $[M + H]^+$ (mass error 5 ppm) signals. Signals corresponding to novel SCs were further investigated applying data dependent MS² measurements (dd-MS²) at resolutions of 60,000 FWHM (Full MS) and 15,000 FWHM (MS²), with normalized stepped collision energies of 10, 17.5, and 35 (normalized to m/z 500 [$z = 1$]). Where available, the MS² spectra were compared with published product ion spectra. To confirm the obtained results, reference materials (where available) were obtained, allowing full verification of the result.

The screening method for SCs was validated concerning limit of detection (LOD), specificity, and selectivity for 63 SCs (status: June 2021, Table S2). The respective LODs were determined in both the matrix (spiked pool of six hashish and six cannabis flower extracts) and MeOH. LODs were investigated using FreeStyle™ (version 1.7, SP1, Thermo Scientific™) software. The formal criterion for LODs was signal to noise (S/N) of greater than three to one, although, due to the applied low noise system, much higher S/N at LOD were achieved.

Specificity and selectivity were verified by measuring six hashish and six cannabis flower preparations (low- and high-THC), accompanied by investigation of injections of mixtures and individual SCs, with a focus on the resolution and distinction of structural isomers (e.g. 5F-MDMB-PICA and 5F-MDMB-P7AICA), isobaric compounds, and possible interfering signals (i.e., isotopes). The recoveries of the herein applied sample preparation procedure (filtration and dilution) were evaluated by applying a spiking experiment. This experiment was conducted with three SCs (5F-MDMB-PICA, 4F-MDMB-BINACA, and MDMB-4en-PINACA), as sufficient amounts of reference material were available for these compounds. In brief, 50 mg of low-THC cannabis flowers were spiked in triplicates using standard solutions of the respective SCs at concentrations translating to 5 µg/mg plant material (0.25 mg/ml) to which ISTD was added (0.25 mg/ml). The area ratios obtained after sample preparation were compared with the ratios obtained after direct dilution of the analytical standards in MeOH.

2.6 | Semi-quantification of selected SCs

5F-MDMB-PICA, 4F-MDMB-BINACA, MDMB-4en-PINACA, and ADB-BUTINACA, which were most frequently detected in this study (≥ 4 detections), were additionally subjected to semi-quantification. Therefore, the previously described screening method was expanded. In a preliminary experiment investigating the influence of the matrix, calibrator solutions (5 ng/ml, 25 ng/ml, 50 ng/ml, and 75 ng/ml translating to 1 µg/mg, 5 µg/mg, 10 µg/mg, and 15 µg/mg with a dilution-factor of 1:10,000) were prepared in matrix (diluted low-THC cannabis flower extract) and MeOH (solvent). Recoveries were calculated via comparison of area ratios obtained in matrix and solvent. The calibrators (levels as described above) used for semi-quantification were prepared in solvent. In addition to the initial screening, samples were also subject to semi-quantification, where

sufficient sample material was available. In cases where the signal was below the lowest calibrator, the sample was remeasured applying a smaller dilution factor. For semi-quantification the TraceFinder™ (version 5.1, Thermo Scientific™), software was used. The respective semi-quantitative contents for each SC were calculated by comparison of area ratios between sample and calibration curve (internal standard method).

2.7 | Quantification of THC and CBD

For the quantification of THC and CBD, an accredited method (according to the guidelines of the Swiss Society of Forensic Medicine, SGRM⁵¹), routinely applied for the forensic chemical analysis of cannabis material, was used. LODs and limits of quantification (LOQs) are 0.1% (w/w, corresponding to 1 mg/g) and 0.3% (w/w, corresponding to 3 mg/g) for both analytes, CBD and THC, respectively. The homogenized samples were weighed (30–50 mg) into 4-ml glass screw top vials obtained from BGB Analytik AG (Boeckten, Switzerland) to which 2 ml ISTD-solution (0.5 mg/ml docosane in EtOAc) was added. After sonification for 15 min at room temperature, using a SW3H ultrasonic bath from Sonoswiss AG (Ramsen, Switzerland), the extracts were set aside for 10 min to allow insoluble parts to settle. The supernatant was then diluted 4:1 with EtOAc, resulting in a final concentration of the ISTD-solution of 0.125 mg/ml. For the subsequent analysis, 1 µl of the diluted sample was injected using an AI 3000 autosampler from Thermo Fisher Scientific™ (Reinach, Switzerland). The Inlet temperature was 210°C, and the split/splitless (SSL) injector was operated with a split ratio of 1:50. Chromatographic separation and analysis were achieved using a FOCUS GC gas chromatograph with flame ionization detector (FID), obtained from Thermo Fisher Scientific™ (Reinach, Switzerland). For the chromatographic separation, an Agilent J&W DB-5MS column (15 m × 0.250 mm, inner diameter 0.25 µm) was used. Starting temperature of the GC oven was 120°C. This temperature was held for 2 min after which it was ramped at 15°C/min until the final temperature of 280°C was reached, which then was held for further 2 min. The GC was used in constant flow mode at a flow rate of 0.8 ml/min with helium as carrier gas. The FID detector was operated at 300°C with nitrogen as makeup gas. Quantitative results were calculated using the analyte/internal standard response ratio.

3 | RESULTS AND DISCUSSION

3.1 | Validation of the SCs screening method

In the measured solutions, the LODs ranged from 0.3 ng/ml to 0.6 ng/ml, with the exception of ADB-PINACA (LOD = 2 ng/ml), translating into concentrations at the product level, when applying a 1:10,000 dilution factor, of 0.06 µg/mg and 0.12 µg/mg, respectively (analyte loss during sample preparation not considered). LODs and respective S/N ratios at LOD are summarized in Table S2. The spiking

experiment revealed mean recoveries of $94.4 \pm 1.7\%$, $99.5 \pm 0.5\%$, and $103.8 \pm 2.1\%$, for 5F-MDMB-PICA, 4F-MDMB-BINACA, and MDMB-4en-PINACA, respectively.

3.2 | SCs prevalence over time

Of all cannabis samples ($n = 94$), 50% ($n = 47$) were found to contain up to three, of the following SCs, namely, 4F-MDMB-BICA (4F-MDMB-BUTICA), 4F-MDMB-BINACA, 5F-MDMB-PICA (5F-MDMB-2201), 5F-MDMB-PINACA (5F-ADB), ADB-BUTINACA (ADB-BINACA), MPHP-2201 (5F-MPP-PICA, 5F-MPhP-PICA), and MDMB-4en-PINACA. Structures of all herein detected SCs are presented in Figure 1. The absolute numbers of detections for each SCs over time are presented in Figure 2 and listed in Table 1.

Mixtures were merely applied onto cannabis flowers, while hashish was always adulterated using a single SC. A tendency from mixtures towards the use of single SCs was observed for cannabis flowers in this study. Of all SC positive cannabis flowers collected in 2020 ($n = 17$), 47% ($n = 8$) contained mixtures of up to three different SCs. In the first half of 2021, the percentage of cannabis flowers containing more than one SC decreased to 25% ($n = 2$), with mixtures containing a maximum of two SCs.

MDMB-4en-PINACA was most commonly found. It was detected in 40% ($n = 38$) of all analysed cannabis samples ($n = 94$) and in 81% ($n = 38$) of all adulterated samples ($n = 47$, including mixtures). Oomen et al.²² reported the presence of the SC MDMB-4en-PINACA in 23.6% ($n = 270$) of all analysed cannabis samples collected at various drug checking services throughout Europe.

Regarding the collected data about MDMB-4en-PINACA, 5F-MDMB-PICA, and 4F-MDMB-BINACA in 2020, the results of this study match previously reported SC prevalence on transnational

levels.^{12,20,52,53} Over the period of this study, 4F-MDMB-BINACA and 5F-MDMB-PICA were only detected as adulterants in 2020. The ever-changing SCs market is also illustrated in this study by the first detection of ADB-BUTINACA in February 2021. ADB-BUTINACA has since been repeatedly detected, with additional seven detections in the timeframe up to the end of June 2021 (end of study). The emergence of ADB-BUTINACA has also been reported in other countries.^{22,54,55} Thus, ADB-BUTINACA could become increasingly popular on the drug market in the near future and replace earlier SCs.

3.3 | Semi-quantification of selected SCs

When comparing the area ratios obtained in matrix and solvent, mean recoveries of $97.5 \pm 4.0\%$, $102.8 \pm 1.5\%$, $98.4 \pm 1.9\%$, and $92.6 \pm 4.6\%$ were achieved for 5FMDMB-PICA, 4F-MDMB-BINACA, MDMB-4en-PINACA, and ADB-BUTINACA, respectively. The correlation factors of all calibrations used for semi-quantification were >0.998 .

Of the adulterated samples, 79% ($n = 37$) were subjected to semi-quantification. Mean values and standard deviations (SDs) of $2.0 \pm 1.1 \mu\text{g}/\text{mg}$ (range 0.6–4.2 $\mu\text{g}/\text{mg}$), $4.3 \pm 2.2 \mu\text{g}/\text{mg}$ (range 0.1–7.2 $\mu\text{g}/\text{mg}$), $5.6 \pm 2.2 \mu\text{g}/\text{mg}$ (range 1.0–9.9 $\mu\text{g}/\text{mg}$), and 2.5 $\mu\text{g}/\text{mg}$ (only quantifiable in one sample) were found for 5F-MDMB-PICA, MDMB-4en-PINACA, ADB-BUTINACA, and 4F-MDMB-BINACA, respectively. The highest SC concentrations were detected for ADB-BUTINACA. The SC and phytocannabinoid contents are summarized in Table 1. Two cannabis flower samples (14 and 22) contained 4F-MDMB-BINACA and MDMB-4en-PINACA, respectively, in trace amounts. The low contents probably originated from contamination during manufacturing, ultimately resulting in signals below limit of quantification (LOQ). Previous studies reported SC contents for herbal

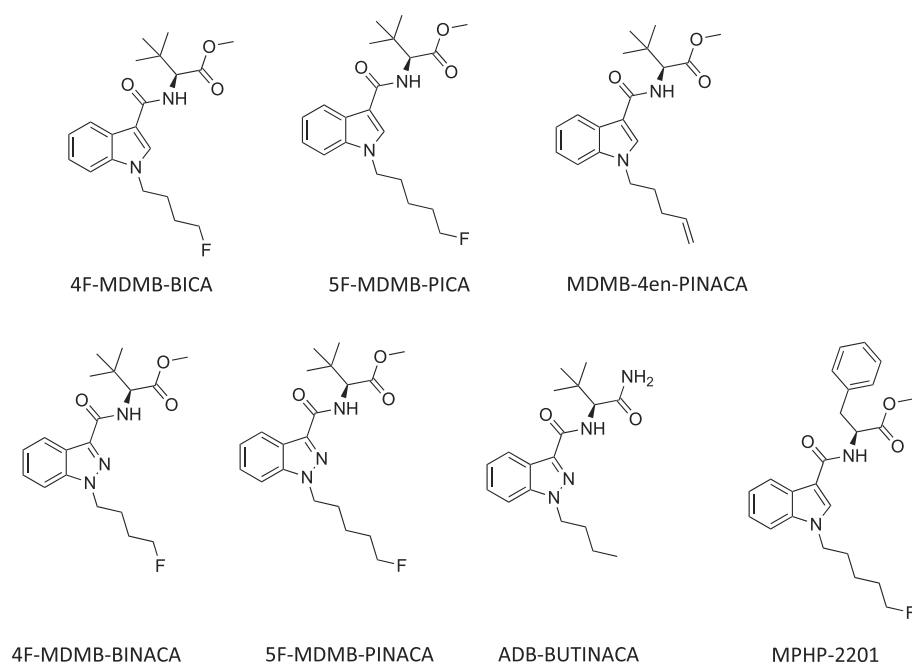
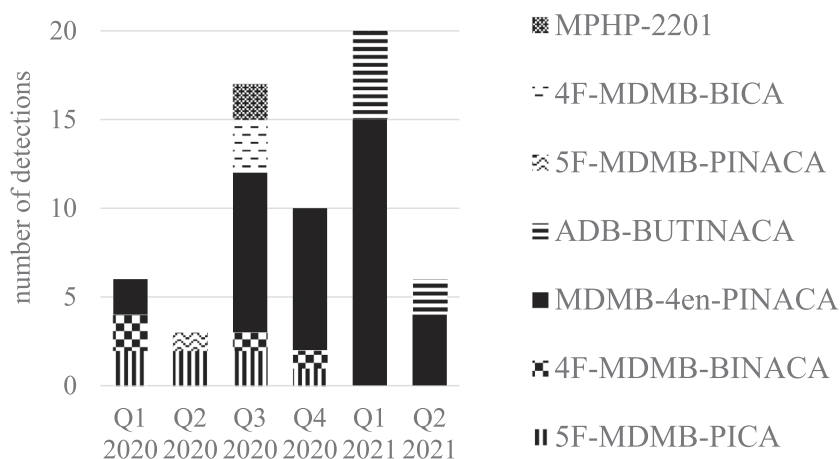


FIGURE 1 Chemical structures of detected SCs

FIGURE 2 Detected SCs (mixtures included) over time

blends (“spice”),^{16,17,21,56} of different SCs than detected in the presented study. Direct comparability of quantitative results is difficult. For instance, differences in the potency of SCs might influence required dosages. Despite the existence of data on potency and efficacy of selected SCs at CB1,^{4,27,57} one drawback is the limited comparability between different *in vitro* assays. Further, pharmacokinetic parameters of SCs are largely unknown,⁵⁸ ultimately rendering dose estimates currently unfeasible. Concerning the herein detected SCs, Cannaert et al.²⁷ reported EC₅₀ values at CB1, obtained via a β -Arrestin 2 recruitment assay, for 5F-MDMB-PICA (3.26 nM), MDMB-4en-PINACA (2.33 nM), 4F-MDMB-BINACA (7.39 nM), ADB-BUTINACA (6.36 nM, referred to by the authors as ABD-BINACA), 5F-MDMB-PINACA (1.78 nM), MPHP-2201 (32.9 nM, referred to by the authors as 5F-MPP-PICA), and 4F-MDMB-BICA (121 nM). Therefore, the SCs detected in this study presented high potencies at CB1 in the mid- to low-nM range. The overall seemingly lower contents detected in this study, when compared with earlier results for spice preparations,^{16,17,21,56} may be explained by the dosages being adjusted, as the adulterated products encountered in this study are intended to mimic regular cannabis preparations; thus, the effects should comply as closely as possible with those encountered from THC-rich cannabis preparations.

A study conducted in 2014 by Moosmann et al.²¹ investigated the SC contents in 311 herbal blends from 31 different brands. Considerable inter- and intra-package variances in SC contents were shown, ultimately resulting in increased risks for accidental overdosing. A study from 2019, addressing the same question via the analysis of 20 herbal blends, presented less variation, indicating that the risk for consumers has slightly decreased.⁵⁶ Inhomogeneities regarding SC content were also expected in this study, especially in the case of adulterated cannabis flowers, which presumably are sprayed during adulteration. This would likely result in uneven distribution of SC, given the morphologic shape of cannabis flowers. For MDMB-4en-PINACA, however, eight hashish samples showing strikingly similar contents of MDMB-4en-PINACA with mean value of $6.5 \pm 0.3 \mu\text{g}/\text{mg}$ were detected between December 2020 and June 2021 (formatted bold in Table 1). These products, obtained over an interval of half a year, showed varying CBD and THC contents, thus implying different

production batches. It can be hypothesized that the producer(s) applied a standardized process, which resulted in reproducible SC contents—however, this will need to be proven by further studies.

3.4 | Carrier material

A total of 94 cannabis samples, comprised of 55% cannabis flowers ($n = 52$) and 45% hashish ($n = 42$), were collected during the time course of this study. Of all adulterated samples ($n = 47$), 53% ($n = 25$) were cannabis flowers, and 47% ($n = 22$) were hashish. For the adulterated hashish samples, the presence of trichomes, demonstrating that the samples originated from cannabis plant material, was verified applying microscopy (data not shown). Figure 3 shows the distribution over time of the adulterated carrier material. In the first three quarters of 2020, cannabis flowers were predominantly handed in for analysis. All adulterated cannabis flowers, where sufficient sample material enabled natural cannabinoid quantification, presented low THC and high CBD contents (in relation to each other), with mean THC and CBD concentrations of 0.6% (range <0.3–1%) and 14% (range 2.7–19.3%), respectively. In consideration of the Swiss harmonized measurement uncertainty, published by the SGRM,⁵⁹ the obtained THC-values of the analysed cannabis flowers were below the Swiss legal THC threshold of 1%.⁴⁰ The presented results are in accordance with recently published data on the phytocannabinoid contents of cannabis flowers adulterated with the SC MDMB-4en-PINACA.²² The use of low-THC cannabis flowers might be explained as that, in the view of producers, it is attractive to obtain and store a legal product (low-THC cannabis flowers), which is then altered into a psychoactive and illegal product only prior to releasing the product on to the market. The adulterated low-THC cannabis flowers are not distinguishable from the non-altered cannabis by the routinely used colour reagent test used by the Swiss police. Therefore, those products are less likely to be detected by police forces as the test result will indicate a supposedly legal product.³⁸

Additionally, economic motives might have promoted the production of adulterated cannabis products, as the market price of low-THC cannabis flowers is typically lower than that of (illegal) high-THC

TABLE 1 Quantitative results for CBD and THC (percentage w/w) and semi-quantitative results for SCs

Cannabis flower sample	Period	THC (%)	CBD (%)	5F-MDMB-PICA (µg/mg)	MDMB-4en-PINACA (µg/mg)	ADB-BUTINACA (µg/mg)	4F-MDMB-BINACA (µg/mg)	4F-MDMB-BICA (qualitative)	5F-MDMB-PINACA (qualitative)	5F-MPHP-2201 (qualitative)
1	Q1 2020	-	-	>LOD ^a	>LOD ^a	n.d.	>LOD ^a	n.d.	n.d.	n.d.
2	Q1 2020	0.6	18.1	0.6	0.3	n.d.	2.5	n.d.	n.d.	n.d.
3	Q2 2020	0.3	8.5	2.0	n.d.	n.d.	n.d.	n.d.	n.d.	n.d.
4	Q2 2020	0.5	14.4	n.d.	n.d.	n.d.	n.d.	n.d.	>LOD ^b	n.d.
5	Q3 2020	0.5	12.5	1.4	4.5	n.d.	n.d.	n.d.	n.d.	n.d.
6	Q3 2020	0.7	17.1	n.d.	2.3	n.d.	n.d.	n.d.	n.d.	n.d.
7	Q3 2020	0.7	19.3	n.d.	3.2	n.d.	n.d.	>LOD ^b	n.d.	>LOD ^b
8	Q3 2020	0.6	10.6	n.d.	1.8	n.d.	n.d.	n.d.	n.d.	n.d.
9	Q3 2020	-	-	n.d.	>LOD ^a	n.d.	n.d.	n.d.	n.d.	n.d.
10	Q3 2020	0.6	18.4	>LOD ^a	>LOD ^a	n.d.	>LOD ^a	n.d.	n.d.	n.d.
11	Q3 2020	0.6	12.1	n.d.	4.6	n.d.	n.d.	n.d.	n.d.	n.d.
12	Q3 2020	0.7	13.1	2.4	n.d.	n.d.	n.d.	>LOD ^b	n.d.	n.d.
13	Q3 2020	0.6	13.4	n.d.	3.0	n.d.	n.d.	>LOD ^b	n.d.	>LOD ^b
14	Q4 2020	0.7	14.1	1.1	1.1	n.d.	<LOQ	n.d.	n.d.	n.d.
15	Q4 2020	0.9	16.4	n.d.	2.2	n.d.	n.d.	n.d.	n.d.	n.d.
16	Q4 2020	-	-	n.d.	>LOD ^a	n.d.	n.d.	n.d.	n.d.	n.d.
17	Q1 2021	-	-	n.d.	>LOD ^a	n.d.	n.d.	n.d.	n.d.	n.d.
18	Q1 2021	0.8	18.0	n.d.	n.d.	1.6	n.d.	n.d.	n.d.	n.d.
19	Q1 2021	0.6	12.8	n.d.	>LOD ^a	n.d.	n.d.	n.d.	n.d.	n.d.
20	Q1 2021	0.6	10.8	n.d.	>LOD ^a	n.d.	n.d.	n.d.	n.d.	n.d.
21	Q1 2021	0.5	11.6	n.d.	0.1	9.9	n.d.	n.d.	n.d.	n.d.
22	Q1 2021	0.8	16.9	n.d.	<LOQ	9.1	n.d.	n.d.	n.d.	n.d.
23	Q1 2021	0.7	14.0	n.d.	n.d.	1.0	n.d.	n.d.	n.d.	n.d.
24	Q2 2021	<0.3	2.7	n.d.	3.4	n.d.	n.d.	n.d.	n.d.	n.d.
25	Q2 2021	1.0	18.5	n.d.	n.d.	3.6	n.d.	n.d.	n.d.	n.d.

(B)							
Hashish sample	Period	THC (%)	CBD (%)	5F-MDMB-PICA (µg/mg)	MDMB-4en-PINACA (µg/mg)	ADB-BUTINACA (µg/mg)	
1	Q2 2020	0.5	23.1	4.2	n.d.	n.d.	
2	Q3 2020	0.4	14.1	n.d.	7.2	n.d.	
3	Q4 2020	-	-	n.d.	>LOD ^a	n.d.	
4	Q4 2020	0.5	13.6	n.d.	3.4	n.d.	
5	Q4 2020	0.6	15.0	n.d.	1.7	n.d.	
6	Q4 2020	0.5	18.3	n.d.	6.5	n.d.	
7	Q4 2020	0.4	14.6	n.d.	6.7	n.d.	
8	Q1 2021	0.5	14.2	n.d.	6.7	n.d.	
9	Q1 2021	0.7	14.7	n.d.	6.1	n.d.	
10	Q1 2021	0.8	23.4	n.d.	6.7	n.d.	
11	Q1 2021	8.7	25.0	n.d.	>LOD ^a	n.d.	
12	Q1 2021	1.6	39.3	n.d.	6.2	n.d.	
13	Q1 2021	1.6	38.9	n.d.	6.1	n.d.	
14	Q1 2021	0.5	13.5	n.d.	3.7	n.d.	
15	Q1 2021	27.0	11.4	n.d.	3.0	n.d.	
16	Q1 2021	0.8	20.4	n.d.	n.d.	6.5	
17	Q1 2021	1.4	35.0	n.d.	5.8	n.d.	
18	Q1 2021	1.4	37.4	n.d.	5.8	n.d.	
19	Q2 2021	0.9	20.1	n.d.	n.d.	7.7	
20	Q2 2021	0.9	14.9	n.d.	7.0	n.d.	
21	Q2 2021	0.7	14.2	n.d.	5.0	n.d.	
22	Q2 2021	1.5	33.7	n.d.	6.8	n.d.	

Note: (A) Adulterated cannabis flowers and (B) adulterated hashish samples. “-” indicates samples, where insufficient material was available for phytocannabinoid quantification but tested positive with HRMS. “n.d.” stands for “not detected”. In bold: samples with similar MDMB-4en-PINACA content. 4F-MDMB-BICA, 4F-MDMB-BINACA, 4F-MDMB-PINACA, and 5F-MPH-2201 were not detected in any hashish samples (Table B).

^aDetected during initial screening, due to insufficient sample amounts not quantified.

^bSeldomly detected, therefore not quantified.

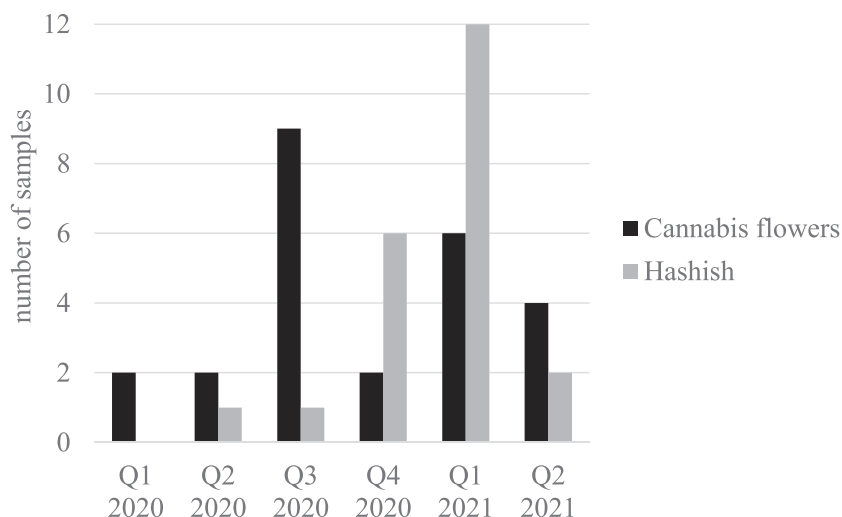


FIGURE 3 Distribution of adulterated cannabis flower samples and adulterated hashish samples

cannabis flowers.⁴⁹ Because of the high potency of many SCs, only small quantities of pure SCs are required to fabricate the final products, which then can be sold at standard market prices of drug-type cannabis.

The discussed advantages for producers and sellers of adulterated cannabis products are reduced, when hashish, instead of low-THC cannabis flowers, is used, particularly with regard to distribution of the final product. Hashish is illegal in Switzerland, regardless of its THC content.⁴⁰ Nevertheless, as with the exception of two samples, which contained higher levels of THC (8.7% and 27% THC), the THC content of adulterated hashish samples was very low. The median THC content was 0.8% THC (range: 0.4–27.0%), with 66.7% of samples containing <1% THC. This indicates that the utilized raw material was very likely industrial-type cannabis. In the study by Oomen et al.,²² six hashish samples, for which phytocannabinoid contents were available, showed low THC levels of <1%,²² therefore agreeing with our findings. While in the present study the number of adulterated hashish samples (47%) was nearly equal to the number of adulterated cannabis flowers (53%), this largely differed from the observations by Oomen et al.²² Of all adulterated samples, only 8.5% ($n = 23$) were hashish samples, the rest being comprised of cannabis flowers (73%, $n = 197$) or e-liquids (19%, $n = 50$). This could either indicate that adulterated hashish is less prominent in other regions or that adulterated hashish samples are less often handed for analysis and, therefore, underreported. Concerning the present study, the observed emerging use of hashish as carrier material might have been a reaction to the public and law enforcement being increasingly sensitized to the presence of adulterated cannabis flowers.

3.5 | Evaluation of self-reports

Self-reports were available whenever an individual had already consumed the respective product before handing a sample in. This was the case for 75% ($n = 36$) of samples containing SCs and for 66% ($n = 31$) of unadulterated samples. The reports belonging to two

TABLE 2 List of the five most frequently reported experiences for the SC- and THC-group

SC-Group	n (%)
Exceptional strong effect	16 (44)
Short duration	15 (42)
Palpitations	9 (25)
Anxiety	8 (22)
Psychologic discomfort or stress	8 (22)
THC-Group	n (%)
Exceptional strong effect	9 (29)
Normal	5 (16)
Headache	5 (16)
Palpitations	4 (13)
Dizziness	4 (13)
Nausea	4 (13)
Weak	4 (13)
Short duration	4 (13)
Strange taste	4 (13)

adulterated hashish samples, with elevated THC-levels (8.7% and 27%), were excluded, as they could not be exclusively assigned to one group. A list of the top five most frequent statements for the SC- and THC-group is shown in Table 2. For both groups the most often described experience was “exceptional strong effect.” This was described by 44% ($n = 16$) of the SC- and 29% ($n = 9$) of the THC-group, resulting in no statistical difference between groups ($p = 0.21$). However, “short effect duration” was described by 42% ($n = 15$) of the SC-group and was the second most reported observation for this group. This attribute was less often described for the THC-group ($p = 0.013$), as it was reported by 13% ($n = 4$) of the THC-group. Shorter effect durations of SCs, when compared with natural cannabis, have been previously reported in a study investigating reports of recreational drug users.⁶⁰

TABLE 3 Statistical evaluation of adverse events and adverse effect (ae) subcategories

	SC n (%) (n = 36)	THC n (%) (n = 31)	p value	OR	CI (95%)
Adverse event	27 (75)	15 (48)	0.041	3.1	1.0–10.3
Cardiovascular ae	14 (39)	4 (13)	0.020	3.7	1.2–12.4
Psychologic ae	19 (53)	4 (13)	0.0007	7.3	1.9–34.7
Neurologic ae	15 (42)	9 (29)	0.31	1.7	0.6–5.6

Note: Listed are the number of individuals reporting an adverse event or adverse effect, p values, odds ratios (ORs), and 95% confidence intervals (CIs).

The statistical evaluation of adverse events and adverse effect subcategories is presented in Table 3. A higher likelihood ($p = 0.041$) for the occurrence of adverse events was shown for the SC-group when compared with the THC-group, as 75% ($n = 27$) of the reports from SC-group and 48% ($n = 15$) of the reports from the THC-group were classified to describe an adverse event. Neurologic effects, however, were shown to be independent of the consumed product ($p = 0.31$). The most prominent neurologic adverse effects in this study were headache for the THC-group (16%, $n = 5$) and dizziness for the SC-group (14%, $n = 5$).

Psychologic adverse effects were found to be more profound in the SC-group than the in THC-group ($p = 0.0007$). Severe psychologic adverse effects resulted in the admittance of two independent individuals of the SC-group to the emergency department. Both users reported strong psychologic adverse effects, including panic attacks and fear of death. A study comparing the clinical conditions of SCs and cannabis users found SCs to be associated with significantly more psychotic symptoms.⁶¹ Paranoia, hallucinations, and psychosis are symptoms frequently associated with SC intoxication.^{62–64}

In this study, SCs were additionally associated with a higher risk for cardiovascular adverse effects ($p = 0.020$). This is in accordance with existing literature on SCs as, ever since their emergence on the drug market, many SCs have been widely associated with cardiovascular adverse effects, including severe outcomes.^{5,29,63,65–68} The mechanisms behind the cardiac effects of SCs are still not completely understood.⁶³ The often-observed higher activities of many SCs at CB1, when compared with THC, have been described as a contributing factor.⁶⁷ However, other pathways may exist, as further toxicologically relevant receptors have not been thoroughly investigated.⁶³ Toxicologically relevant pathways might be substance-dependent and not transferable to the whole class of SCs. Furthermore, CBD has been discussed to alter THC-effects.⁶⁹ As the adulterated samples detected in this study contained CBD ranging from 2.7% up to 39.3%, a potential modulation of SC-effects cannot be excluded.

The herein presented adverse effects are largely in agreement with the reported adverse effects after consumption of adulterated cannabis products with MDMB-4en-PINACA reported by Oomen et al.²² The publication included a descriptive summary of reported adverse effects. Adverse effects stated by drug checking users comprised nausea, vomiting, paranoia, anxiety, hallucinations, tremors, paralysis, aggressiveness, insomnia, loss of consciousness, and

palpitations. Information on the observed frequency of the stated adverse effects were not given. The authors reported on three individuals requiring emergency hospital treatment, due to adverse effects including excessive emesis, perspiration, panic attacks, tachycardia, amnesia, and seizures.

3.6 | Limitations

Concerning chemical analyses, potential degradation of natural cannabinoids and SCs cannot be ruled out, as some samples were stored for up to one and a half years before being subjected to semi-quantification. Three expected degradation products of detected SCs were screened (i.e., MDMB-4en-butanoic acid, 4F-MDMB-BICA-butanoic acid, and 5F-MDMB-PICA-butanoic acid). Results showed no detectable signals, thus implying little to no degradation of the corresponding SCs. A full validation for a quantitative method according to guidelines applied in forensic chemistry (e.g., SGRM) was omitted as a comparison of the content was still possible. Due to the limited sample material, samples were subjected to single measurements after being homogenized.

A limitation regarding the self-reported adverse effects was that medical confirmation (e.g., cardiovascular parameters and psychological screenings) of these symptoms were lacking. Also, dosages and co-ingestion of other relevant drugs were not accessible. Additionally, due to the study design involving volunteers using drug checking services, the study group was not randomized (e.g., age and gender). As people submitting cannabis samples at drug checking services often suspect sample adulteration when they experience unwanted or unexpected effects, this might have resulted in a preselection bias of the study group. Finally, the observed prevalence of adulterated products may not be representative for the whole drug market.

4 | CONCLUSION

Higher likelihoods for adverse events in general, in particular for psychologic and cardiologic adverse effects, were observed after the uptake of cannabis products adulterated with SCs, when compared with untreated cannabis products. This underlines the increased public health concerns associated with this new phenomenon. For

adulterated hashish samples, a relatively homogenous picture for MDMB-4en-PINACA was observed, while the results for cannabis flowers differed considerably.

Drug checking services enabled a unique insight into the drug market, as well as the timely detection of new developments surrounding NPS, as demonstrated in this study by the example of SCs. Thus, drug checking services, besides being an important harm-reduction tool in the sense of public health and prevention, offer the possibility to act as a market monitoring tool and further may give information on NPS, on which toxicological data are typically scarce. The data gained through drug checking services, whilst not validated or standardised, bear the potential to expand present knowledge gained through more established routes, as in, for example, case reports and case series after intoxication, helping to fill the gap between product and effects.

ACKNOWLEDGEMENTS

We would like to thank all cooperating drug checking parties (DIBS [Drogeninformation Basel], DILU [Drogeninformation Luzern], and Suchthilfe Ost), with special thanks to all persons involved during counselling, sample collection, and reporting of results. The authors also want to thank Christian Bissig of the Zurich Forensic Science Institute and Andrea Jacobsen-Bauer, State Office of Criminal Investigation (LKA) Baden-Württemberg, for supplying reference material and Christian Bissig for his always well-appreciated scientific input. Special thanks goes to the staff of the Forensic Chemistry and Toxicology Department of the Institute of Forensic Medicine, University of Basel, for the valuable support in sample documentation and chemical analysis. Finally, we would like to thank Florian Franz for his input during data evaluation and manuscript preparation and June Mercer-Chalmers-Bender for language editing.

DATA AVAILABILITY STATEMENT

The data that supports the findings of this study are available in the supplementary material of this article or available from the corresponding author upon reasonable request.

ORCID

Manuela Carla Monti  <https://orcid.org/0000-0002-9959-398X>

Katja Mercer-Chalmers-Bender  <https://orcid.org/0000-0002-3843-9065>

REFERENCES

- European Monitoring Centre for Drugs and Drug Addiction. European Drug Report 2021: Trends and developments. https://www.emcdda.europa.eu/publications/edr/trends-developments/2021_en. Accessed September 13, 2021.
- Gatch MB, Forster M. Cannabinoid-like effects of five novel carboxamide synthetic cannabinoids. *Neurotoxicology*. 2019;70:72-79. doi:10.1016/j.neuro.2018.11.004
- Castaneto MS, Gorelick DA, Desrosiers NA, Hartman RL, Pirard S, Huestis MA. Synthetic cannabinoids: epidemiology, pharmacodynamics, and clinical implications. *Drug Alcohol Depend*. 2014;144:12-41. doi:10.1016/j.drugalcdep.2014.08.005
- Pike E, Grafinger KE, Cannaeert A, et al. Systematic evaluation of a panel of 30 synthetic cannabinoid receptor agonists structurally related to MMB-4en-PICA, MDMB-4en-PINACA, ADB-4en-PINACA, and MMB-4CN-BUTINACA using a combination of binding and different CB(1) receptor activation assays: Part I-Synthesis, analytical characterization, and binding affinity for human CB(1) receptors. *Drug Test Anal*. 2021;13(7):1383-1401. doi:10.1002/dta.3037
- Zaurova M, Hoffman RS, Vlahov D, Manini AF. Clinical effects of synthetic cannabinoid receptor agonists compared with marijuana in emergency department patients with acute drug overdose. *J Med Toxicol*. 2016;12(4):335-340. doi:10.1007/s13181-016-0558-4
- Giorgetti A, Busardò FP, Tittarelli R, Auwärter V, Giorgetti R. Post-mortem toxicology: a systematic review of death cases involving synthetic cannabinoid receptor agonists. *Front Psych*. 2020;11:464-464. doi:10.3389/fpsy.2020.00464
- Maida NL, Papaseit E, Martínez L, et al. Acute pharmacological effects and oral fluid biomarkers of the synthetic cannabinoid UR-144 and THC in recreational users. *Biology (Basel)*. 2021;10(4):257 doi:10.3390/biology10040257
- Wood DM, Hill SL, Thomas SH, Dargan PI. Using poisons information service data to assess the acute harms associated with novel psychoactive substances. *Drug Test Anal*. 2014;6(7-8):850-860. doi:10.1002/dta.1671
- Beharry S, Gibbons S. An overview of emerging and new psychoactive substances in the United Kingdom. *Forensic Sci Int*. 2016;267:25-34. doi:10.1016/j.forsciint.2016.08.013
- Angerer V, Jacobi S, Franz F, Auwärter V, Pietsch J. Three fatalities associated with the synthetic cannabinoids 5F-ADB, 5F-PB-22, and AB-CHMINACA. *Forensic Sci Int*. 2017;281:e9-e15. doi:10.1016/j.forsciint.2017.10.042
- Adamowicz P, Gieron J, Gil D, Lechowicz W, Skulska A, Tokarczyk B. The effects of synthetic cannabinoid UR-144 on the human body—a review of 39 cases. *Forensic Sci Int*. 2017;273:e18-e21. doi:10.1016/j.forsciint.2017.02.031
- Krotulski AJ, Cannaeert A, Stove C, Logan BK. The next generation of synthetic cannabinoids: Detection, activity, and potential toxicity of pent-4en and but-3en analogues including MDMB-4en-PINACA. *Drug Test Anal*. 2021;13(2):427-438. doi:10.1002/dta.2935
- Andersson M, Kjellgren A. The slippery slope of flubromazolam: experiences of a novel psychoactive benzodiazepine as discussed on a Swedish online forum. *Nordisk Alkohol Nark*. 2017;34(3):217-229. doi:10.1177/1455072517706304
- Antonides LH, Cannaeert A, Norman C, et al. Shape matters: the application of activity-based in vitro bioassays and chiral profiling to the pharmacological evaluation of synthetic cannabinoid receptor agonists in drug-infused papers seized in prisons. *Drug Test Anal*. 2021;13(3):628-643. doi:10.1002/dta.2965
- Angerer V, Franz F, Moosmann B, Bisel P, Auwärter V. 5F-Cumyl-PINACA in 'e-liquids' for electronic cigarettes: comprehensive characterization of a new type of synthetic cannabinoid in a trendy product including investigations on the in vitro and in vivo phase I metabolism of 5F-Cumyl-PINACA and its non-fluorinated analog Cumyl-PINACA. *Forensic Toxicol*. 2019;37(1):186-196. doi:10.1007/s11419-018-0451-8
- Ernst L, Langer N, Bockelmann A, Salkhordeh E, Beuerle T. Identification and quantification of synthetic cannabinoids in 'spice-like' herbal mixtures: update of the German situation in summer 2018. *Forensic Sci Int*. 2019;294:96-102. doi:10.1016/j.forsciint.2018.11.001
- Langer N, Lindigkeit R, Schiebel H-M, Papke U, Ernst L, Beuerle T. Identification and quantification of synthetic cannabinoids in "spice-like" herbal mixtures: update of the German situation for the spring of 2016. *Forensic Sci Int*. 2016;269:31-41. doi:10.1016/j.forsciint.2016.10.023
- Schoeder CT, Hess C, Madea B, Meiler J, Müller CE. Pharmacological evaluation of new constituents of "Spice": synthetic cannabinoids

- based on indole, indazole, benzimidazole and carbazole scaffolds. *Forensic Toxicol.* 2018;36(2):385-403. doi:10.1007/s11419-018-0415-z
19. Münster-Müller S, Matzenbach I, Knepper T, Zimmermann R, Pütz M. Profiling of synthesis-related impurities of the synthetic cannabinoid Cumyl-5F-PINACA in seized samples of e-liquids via multivariate analysis of UHPLC–MSn data. *Drug Testing and Analysis.* 2020;12(1):119-126. doi:10.1002/dta.2673
 20. Norman C, Halter S, Haschimi B, et al. A transnational perspective on the evolution of the synthetic cannabinoid receptor agonists market: comparing prison and general populations. *Drug Test Anal.* 2021;13(4):841-852. doi:10.1002/dta.3002
 21. Moosmann B, Angerer V, Auwärter V. Inhomogeneities in herbal mixtures: a serious risk for consumers. *Forensic Toxicol.* 2015;33(1):54-60. doi:10.1007/s11419-014-0247-4
 22. Oomen PE, Schori D, Tögel-Lins K, et al. Cannabis adulterated with the synthetic cannabinoid receptor agonist MDMB-4en-PINACA and the role of European drug checking services. *Int J Drug Policy.* 2022;100:103493 doi:10.1016/j.drugpo.2021.103493
 23. Hess C, Schoeder CT, Pillaiyar T, Madea B, Müller CE. Pharmacological evaluation of synthetic cannabinoids identified as constituents of spice. *Forensic Toxicol.* 2016;34(2):329-343. doi:10.1007/s11419-016-0320-2
 24. Noble C, Cannaeert A, Linnet K, Stove CP. Application of an activity-based receptor bioassay to investigate the in vitro activity of selected indole- and indazole-3-carboxamide-based synthetic cannabinoids at CB1 and CB2 receptors. *Drug Testing and Analysis.* 2019;11(3):501-511. doi:10.1002/dta.2517
 25. Asada A, Doi T, Tagami T, et al. Cannabimimetic activities of cumyl carboxamide-type synthetic cannabinoids. *Forensic Toxicol.* 2018;36(1):170-177. doi:10.1007/s11419-017-0374-9
 26. Andre CM, Hausman J-F, Guerriero G. Cannabis sativa: The plant of the thousand and one molecules. *Front Plant Sci.* 2016;7:19-19. doi:10.3389/fpls.2016.00019
 27. Cannaeert A, Sparkes E, Pike E, et al. Synthesis and in vitro cannabinoid receptor 1 activity of recently detected synthetic cannabinoids 4F-MDMB-BICA, 5F-MPP-PICA, MMB-4en-PICA, CUMYL-CBMICA, ADB-BINACA, APP-BINACA, 4F-MDMB-BINACA, MDMB-4en-PINACA, A-CHMINACA, 5F-AB-P7AICA, 5F-MDMB-P7AICA, and 5F-AP7AICA. *ACS Chem Neurosci.* 2020;11(24):4434-4446. doi:10.1021/acschemneuro.0c00644
 28. Darke S, Banister S, Farrell M, Duffou J, Lappin J. 'Synthetic cannabis': a dangerous misnomer. *Int J Drug Policy.* 2021;98:103396 doi:10.1016/j.drugpo.2021.103396
 29. Ozturk HM, Yetkin E, Ozturk S. Synthetic cannabinoids and cardiac arrhythmia risk: review of the literature. *Cardiovasc Toxicol.* 2019;19(3):191-197. doi:10.1007/s12012-019-09522-z
 30. European Monitoring Centre for Drugs and Drug Addiction. EMCDDA initial report on the new psychoactive substance methyl 3,3-dimethyl-2-(1-(pent-4-en-1-yl)-1H-indazole-3-carboxamido)butanoate (MDMB-4en-PINACA). <https://www.emcdda.europa.eu/system/files/publications/13363/emcdda-initial-report-MDMB-4en-PINACA.pdf>. Accessed February 1, 2021.
 31. European Monitoring Centre for Drugs and Drug Addiction. Synthetic cannabinoids in Europe—a review. <https://www.emcdda.europa.eu/system/files/publications/14035/Synthetic-cannabinoids-in-Europe-EMCDDA-technical-report.pdf>. Accessed September 16, 2021.
 32. European Monitoring Centre for Drugs and Drug Addiction. Drug checking as a harm reduction tool for recreational drug users: opportunities and challenges. https://www.emcdda.europa.eu/system/files/attachments/6339/EuropeanResponsesGuide2017_BackgroundPaper-Drug-checking-harm-reduction_0.pdf. Accessed May 10, 2021.
 33. La Mantia A, Oechslin L, Duarte M, Laubereau B, Fabian C. Studie zu den Effekten der Drug-Checking-Angebote in der Schweiz - Bericht zuhanden des Bundesamts für Gesundheit (BAG). https://www.bag.admin.ch/dam/bag/de/dokumente/npp/forschungsberichte/forschungsberichte_drogen/studie_effekte_drug-checking.pdf. download.pdf/studie_effekte_drugchecking_2020.pdf. Accessed February 1, 2021.
 34. Green TC, Park JN, Gilbert M, et al. An assessment of the limits of detection, sensitivity and specificity of three devices for public health-based drug checking of fentanyl in street-acquired samples. *Int J Drug Policy.* 2020;77:102661. doi:10.1016/j.drugpo.2020.102661
 35. Wallace B, Hills R, Rothwell J, et al. Implementing an integrated multi-technology platform for drug checking: social, scientific, and technological considerations. *Drug Test Anal.* 2021;13(4):734-746. doi:10.1002/dta.3022
 36. Fregonese M, Albino A, Covino C, et al. Drug checking as strategy for harm reduction in recreational contests: evaluation of two different drug analysis methodologies. *Front Psych.* 2021;12:596895. doi:10.3389/fpsy.2021.596895
 37. Harper L, Powell J, Pijl EM. An overview of forensic drug testing methods and their suitability for harm reduction point-of-care services. *Harm Reduct J.* 2017;14(1):52. doi:10.1186/s12954-017-0179-5
 38. European Monitoring Centre for Drugs and Drug Addiction. Low-THC cannabis products in Europe. <https://www.emcdda.europa.eu/system/files/publications/13471/TD0320749ENN01.pdf>. Accessed February 1, 2021.
 39. McGregor IS, Cairns EA, Abelev S, et al. Access to cannabidiol without a prescription: a cross-country comparison and analysis. *Int J Drug Policy.* 2020;85:102935. doi:10.1016/j.drugpo.2020.102935
 40. Federal Department of Home Affairs. Verordnung des EDI über die Verzeichnisse der Betäubungsmittel, psychotropen Stoffe, Vorläuferstoffe und Hilfschemikalien (Betäubungsmittelverzeichnisverordnung, BetmVV-EDI, Stand: 15.12.2020). <https://www.fedlex.admin.ch/eli/cc/2011/363/de>. Accessed August 2, 2021.
 41. Manthey J. Cannabis use in Europe: current trends and public health concerns. *Int J Drug Policy.* 2019;68:93-96. doi:10.1016/j.drugpo.2019.03.006
 42. Hazekamp A. The trouble with CBD oil. *Med Cannabis Cannabinoids.* 2018;1(1):65-72. doi:10.1159/000489287
 43. Pichini S, Mannocchi G, Berretta P, et al. Δ^9 -tetrahydrocannabinol and cannabidiol time courses in the sera of "light cannabis" smokers: discriminating light cannabis use from illegal and medical cannabis use. *Ther Drug Monit.* 2020;42(1):151-156.
 44. Arnold JC. A primer on medicinal cannabis safety and potential adverse effects. *Aust J Gen Pract.* 2021;50(6):345-350. doi:10.31128/ajgp-02-21-5845
 45. Arkell TR, Vinckenbosch F, Kevin RC, Theunissen EL, McGregor IS, Ramaekers JG. Effect of cannabidiol and Δ^9 -tetrahydrocannabinol on driving performance: a randomized clinical trial. *JAMA.* 2020;324(21):2177-2186. doi:10.1001/jama.2020.21218
 46. Hädener M, Gelmi TJ, Martin-Fabritius M, Weinmann W, Pfäffli M. Cannabinoid concentrations in confiscated cannabis samples and in whole blood and urine after smoking CBD-rich cannabis as a "tobacco substitute". *Int J Leg Med.* 2019;133(3):821-832. doi:10.1007/s00414-018-01994-y
 47. Meier U, Dussy F, Scheurer E, Mercer-Chalmers-Bender K, Hangartner S. Cannabinoid concentrations in blood and urine after smoking cannabidiol joints. *Forensic Sci Int.* 2018;291:62-67. doi:10.1016/j.forsci.2018.08.009
 48. Die Stellen für Suchtprävention Kanton Zürich. Factsheet April 2020 - Synthetische Cannabinoide und ihre Risiken. https://www.suchtfachstelle.zuerich/images/PDFs/Factsheet_Cannabinoide_Suchtpraevention.pdf. Accessed September 13, 2021.
 49. Infodrog Schweizerische Koordinations- und Fachstelle Sucht. Synthetische Cannabinoide - Informationen für Suchtfachleute.

- https://www.infodrog.ch/files/content/schadensminderung_de/2020-12_fiche-cannabinoides-prof_de.pdf. Accessed August 2, 2021.
50. Abteilung Sucht Gesundheitsdepartement des Kantons Basel-Stadt. Factsheet Mai 2020 - Synthetische Cannabinoide und ihre Risiken. https://www.sucht.bs.ch/dam/jcr:eae1f8c4-7947-4171-bd53-080cfe5fdf62/Abt_Sucht_Syn_Cannabinoide.pdf
51. Schweizerische Gesellschaft für Rechtsmedizin SGRM. <https://www.sgrm.ch/de/allgemein/uebersicht/>. Accessed December 1, 2020.
52. Norman C, Walker G, McKirdy B, et al. Detection and quantitation of synthetic cannabinoid receptor agonists in infused papers from prisons in a constantly evolving illicit market. *Drug Test Anal.* 2020;12(4):538-554. doi:10.1002/dta.2767
53. Krotulski AJ, Mohr ALA, Kacinko SL, et al. 4F-MDMB-BINACA: a new synthetic cannabinoid widely implicated in forensic casework. *Journal of Forensic Sciences.* 2019;64(5):1451-1461. doi:10.1111/1556-4029.14101
54. Kavanagh P, Pechnikov A, Nikolaev I, Dowling G, Kolosova M, Grigoryev A. Detection of ADB-BUTINACA metabolites in human urine, blood, kidney and liver. *J Anal Toxicol.* 2021. doi:10.1093/jat/bkab088
55. Sia CH, Wang Z, Goh EML, et al. Urinary metabolite biomarkers for the detection of synthetic cannabinoid ADB-BUTINACA abuse. *Clin Chem.* 2021;67(11):1534-1544. doi:10.1093/clinchem/hvab134
56. Halter S, Mogler L, Auwärter V. Quantification of herbal mixtures containing cumyl-PEGACLONE—is inhomogeneity still an issue? *J Anal Toxicol.* 2019;44(1):81-85. doi:10.1093/jat/bkz028
57. Janssens L, Cannaert A, Connolly MJ, Liu H, Stove CP. In vitro activity profiling of cumyl-PEGACLONE variants at the CB(1) receptor: fluorination versus isomer exploration. *Drug Test Anal.* 2020;12(9):1336-1343. doi:10.1002/dta.2870
58. Schaefer N, Wojtyniak J-G, Kettner M, et al. Pharmacokinetics of (synthetic) cannabinoids in pigs and their relevance for clinical and forensic toxicology. *Toxicol Lett.* 2016;253:7-16. doi:10.1016/j.toxlet.2016.04.021
59. Schweizerische Gesellschaft für Rechtsmedizin SGRM. Empfehlung zur Angabe der Messergebnisse für Gehaltsbestimmungen von Stoffproben. https://www.sgrm.ch/inhalte/Forensische-Chemie-und-Toxikologie/Angabe_Messresultate.pdf. Accessed September 1, 2021.
60. Winstock AR, Barratt MJ. Synthetic cannabis: a comparison of patterns of use and effect profile with natural cannabis in a large global sample. *Drug Alcohol Depend.* 2013;131(1):106-111. doi:10.1016/j.drugalcdep.2012.12.011
61. Bassir Nia A, Medrano B, Perkel C, Galynker I, Hurd YL. Psychiatric comorbidity associated with synthetic cannabinoid use compared to cannabis. *J Psychopharmacol.* 2016;30(12):1321-1330. doi:10.1177/0269881116658990
62. Cooper ZD, Williams AR. Cannabis and cannabinoid intoxication and toxicity. In: *Cannabis Use Disorders*. Springer International Publishing; 2019:103-111.
63. Luethi D, Liechti ME. Designer drugs: mechanism of action and adverse effects. *Arch Toxicol.* 2020;94(4):1085-1133. doi:10.1007/s00204-020-02693-7
64. Cohen K, Weinstein AM. Synthetic and non-synthetic cannabinoid drugs and their adverse effects—a review from public health prospective. *Front Public Health.* 2018;6(162): doi:10.3389/fpubh.2018.00162
65. Seely KA, Lapoint J, Moran JH, Fattore L. Spice drugs are more than harmless herbal blends: a review of the pharmacology and toxicology of synthetic cannabinoids. *Prog Neuropsychopharmacol Biol Psychiatry.* 2012;39(2):234-243. doi:10.1016/j.pnpbp.2012.04.017
66. Pacher P, Steffens S, Haskó G, Schindler TH, Kunos G. Cardiovascular effects of marijuana and synthetic cannabinoids: the good, the bad, and the ugly. *Nat Rev Cardiol.* 2018;15(3):151-166. doi:10.1038/nrcardio.2017.130
67. Radaelli D, Manfredi A, Zanon M, et al. Synthetic cannabinoids and cathinones cardiotoxicity: evidences actualities and perspectives. *Curr Neuroparmacol.* 2021;19(11):2038-2048. doi:10.2174/1570159x19666210412101929
68. Lobato-Freitas C, Brito-da-Costa AM, Dinis-Oliveira RJ, et al. Overview of synthetic cannabinoids ADB-FUBINACA and AMB-FUBINACA: clinical, analytical, and forensic implications. *Pharmaceutics.* 2021;14(3):186 doi:10.3390/ph14030186
69. Freeman AM, Petrilli K, Lees R, et al. How does cannabidiol (CBD) influence the acute effects of delta-9-tetrahydrocannabinol (THC) in humans? A systematic review. *Neurosci Biobehav Rev.* 2019;107:696-712. doi:10.1016/j.neubiorev.2019.09.036

SUPPORTING INFORMATION

Additional supporting information may be found in the online version of the article at the publisher's website.

How to cite this article: Monti MC, Zeugin J, Koch K, Milenkovic N, Scheurer E, Mercer-Chalmers-Bender K. Adulteration of low-delta-9-tetrahydrocannabinol products with synthetic cannabinoids: Results from drug checking services. *Drug Test Anal.* 2022;1-14. doi:10.1002/dta.3220

Supplementary material of the manuscript:

Adulteration of low-delta-9-tetrahydrocannabinol products with synthetic cannabinoids: Results from drug checking services

Manuela Carla Monti¹, Jill Zeugin², Konrad Koch¹, Natasa Milenkovic³, Eva Scheurer¹, Katja Mercer-Chalmers-Bender^{*1}

*Corresponding author

¹ Institute of Forensic Medicine, Department of Biomedical Engineering, University of Basel, Basel, Switzerland

² Addiction Support – Region Basel (Suchthilfe Region Basel), Basel, Switzerland

³ Addiction Services (Abteilung Sucht), Health Department Kanton Basel-Stadt, Basel, Switzerland

Table S1. Synthetic cannabinoids (SCs) contained in the qualitative screening.

Compound	CAS	Formal name	Vendor
"Synthetic cannabinoid Mixture 1" (commercially available mixture)	1445577-42-3	(1-(5-chloropentyl)-1H-indol-3-yl)(2,2,3,3-tetramethylcyclopropyl)methanone	Cayman chemical
UR-144 N-(5-chloropentyl) analog	335161-24-5	[1-(5-fluoropentyl)-1H-indol-3-yl]-1-naphthalenyl-methanone	Cayman chemical
AMM201	209414-07-3	1-naphthalenyl(1-pentyl-1H-indol-3-yl)-methanone	Cayman chemical
JWH 018	1400742-39-3	1-pentyl-N-8-quinolinyl-1H-indole-3-carboxamide	Cayman chemical
JWH 018 8-quinolinyl carboxamide	208987-48-8	(1-butyl-1H-indol-3-yl)-1-naphthalenyl-methanone	Cayman chemical
JWH-122	619294-47-2	(4-methyl-1-naphthalenyl)(1-pentyl-1H-indol-3-yl)-methanone	Cayman chemical
JWH 210	824959-81-1	(4-ethyl-1-naphthalenyl)(1-pentyl-1H-indol-3-yl)-methanone	Cayman chemical
JWH 250	864445-43-2	1-(1-pentyl-1H-indol-3-yl)-2-(2-methoxyphenyl)-ethanone	Cayman chemical
MAMM201	1354631-24-5	[1-(5-fluoropentyl)-1H-indol-3-yl]([4-methyl-1-naphthalenyl)-methanone	Cayman chemical
UR-144	1199943-44-6	(1-pentyl-1H-indol-3-yl)(2,2,3,3-tetramethylcyclopropyl)-methanone	Cayman chemical
UR-144 degradant	1609273-88-2	3,3,4-trimethyl-1-(1-pentyl-1H-indol-3-yl)pent-4-en-1-one	Cayman chemical
XLR11	1364933-54-9	(1-(5-fluoropentyl)-1H-indol-3-yl)(2,2,3,3-tetramethylcyclopropyl)methanone	Cayman chemical
XLR11 degradant	1616469-09-0	1-[1-(5-fluoropentyl)-1H-indol-3-yl]-3,3,4-trimethyl-4-penten-1-one	Cayman chemical
"Synthetic cannabinoid Mixture 3" (commercially available mixture)	1445580-60-8	1-(5-fluoropentyl)-N-(naphthalen-1-yl)-1H-indole-3-carboxamide	Cayman chemical
SF-NNEI	1400742-41-7	1-(5-fluoropentyl)-8-quinolinyl ester-1H-indole-3-carboxylic acid	Cayman chemical
5-Fluoro-PB22*	n.a.	quinolin-3-yl-1-(5-fluoropentyl)-1H-indole-3-carboxylate	Cayman chemical
5-Fluoro-PB22-3-hydroxyquinoline isomer*	2185863-15-2	(1-(4-fluorobenzyl)-1H-indol-3-yl)(2,2,3,3-tetramethylcyclopropyl)methanone	Cayman chemical
FUB-144	1971007-92-7	N-[[1-[(4-fluorophenyl)methyl]-1H-indazol-3-yl]carbonyl]-L-valine, methyl ester	Cayman chemical
MMB-FUBINACA = AMB-FUBINACA	1800098-36-5	1-[(4-fluorophenyl)methyl]-1H-indole-3-carboxylic acid, 8-quinolinyl ester	Cayman chemical
FUB-PB-22	837112-21-7	naphthalen-1-yl-1-(5-fluoropentyl)-1H-indole-3-carboxylate	Cayman chemical
NM-2201	1400742-17-7	1-pentyl-8-quinolinyl ester-1H-indole-3-carboxylic acid	Cayman chemical
PB-22	1801552-01-1	[1-(5-fluoropentyl)-1H-indazol-3-yl]-1-naphthalenyl-methanone	Cayman chemical
THI-2201 = AMM201 indazole analogue			

4-cyano CUMYL-BUTINACA	1631074-54-8	1-(4-cyanobutyl)-N-(1-methyl-1-phenylethyl)-1H-indazole-3-carboxamide	Cayman chemical
(R)-5F-MDMB-PINACA = (5F-ADB)	1838134-16-9	N-[[1-(5-fluoropentyl)-1H-indazol-3-yl]carbonyl]-3-methyl-D-valine, methyl ester	Cayman chemical
4-Fluoro MDMB-BICA (=4-Fluoro-MDMB-BUTICA)	n.a.	methyl (S)-2-(1-(4-fluorobutyl)-1H-indole-3-carboxamido)-3,3-dimethylbutanoate	Cayman chemical
4-Fluoro-MDMB-BINACA (=4-fluoro MDMB-BUTINACA)	2390036-46-9	N-[[1-(4-fluorobutyl)-1H-indazol-3-yl]carbonyl]-3-methyl-L-valine, methyl ester	Cayman chemical
5-Chloro AKB48	2160555-52-0	1-(5-chloropentyl)-N-tricyclo[3.3.1.1 ^{3,3} .7]dec-1-yl-1H-indazole-3-carboxamide	Cayman chemical
5-Chloro TH-018	n.a.	1-(5-chloropentyl)-1H-indazol-3-yl]naphthalen-1-yl]methanone	Cayman chemical
5-Fluoro-CUMYL-PegACLONE	2377403-49-9	5-(5-fluoropentyl)-2,5-dihydro-2-(1-methyl-1-phenylethyl)-1H-pyridol[4,3-b]indol-1-one	Zurich Forensic Science Institute
5-Fluoro-EMB-PINACA	n.a.	(S)-ethyl 2-(1-(5-fluoropentyl)-1H-indazole-3-carboxamido)-3-methylbutanoate	Zurich Forensic Science Institute
5-Fluoro ADBICA	1863065-82-0	N-[1-(aminocarbonyl)-2,2-dimethylpropyl]-1-(5-fluoropentyl)-1H-indole-3-carboxamide	Cayman chemical
5-Fluoro AKB48	1400742-13-3	N-[(3S,5S,7S)-adamantan-1-yl]-1-(5-fluoropentyl)-1H-indazole-3-carboxamide	Zurich Forensic Science Institute
5-Fluoro APINAC = 5F-AKB57	n.a.	(3S,5S,7S)-adamantan-1-yl]-1-(5-fluoropentyl)-1H-indazole-3-carboxylate	Cayman chemical
5-Fluoro CUMYL-P7AICA	2171492-36-5	1-(5-fluoropentyl)-N-(2-phenylpropan-2-yl)-1H-pyridol[2,3-b]pyridine-3-carboxamide	Cayman chemical
5-Fluoro CUMYL-PINACA	1400742-16-6	1-(5-fluoropentyl)-N-(1-methyl-1-phenylethyl)-1H-indazole-3-carboxamide	Cayman chemical
5-Fluoro MDMB-P7AICA	n.a.	methyl (S)-2-(1-(5-fluoropentyl)-1H-pyridol[2,3-b]pyridine-3-carboxamido)-3,3-dimethylbutanoate	Cayman chemical
5-Fluoro-MDMB-PICA	1971007-88-1	methyl (2S)-2-[[1-(5-fluoropentyl)indole-3-carboxyl]amino]-3,3-dimethylbutanoate	state criminal investigation office
AB-CHMINACA	1185887-21-1	N-[[1S)-1-(aminocarbonyl)-2-methylpropyl]-1-(cyclohexylmethyl)-1H-indazole-3-carboxamide	Baden-Württemberg
AB-FUBINACA	1185282-01-2	N-[[1S)-1-(aminocarbonyl)-2-methylpropyl]-1-[[4-fluorophenyl]methyl]-1H-indazole-3-carboxamide	Cayman chemical
ACHMINACA	1400742-33-7	1-(cyclohexylmethyl)-N-tricyclo[3.3.1.1 ^{3,3} .7]dec-1-yl-1H-indazole-3-carboxamide	Cayman chemical
ADAMANTYL-THPINACA	1400742-48-4	N-(2-adamantyl)-1-(oxan-4-ylmethyl)indazole-3-carboxamide	Cayman chemical
ADB-BUTINACA	n.a.	(S)-N-(1-amino-3,3-dimethyl-1-oxobutan-2-yl)-1-butyl-1H-indazole-3-carboxamide	Zurich Forensic Science Institute
ADBICA (=ADB-PICA)	1445583-48-1	N-(1-amino-3,3-dimethyl-1-oxobutan-2-yl)-1-pentyl-1H-indole-3-carboxamide	Zurich Forensic Science Institute
ADB-PINACA	1633766-73-0	N-[1-(aminocarbonyl)-2,2-dimethylpropyl]-1-pentyl-1H-indazole-3-carboxamide	Cayman chemical
AKB48 = APINACA	1345973-53-6	1-pentyl-N-tricyclo[3.3.1.1 ^{3,3} .7]dec-1-yl-1H-indazole-3-carboxamide	Zurich Forensic Science Institute
AKB57 (APINAC)	n.a.	(3S,5S,7S)-adamantan-1-yl]-1-pentyl-1H-indazole-3-carboxylate	Cayman chemical
CUMYL-CBMICA	n.a.	1-(cyclobutylmethyl)-N-(2-phenylpropan-2-yl)-1H-indole-3-carboxamide	Zurich Forensic Science Institute
CUMYL-PegACLONE	2160555-55-3	2,5-dihydro-2-(1-methyl-1-phenylethyl)-5-pentyl-1H-pyridol[4,3-b]indol-1-one	Cayman chemical
CUMYL-THPINACA	1400742-50-8	N-(1-methyl-1-phenylethyl)-1-(tetrahydro-2H-pyran-4-yl)methyl]-1H-indazole-3-carboxamide	Cayman chemical
EMB-FUBINACA	n.a.	N-[[1-(4-fluorophenyl)methyl]-1H-indazol-3-yl]carbonyl]-L-valine, ethyl ester	Cayman chemical
FUB-AKB48	2180933-90-6	N-(3S,5S,7S)-adamantan-1-yl)-1-(4-fluorobenzyl)-1H-indazole-3-carboxamide	Cayman chemical
JWH-398	1292765-18-4	(4-chloro-1-naphthalenyl)(1-pentyl-1H-indol-3-yl)-methanone	Cayman chemical
MAB-CHMINACA = ADB-CHMINACA	1863065-92-2	N-[1-(aminocarbonyl)-2,2-dimethylpropyl]-1-(cyclohexylmethyl)-1H-indazole-3-carboxamide	Cayman chemical
MDMB-4en-PINACA	2504100-70-1	methyl 3,3-dimethyl-2-[1-(pent-4-en-1-yl)-1H-indazole-3-carboxamido] butanoate	Cayman chemical
MDMB-CHMCZCA	2219324-32-8	N-[[9-(cyclohexylmethyl)-9H-carbazol-3-yl]carbonyl]-3-methyl-L-valine, methyl ester	Cayman chemical
MDMB-CHMICA	1971007-95-0	N-[[1-(cyclohexylmethyl)-1H-indol-3-yl]carbonyl]-3-methyl-L-valine, methyl ester	Cayman chemical
MDMB-CHMICA	1185888-32-7	N-[[1-(cyclohexylmethyl)-1H-indazol-3-yl]carbonyl]-3-methyl-L-valine, methyl ester	Cayman chemical
MDMB-CHMINACA	1971007-94-9	methyl 1-(1-(cyclohexylmethyl)-1H-indole-3-carboxyl)-L-valinate	Cayman chemical
MMB-CHMICA = AMB-CHMICA	1971007-92-7	N-[[1-(4-fluorophenyl)methyl]-1H-indazol-3-yl]carbonyl]-L-valine, methyl ester	Cayman chemical
MMB-FUBINACA = AMB-FUBINACA	n.a.	2-(1-(5-fluoropentyl)-1H-indole-3-carboxamido) propanoic acid methyl ester	Zurich Forensic Science Institute

THU	n.a.	1-pentyl-N-(quinolin-8-yl)-1H-indazole-3-carboxamide	Cayman chemical
THU-018	1364933-55-0	1-naphthalenyl[1-pentyl-1H-indazol-3-yl]-methanone	Cayman chemical

Table S2. Parameters and results, i.e. limits of detection (LODs) and signal to noise ratios (S/N) at LOD, of the qualitative screening method for SCs. Limits of detection were not determined for THC, THCA, CBD, and CBDA as these compounds were merely screened in order to estimate cannabis type (high vs. low THC and CBD). INF stands for “infinite”.

Compound	Formula	[M+H] ⁺ [m/z]	retention time [min]	LOD [ng/mL]	S/N at LOD
UR-144 N-(5-chloropentyl) analog	C21H28ClNO	346.1932	6.04	0.3	INF
5F-MDMB-PINACA (= 5F-ADB)	C20H28FN3O3	378.2187	4.43	0.3	56
4-cyano CUMYL-BUTINACA	C22H24N4O	361.2023	3.89	0.3	INF
4-Fluoro MDMB-BICA (=4-Fluoro-MDMB-BUTICA)	C20H27FN2O3	363.2078	3.66	0.3	45
4-Fluoro-MDMB-BINACA (= 4-fluoro MDMB-BUTINACA)	C19H26FN3O3	364.2031	4.07	0.3	INF
5-Chloro AKB48	C23H30ClN3O	400.215	6.48	0.3	INF
5-Chloro THU-018	C23H21ClN2O	377.1415	6.15	0.6	INF
5-Fluoro-CUMYL-PeGACLONE	C25H27FN2O	391.218	4.59	0.3	203
5-Fluoro-EMB-PINACA	C20H28FN3O3	378.2187	4.36	0.3	93
5-Fluoro ADBICA	C20H28FN3O2	362.2238	2.63	0.3	INF
5-Fluoro AKB48	C23H30FN3O	384.2446	5.82	0.3	INF
5-Fluoro APINAC (= 5F-AKB57)	C23H29FN2O2	385.2286	6.23	0.3	121
5-Fluoro CUMYL-P7AICA	C22H26FN3O	368.2133	3.37	0.3	166
5-Fluoro CUMYL-PINACA	C22H26FN3O	368.2133	4.83	0.3	158
5-Fluoro MDMB-P7AICA	C20H28FN3O3	378.2187	3.02	0.3	130
5-Fluoro-PB22 3-hydroxyquinoline isomer*	C23H21FN2O2	377.1660	4.37/4.81	0.3	INF
5-Fluoro-PB22*	C23H21FN2O2	377.1660	4.37/4.81	0.3	INF
5-Fluoro-MDMB-PIICA	C21H29FN2O3	377.2235	4.06	0.3	INF
5F-NNEI	C24H23FN2O	375.1867	4.58	0.3	124
AB-CHMINACA	C20H28N4O2	357.2285	3.38	0.3	41
AB-FUBINACA	C20H21FN4O2	369.1721	2.71	0.3	INF
ACHMINACA	C25H33N3O	392.2696	7.16	0.3	INF

ADAMANTYL-THPINACA	C24H31N3O2	394.2489	4.82	0.4	95
ADB-BUTINACA	C18H26N4O2	331.2129	2.83	0.4	50
ADBICA (= ADB-PICA)	C20H29N3O2	344.2333	3.14	0.3	INF
ADB-PINACA	C19H28N4O2	345.2285	3.31	2	136
AKB48 = APINACA	C23H31N3O	366.254	6.57	0.4	636
AKB57 (= APINAC)	C23H30N2O2	367.238	6.86	0.3	INF
AM2201	C24H22FNO	360.1758	5.36	0.3	112
CUMYL-CBMICA	C23H26N2O	347.2118	4.76	0.3	INF
CUMYL-PEGACLONE	C25H28N2O	373.2274	5.32	0.3	114
CUMYL-THPINACA	C23H27N3O2	378.2176	3.8	0.3	INF
EMB-FUBINACA	C22H24FN3O3	398.1874	4.78	0.3	INF
FUB-144	C23H24FNO	350.1915	5.83	0.3	97
FUB-AKB48	C25H26FN3O	404.2133	6.2	0.3	INF
FUB-PB-22	C25H17FN2O2	397.1347	4.79	0.3	82
JWH 018	C24H23NO	342.1852	6.06	0.3	45
JWH 018 8-quinolinyl carboxamide	C23H23N3O	358.1914	5.82	0.3	69
JWH 073	C23H21NO	328.1696	5.58	0.3	INF
JWH 210	C26H27NO	370.2165	6.88	0.3	INF
JWH 250	C22H25NO2	336.1958	5.37	0.3	130
JWH-122	C25H25NO	356.2009	6.41	0.3	104
JWH-398	C24H22ClNO	376.1463	6.8	0.3	INF
MAB-CHMINACA (= ADB-CHMINACA)	C21H30N4O2	371.2442	3.84	0.4	148
MAM2201	C25H24FNO	374.1915	5.7	0.3	59
MADB-4en-PINACA	C20H27N3O3	358.2125	4.72	0.4	133
MADB-CHMCZA	C27H34N2O3	435.2642	6.28	0.4	INF
MADB-CHMICA	C23H32N2O3	385.2486	5.38	0.4	INF
MADB-CHMINACA	C22H31N3O3	386.2438	5.7	0.4	49
MMB-CHMICA (= AMB-CHMICA)	C22H30N2O3	371.2329	4.77	0.4	INF
MMB-FUBINACA (= AMB-FUBINACA)	C21H22FN3O3	384.1718	4.32	0.3	85

MMB-FUBINACA (= AMB-FUBINACA)	C21H22FN3O3	384.1718	4.32	0.4	INF
MPPH-2201 (= 5F-MPPH-PICA)	C24H27FN2O3	411.2078	4.14	0.3	363
NM-2201	C24H22FN2O2	376.1707	6.09	0.6	27
PB-22	C23H22N2O2	359.1754	5.08	0.3	INF
THI	C22H22N4O	359.1866	6.28	0.3	62
THI-018	C23H22N2O	343.1805	6.21	0.3	70
THI-2201 (= AM2201 indazole analog)	C23H21FN2O	361.1711	5.53	0.3	37
UR-144	C21H29NO	312.2322	6.1	0.3	375
UR-144 degradant	C21H29NO	312.2322	5.72	0.3	254
XLR11	C21H28FNO	330.2228	5.45	0.3	101
Cannabidiol (CBD)	C21H30O2	315.2319	5.41	not determined	not determined
CBD acid (CBDA)	C22H30O4	359.2217	5.14	not determined	not determined
(-)-trans- Δ -9-tetrahydrocannabinol (THC)	C21H30O2	315.2319	6.12	not determined	not determined
THC acid (THCA)	C22H30O4	359.2217	6.38	not determined	not determined

*The isobaric compounds 5-Fluoro-PB22 and 5-Fluoro-PB22 3-hydroxyquinoline isomer could not be unambiguously assigned, as these compounds were contained in a commercial mixture.



Beyond Δ^9 -tetrahydrocannabinol and cannabidiol: chemical differentiation of cannabis varieties applying targeted and untargeted analysis

Manuela Carla Monti¹ · Priska Frei¹ · Sophie Weber¹ · Eva Scheurer¹ · Katja Mercer-Chalmers-Bender¹

Received: 8 February 2022 / Revised: 10 March 2022 / Accepted: 16 March 2022
© The Author(s) 2022

Abstract

Cannabis sativa (*C. sativa*) is commonly chemically classified based on its Δ^9 -tetrahydrocannabinol (THC) and cannabidiol (CBD) content ratios. However, the plant contains nearly 150 additional cannabinoids, referred to as minor cannabinoids. Minor cannabinoids are gaining interest for improved plant and product characterization, e.g., for medical use, and bioanalytical questions in the medico-legal field. This study describes the development and validation of an analytical method for the elucidation of minor cannabinoid fingerprints, employing liquid chromatography coupled to high-resolution mass spectrometry. The method was used to characterize inflorescences from 18 different varieties of *C. sativa*, which were cultivated under the same standardized conditions. Complementing the targeted detection of 15 cannabinoids, untargeted metabolomics employing *in silico* assisted data analysis was used to detect additional plant ingredients with focus on cannabinoids. Principal component analysis (PCA) was used to evaluate differences between varieties. The overall purpose of this study was to examine the ability of targeted and non-targeted metabolomics using the mentioned techniques to distinguish cannabis varieties from each other by their minor cannabinoid fingerprint. Quantitative determination of targeted cannabinoids already gave valuable information on cannabinoid fingerprints as well as inter- and intra-variety variability of cannabinoid contents. The untargeted workflow led to the detection of 19 additional compounds. PCA of the targeted and untargeted datasets revealed further subgroups extending commonly applied phenotype classification systems of cannabis. This study presents an analytical method for the comprehensive characterization of *C. sativa* varieties.

Keywords Principal component analysis · Minor cannabinoids · High-resolution mass spectrometry · Cannabinomics · Metabolomics · Chemotaxonomy

Introduction

Cannabis sativa (*C. sativa*) has been cultivated by humans for millennia as a source of fiber (e.g., paper and fabrics), food, and oil. Reports on the medicinal use of *C. sativa* date back to 500 B.C. Arising from the psychoactive effects exerted by Δ^9 -tetrahydrocannabinol (THC), the cannabis plant has a long history of abuse [1]. In recent years, several countries have authorized the dispensing and use of herbal cannabis and cannabis preparations for medical and recreational

purposes [2–7]. In 2020, the United Nations reported over 50 countries enrolled in medical cannabis programs and over 15 countries allowing the recreational use of cannabis [8].

C. sativa contains hundreds of chemical compounds, of which phytocannabinoids (from here one referred to as cannabinoids) constitute one major class [9]. The best-known cannabinoids are THC and cannabidiol (CBD). In contrast to THC, CBD is regarded as non-intoxicating [10], while exerting various other effects. CBD is, for example, licensed for the treatment of rare forms of childhood epilepsy [11–14]. Even though THC and CBD comprised the main focus of cannabis research so far, nearly 150 additional cannabinoids, often referred to as minor cannabinoids, are known today [15]. The highest cannabinoid concentrations are found in the flowering parts of the female plant [2]. Following a widely accepted [6, 16] chemical classification system that was first introduced in 1973 [17], cannabis

✉ Katja Mercer-Chalmers-Bender
katja.mercer-chalmers-bender@unibas.ch

¹ Institute of Forensic Medicine, Department of Biomedical Engineering, University of Basel, Pestalozzistrasse 22, 4056 Basel, Switzerland

phenotypes, also referred to as chemotypes, can be classified based on their content of the two major cannabinoids THC and CBD. Hereby, phenotype I is characterized by $\text{THC} > \text{CBD}$ ($> 0.3\% \text{ THC}, < 0.5\% \text{ CBD}$), phenotype II by $\text{THC} \approx \text{CBD}$ ($> 0.3 \text{ THC}, > 0.5\% \text{ CBD}$), and phenotype III by $\text{THC} < \text{CBD}$ (“fiber type,” $< 0.3\% \text{ THC}, > 0.5\% \text{ CBD}$) [17–19]. Meanwhile, additional phenotypes have been described, with one phenotype presenting cannabigerol (CBG) as major cannabinoid [20]. In the legal context, THC is the main focus of regulatory thresholds, often used to classify a plant or derived product as a narcotic [6, 21]. However, these simple approaches might not be sufficient to characterize a product, which is known to comprise a diversity of bioactive compounds, especially regarding its use as a medicinal product [7]. It is still a subject of ongoing research to what extent pharmacologic effects depend on the chemical profile of a cannabis product. The focus, therefore, shifted from THC and CBD towards more comprehensive approaches with growing interest in the often-overlooked minor cannabinoids, as well as in other compound classes such as flavonoids and terpenoids [7, 18, 22–29].

The growing industry around cannabis and the availability of cannabis products for medicinal and recreational uses necessitates improved product characterization [30, 31] that will enable enhanced product standardization and quality control [31]. The detection of cannabis intake comprises a major task in clinical and forensic toxicology, e.g., in traffic drug testing, abstinence control, and doping control, which is likely to become even more relevant due to increasing medical use and legalization of cannabis products [32]. In forensic toxicology, CBD and minor cannabinoids have been examined as possible markers to distinguish between medicinal and recreational cannabis intake [32–34]. Furthermore, some minor cannabinoids have been investigated as markers for recent cannabis consumption [35, 36] as well as tools to discriminate occasional from frequent consumers [32].

Breeding and selection of *C. sativa* strains resulted in currently over 700 described varieties (also known as cultivars). Even though these varieties might differ in morphologic and organoleptic features and are commonly distinguished by names, it is inconclusive to which extent these varieties present true differences in chemical composition [18]. There are some studies [6, 24, 27, 37–39] addressing this specific question. Fishedick et al. [37] cultivated eleven different varieties under equal and controlled conditions and then analyzed 36 different plant ingredients, seven of which were cannabinoids. Ultimately, the authors were able to distinguish between the investigated varieties. Berman et al. [24] analyzed 36 of the most commonly used cannabis plant varieties prescribed to patients in Israel. They found that despite similar CBD content, not all varieties exerted the same anticonvulsive effect [24], clearly highlighting the need for the determination of further plant ingredients. A recent

study conducted by Vasquez-Ocmín et al. [6], which investigated 20 varieties, found minor phytochemicals to play a significant role in the differentiation of *C. sativa* varieties. Cerrato et al. [27] presented an untargeted metabolomics approach, labelled as *phytocannabinomics*, which was tested on 50 cannabis varieties, ultimately proving the existence of chemical subgroups that extend traditional classification systems. Slosse et al. [40] investigated intra- and inter-plantation variabilities by means of chemical fingerprints with the aim of elaborating on common sample sources, e.g., linking seized material to plantations [40]. Finally, Capriotti et al. [30] recently reviewed analytical applications for the characterization of cannabis products applying mass spectrometry. The increasing use of untargeted approaches to achieve better product characterization has been pointed out, while the lack of standardization for untargeted analyses was mentioned as a potential hurdle.

In order to interpret data comprising a large set of analytes, multivariate analyses are commonly used. The aim of such statistical analyses is to identify underlying patterns indicating differences and similarities in the chemical fingerprints. Those patterns would otherwise not be easily recognizable, due to the complexity of the data arising from the large number of analytes (i.e., observations) per sample. Principal component analysis (PCA) describes a mathematical procedure allowing multicomponent data to be reduced in its dimensions. Thereby, PCA enables multidimensional data to be presented in a two-dimensional manner, facilitating data interpretation [41].

On a rudimentary level, the analytical method clearly has an impact on the detectability of cannabis ingredients and, therefore, the knowledge of their composition in the cannabis products [42, 43]. In the cannabis plant, cannabinoids are mainly biosynthesized in their acidic forms, e.g., THC-acid (THCA). These acidic precursors are heat-labile. Chromatographic separation by gas chromatography (GC) typically results in the decarboxylation of cannabinoids in the injection port [24]. In order to investigate acid precursors, high-performance liquid chromatography (HPLC) is preferred [24]. Furthermore, when applying mass spectrometry, the ionization mode substantially influences the ionization efficiency of analytes. While positive ionization mode could be more suitable for the detection of neutral cannabinoids, acidic cannabinoids, which are predominantly found in native plant extracts, are commonly analyzed using negative ionization mode [30]. Therefore, positive and negative ionization modes have been used in the presented work for neutral and acidic cannabinoids, respectively. Finally, the herein used electrospray ionization (ESI) is the most common ionization technique used for HPLC coupled to mass spectrometry [44].

This work reports on the implementation, validation, and application of an analytical method employing HPLC

coupled to high-resolution mass spectrometry (HRMS). The method was validated for the quantification of 15 cannabinoids. The application of a full scan acquisition enabled retrospective identification of additional plant ingredients applying an untargeted metabolomics workflow. In-depth cannabinoid fingerprint characterization was conducted for 45 individual plants belonging to 18 cannabis varieties grown under standardized conditions, applying PCA to determine similarities and differences between the investigated varieties. Study aims included the assessment of intra- and inter-variety differences in cannabinoid contents of cannabis plants cultivated and stored under identical conditions.

Materials and methods

Materials

Certified reference materials (CRMs) were purchased from Merck (Buchs, Switzerland), Lipomed AG (Arlesheim, Switzerland), or Cayman Chemical Company (MI, USA). Detailed information is found in the supplementary Table S1. LC–MS grade methanol (MeOH), acetonitrile (ACN), and water were purchased from Macherey Nagel (Oensingen, Switzerland). Formic acid (purity 98–100%) was purchased from Merck (Zug, Switzerland). Dried flowers of hops PhEur were purchased from TeeFischer (Tägerwilten, Switzerland); organic peppermint and stinging nettles herbal tea were both purchased from Coop supermarket-chain (Basel, Switzerland).

Cannabis plant cultivation and harvest

Cannabis inflorescences were kindly provided by Suisse BioHemp AG (Ried bei Kerzers, Switzerland). Cannabis plants were planted in the beginning of July 2020 and harvested by mid-October (98 days). Cultivation took place in a greenhouse of 10,000 m², of which 320 m² were used for the investigated strains. No artificial lighting was applied, temperatures ranged from 10 to 33 °C, and relative humidity ranged from 40 to 75%. Cannabis inflorescences were harvested manually and dried at 38 °C for 36 h until residual water content was 14%. Thereafter, cannabis inflorescences were openly stored at 20 °C and 50% relative humidity in the dark for 2 weeks and finally packaged in separate pressure lock bags, stored in the dark at room temperature until analysis. Samples derived from 45 individual plants belonging to 18 varieties were obtained. A list of all varieties, number of plants per variety, and detailed information on cultivation, i.e., if a plant was grown from seeds or cuttings, are shown in Table 1. Authorization for cultivation and analysis of the herein presented plants and derived samples for research purposes was granted by Swiss regulatory instances.

Table 1 Overview of investigated varieties and number of individual plants per variety (*n*). Strains presenting names connected by an “×” were obtained via crossbreeding of the respective varieties

	<i>n</i>	Cultivation method
Amnesia	1	Cuttings
Amnesia S5 ^a	3	Cuttings
Amnesia × SFV	2	Seeds
Big Bud	3	Cuttings
Bubba Kush	3	Cuttings
C7	1	Cuttings
C7 × Thai	1	Cuttings
Durban × Malawi	8	Seeds
GWS	1	Cuttings
Lebi 2	3	Cuttings
Malawi × Super Skunk	1	Cuttings
OG Kush	3	Cuttings
Pot of Gold	2	Cuttings
Pot of Gold nr. 11 ^b	1	Cuttings
Purple Punch	3	Cuttings
Rascal OG	3	Cuttings
SFV OG	3	Seeds
Wappa	3	Cuttings

^aSelection of the Amnesia variety

^bSelection of the Pot of Gold variety

Sample extraction

Dried cannabis inflorescences (5 g per individual plant) were homogenized using a Grindomix GM 200 knife mill from Retsch (Haan, Germany). For sample extraction, 50 mg of homogenized cannabis inflorescence were mixed with 2 mL MeOH in glass vials and ultra-sonicated for 15 min. The extract was filtered using a Simplepure™ syringe filter (13 mm, 0.45 μm) obtained from BGB Analytik AG (Boeckten, Switzerland). In a preliminary experiment, the herein applied extraction procedure was evaluated by comparison of the cannabinoid levels obtained after single extraction to a procedure applying an exhaustive extraction comprised of five subsequent extraction steps. The analysis of the combined extract did not result in higher cannabinoid levels compared to the presented protocol (data not shown). Before chromatographic analysis, the extracts were diluted with MeOH to the appropriate concentrations for analysis and calibration range (1:10,000, selected samples were reinjected at 1:5000 or 1:15,000). For each individual plant, extraction was done in duplicate.

LC-HRMS analysis

Chromatographic separation was achieved using a Dionex UltiMate 3000 UHPLC System equipped with a

MultiSLEEVE column heater (Analytical SALES & SERVICES, Inc.), a Triplus RSH Autosampler (CTC Analytics AG), and a Hypersil GOLD™ column (100×2.1 mm, 1.9 μm), all purchased from Thermo Fisher Scientific (Reinach, Switzerland). The Autosampler temperature was 10 °C. An injection volume of 5 μL, column temperature of 40 °C, and flow rate of 0.6 mL/min were applied. Mobile phase A consisted of 0.1% (v/v) formic acid in water. Mobile phase B consisted of 50:50% (v/v) ACN and MeOH with 0.1% (v/v) formic acid. The gradient started at 65% of phase B and then increased to 76% over 8.5 min and ramped up to 100% of phase B within the next minute. This condition was maintained for 2 min and followed by 1.5 min reequilibration at starting conditions. For the subsequent analysis, a Q Exactive™ HF mass spectrometer operated with a HESI-II probe all purchased from Thermo Fisher Scientific (Reinach, Switzerland) was used. Transfer capillary temperature was set to 300 °C, spray voltage was set to 3.5 kV, sheath gas flow rate was set to 50 arbitrary units (AU), auxiliary gas flow rate was set to 15 AU, and auxiliary gas heater temperature was 350 °C.

A full scan acquisition over a range of 250–400 *m/z* was performed at a resolution of 120,000 at full width at half maximum (FWHM). To be able to measure at high mass-resolution (> 100,000 FWHM) while maintaining a reasonable cycle time and, thus, sufficient data points per peak, the positive and negative ionization modes were defined in two separate instrument methods, requiring two injections per sample. Maximum injection time (IT) was set to 200 ms. Automatic gain control (AGC) target values of 1e6 and 1e5 were used for the positive and negative ionization modes, respectively. Instruments were controlled and data were processed employing Aria MX, TraceFinder (version 4.1), and FreeStyle™ (version 1.7 SP1) all by Thermo Fisher Scientific (Reinach, Switzerland). To prevent carry-over, blank injections (100% MeOH) were interposed in-between analyses of each plant.

Quantification of targeted cannabinoids

An overview of the 15 quantified analytes and abbreviations, applied calibration ranges, including weighing factors, referenced internal standards (ISTDs), screened theoretical mass traces, ionization modes, and retention times is given in Table 2. Structures of the targeted cannabinoids are shown in supplementary Table S2. Exemplary chromatograms obtained after injection of quality control (QC) samples are presented in supplementary Fig. S1. QC samples and calibrators were independently from each other generated by dilution of CRM in MeOH. QC samples and calibrators were prepared from separate pooled stock solutions (10 μg/mL in MeOH, stored at –20 °C) containing either all analytes measured in positive or negative ionization mode. ISTDs

were added to calibrators, QC samples, and extracted inflorescences at 100 ng/mL and 500 ng/mL (only THC-COOH) final concentration during the final dilution step. The calibration range for all cannabinoids measured in positive and negative ionization modes, except for THCA and CBDA, was defined from 0.5 to 100 ng/mL. THCA and CBDA were quantified using two separate calibration ranges: 0.5–100 ng/mL (THCA_{low}, CBDA_{low}) referenced to THC-COOH-D₉ at 100 ng/mL; 50–500 ng/mL (THCA_{high}, CBDA_{high}) referenced to the ISTD THC-COOH at 500 ng/mL. Signals falling in between 50 and 100 ng/mL were calculated using the THCA_{low} and CBDA_{low} calibration ranges. For quantification, the analytes were identified via their retention time with a detection window of ±30 s as well as acceptable mass error ±5 ppm. During each sequence, QC samples spanning the calibration range (0.8 ng/mL, 3 ng/mL, 80 ng/mL, for all analytes, THCA and CBDA additionally: 425 ng/mL) were measured in order to assure functionality of the analysis, accurate retention times and suitability, and correctness of calibration. For each individual plant, mean values of analyses of the duplicate extractions were used to describe the cannabinoid content.

Selectivity and specificity were evaluated by investigating interfering signals in diluted extracts of dried flowers of hops, dried peppermint leaves, and dried stinging nettles as well as blank measurements, with and without the addition of ISTDs. Additionally, Δ8-THC was injected to investigate the separation power between Δ9-THC (here referred to as THC) and its isomer Δ8-THC. Limits of detection (LODs) were investigated after serial dilution of CRM at ranges at suspected LODs. The required root mean square signal to noise (S/N) ratio at the LOD was defined to be ≥3. For the evaluation of LOQs, five repeated measurements of the target analytes at 0.5 ng/mL were conducted, followed by evaluation of bias and repeatability as relative standard deviation (RSD), whereby bias within ±20% and RSD ≤20% were considered acceptable. Linearity was tested by measurement of the calibration curves and assessment of the resulting coefficients of correlation (*R*²) with a resulting value of >0.99 regarded sufficient. Accuracy with precision and trueness was evaluated by duplicate measurements of QC samples at different concentration levels on eight different days (0.8 ng/mL, 3 ng/mL, 80 ng/mL, CBDA and THCA additionally: 400 ng/mL). Intra- and inter-day precision (RSD_r and RSD_(T)) and trueness (as bias) were examined, with validation criteria being RSD_r and RSD_(T) <20% and bias within ±20%.

Untargeted screening

The high-resolution full scan measurement enabled the retrospective analysis of chromatograms regarding initially untargeted, additional compounds. Due to the overall higher

Table 2 Overview of the retention times, chemical formula, measured polarity and respective $[M+H]^+$ or $[M-H]^-$ signals, calibration ranges, weighing of the calibration curve, and internal standards (ISTDs) used for the quantitative analysis. Cannabinoids are orderedbased on retention time (RT). THC-OH-D₃: deuterated 11-hydroxy-THC (human THC metabolite); THC-COOH and THC-COOH-D₉: (deuterated) 11-nor-9-carboxy-THC (human THC metabolite)

Cannabinoid	Abbreviation	RT	Formula	Mass trace [m/z]	Calibration range [ng/mL]	Weighing of calibration curve	ISTD
Cannabidivarin	CBDV	1.30	C ₁₉ H ₂₆ O ₂	$[M+H]^+$ 287.2006	0.5–100	1/x	OH-THC-D ₃
Cannabidivarinic acid	CBDVA	1.75	C ₂₀ H ₂₆ O ₄	$[M-H]^-$ 329.1758	0.5–100	1/x	THC-COOH-D ₉
Cannabidiol	CBD	3.00	C ₂₁ H ₃₀ O ₂	$[M+H]^+$ 315.2319	0.5–100	1/x	CBD-D ₃
Tetrahydrocannabivarin	THCV	3.10	C ₁₉ H ₂₆ O ₂	$[M+H]^+$ 287.2006	0.5–100	1/x	THC-D ₃
Cannabigerol	CBG	3.20	C ₂₁ H ₃₂ O ₂	$[M+H]^+$ 317.2475	0.5–100	1/x	CBD-D ₃
Cannabidiolic acid	CBDA _{low}	3.40	C ₂₂ H ₃₀ O ₄	$[M-H]^-$ 357.2071	0.5–100	1/x	THC-COOH-D ₉
	CBDA _{high}	3.40	C ₂₂ H ₃₀ O ₄	$[M-H]^-$ 357.2071	50–500	1/x	THC-COOH
Cannabigerolic acid	CBGA	4.25	C ₂₂ H ₃₂ O ₄	$[M-H]^-$ 359.2228	0.5–100	1/x	THC-COOH-D ₉
Cannabinol	CBN	5.00	C ₂₁ H ₂₆ O ₂	$[M+H]^+$ 311.2006	0.5–100	1/x	CBN-D ₃
Tetrahydrocannabivarinic acid	THCVA	5.71	C ₂₂ H ₂₆ O ₄	$[M-H]^-$ 329.1758	0.5–100	1/x	THC-COOH-D ₉
Tetrahydrocannabinol	THC	5.90	C ₂₁ H ₃₀ O ₂	$[M+H]^+$ 315.2319	0.5–100	1/x	THC-D ₃
Cannabicyclol	CBL	6.65	C ₂₁ H ₃₀ O ₂	$[M+H]^+$ 315.2319	0.5–100	1/x	THC-D ₃
Cannabinolic acid	CBNA	7.66	C ₂₂ H ₂₆ O ₄	$[M+H]^+$ 353.1758	0.5–100	1/x	THC-COOH-D ₉
Cannabichromene	CBC	7.95	C ₂₁ H ₃₀ O ₂	$[M+H]^+$ 315.2319	0.5–100	1/x	CBC-D ₉
Tetrahydrocannabinolic acid	THCA _{low}	8.75	C ₂₂ H ₃₀ O ₄	$[M-H]^-$ 357.2071	0.5–100	1/x	THC-COOH-D ₉
	THCA _{high}	8.75	C ₂₂ H ₃₀ O ₄	$[M-H]^-$ 357.2071	50–500	None	THC-COOH
Cannabichromenic acid	CBCA	9.05	C ₂₂ H ₃₀ O ₄	$[M-H]^-$ 357.2071	0.5–100	1/x	THC-COOH-D ₉
ISTD							
THC-OH-D ₃		2.12	C ₂₁ H ₂₇ O ₃ D ₃	$[M+H]^+$ 334.2456	100		
THC-COOH-D ₉		2.70	C ₂₁ H ₁₉ O ₄ D ₉	$[M-H]^-$ 352.2480	100		
THC-COOH		2.70	C ₂₁ H ₂₈ O ₄	$[M-H]^-$ 343.1915	500		
CBD-D ₃		3.00	C ₂₁ H ₂₇ O ₂ D ₃	$[M+H]^+$ 318.2507	100		
CBN-D ₃		5.00	C ₂₁ H ₂₃ O ₂ D ₃	$[M+H]^+$ 314.2194	100		
THC-D ₃		5.90	C ₂₁ H ₂₇ O ₂ D ₃	$[M+H]^+$ 318.2507	100		
CBC-D ₉		7.95	C ₂₁ H ₂₁ O ₂ D ₉	$[M+H]^+$ 324.2883	100		

abundance of acidic cannabinoids in native plant extracts, untargeted data analysis in negative ionization mode yielded more promising results regarding the number of detected compounds and signal intensities, than seen in a preliminary analysis conducted for the positive ionization mode (data not shown). Thus, the untargeted workflow was conducted for the negative ionization mode only. A so-called *unexpected workflow* (predefined workflow within the used software) was adapted in the Compound Discoverer™ (version 3.1.0.305) software from Thermo Fisher Scientific (Reinach, Switzerland). The full scan data was investigated applying an untargeted metabolomics workflow, in which retention times were aligned between samples, mass traces detected, background compounds extracted (comparison to a blank injection), and initially targeted compounds, of where CRMs were available, were detected based on a mass list containing the corresponding retention times and molecular formulas. Supplementary Fig. S2 depicts the complete workflow including advanced parameters used for data processing in

the Compound Discoverer™ software. In a second step, the processed and visualized results for tentatively identified compounds were manually validated. Signals likely corresponding to cannabinoids or other additional plant metabolites were marked for further evaluation and finally exported by means of an inclusion list for additional structure elucidation.

Structure elucidation of additional compounds

For further characterization of additional compounds, selected samples containing the compounds of interest were reinjected applying a full scan measurement with a data-dependent-MS² (dd-MS²) acquisition. The resolution of the full scan measurement was 120,000 FWHM, with AGC target value of 1e6 and maximum IT of 200 ms. Method parameters for the dd-MS² acquisition were resolution of 30,000, AGC target value of 1e5, maximum IT of 20 ms, and isolation window of 2.0 m/z. Suitable collision energy

(CE) was determined in a preliminary experiment via measurement of CBDA, THCA, and CBCA at 100 ng/mL applying varying CEs (20, 30, 40, 50, 60), after which CE 40 was chosen as best (data not shown). Tentatively identified compounds were compared to literature based on proposed elemental composition derived from the $[M-H]^-$ signal and MS^2 spectra.

Multivariate analyses

PCA was conducted in R (version 3.4.3). Source codes for analyses conducted in R are presented in supplementary Figs. S3 and S4. Statistical analyses were conducted for the results of the targeted analysis (mass content) as well as for exported and weight normalized mean peak areas (exported from the Compound Discoverer™ software) for the untargeted approach. PCA analysis using the R package FactoMineR [45] included data normalization (z-transformations; autoscaling) as a data pretreatment, meaning that the result of each analyte (i.e., observation; content w/w or weight normalized peak area) is mean-centered and divided by its standard deviation. Ultimately, this results in a mean value equaling zero and a standard deviation of one. Scatter plots, generated by plotting PC1 against PC2, offered the possibility to assess similarities and differences between varieties (plotted as individual data points per plant). If varieties show up close to each other, this indicates a high degree of similarity, if they spread apart, this means that these varieties are considerably different regarding their chemical composition. The contribution of individual analytes is made visible by additionally plotting their corresponding eigenvectors (e.g., biplots, loading plots). Thereby, the direction and length of an eigenvector represent its contribution to the construction of the dimensions (PC1 and PC2), allowing to identify which analytes are contributing the most. Analytes that largely add to a dimension are interesting, as they are acting as distinguishing markers between varieties. Detailed information concerning PCA in general [41] and specifically the applied package [45] are found under the indicated literature sources. Complementing the PCA additionally, heatmaps applying hierarchical clustering of the z-transformed data were computed in R using the ggplot2 package. These heatmaps allow a complementary representation of the data.

Results

HPLC-HRMS analysis and method validation

Selectivity and specificity of the method were shown by analysis of tea extracts, solvent blanks, and solvent blanks containing ISTDs, as no signals were detected in the defined time frames and corresponding mass traces of the targeted

analytes. With the presented method THC (Δ^9 -THC) and its isomer Δ^8 -THC are chromatographically separated. However, due to the close elution of Δ^8 -THC which ultimately coelutes within the tail of the THC peak, full quantification of Δ^8 -THC, which is expected to occur at much lower levels compared to THC [24], was omitted. The LOD for Δ^8 -THC was determined to be 5 ng/mL if 500 ng/mL THC was contained in a spiked sample, corresponding to 0.2% Δ^8 -THC and 20% THC (w/w; 1:10,000 dilution when 50 mg plant material are extracted with 2 mL MeOH). An exemplary chromatogram is shown in supplementary Fig. S5. For all analytes measured in negative ionization mode, an LOD of 0.2 ng/mL was observed, translating to cannabinoid contents at product level of 0.008% (w/w; 1:10,000 dilution when 50 mg plant material are extracted with 2 mL MeOH). LODs of analytes measured in positive ionization mode ranged from 0.3 to 0.5 ng/mL, translating to 0.012% and 0.02% (1:10,000 dilution), respectively. Biases and RSDs at the evaluated LOQs of 0.5 ng/mL, referring to 0.02% at the product level (1:10,000 dilution), lay within the acceptable range for all analytes. Linearity was shown with correlation factors (R^2) of > 0.99 for calibrations of all analytes. The results for accuracy with precision and trueness met the defined criteria for all analytes at the investigated QC levels. All analytes met the defined criteria with maximum RSD_p , RSD_T , and bias of 16.8%, 16.0%, and -19.3% , respectively. For detailed information on the validation results, see supplementary Table S3.

Quantification of targeted cannabinoids

Mean contents (percentage; w/w) of the quantified cannabinoids for each variety are shown in Table 3. Detailed results including content ranges and corresponding standard deviations (SDs) can be found in the supplementary Table S4 (neutral and acid presented separately) and S5 (calculated total cannabinoid content, i.e., neutral + acid). Plant extractions were conducted in duplicate. The mean relative deviation of extracts of the same plant was $\leq 6.8\%$ (median: 3.8%). RSD of the ISTDs was $\leq 2.3\%$ throughout the presented analyses. When classifying into phenotypes I, II, and III [17], 14 varieties belonged to phenotype I (high-THC). The other four namely Pot of Gold nr. 11, Pot of Gold, GWS, and C7×Thai additionally presented elevated CBD levels, therefore, belonging to phenotype II (intermediate type). CBDA (range: 0.03–9.5%), CBGA (range $< LOQ$ –1.6%), CBCA (range: 0.11–0.26%), and THCVA (range: 0.03–1.7%) were detectable in all samples. CBDVA was only detectable in plants belonging to phenotype II. Several neutral cannabinoids were detected, but in considerably lower amounts than the corresponding acidic precursor. The neutral cannabinoid THC was detected at approximate levels $\leq 2.1\%$ (range: 0.71–2.1%), CBG $< 0.2\%$ (range: 0.04–0.16%), and

Table 3 Mean quantitative results (two replicas per individual plant) expressed as content (% w/w) for the investigated varieties. Columns are ordered from highest to lowest overall observed content; varieties are ordered from highest to lowest THCA content. CBL and Δ^8 -THC (qualitatively screened) were not detected above respective LODs in any sample and are therefore not shown. "n.d." stands for "not detected" (<LOD)

Variety (n ^a)	THCA	CBDA	THC	CBD	CBGA	CBCA	THCVA	CBNA	CBG	CBC	CBN	CBDVA	THCV	CBDV
Amnesia S5 (3)	19.6	0.04	1.38	n.d	1.62	0.26	0.08	0.20	0.16	0.04	0.03	n.d	n.d	n.d
Lebi 2 (3)	19.3	0.04	1.15	n.d	0.42	0.24	0.07	0.19	0.15	0.02	0.03	n.d	n.d	n.d
Amnesia x SFV (2)	17.4	0.26	0.87	0.03	0.70	0.17	0.10	0.17	0.12	0.02	<LOQ	n.d	n.d	n.d
Purple Punch (3)	16.8	0.04	0.59	n.d	0.14	0.22	0.06	0.18	0.04	0.01	<LOQ	n.d	n.d	n.d
C7 (1)	15.6	0.05	0.93	n.d	0.20	0.13	0.10	0.23	0.08	0.01	0.04	n.d	n.d	n.d
Big Bud (3)	15.5	0.03	0.67	n.d	0.26	0.13	0.07	0.20	0.12	n.d	<LOQ	n.d	n.d	n.d
Amnesia (1)	15.5	0.03	0.93	n.d	0.62	0.14	0.05	0.16	0.08	0.02	0.03	n.d	n.d	n.d
Durban x Malawi (8)	15.4	0.05	1.04	<LOQ	0.18	0.13	0.17	0.14	0.05	<LOQ	<LOQ	n.d	<LOQ	n.d
Rascal OG (3)	13.4	0.03	1.94	n.d	0.10	0.19	0.04	0.17	0.04	0.03	0.06	n.d	n.d	n.d
Bubba Kush (3)	11.9	0.04	0.94	n.d	0.09	0.17	0.05	0.08	0.08	0.02	0.02	n.d	n.d	n.d
Malawi x Super Skunk (1)	11.5	0.03	1.46	n.d	1.07	0.43	1.73	0.11	0.26	0.03	0.03	n.d	0.24	n.d
Wappa (3)	11.3	0.03	1.85	n.d	0.22	0.18	0.26	0.16	0.05	0.04	0.06	n.d	0.05	n.d
SFV OG (3)	9.67	<LOQ	2.10	n.d	0.23	0.11	0.03	0.10	0.05	0.02	0.04	n.d	n.d	n.d
OG Kush (3)	8.68	<LOQ	0.65	n.d	<LOQ	0.17	<LOQ	0.08	0.04	<LOQ	<LOQ	n.d	n.d	n.d
Pot of Gold nr. 11 (2)	7.78	9.29	1.06	0.61	0.31	0.57	0.47	0.10	0.05	0.04	0.03	0.40	0.07	0.02
Pot of Gold (1)	7.54	9.48	1.26	0.72	0.37	0.57	0.47	0.09	0.06	0.05	0.03	0.42	0.08	<LOQ
GWS (1)	2.90	5.54	0.73	0.55	0.07	0.33	0.03	0.07	0.06	0.03	0.03	0.03	n.d	n.d
C7 x Thai (1)	2.88	6.12	0.71	0.60	0.05	0.42	0.03	0.06	0.05	0.04	0.03	0.04	n.d	n.d

^an total number of individual plants analyzed and available per variety

CBD < 1% (range: n.d.–0.6%), while the remaining cannabinoids (CBC, CBN, CBDV, THCV), if detected, were found at amounts < 0.1%. CBL and Δ 8-THC (qualitatively screened) were not detected above their respective LODs in any sample. Inter-variety cannabinoid variability is assessable via the obtained SDs shown in Tables S2 and S3. The SDs of THC_{Total} (Table S3) ranged from \pm 0.41% (Purple Punch, $n=3$), showing the lowest variability, to \pm 2.05% (Durban \times Malawi, $n=8$), presenting the highest SD. The highest difference between individual plants was observed for Amnesia \times SFV ($n=2$), with a mean THC_{Total} of 11.5% for plant 1 and 20.8% for plant 2.

Identification of untargeted additional compounds

The untargeted workflow detected 19 additional compounds. Including the 7 acidic cannabinoids, initially targeted in the negative ionization mode, a total of 26 compounds were detected. Table 4 shows all identified compounds, including theoretical molecular weights, measured [M-H]⁻ and mass errors as well as the herein detected MS² fragments compared to MS² fragments found in literature. Based on exact mass and matching MS² spectra, nine compounds could be assigned to previously reported cannabinoids described in the literature [24, 46]. These compounds are therefore assigned with high confidence. For full verification of these results, however, analytical reference standards are required. Additional detected cannabinoids belonging to the THC family were two homologues of THCA, presenting different alkyl side chain lengths (THCA-C₁, THCA-C₄; also referred to as tetrahydrocannabinol abbreviated THCBA). Low signal intensities of these aforementioned compounds resulted in the detection of only one fragment each. This renders the annotation for THCA-C₁ and THCA-C₄ with higher uncertainty than for the other compounds that produced more characteristic MS² spectra. THCA monomethyl ether (THCMA) was also detected. Cannabichromevarinic acid (CBCVA) and cannabigerovarinic acid (CBGVA) were identified as well. Additionally, two chromatographically separated isomers of the cannabinoid 6,7-epoxy-CBGA were found, as well as cannabigerolic acid monomethyl ether (CBGMA). Finally, cannabitrilic acid (CBTA) was identified. For 10 compounds (from here on termed *unknown 1* to *10*), the conclusive assignment was not possible due to missing MS² spectra, resulting from low signal intensities and/or the lack of a matching known compound in literature. *Unknown 3* and *unknown 7*, both presenting a parent ion at [M-H]⁻ = 373.202 (m/z), match the signal of cannabielsoic acid (CBEA) as well as of other compounds reported by Berman et al. [24] Unfortunately, no MS² spectra could be obtained for *unknown 3* and *unknown 7*, making a more conclusive assignment impossible. *Unknown 5* and *unknown 8* had the same elemental composition as the major

cannabinoids THCA and CBDA, therefore, likely belonging to the cannabinoid class. A similar compound matching *unknown 5* and *unknown 8* was again reported by a study from Berman et al. [24]. Montone et al. [47] detected various isomers of cannabinoids applying an untargeted analysis. Accordingly, *unknown 8* that generated the same fragment at m/z 313 as THCA could be an isomer of THCA. *Unknown 10* with parent ion [M-H]⁻ at 325.145 (m/z) and proposed chemical formula of C₂₀H₂₂O₄ matched the one expected for cannabivarinic acid (CBNVA). Structures of the herein tentatively detected cannabinoids are shown in supplementary material Table S2.

Comparison of varieties – PCA resulting from the targeted and untargeted analysis

The obtained PCA scatter plots are presented in Fig. 1. The loading plot for the targeted analysis is presented in Fig. 2. The loading plot for the untargeted analysis is shown in Fig. 3. For the targeted approach, PC1 is contributing to 38.3% of variance and PC2 to 21.3%. Based on PCA of the data from the targeted workflow, the varieties belonging to the phenotype II, namely Pot of Gold, Pot of Gold nr. 11, GWS, and C7 \times Thai, group in the first and fourth quadrants (counted from top right counterclockwise) of the scatter plot. The loading plot shows that the cannabinoids from the CBD family (CBD, CBDA, CBDV, CBDVA) are mostly contributing to the grouping of these varieties. CBCA is an additional eigenvector showing in this direction, meaning that CBCA was detected at higher levels in plants of phenotype II. In contrast, the eigenvectors for THCA and CBNA are pointing in the opposite direction of the ones of the CBD-type cannabinoids, indicating that these analytes behave counter-directional for these varieties. GWS and C7 \times Thai presented similar chemical fingerprints, thus clustering in a distinct subgroup on the bottom right (fourth quadrant), attributable to their low contents of THCA. Cannabis varieties high in THC and, thus, belonging to phenotype I form one large cluster, which, apart from Wappa and Malawi \times Super Skunk, are found in the second and third quadrant of the plot. Malawi \times Super Skunk, not clustering with other varieties, expresses a unique chemical fingerprint compared to the other varieties. This is largely explained by its elevated THCVA levels, as seen in the loading plot. Nevertheless, additional subgroups within the large phenotype I cluster can be distinguished. For instance, Amnesia S5 and OG Kush are found on each end (top and bottom) of the cluster belonging to two different quadrants (second and third), thus, implying considerable differences in their chemical fingerprints largely attributable to their differences in their overall cannabinoid content, with Amnesia S5 presenting higher cannabinoid levels than OG Kush, e.g., THCA, THCVA, CBGA, CBG, and CBNA. Elevated CBGA

Table 4 List of all detected compounds using the untargeted data analysis. The herein detected fragments and (where indicated) published fragments are given in decreasing signal abundancies (excluding signals belonging to the unfragmented parent ion)

Compound	Formula	Theoretical [M-H] ⁻ [m/z]	Measured [M-H] ⁻ [m/z]	Mass error [ppm]	RT [min]	Detected fragments [m/z]	Published fragments [m/z]
6-7-Epoxy-CBGA (isomer 1) ^b	C ₂₂ H ₃₂ O ₅	375.2177	375.2179	0.4	1.02	357.21, 222.09, 273.19, 178.10	273, 357, 222, 313, 179 [46]
6-7-Epoxy-CBGA (isomer 2) ^b	C ₂₂ H ₃₂ O ₅	375.2177	375.2180	0.8	0.85	357.21 ^c	273, 357, 222, 313, 179 [46]
CBCA ^a	C ₂₂ H ₃₀ O ₄	357.2071	357.2074	0.7	9.00	191.11, 313.22, 339.20, 179.11	191, 313, 339 [24]
CBCVA ^b	C ₂₀ H ₂₆ O ₄	329.1758	329.1758	-0.3	6.84	185.01, 285.19, 311.16	163, 311, 285, 151 [24]
CBDA ^a	C ₂₂ H ₃₀ O ₄	357.2071	357.2073	0.5	3.39	245.15, 339.20, 179.11, 311.20	245, 339, 311, 179 [24]
CBDVA ^a	C ₂₀ H ₂₆ O ₄	329.1758	329.1760	0.4	1.78	217.12, 311.17, 151.08, 283.17	217, 311, 151, 283 [24]
CBGA ^a	C ₂₂ H ₃₂ O ₄	359.2228	359.2229	0.3	4.31	341.21, 315.23, 297.22, 191.11	341, 315, 191, 297 [24]
CBGMA ^b	C ₂₃ H ₃₄ O ₄	373.2384	373.2387	0.7	9.07	329.25, 191.11, 245.15	355, 374, 329, 205 [24]
CBGVA ^b	C ₂₀ H ₂₈ O ₄	331.1915	331.1915	0.1	2.50	164.93, 313.18, 287.20, 217.19	313, 287, 164 [25]
CBNA ^a	C ₂₂ H ₂₆ O ₄	353.1758	353.1760	0.4	7.77	309.19, 279.14, 171.08	309, 279, 171 [25]
CBTA ^b	C ₂₂ H ₃₀ O ₆	389.1970	389.1969	-0.2	1.18	191.11, 327.21	309, 327, 285, 191 [25]
THCA ^a	C ₂₂ H ₃₀ O ₄	357.2071	357.2072	0.2	8.77	313.22, 245.15, 179.11	313, 339, 245 [25]
THCA-C ₁ ^c	C ₁₈ H ₂₂ O ₄	301.1445	301.1446	0.2	3.40	257.16	257, 283, 189 [25]
THCA-C ₄ ^c	C ₂₁ H ₂₈ O ₄	343.1915	343.1914	-0.4	7.47	257.16	299, 325, 231, 177 [25]
THCMA ^b	C ₂₃ H ₃₂ O ₄	371.2228	371.2229	0.3	8.48	259.17, 311.17, 193.12, 327.23	327, 371, 259, 205, 193 [25]
THCVA ^a	C ₂₀ H ₂₆ O ₄	329.1758	329.1758	-0.1	5.76	285.19, 217.12, 163.08	285, 311, 217, 163 [25]
Unknown 1	C ₂₆ H ₃₈ O ₃	397.2748	397.2745	-0.7	9.32	No MS ² obtained	n.a
Unknown 2	C ₂₀ H ₁₈ O ₅	337.1081	337.1083	0.4	0.66	No MS ² obtained	n.a
Unknown 3	C ₂₂ H ₃₀ O ₅	373.2020	373.2021	0.2	2.81	No MS ² obtained	n.a
Unknown 4	C ₂₂ H ₂₈ O ₄	355.1915	355.1917	0.6	8.64	No MS ² obtained	n.a
Unknown 5	C ₂₂ H ₃₀ O ₄	357.2071	357.2073	0.5	1.37	No MS ² obtained	n.a
Unknown 6	C ₂₁ H ₂₈ O ₃	327.1966	327.1964	-0.8	5.23	No MS ² obtained	n.a
Unknown 7	C ₂₂ H ₃₀ O ₅	373.2020	373.2020	0	3.14	No MS ² obtained	n.a
Unknown 8	C ₂₂ H ₃₀ O ₄	357.2071	357.2073	0.7	8.50	313.22, 215.45, 357.21	n.a
Unknown 9	C ₂₂ H ₃₂ O ₆	391.2126	391.2127	0.1	1.30	No MS ² obtained	n.a
Unknown 10	C ₂₀ H ₂₂ O ₄	325.1445	325.1450	1.6	4.50	No MS ² obtained	n.a

^aVerified via comparison to certified reference material. ^bAnnotated via comparison to published [M-H]⁻ and MS² spectra. ^cLow signal intensity resulted in the detection of only one fragment that was distinguishable from noise, resulting in higher uncertainty in annotation. "n.a." stands for not applicable

and CBG levels are indicative for the variety Amnesia S5, as seen in the loading plot. Due to the small sample size of individual plants per variety (1–3 plants), calculation of the 95% confidence interval (95% CI) was only possible for the variety Durban × Malawi ($n=8$). PCA scatter plots showing

the 95% CI of Durban × Malawi are shown in supplementary Figs. S6 and S7.

PCA of the untargeted workflow showed similar results to the ones obtained with the targeted approach. The percentage of variance explained by PC1 and PC2 is

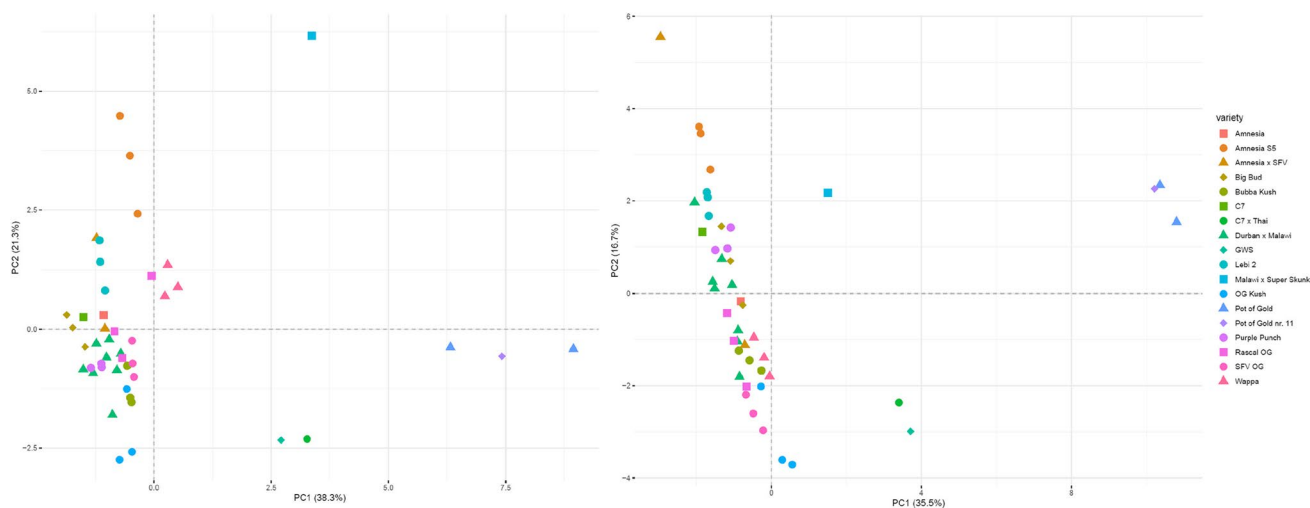


Fig. 1 Scatter plots for the targeted analytes (left) and for the untargeted approach (right). Varieties presenting similar chemical fingerprints are clustering together, while distinct varieties are plotted further apart. Varieties belonging to phenotype II (Pot of Gold

nr. 11, Pot of Gold, GWS, and C7×Thai) are clearly distinguished from varieties of phenotype I. Slight differences between the resulting clusters are seen between the targeted (left) and untargeted (right) approach. Chemical subgroups are observable in both plots

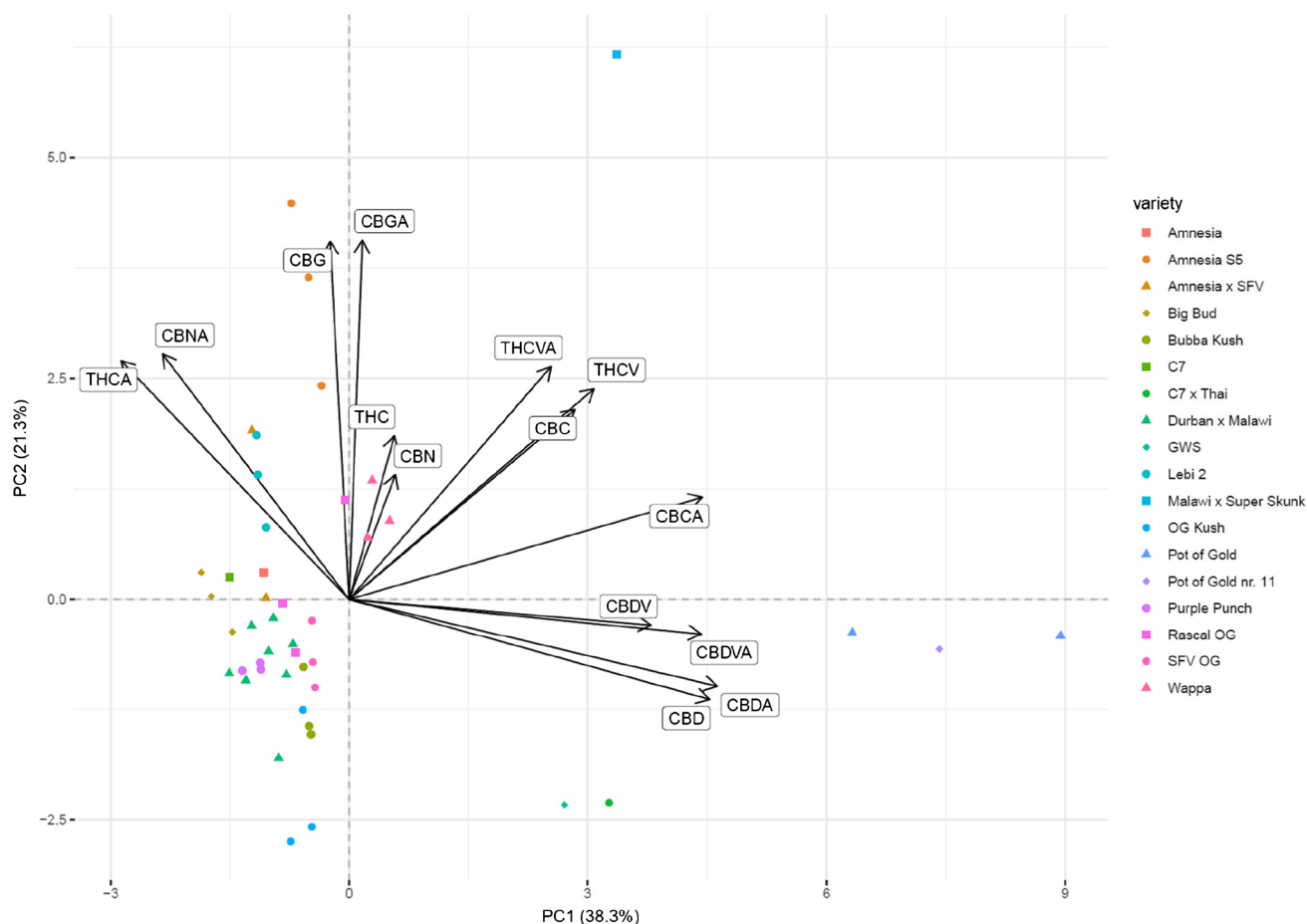


Fig. 2 Loading plot (biplot) for the PCA of the targeted workflow. Eigenvectors are indicated by black arrows. The length and direction of these eigenvectors correspond to their contribution to the dimensions PC1 and PC2. Cannabinoids of the CBD type are largely con-

tributing to the distinction between phenotypes I and II. THCA and CBNA are pointing in the opposite direction and are therefore more indicative for varieties belonging to phenotype I. CBG and CBGA are expressed at elevated levels for the variety Amnesia S5

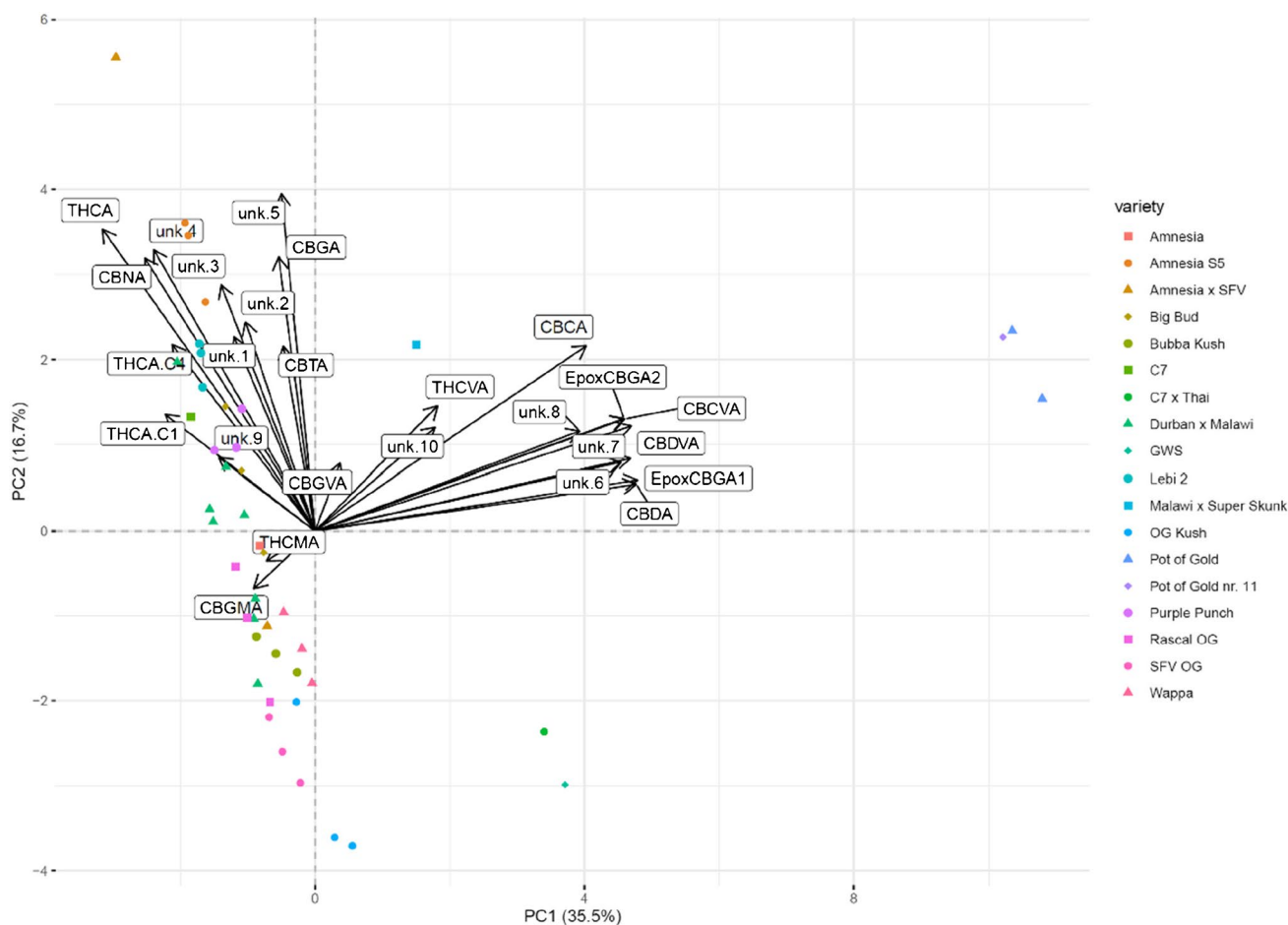


Fig. 3 Loading plot (biplot) for the PCA of the targeted workflow. Eigenvectors are indicated by black arrows. The length and direction of these eigenvectors correspond to their contribution to the dimensions PC1 and PC2. Besides cannabinoids of the CBD family,

6,7-epoxy-CBGA isomers 1 and 2 were found to be highly indicative of the varieties Pot of Gold and Pot of Gold nr. 11. Note: “unkw.” stands for “unknown compound,” EpoxyCBGA1 = 6,7-epoxy-CBGA isomer 1, EpoxyCBGA2 = 6,7-epoxy-CBGA isomer 2

slightly reduced to 35.5% and 16.7%, respectively. This can be explained by the introduction of a higher number of observations (i.e., compounds) with mixed discriminative value (reflected by compounds expressing short eigenvectors), which ultimately rendered the explanation of the variance of the whole dataset more difficult. Using the untargeted dataset, some varieties, for instance, Pot of Gold, Lebi 2, and OG Kush, clustered closer together than in the PCA plot generated from the targeted dataset. Thus, these varieties are better discriminated using the untargeted dataset. Others, however, are losing similarity when using the untargeted dataset, as seen for Amnesia S5 and Durban \times Malawi. For these varieties, the additionally introduced compounds are showing higher variability than observed for the targeted analytes. Malawi \times Super Skunk contained elevated levels of additional propylcannabinoids (C_3) besides THCVA, namely CBGVA and *unknown 10* (likely to be CBNVA). Regarding the varieties Pot of Gold and Pot of Gold nr. 11 (a selection of Pot of

Gold made by the producer with no given further information), as expected, very similar cannabinoid profiles were obtained. Upon investigation of the loading plot, the two 6,7-epoxy-CBGA isomers were shown to be indicative for these varieties. The relatively short eigenvectors belonging to CBGMA and THCMA point into a new direction (third quadrant), which has not been covered by any eigenvector for the targeted dataset. The variety Wappa did not express elevated CBGMA nor THCMA levels (Figure S9); thus, other low abundant or absent compounds of the newly introduced compounds with eigenvectors pointing to the top right has resulted in this variety being present in the untargeted approach in the third quadrant (while it was in the first quadrant for the targeted analysis). Additionally to Figs. 1, 2 and 3, heatmaps applying hierarchical clustering are shown in supplementary Figs. S8 and S9. These complementary multivariate analyses offer additional visualization of the data.

Discussion

Method validation

Despite the increasing demand for comprehensive product characterization [30], only a limited number of quantitative methods for the analysis of cannabis plant material spanning the range of 15 or more cannabinoids have been published so far [34, 48]. While ultraviolet (UV) or flame ionization detectors (FID) are commonly used for the robust quantification of major cannabinoids, the use of mass spectrometry has been suggested to improve specificity and widen the dynamic range [30, 48]. The latter is a prerequisite for the analysis of the lower abundant minor cannabinoids together with the typically high concentrated major cannabinoids [48].

For the presented study, deuterated and non-deuterated THC-metabolites 11-hydroxy-THC (OH-THC) and 11-nor-9-carboxy-THC (THC-COOH) were included as ISTDs for those cannabinoids where deuterated analogues were not commercially available. THCA and CBDA were calibrated using two separate calibration ranges, arising from the large concentration ranges required for these compounds. Although it would be most favorable to add the deuterated ISTDs before sample extraction, due to the required lower quantities and therefore reasonable costs, the addition of ISTDs at the final dilution step was chosen.

Sample dilution prior to analysis clearly influences the achievable LODs and LOQs. To fit analytes within a calibrated range, the injection of various dilutions poses an option; however, contamination of the analytical system and carry-over are limiting factors while, additionally, higher costs (resulting from material and longer runtimes) are disadvantageous. In the presented study, 14 out of the 15 validated analytes were detected, after applying a dilution of minimally 1:5000 to a sample of 50 mg plant material in 2 mL MeOH, which resulted in no contamination of the analytical system and no carry-over (assessed via blank injections between samples). The injection of higher concentrated samples was not possible due to the aforementioned limitations (contamination of the analytical system and carry-over). Selectivity was assessed via the measurement of diluted tea extracts and blank injections. The lack of a cannabinoid-free matrix hinders classical selectivity testing, which typically requires the measurement of blank matrices. Due to the same reason, preparation of matrix calibrators was not possible, requiring calibrators to be prepared in the solvent [48].

Cannabinoid quantification

For the varieties belonging to phenotype I, the mean $\text{THC}_{\text{Total}}$ content ranged from 10.6 to 18.5%. The United Nations Office on Drugs and Crime (UNODC) reported

increasing $\text{THC}_{\text{Total}}$ contents over the past decades in cannabis herbal preparations, with mean THC contents of approximately 10% in Europe and 15% in the USA in 2019 [21]. Thus, the herein investigated varieties belonging to phenotype I can be considered to span the range from average to high potency cannabis. Four varieties belonged to phenotype II, which is not believed to be commonly found on the recreational drug market [49]. Nonetheless, the varieties Pot of Gold and Pot of Gold nr. 11 both produced nearly equaling $\text{THC}_{\text{Total}}$ and $\text{CBD}_{\text{Total}}$ contents, therefore exhibited a similar THC/CBD profile as the marketed medicinal preparation Sativex® [34]. CBD itself is being investigated for various implications. It has been shown that CBD modulates the effects of THC; however, the interplaying effects of THC and CBD are not entirely understood [50]. In this study, CBL was not detectable in any samples. CBL is produced from CBC under heating, e.g., during smoking [1]. Therefore, under suitable storage conditions (cool and dry), the CBL content is expected to be very low.

The herein analyzed plants were cultivated and stored under identical and standardized conditions, therefore, eliminating changes introduced via heat, radiation, and prolonged storage periods, all influences which are believed to alter cannabinoid composition, e.g., by decarboxylation of acidic cannabinoids [2]. The standardized cultivation and storage conditions enable the assessment of inter-variety differences. In the presented study, Durban × Malawi and Amnesia × SFV showed high variability in their cannabinoid contents (as also seen in the PCA plots). In contrast to the other varieties, Durban × Malawi and Amnesia × SFV were grown from seeds and not cultivated from cuttings. Therefore, a higher variability of plant constituents was expected [1].

In a recent study, Scheunemann et al. [34] examined potential markers to distinguish medicinal from recreational cannabis intake, based on the analysis of 27 seized cannabis samples (all belonging to phenotype I) and various medicinal preparations, including Sativex®. The aforementioned authors developed and validated an analytical method for the detection and quantification of 16 cannabinoids, expanding the herein presented method with the analyte CBLA. Similar quantitative results as obtained in this study were obtained.

Untargeted workflow

The introduction of high-resolution mass spectrometry considerably changed the field of cannabinoid analytics, largely due to the new possibility of complementing targeted approaches with untargeted analyses [30]. The untargeted analysis applied herein resulted in the detection of 19 additional compounds. Of those additional compounds, 9 were assigned to cannabinoids described in literature. However, as of today, reference materials of many minor cannabinoids are not readily available, especially for the acidic precursors

(e.g., CBEA, CBTA, CBGMA) [30]. For full substance identification, regarding these tentatively assigned compounds, reference standards becoming available in the future should be measured. In recent years, the discovery of cannabidibutol (CBDB, CBD-C₄) [51], Δ^9 -tetrahydrocannabinol (THCB, THC-C₄) [52], cannabidiphorol (CBDP, CBD-C₇), and Δ^9 -tetrahydrocannabiphorol (THCP, THC-C₇) [53] in cannabis inflorescences attracted a lot of attention in the scientific community [54]. THCP levels in cannabis inflorescences after heating-induced decarboxylation have recently been published by Bueno et al. [54], who reported THCP levels ranging from 0.0023 to 0.0136%. In the presented study, THCBA (referred to as THCA-C₄ in the presented study) was detected in 17 out of 18 varieties. CBDDBA, CBDPA, and THCPA remained undetected, probably due to LODs not being low enough. Nonetheless, various additional cannabinoids have been tentatively identified using the herein presented approach. In a recent study, Montone et al. [47] employed a similar workflow using the Compound Discoverer™ software. The aforementioned authors were able to identify 121 phytocannabinoids, highlighting the potential of untargeted analyses in phytocannabinoid characterization.

Comparison of varieties

Traditional classification based on THC and CBD contents [6, 16, 17] allowed differentiation of the investigated cannabis varieties into phenotypes I and II. As previously observed in other studies [6, 18, 24, 25, 27, 37, 39, 55], comprehensive analytical methods combined with multivariate statistical analyses, e.g., PCA, enabled for further subgrouping of cannabis varieties. The presented data concerning the PCA complemented the traditionally applied classification into phenotypes I, II, and III. The targeted and untargeted approach inarguably displayed a more refined and detailed image of the cannabinoid fingerprint. However, PCA also confirmed the important role of THCA and CBDA in the distinction of varieties, as these eigenvectors presented the highest divergence in the presented loading plot for the targeted data (Fig. 2). Comparing the PCA results obtained from the targeted versus the untargeted approach, slight differences in the observed clusters were seen: clustering was enhanced for some varieties, while it decreased for others depending on the dataset used. The untargeted approach resulted in the additional detection of further compounds, whereas the targeted approach has undergone method validation resulting in higher confidence in the obtained results and offering quantitative information. Consequently, regarding the characterization of cannabis varieties, both approaches have their eligibility.

Selected compounds were shown to be rather specific for some varieties, making them interesting as potential distinguishing markers. For instance, the 6,7-epoxy-CBGA

isomers 1 and 2 are markers for the varieties Pot of Gold and Pot of Gold nr. 11 belonging to the phenotype II. Interestingly, THCA and CBGMA resulted in eigenvectors pointing in a new direction in the loading plot (Fig. 3); however, the short length of the eigenvectors implies little discriminative value overall. The shorter alkyl-chain homologues of THC (THC-C1, THC-C4) were additional markers, distinct for plants of the phenotypes I, which was expected due to the close relation to THCA. CBGA and CBG levels contributed largely to the distinction within varieties belonging to phenotype I. THCA was highly indicative for the variety Malawi × Super Skunk, which presented a unique chemical fingerprint.

Limitations

The presented study was limited by the small number of samples per variety. As a result, the 95% CI for the PCA could only be calculated for one variety. The analytical procedure (e.g., chromatography and mass range of 200–400 m/z) was developed and optimized for cannabinoids. Other compound families (terpenoids and flavonoids) and other plant metabolites were, therefore, not the subject of this study.

While the standardized cultivation and storage conditions are regarded as an advantage in order to detect inter-variety differences, they might not be representative for the (illicit) recreational cannabis market. Ultimately, this limits the transferability of the presented results to settings encountered in forensic chemistry, where storage times and conditions of seized samples are generally not accessible. Finally, although popular names, e.g., Amnesia or White Widow [18], are commonly used to describe varieties, lack of classification as well as crossbreeding (especially for plants grown from seeds) must be considered when comparing results. The comparability of similar varieties obtained from various sources was beyond the scope of this study but is required to prove whether the herein reported results are transferable or not.

Conclusion

The increasing availability of cannabis and derived products are posing the need for comprehensive analytical methods. The presented workflow comprised the expansion of a targeted method used for the quantification of 15 cannabinoids with an untargeted approach, employing *in silico* assisted identification of additional compounds. Thereby, new possibilities arising from high-resolution mass spectrometry in the field of *cannabinomics* are highlighted. PCA revealed additional subgroups, indicating distinct chemical composition of some varieties. Selected compounds, e.g., THVA, THCA homologues, and 6,7-epoxy-CBGA isomers 1 and 2,

showed the potential to be used as distinguishing markers. Controlled cultivation and storage conditions enabled the assessment of intra- and inter-variety variability between plants. Expansion of the presented methodologies for chemical characterization of other materials than cannabis inflorescences, such as extracts, is conceivable, although requiring further validation. The presented approach provides a comprehensive and versatile means for cannabinoid fingerprinting on the product level. In-depth knowledge at the product level is key for product standardization, considered fundamental to ensure reproducible effects in humans (e.g., medicinal products) and may result in improved bioanalytical data interpretation in the medico-legal field.

Supplementary Information The online version contains supplementary material available at <https://doi.org/10.1007/s00216-022-04026-2>.

Acknowledgements We thank Suisse BioHemp AG for providing cannabis sample material. We also express our gratitude to Remo Monti for his assistance in statistical data evaluation.

Funding Open access funding provided by University of Basel

Declarations

Conflict of interest The authors declare no competing interests.

Open Access This article is licensed under a Creative Commons Attribution 4.0 International License, which permits use, sharing, adaptation, distribution and reproduction in any medium or format, as long as you give appropriate credit to the original author(s) and the source, provide a link to the Creative Commons licence, and indicate if changes were made. The images or other third party material in this article are included in the article's Creative Commons licence, unless indicated otherwise in a credit line to the material. If material is not included in the article's Creative Commons licence and your intended use is not permitted by statutory regulation or exceeds the permitted use, you will need to obtain permission directly from the copyright holder. To view a copy of this licence, visit <http://creativecommons.org/licenses/by/4.0/>.

References

1. ElSohly MA, Radwan MM, Gul W, Chandra S, Galal A. Phytochemistry of Cannabis sativa L. In: Kinghorn AD, Falk H, Gibbons S, Ji K, editors. *Phytocannabinoids: unraveling the complex chemistry and pharmacology of Cannabis sativa*. Cham: Springer International Publishing; 2017. p. 1–36.
2. Gülcük T, Møller BL. Phytocannabinoids: origins and biosynthesis. *Trends Plant Sci*. 2020;25(10):985–1004. <https://doi.org/10.1016/j.tplants.2020.05.005>.
3. Carliner H, Brown QL, Sarvet AL, Hasin DS. Cannabis use, attitudes, and legal status in the U.S.: a review. *Prev Med*. 2017;104:13–23. <https://doi.org/10.1016/j.ypmed.2017.07.008>.
4. Shanahan M, Cyrenne P. Cannabis policies in Canada: how will we know which is best? *Int J Drug Policy*. 2021;91:102556. <https://doi.org/10.1016/j.drugpo.2019.09.004>.
5. Manthey J, Freeman TP, Kilian C, López-Pelayo H, Rehm J. Public health monitoring of cannabis use in Europe: prevalence of use, cannabis potency, and treatment rates. *Lancet Reg Health Eur*. 2021;10:100227. <https://doi.org/10.1016/j.lanepe.2021.100227>.
6. Vásquez-Ocmín PG, Marti G, Bonhomme M, Mathis F, Fournier S, Bertani S, et al. Cannabinoids vs. whole metabolome: relevance of cannabinomics in analyzing Cannabis varieties. *Anal Chim Acta*. 2021;1184:339020. <https://doi.org/10.1016/j.aca.2021.339020>.
7. Ladha KS, Ajrawat P, Yang Y, Clarke H. Understanding the medical chemistry of the cannabis plant is critical to guiding real world clinical evidence. *Molecules*. 2020;25(18):4042. <https://doi.org/10.3390/molecules25184042>.
8. United Nations. UN commission reclassifies cannabis, yet still considered harmful. <https://news.un.org/en/story/2020/12/1079132>. Accessed 5 Jan 2022.
9. Gould J. The cannabis crop. *Nature*. 2015;525:S2. <https://doi.org/10.1038/525S2a>.
10. Russo EB. Cannabidiol claims and misconceptions. *Trends Pharmacol Sci*. 2017;38(3):198–201. <https://doi.org/10.1016/j.tips.2016.12.004>.
11. Izzo AA, Borrelli F, Capasso R, Di Marzo V, Mechoulam R. Non-psychoactive plant cannabinoids: new therapeutic opportunities from an ancient herb. *Trends Pharmacol Sci*. 2009;30(10):515–27. <https://doi.org/10.1016/j.tips.2009.07.006>.
12. Pisanti S, Malfitano AM, Ciaglia E, Lamberti A, Ranieri R, Cuomo G, et al. Cannabidiol: state of the art and new challenges for therapeutic applications. *Pharmacol Ther*. 2017;175:133–50. <https://doi.org/10.1016/j.pharmthera.2017.02.041>.
13. Crippa JA, Guimarães FS, Campos AC, Zuardi AW. Translational investigation of the therapeutic potential of cannabidiol (CBD): toward a new age. *Front Immunol*. 2018;9:2009. <https://doi.org/10.3389/fimmu.2018.02009>.
14. Freeman TP, Hindocha C, Green SF, Bloomfield MAP. Medicinal use of cannabis based products and cannabinoids. *BMJ*. 2019;365:11141-1. <https://doi.org/10.1136/bmj.11141>.
15. Hanuš LO, Meyer SM, Muñoz E, Tagliatalata-Scafati O, Appendino G. Phytocannabinoids: a unified critical inventory. *Nat Prod Rep*. 2016;33(12):1357–92. <https://doi.org/10.1039/C6NP00074F>.
16. Small E. Classification of Cannabis sativa L. in relation to agricultural, biotechnological, medical and recreational utilization. In: Chandra S, Lata H, ElSohly MA, editors. *Cannabis sativa L - botany and biotechnology*. Cham: Springer International Publishing; 2017. p. 1–62.
17. Small E, Beckstead HD. Cannabinoid phenotypes in Cannabis sativa. *Nature*. 1973;245(5421):147–8. <https://doi.org/10.1038/245147a0>.
18. Hazekamp A, Fishedick JT. Cannabis - from cultivar to chemovar. *Drug Test Anal*. 2012;4(7–8):660–7. <https://doi.org/10.1002/dta.407>.
19. Fishedick JT. Identification of terpenoid chemotypes among high (-)-trans- $\Delta(9)$ -tetrahydrocannabinol-producing Cannabis sativa L. cultivars. *Cannabis Cannabinoid Res*. 2017;2(1):34–47. <https://doi.org/10.1089/can.2016.0040>.
20. Fournier G, Richez-Dumanois C, Duvezin J, Mathieu JP, Paris M. Identification of a new chemotype in Cannabis sativa: cannabigerol - dominant plants, biogenetic and agronomic prospects. *Planta Med*. 1987;53(03):277–80. <https://doi.org/10.1055/s-2006-962705>.
21. United Nations Office on Drugs and Crime. *World Drug Report 2021. Booklet 3 - Drug market trends: Opioids, Cannabis*. https://www.unodc.org/res/wdr2021/field/WDR21_Booklet_3.pdf. Accessed 3 Jan 2022.
22. Baron EP. Medicinal properties of cannabinoids, terpenes, and flavonoids in cannabis, and benefits in migraine, headache, and pain: an update on current evidence and cannabis science. *Headache*. 2018;58(7):1139–86. <https://doi.org/10.1111/head.13345>.

23. Andre CM, Hausman J-F, Guerriero G. Cannabis sativa: the plant of the thousand and one molecules. *Front Plant Sci.* 2016;7:19. <https://doi.org/10.3389/fpls.2016.00019>.
24. Berman P, Futoran K, Lewitus GM, Mukha D, Benami M, Shlomi T, et al. A new ESI-LC/MS approach for comprehensive metabolic profiling of phytocannabinoids in Cannabis. *Sci Rep.* 2018;8(1):14280. <https://doi.org/10.1038/s41598-018-32651-4>.
25. Berman P, Sulimani L, Gelfand A, Amsalem K, Lewitus GM, Meiri D. Cannabinoidomics – an analytical approach to understand the effect of medical cannabis treatment on the endocannabinoid metabolome. *Talanta.* 2020;219:121336. <https://doi.org/10.1016/j.talanta.2020.121336>.
26. Russo EB. Taming THC: potential cannabis synergy and phytocannabinoid-terpenoid entourage effects. *Br J Pharmacol.* 2011;163(7):1344–64. <https://doi.org/10.1111/j.1476-5381.2011.01238.x>.
27. Cerrato A, Citti C, Cannazza G, Capriotti AL, Cavaliere C, Grassi G, et al. Phytocannabinomics: untargeted metabolomics as a tool for cannabis chemovar differentiation. *Talanta.* 2021;230:122313. <https://doi.org/10.1016/j.talanta.2021.122313>.
28. Namdar D, Mazuz M, Ion A, Koltai H. Variation in the compositions of cannabinoid and terpenoids in Cannabis sativa derived from inflorescence position along the stem and extraction methods. *Ind Crops Prod.* 2018;113:376–82. <https://doi.org/10.1016/j.indcrop.2018.01.060>.
29. Aliferis KA, Bernard-Perron D. Cannabinomics: application of metabolomics in Cannabis (Cannabis sativa L.) research and development. *Front Plant Sci.* 2020;11(554). <https://doi.org/10.3389/fpls.2020.00554>.
30. Capriotti AL, Cannazza G, Catani M, Cavaliere C, Cavazzini A, Cerrato A, et al. Recent applications of mass spectrometry for the characterization of cannabis and hemp phytocannabinoids: from targeted to untargeted analysis. *J Chromatogr A.* 2021;1655:462492. <https://doi.org/10.1016/j.chroma.2021.462492>.
31. Calvi L, Pentimalli D, Panseri S, Giupponi L, Gelmini F, Beretta G, et al. Comprehensive quality evaluation of medical Cannabis sativa L. inflorescence and macerated oils based on HS-SPME coupled to GC–MS and LC–HRMS (q-exactive orbitrap®) approach. *J Pharm Biomed Anal.* 2018;150:208–19. <https://doi.org/10.1016/j.jpba.2017.11.073>.
32. Karschner EL, Swortwood-Gates MJ, Huestis MA. Identifying and quantifying cannabinoids in biological matrices in the medical and legal cannabis era. *Clin Chem.* 2020;66(7):888–914. <https://doi.org/10.1093/clinchem/hvaa113>.
33. Scheunemann A, Elsner K, Germerott T, Groppa S, Hess C, Miederer I, et al. Identification of potential distinguishing markers for the use of cannabis-based medicines or street cannabis in serum samples. *Metabolites.* 2021;11(5):316. <https://doi.org/10.3390/metabo11050316>.
34. Scheunemann A, Elsner K, Germerott T, Hess C, Zörntlein S, Röhrich J. Extensive phytocannabinoid profiles of seized cannabis and cannabis-based medicines – identification of potential distinguishing markers. *Forensic Sci Int.* 2021;322:110773. <https://doi.org/10.1016/j.forsciint.2021.110773>.
35. Kraemer M, Madea B, Hess C. Detectability of various cannabinoids in plasma samples of cannabis users: Indicators of recent cannabis use? *Drug Test Anal.* 2019;11(10):1498–506. <https://doi.org/10.1002/dta.2682>.
36. Levin FR, Mariani JJ, Brooks DJ, Xie S, Murray KA. Δ^9 -Tetrahydrocannabinol testing may not have the sensitivity to detect marijuana use among individuals ingesting dronabinol. *Drug Alcohol Depend.* 2010;106(1):65–8. <https://doi.org/10.1016/j.drugalcdep.2009.07.021>.
37. Fishedick JT, Hazekamp A, Erkelens T, Choi YH, Verpoorte R. Metabolic fingerprinting of Cannabis sativa L., cannabinoids and terpenoids for chemotaxonomic and drug standardization purposes. *Phytochemistry.* 2010;71(17):2058–73. <https://doi.org/10.1016/j.phytochem.2010.10.001>.
38. Elzinga S, Fishedick J, Podkolinski R, Raber J. Cannabinoids and terpenes as chemotaxonomic markers in cannabis. *Nat Prod Chem Res.* 2015;3(4). <https://doi.org/10.4172/2329-6836.1000181>.
39. Hazekamp A, Tejkalová K, Papadimitriou S. Cannabis: from cultivar to chemovar II—a metabolomics approach to cannabis classification. *Cannabis Cannabinoid Res.* 2016;1(1):202–15. <https://doi.org/10.1089/can.2016.0017>.
40. Slosse A, Van Durme F, Samyn N, Mangelings D, Vander HY. Evaluation of data preprocessings for the comparison of GC–MS chemical profiles of seized cannabis samples. *Forensic Sci Int.* 2020;310:110228. <https://doi.org/10.1016/j.forsciint.2020.110228>.
41. Pinto RC. Chemometrics methods and strategies in metabolomics. In: Sussulini A, editor. *Metabolomics: from fundamentals to clinical applications.* Cham: Springer International Publishing; 2017. p. 163–90.
42. Raharjo TJ, Verpoorte R. Methods for the analysis of cannabinoids in biological materials: a review. *Phytochem Anal.* 2004;15(2):79–94. <https://doi.org/10.1002/pca.753>.
43. Hazekamp A, Peltenburg A, Verpoorte R, Giroud C. Chromatographic and spectroscopic data of cannabinoids from Cannabis sativa L. *J Liq Chromatogr Relat Technol.* 2005;28(15):2361–82. <https://doi.org/10.1080/10826070500187558>.
44. De Vijlder T, Valkenburg D, Lemièrre F, Romijn EP, Laukens K, Cuyckens F. A tutorial in small molecule identification via electrospray ionization-mass spectrometry: the practical art of structural elucidation. *Mass Spectrom Rev.* 2018;37(5):607–29. <https://doi.org/10.1002/mas.21551>.
45. Lê S, Josse J, Husson F. FactoMineR: An R package for multivariate analysis. *J Stat Softw.* 2008;25(1):1–18. <https://doi.org/10.18637/jss.v025.i01>.
46. Piccolella S, Crescente G, Formato M, Pacifico S. A cup of hemp coffee by Moka Pot from Southern Italy: an UHPLC–HRMS investigation. *Foods.* 2020;9(8). <https://doi.org/10.3390/foods9081123>.
47. Montone CM, Cerrato A, Botta B, Cannazza G, Capriotti AL, Cavaliere C, et al. Improved identification of phytocannabinoids using a dedicated structure-based workflow. *Talanta.* 2020;219:121310. <https://doi.org/10.1016/j.talanta.2020.121310>.
48. McRae G, Melanson JE. Quantitative determination and validation of 17 cannabinoids in cannabis and hemp using liquid chromatography–tandem mass spectrometry. *Anal Bioanal Chem.* 2020;412(27):7381–93. <https://doi.org/10.1007/s00216-020-02862-8>.
49. ElSohly MA, Mehmedic Z, Foster S, Gon C, Chandra S, Church JC. Changes in cannabis potency over the last 2 decades (1995–2014): analysis of current data in the United States. *Biol Psychiatry.* 2016;79(7):613–9. <https://doi.org/10.1016/j.biopsych.2016.01.004>.
50. Freeman AM, Petrilli K, Lees R, Hindocha C, Mokrysz C, Curran HV, et al. How does cannabidiol (CBD) influence the acute effects of delta-9-tetrahydrocannabinol (THC) in humans? A systematic review. *Neurosci Biobehav Rev.* 2019;107:696–712. <https://doi.org/10.1016/j.neubiorev.2019.09.036>.
51. Citti C, Linciano P, Forni F, Vandelli MA, Gigli G, Laganà A, et al. Analysis of impurities of cannabidiol from hemp. Isolation, characterization and synthesis of cannabidibutol, the novel cannabidiol butyl analog. *J Pharm Biomed Anal.* 2019;175:112752. <https://doi.org/10.1016/j.jpba.2019.06.049>.

52. Linciano P, Citti C, Russo F, Tolomeo F, Laganà A, Capriotti AL, et al. Identification of a new cannabidiol n-hexyl homolog in a medicinal cannabis variety with an antinociceptive activity in mice: cannabidihexol. *Sci Rep.* 2020;10(1):22019. <https://doi.org/10.1038/s41598-020-79042-2>.
53. Citti C, Linciano P, Russo F, Luongo L, Iannotta M, Maione S, et al. A novel phytocannabinoid isolated from *Cannabis sativa* L. with an in vivo cannabimimetic activity higher than Δ^9 -tetrahydrocannabinol: Δ^9 -tetrahydrocannabiphorol. *Sci Rep.* 2019;9(1):20335. <https://doi.org/10.1038/s41598-019-56785-1>.
54. Bueno J, Greenbaum EA. (–)-trans- Δ^9 -Tetrahydrocannabiphorol content of *Cannabis sativa* inflorescence from various chemotypes. *J Nat Prod.* 2021;84(2):531–6. <https://doi.org/10.1021/acs.jnatprod.0c01034>.
55. Elzinga S, Fishedick J, Podkolinski R, Raber J. Cannabinoids and terpenes as chemotaxonomic markers in cannabis. *Nat Prod Chem Res.* 2015;3. <https://doi.org/10.4172/2329-6836.1000181>.

Publisher's note Springer Nature remains neutral with regard to jurisdictional claims in published maps and institutional affiliations.

Supporting information:

Beyond $\Delta 9$ -tetrahydrocannabinol and cannabidiol: Chemical differentiation of cannabis varieties applying targeted and untargeted analysis

Authors: Manuela Carla Monti; Priska Frei; Sophie Weber; Eva Scheurer; Katja Mercer-Chalmers-Bender*

Affiliation: Institute of Forensic Medicine, Department of Biomedical Engineering, University of Basel, Basel, Switzerland

*Corresponding author, *katja.mercer-chalmers-bender@unibas.ch*

List of Supplementary Figures

- Figure S1 Exemplary extracted ion chromatograms (p. 9)
- Figure S2 Advanced parameters applied for the untargeted data processing in the Compound Discoverer™ Software (p. 10)
- Figure S3 Source code for the principal component analysis (PCA) and plotting (loading plots) in R (p. 11)
- Figure S4 Source code data normalization (z-score transformation) and hierarchical clustering in R (p. 12)
- Figure S5 Exemplary mass trace of $\Delta 9$ -THC and its isomer $\Delta 8$ -THC (p. 12)
- Figure S6 PCA loading plot of the targeted analysis showing 95% confidence interval (95%-CI) for Duban x Malawi (p. 16)
- Figure S7 PCA loading plot of the untargeted analysis showing 95% confidence interval (95%-CI) for Duban x Malawi (p. 17)
- Figure S8 Heatmap applying hierarchical clustering of the targeted dataset (contents) (p. 18)
- Figure S9 Heatmap applying hierarchical clustering of the untargeted dataset (area) (p. 19)

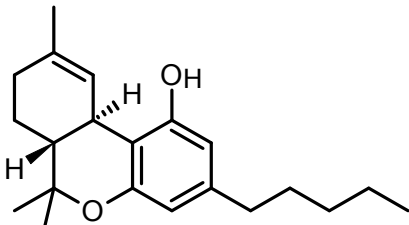
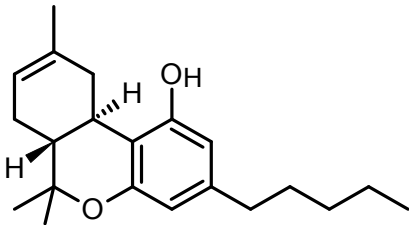
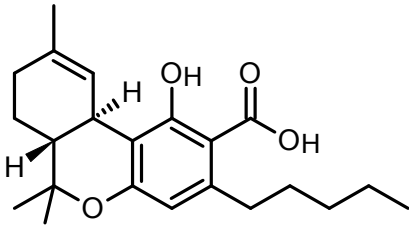
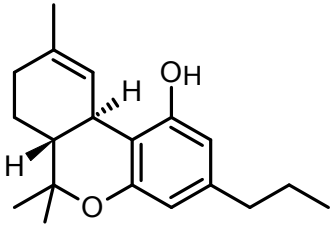
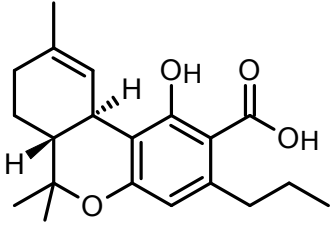
List of Supplementary Tables

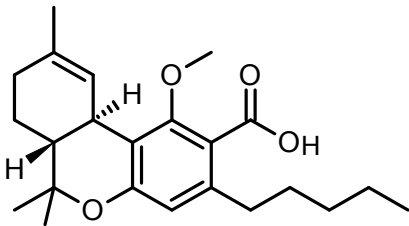
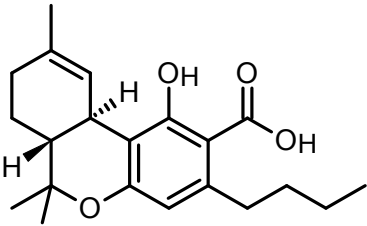
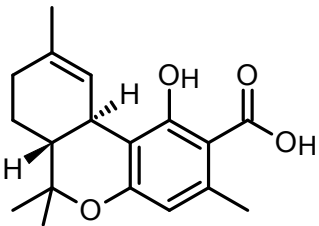
- Table S1 List of certified reference material including vendors (p. 2)
- Table S2 Structures of cannabinoids contained in the targeted method and detected during the untargeted workflow (p. 3 - 8)
- Table S3 Summary of validation results (p. 13)
- Table S4 Cannabinoid contents (acid and free shown separately) of the investigated cannabis varieties (p.14)
- Table S5 Total cannabinoid contents (acid + free) of the investigated cannabis varieties (p. 15)

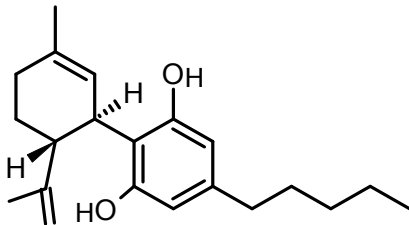
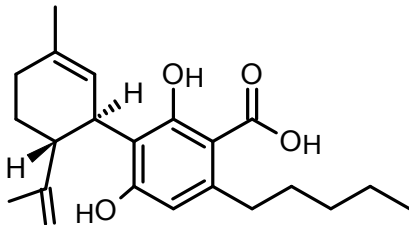
Table S1 List of the used certified reference material (CRM) and respective vendors

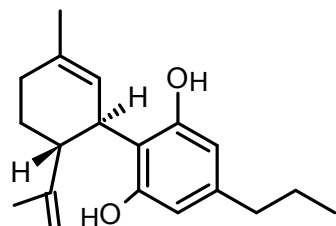
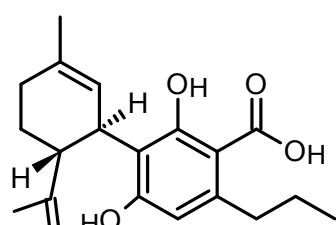
Analyte	Full name	Vendor
Δ^9 -THC (THC)	Δ^9 -Tetrahydrocannabinol	Lipomed (Arlesheim, Switzerland)
Δ^8 -THC	Δ^8 -Tetrahydrocannabinol	Lipomed (Arlesheim, Switzerland)
D_3 - Δ^9 -THC	Deuterated THC	Lipomed (Arlesheim, Switzerland)
THCA	THC-acid	Lipomed (Arlesheim, Switzerland)
THCV	Tetrahydrocannabinolvarin	Merck (Buch, Switzerland)
THCVA	Tetrahydrocannabinolvarin acid	Merck (Buch, Switzerland)
CBD	Cannabidiol	Lipomed (Arlesheim, Switzerland)
D_3 -CBD	Deuterated CBD	Lipomed (Arlesheim, Switzerland)
CBDa	CBD-acid	Lipomed (Arlesheim, Switzerland)
CBDV	Cannabidiolvarin	Merck (Buch, Switzerland)
CBDVA	Cannabidiolvarinic acid	Merck (Buch, Switzerland)
CBN	Cannabinol	Lipomed (Arlesheim, Switzerland)
D_3 -CBN	Deuterated CBN	Lipomed (Arlesheim, Switzerland)
CBNA	CBN-acid	Merck (Buch, Switzerland)
CBC	Cannabichromene	Lipomed (Arlesheim, Switzerland)
D_9 -CBC	Deuterated CBC	Gayman Chemical Company (Michigan, USA)
CBCA	Cannabichromenic acid	Merck (Buch, Switzerland)
CBG	Cannabigerol	Lipomed (Arlesheim, Switzerland)
CBGA	CBG-acid	Merck (Buch, Switzerland)
CBL	Cannabicyclol	Merck (Buch, Switzerland)
OH-THC	11-hydroxy-THC	Lipomed (Arlesheim, Switzerland)
OH-THC-D3	Deuterated 11-hydroxy-THC	Lipomed (Arlesheim, Switzerland)
THC-COOH	11-nor-9-carboxy-THC	Lipomed (Arlesheim, Switzerland)
THC-COOH-D9	Deuterated 11-nor-9-carboxy-THC	Lipomed (Arlesheim, Switzerland)

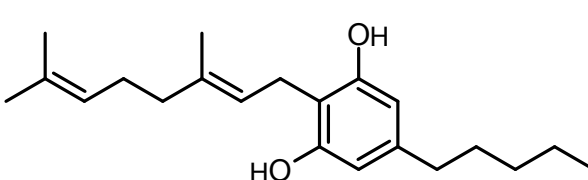
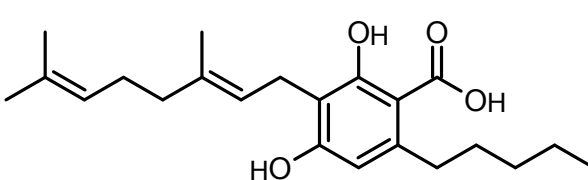
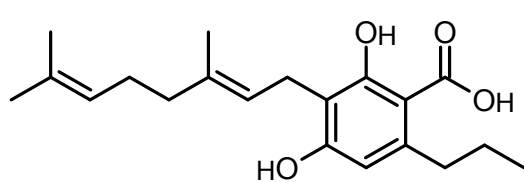
Table S2 Structures, CAS numbers (where available), and chemical formula of cannabinoids contained in the targeted method and detected during the untargeted workflow (tentatively identified). "n.a." stands for not applicable

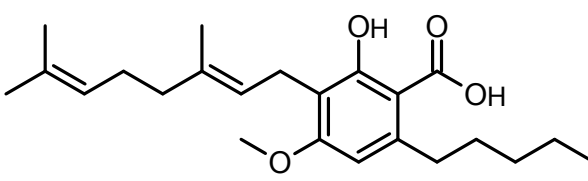
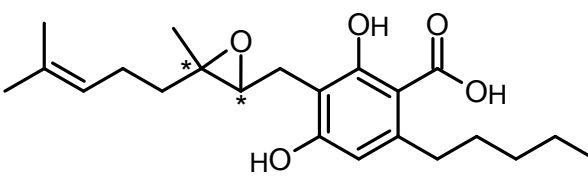
THC-type			
Analyte	CAS	Formula	Full name and chemical structure
Δ^9 -THC	1972-08-3	$C_{21}H_{30}O_2$	<p>Δ^9-Tetrahydrocannabinol</p> 
Δ^8 -THC	5957-75-5	$C_{21}H_{30}O_2$	<p>Δ^8-Tetrahydrocannabinol</p> 
THCA	23978-85-0	$C_{22}H_{30}O_4$	<p>Δ^9-Tetrahydrocannabinolic acid</p> 
THCV	31262-37-0	$C_{19}H_{26}O_2$	<p>Tetrahydrocannabidivarin</p> 
THCVA	39986-26-0	$C_{20}H_{26}O_4$	<p>Tetrahydrocannabidivarin acid</p> 

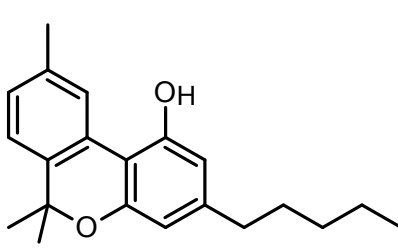
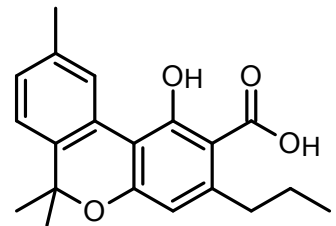
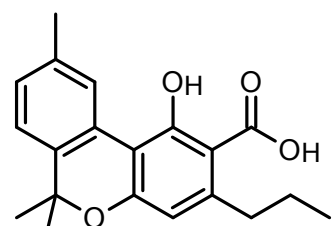
THCMA	n.a.	$C_{23}H_{32}O_4$	<p>Tetrahydrocannabinolic acid monomethyl ester</p> 
THCBA THCA-C4	n.a.	$C_{21}H_{28}O_4$	<p>Tetrahydrocannabutolic acid</p> 
THCA-C1	n.a.	$C_{18}H_{22}O_4$	<p>Tetrahydrocannabinolic acid-C1 = Tetrahydrocannabiorcolic acid</p> 

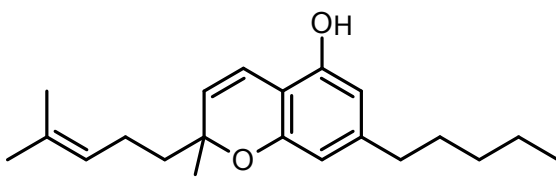
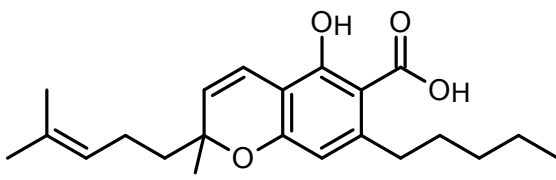
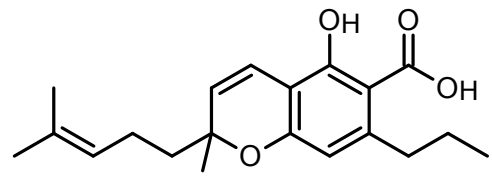
CBD-type			
Analyte	CAS	formula	Full name and chemical structure
CBD	13956-29-1	$C_{21}H_{30}O_2$	<p>Cannabidiol</p> 
CBDA	1244-58-2	$C_{22}H_{30}O_4$	<p>Cannabidiolic acid</p> 

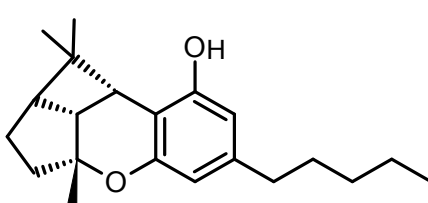
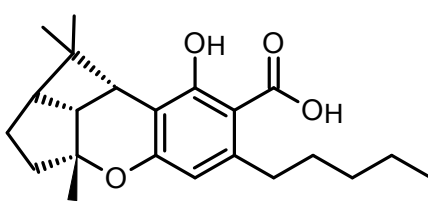
CBDV	24274-48-4	C ₁₉ H ₂₆ O ₂	Cannabidivarin 
CBDVA	31932-13-5	C ₂₀ H ₂₆ O ₄	Cannabidivarinic acid 

CBG-type			
Analyte	CAS		Full name and chemical structure
CBG	25654-31-3	C ₂₁ H ₃₂ O ₂	Cannabigerol 
CBGA	25555-57-1	C ₂₂ H ₃₂ O ₄	Cannabigerolic acid 
CBGVA	64924-07-8	C ₂₀ H ₂₈ O ₄	Cannabigerivarinic acid 

CBGMA	29624-08-6	C ₂₃ H ₃₄ O ₄	Cannabigerolic acid monomethyl ester 
6,7-Epoxy-CBGA	n.a.	C ₂₂ H ₃₂ O ₅	6,7-Epoxy-cannabigerolic acid isomers 1 and 2 

CBN-type			
Analyte	CAS		Full name and chemical structure
CBN	13956-29-1	C ₂₁ H ₂₆ O ₂	Cannabinol 
CBNA	2808-39-1	C ₂₂ H ₂₆ O ₄	Cannabinolic acid 
CBNVA	n.a.	C ₂₀ H ₂₂ O ₄	Cannabinovarinic acid 

CBC-type			
Analyte	CAS		Full name and chemical structure
CBC	20675-51-8	$C_{21}H_{30}O_2$	Cannabichromene 
CBCA	185505-15-1	$C_{22}H_{30}O_4$	Cannabichromenic acid 
CBCVA	64898-02-8	$C_{20}H_{26}O_4$	Cannabichromevarinic acid 

CBL-type			
Analyte	CAS	Formula	Full name and chemical structure
CBL	21366-63-2	$C_{21}H_{30}O_2$	Cannabicyclol 
CBLA	n.a.	$C_{22}H_{30}O_4$	Cannabicycloic acid 

CBT-type			
Analyte	CAS	Formula	Full name and chemical structure
CBTA	n.a.	$C_{22}H_{30}O_6$	<p>Cannabitrilic acid</p>

CBE-type			
Analyte	CAS	Formula	Full name and chemical structure
CBEA	n.a.	$C_{22}H_{30}O_5$	<p>Cannabielsoinic acid</p>

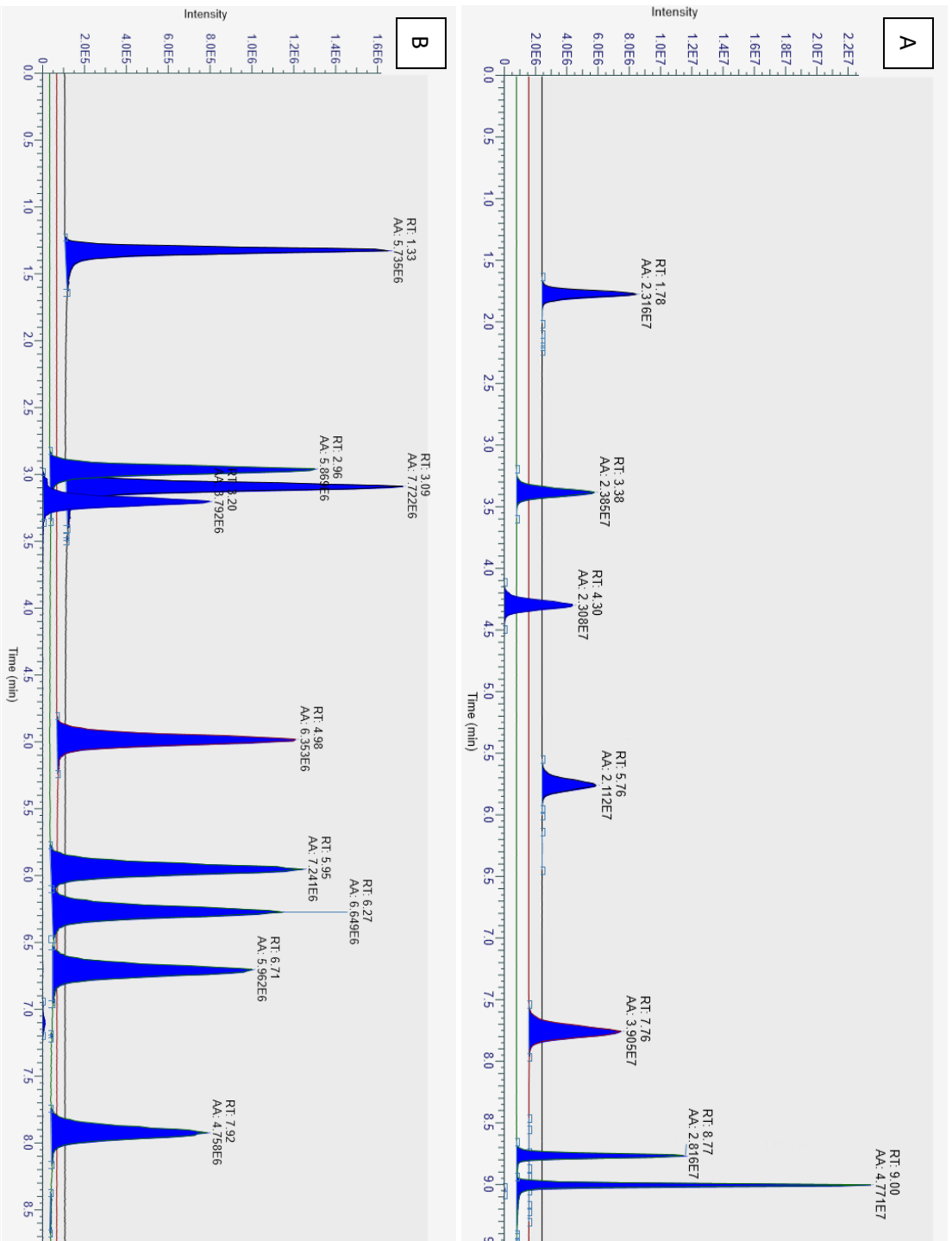


Figure S1 Exemplary extracted ion chromatograms (QC samples at 80 ng/mL including Δ8-THC at 80 ng/mL, 5 ppm mass tolerance). A: negative ionization mode: CBCVA (1.78 min), CBDA (3.38 min), CBGA (4.30 min), THCVA (5.76 min), CBNA (7.76 min), THCA (8.77 min), CBCA (9.05 min). B: positive ionization mode: CBDV (1.33 min), CBD (2.96 min), THCV (3.09 min), CBG (3.20 min), CBN (4.98), Δ9-THC (5.95 min), Δ8-THC (6.27 min), CBL (6.71 min), CBC (7.92 min)

Select Spectra:

- 1. General Settings
 - Precursor Selection Use MSI Precursor
 - Provide Profile Sp: Automatic
- 2. Spectrum Properties Filter
 - Lower RT Limit 0
 - Upper RT Limit 0
 - First Scan 0
 - Last Scan 0
 - Ignore Specified Si
 - Lowest Charge Sta 0
 - Highest Charge Sta 0
 - Min. Precursor Ma 0 Da
 - Max. Precursor Ma 5000 Da
 - Total Intensity Thn 0
 - Minimum Peak Co 1
- 3. Scan Event Filters
 - Mass Analyzer (Not specified)
 - MS Order Any
 - Activation Type (Not specified)
 - Min. Collision Ener 0
 - Max. Collision Ener 1000
 - Scan Type Any
 - Polarity Mode (Not specified)
- 4. Peak Filters
 - S/N Threshold (FT-1.5)
- 5. Replacements for Unrecognized Properties
 - Unrecognized Cha 1
 - Unrecognized Mar MM5
 - Unrecognized MS MS2
 - Unrecognized Acti CID
 - Unrecognized Pol -
 - Unrecognized MS 60000
 - Unrecognized MSI 30000

Align Retention Times:

- 1. General Settings
 - Alignment Model Adaptive curve
 - Maximum Shift (m 2
 - Mass Tolerance 5 ppm

Create Mass Trace:

- 1. General Settings
 - Trace Type BPC
 - MS Order MSI
 - Polarity +
- 2. XIC Settings
 - Mass (Da) 0
 - Mass Tolerance 5 ppm

Group Compounds:

- 1. Compound Consolidation
 - Mass Tolerance 5 ppm
 - RT Tolerance (min) 0.2
- 2. Fragment Data Selection
 - Preferred Ions [M+H]-1

Search Mass Lists:

- 1. Search Settings
 - Mass Lists \Cannabinoids neg\masslist
 - Use Retention Tim True
 - RT Tolerance (min) 0.5
 - Mass Tolerance 5 ppm

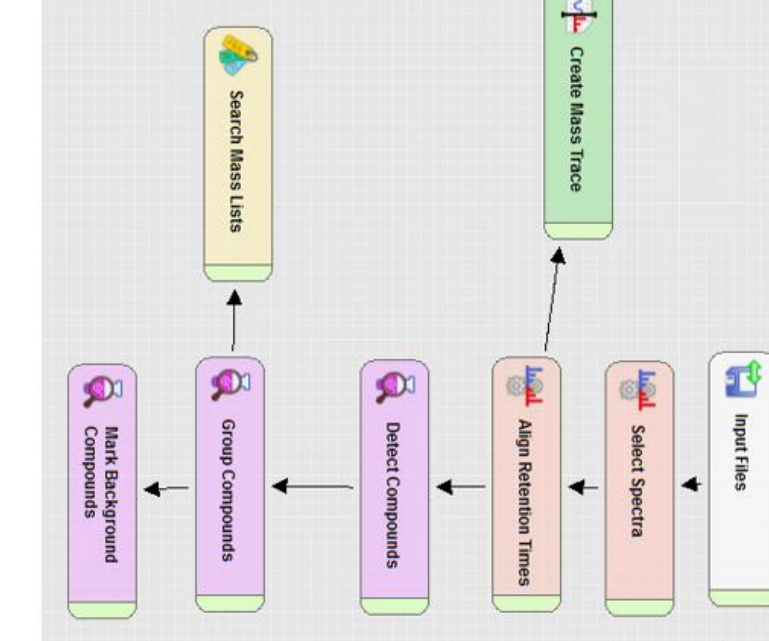


Figure S2 Advanced parameters applied for the untargeted data processing in the Compound Discoverer (Version 3.1.0.305) software from Thermo Fisher Scientific (Reinach, Switzerland)

```

library(ggplot2)
library(FactoMineR)
library(ggrepel)

mydata.pca <- FactoMineR::PCA(mydata, graph = FALSE)
plotdata <- data.frame(mydata.pca$ind$coord)
plotdata$variety <- mydata$Variety
x_dim <- 1
y_dim <- 2
scale_factor <- 5.
loadings <- data.frame(mydata.pca$var$coord) * scale_factor
loadings$label <- row.names(loadings)
loadings$origin <- 0.
ggplot(plotdata, aes_string(x=paste0('Dim.',x_dim), y=paste0('Dim.', y_dim))) +
  geom_vline(xintercept = 0, linetype=2, alpha=0.2) +
  geom_hline(yintercept = 0, linetype=2, alpha=0.2) +
  geom_segment(data = loadings, aes_string(xend=paste0('Dim.',x_dim), yend=paste0('Dim.', y_dim),
x='origin', y='origin'), arrow = arrow(length = unit(10, units = 'pt'))) +
  geom_label_repel(data=loadings, aes_string(x=paste0('Dim.',x_dim), y=paste0('Dim.', y_dim),
label='label'), ) +
  geom_point(aes(col=variety, shape=variety), size=4) +
  theme_bw() +
  xlab(paste0('PC',x_dim,' (',round(mydata.pca$eig[x_dim,'percentage of variance'],1),'%')')) +
  ylab(paste0('PC',y_dim,' (',round(mydata.pca$eig[y_dim,'percentage of variance'],1),'%')')) +
  theme(panel.border = element_blank()) +
  scale_shape_manual(values = rep(c(15:19),length.out=length(unique(plotdata$variety))))

sessionInfo()
gplots_3.1.1    ggrepel_0.9.1    FactoMineR_2.4

```

Figure S3 Source code for the principal component analysis (PCA) and plotting (scatter plots, loading plots; biplots) in R (version 3.4.3)

```

library(ggplot2)
library(cluster)
library(ggrepel)
library(gplots)
library(RColorBrewer)

mydata_norm <- scale(mydata ,center = T,scale = T)
row.names(mydata_norm) <- mydata$Variety
heatmap.2(mydata_norm, cexRow = 0.5, cellnote = mydata[,-15], notecex = 0.5, notecol = 'white', col
= colors, breaks = seq(-3,3,length.out=51), margins = c(5,8), trace = 'none')

sessionInfo()
RColorBrewer_1.1-2   gplots_3.1.1   ggrepel_0.9.1   ggplot2_3.3.5   cluster_2.1.2

```

Figure S4 Source code for data normalization (z-score transformation) and hierarchical clustering in R (version 3.4.3)

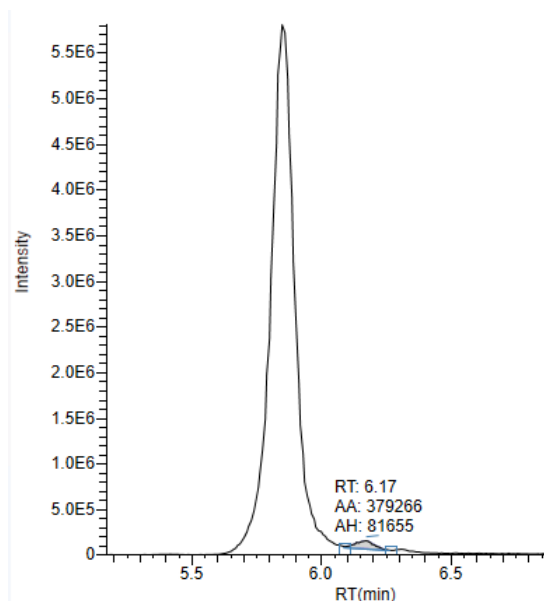


Figure S5 Mass trace (m/z 315.23157; 5 ppm mass error, positive ionization mode) corresponding to Δ 9-THC at 500 ng/mL (5.85 min) and its isomer Δ 8-THC at 5 ng/mL (6.17 min). Sample was produced from certified reference material

Table S3 Summary of validation results, including limit of detection (LOD), limit of quantification (LOQ), intra-day (RSD_r) and inter-day ($RSD_{(T)}$), bias, and linearity range. Target values: $QC_{low1} = 0.8 \text{ ng/mL}$ (0.032%, w/w)*; $QC_{low2} = 3.0 \text{ ng/mL}$ (0.12%, w/w)*; $QC_{medium} = 80 \text{ ng/mL}$ (3.2%, w/w)*; $QC_{high} = 400 \text{ ng/mL}$ (16.0%, w/w)*; *considering a 50 mg sample extracted with 2 mL MeOH and 1 : 10,000 dilution of the sample)

Analyte	LOD [ng/mL]	LOQ [ng/mL]	QC level	RSD_r [%]	$RSD_{(T)}$ [%]	Bias [%]
CBC	0.5	0.5	low ₁	16.8	16.0	-12.4
			low ₂	2.9	7.2	4.3
			medium	1.2	1.3	7.9
CBCA	0.2	0.5	low ₁	4.1	8.8	-19.3
			low ₂	5.7	7.5	-12.0
			medium	2.7	6.0	-7.2
CBD	0.3	0.5	low ₁	4.1	5.0	-2.5
			low ₂	2.9	5.0	0.8
			medium	0.6	0.9	6.6
CBDA	0.2	0.5	low ₁	2.4	6.3	-12.0
			low ₂	3.6	3.6	-0.4
			medium	3.4	6.6	1.0
			high	1.2	2.9	-4.9
CBDV	0.3	0.5	low ₁	4.7	12.9	-4.7
			low ₂	2.7	6.5	1.5
			medium	1.2	1.2	0.8
CBDVA	0.2	0.5	low ₁	2.9	5.4	-9.6
			low ₂	4.0	4.6	-1.7
			medium	3.0	6.6	-0.5
CBG	0.4	0.5	low ₁	7.0	13.9	-13.5
			low ₂	2.7	3.4	2.9
			high	2.3	2.3	1.3
CBGA	0.2	0.5	low ₁	2.1	5.1	-9.7
			low ₂	4.3	4.3	1.0
			medium	2.3	5.4	3.0
CBL	0.4	0.5	low ₁	6.8	12.6	-10.1
			low ₂	2.7	5.9	-3.6
			medium	0.8	1.0	-0.2
CBN	0.4	0.5	low ₁	4.6	12.3	-8.6
			low ₂	2.9	4.1	-0.9
			medium	1.1	1.1	2.3
CBNA	0.2	0.5	low ₁	1.4	7.6	-7.4
			low ₂	8.9	8.9	-4.7
			medium	3.5	5	<0.1
THC	0.3	0.5	low ₁	4.4	9.4	-4.3
			low ₂	4.6	5.1	2.0
			medium	0.5	1.0	2.7
THCA	0.2	0.5	low ₁	4.1	12.0	-17.9
			low ₂	4.8	5.1	1.2
			medium	2.7	3.5	3.9
			high	1.7	3.5	-4.8
THCV	0.3	0.5	low ₁	6.1	7.9	-4.1
			low ₂	3.6	5.8	3.7
			medium	0.7	1.5	3.2
THCVA	0.2	0.5	low ₁	2.8	6.2	-8.4
			low ₂	5.2	5.4	-8.6
			medium	2.4	5.2	-3.7

Table S4 Cannabinoid contents of different cannabis varieties. CBL and Δ8-THC were not detected in any of the samples. Standard deviation and range (shown in brackets) are only given, if number of replicas (n) ≥ 3. Limit of quantification (LOQ) of all analytes was 0.02% (considering a 50 mg sample extracted with 2 mL MeOH and 1 : 10,000 dilution of the sample)

Variety	n	CBC	CBCA	CBD	CBDA	CBDV	CBDVA	CBG	CBGA	CBN	CBNA	Δ ⁹ -THC	Δ ⁹ -THCA	THCV	THCVA	Mean ± standard deviation (range) [%]	
Amnesia 1	1	<LOQ	0.14	n.d.	0.03	n.d.	n.d.	0.08	0.62	0.03	0.16	0.93	15.50	n.d.	0.05		
Amnesia 55 3	3	0.05 ± 0.01 (0.04-0.05)	0.26 ± 0.02 (0.24-0.28)	n.d.	0.04 ± 0.01 (0.04-0.05)	n.d.	n.d.	0.16 ± 0.04 (0.12-0.20)	1.62 ± 0.20 (1.34-1.80)	0.03 ± 0.01 (0.03-0.04)	0.20 ± 0.02 (0.17-0.20)	1.38 ± 0.19 (1.16-1.64)	19.6 ± 1.77 (17.1-20.9)	n.d.	0.08 ± 0.01 (0.08-0.09)		
Amnesia x SFV 2	2	<LOQ	<LOQ	0.06-0.28	n.d., 0.05	0.04, 0.47	n.d., n.d.	n.d., n.d.	0.09, 0.16	0.68, 0.73	<LOQ, 0.03	0.15, 0.20	0.74, 1.00	12.3, 22.6	n.d., n.d.	0.07, 0.13	
Big Bud 3	3	n.d.	0.13 ± 0.01 (0.12-0.14)	n.d.	0.03 ± 0.00 (0.03-0.04)	n.d.	n.d.	0.12 ± 0.01 (0.12-0.14)	0.26 ± 0.03 (0.22-0.28)	detected ^a (<LOQ-0.02)	0.20 ± 0.02 (0.17-0.21)	0.67 ± 0.04 (0.63-0.73)	15.5 ± 1.29 (14.0-17.2)	n.d.	0.07 ± 0.01 (0.06-0.07)		
Bubba Kush 3	3	detected ^b (<LOQ-0.02)	0.17 ± 0.02 (0.15-0.19)	n.d.	0.04 ± 0.02 (0.02-0.06)	n.d.	n.d.	0.08 ± 0.01 (0.07-0.09)	0.09 ± 0.01 (0.07-0.09)	detected ^c (<LOQ-0.02)	0.08 ± 0.01 (0.07-0.09)	0.94 ± 0.14 (0.76-1.09)	11.9 ± 1.46 (10.5-13.9)	n.d.	0.05 ± 0.00 (0.04-0.05)		
C7 1	1	<LOQ	0.13	n.d.	0.05	n.d.	n.d.	0.08	0.20	0.04	0.23	0.93	15.5	n.d.	0.10		
C7 x Thai 1	1	0.04	0.42	0.60	6.12	n.d.	0.04	0.05	0.05	0.03	0.06	0.71	2.88	n.d.	0.03		
Durban x 8	8	detected ^d (n.d.-<LOQ)	0.13 ± 0.01 (0.11-0.15)	detected ^e (n.d.-<LOQ)	0.05 ± 0.02 (0.03-0.10)	n.d.	n.d.	0.05 ± 0.01 (0.03-0.06)	0.18 ± 0.06 (0.09-0.27)	detected ^f (<LOQ-0.03)	0.14 ± 0.02 (0.09-0.16)	1.04 ± 0.35 (0.59-1.21)	15.4 ± 2.51 (11.2-18.8)	detected ^g (n.d.-0.03)	0.17 ± 0.08 (0.08-0.31)		
Malawi 1	1	0.03	0.33	0.55	5.54	n.d.	0.03	0.06	0.07	0.03	0.07	0.73	2.90	n.d.	0.03		
Lebl 2 3	3	detected ^h (<LOQ-0.03)	0.24 ± 0.02 (0.21-0.25)	n.d.	0.04 ± 0.00 (0.04-0.04)	n.d.	n.d.	0.15 ± 0.02 (0.12-0.17)	0.42 ± 0.02 (0.39-0.44)	0.03 ± 0.00 (0.02-0.03)	0.19 ± 0.01 (0.18-0.20)	1.15 ± 0.15 (0.94-1.29)	19.3 ± 1.55 (17.2-20.8)	n.d.	0.07 ± 0.01 (0.06-0.08)		
Malawi x Super Skunk 1	1	0.03	0.43	n.d.	0.03	n.d.	n.d.	0.26	1.07	0.03	0.11	1.46	11.48	0.24	1.73		
OG Kush 3	3	detected ⁱ (n.d.-0.02)	0.17 ± 0.02 (0.14-0.20)	n.d.	detected ^j (<LOQ-0.03)	n.d.	n.d.	0.04 ± 0.02 (0.03-0.06)	detected ^k (<LOQ-0.06)	detected ^l (<LOQ-0.02)	0.08 ± 0.01 (0.07-0.10)	0.65 ± 0.07 (0.58-0.74)	8.68 ± 3.01 (6.15-12.9)	n.d.	detected ^m (<LOQ-0.02)		
Pot of Gold 2	2	0.04, 0.05	0.55, 0.59	0.64, 0.80	9.43, 9.53	<LOQ, 0.03	0.40, 0.44	0.05, 0.06	0.35, 0.38	0.03, 0.02	0.10, 0.08	1.14, 1.39	7.65, 7.44	0.07, 0.09	0.46, 0.49		
Pot of Gold nr. 11 1	1	0.04	0.57	0.61	9.29	0.02	0.40	0.05	0.31	0.03	0.10	1.06	7.8	0.07	0.47		
Purple Punch 3	3	detected ⁿ (<LOQ-<LOQ)	0.22 ± 0.02 (0.19-0.24)	n.d.	0.04 ± 0.00 (0.04-0.04)	n.d.	n.d.	0.04 ± 0.00 (0.04-0.04)	0.14 ± 0.02 (0.13-0.17)	detected ^o (<LOQ-<LOQ)	0.18 ± 0.01 (0.17-0.19)	0.59 ± 0.02 (0.58-0.61)	16.8 ± 0.48 (16.20-16.91)	n.d.	0.06 ± 0.00 (0.06-0.07)		
Rascal OG 3	3	detected ^p (<LOQ-0.05)	0.19 ± 0.03	n.d.	0.03 ± 0.00 (0.03-0.03)	n.d.	n.d.	0.04 ± 0.01 (0.03-0.06)	0.10 ± 0.01 (0.07-0.12)	0.06 ± 0.01 (0.05-0.08)	0.17 ± 0.01 (0.16-0.19)	1.94 ± 0.27 (1.64-2.30)	13.38 ± 1.59 (11.2-13.8)	n.d.	0.04 ± 0.01 (0.03-0.05)		
SFV OG 3	3	detected ^q (<LOQ-0.02)	0.11 ± 0.02 (0.09-0.13)	n.d.	detected ^r (<LOQ-0.02)	n.d.	n.d.	0.05 ± 0.00 (0.05-0.05)	0.23 ± 0.04 (0.17-0.27)	0.04 ± 0.00 (0.04-0.05)	0.10 ± 0.01 (0.08-0.11)	2.10 ± 0.26 (1.79-2.42)	9.67 ± 0.89 (8.93-10.9)	n.d.	0.03 ± 0.00 (0.03-0.03)		
Wappa 3	3	0.04 ± 0.01 (0.04-0.05)	0.18 ± 0.01 (0.17-0.19)	n.d.	0.03 ± 0.00 (0.02-0.03)	n.d.	n.d.	0.05 ± 0.00 (0.05-0.05)	0.22 ± 0.01 (0.21-0.23)	0.06 ± 0.01 (0.05-0.07)	0.16 ± 0.02 (0.15-0.19)	1.85 ± 0.19 (1.59-2.09)	11.3 ± 0.71 (10.6-12.3)	0.05 ± 0.00 (0.01-0.05)	0.26 ± 0.01 (0.25-0.26)		

Analyte detected in a) n = 3 (100%); b) n = 3 (100%); c) n = 3 (100%); d) n = 6 (75%); e) n = 1 (13%); f) n = 8 (100%); g) n = 5 (63%); h) n = 3 (100%); i) n = 2 (67%); j) n = 3 (100%); k) n = 3 (100%); l) n = 3 (100%); m) n = 3 (100%); n) n = 3 (100%); o) n = 3 (100%); p) n = 3 (100%); q) n = 3 (100%); r) n = 3 (100%) of samples

Table S5 Total cannabinoid contents of varieties. CBL and $\Delta 8$ -THC were not detected in any of the samples. Standard deviation and range are only given, if $n \leq 3$. Limit of quantification (LOQ) of all analytes was 0.02% (considering a 50 mg sample extracted with 2 mL MeOH and 1 : 10,000 dilution of the sample). For calculation of means and standard deviations, levels <LOQ were excluded

Mean \pm standard deviation (range) [%]								
Variety	n	CBC _{total}	CBD _{total}	CBDV _{total}	CBG _{total}	CBN _{total}	Δ^9 -THC _{total}	THCV _{total}
Amnesia	1	0.14	0.03	n.d.	0.62	0.17	14.5	0.04
Amnesia S5	3	0.27 \pm 0.02 (0.25-0.29)	0.04 \pm 0.01 (0.03-0.04)	n.d.	1.58 \pm 0.21 (1.29-1.78)	n.d.	18.5 \pm 1.72 (16.1-20.0)	n.d.
Amnesia x SFV	2	0.15, 0.26	0.47, 0.04	n.d.	0.68, 0.80	0.16, 0.20 ^a	11.5, 20.8	0.07, 0.11
Big Bud	3	0.11 \pm 0.01 (0.10-0.13)	0.03 \pm 0.00 (0.03-0.03)	n.d.	0.35 \pm 0.03 (0.37-0.31)	0.18 \pm 0.02 ^b (0.17-0.20)	14.3 \pm 1.17 (12.9-15.8)	0.06 \pm 0.00 (0.05-0.07)
Bubba Kush	3	0.17 \pm 0.02 (0.14-0.19)	0.03 \pm 0.02 (0.02-0.06)	n.d.	0.15 \pm 0.01 (0.13-0.17)	0.08 \pm 0.01 (0.07-0.10)	11.4 \pm 1.37 (10.2-13.3)	0.04 \pm 0.00 (0.04-0.05)
C7	1	0.13	0.05	n.d.	0.25	0.24	14.59	0.08
C7 x Thai	1	0.41	5.97	0.04	0.09	0.08	3.23	0.03
Durban x Malawi	8	0.12 \pm 0.01 (0.10-0.14)	0.04 \pm 0.02 ^c (0.02-0.04)	n.d.	0.21 \pm 0.06 (0.14-0.27)	0.14 \pm 0.03 ^d (0.08-0.17)	14.6 \pm 2.05 (11.6-17.2)	0.15 \pm 0.07 ^e (0.07-0.30)
GWS	1	0.32	5.41	0.03	0.12	0.09	3.27	0.02
Lebi 2	3	0.23 \pm 0.02 ^f (0.21-0.25)	0.04 \pm 0.00	n.d.	0.52 \pm 0.03	0.20 \pm 0.01	18.11 \pm 1.35	0.06 \pm 0.01
Malawi x Super Skunk	1	0.40	0.03	n.d.	1.20	0.13	11.53	1.75
OG Kush	3	0.15 \pm 0.03 (0.13-0.19)	0.02 ^g (<LOQ-0.02)	n.d.	0.06 \pm 0.04 ^h (0.03-0.11)	0.08 \pm 0.02 ⁱ (0.07-0.11)	8.26 \pm 2.71 (5.98-12.06)	0.02 ^j (<LOQ-0.02)
Pot of Gold	2	0.56, 0.54	8.90, 9.16	0.35 ^k , 0.41	0.36, 0.40	0.12, 0.09	7.84, 7.92	0.47, 0.52
Pot of Gold nr. 11	1	0.54	8.8	0.36	0.32	0.12	7.90	0.48
Purple Punch	3	0.20 \pm 0.02 (0.18-0.22)	0.03 \pm 0.00 (0.03-0.04)	n.d.	0.16 \pm 0.02 (0.15-0.19)	0.17 \pm 0.00 ^l (0.16-0.17)	15.4 \pm 0.41 (14.8-15.8)	0.06 \pm 0.00 (0.05-0.06)
Rascal OG	3	0.19 \pm 0.03 (0.16-0.24)	0.03 \pm 0.00 (0.03-0.03)	n.d.	0.13 \pm 0.03 (0.09-0.17)	0.21 \pm 0.01 (0.19-0.22)	13.7 \pm 1.65 (11.5-15.5)	0.04 \pm 0.01 (0.03-0.04)
SFV OG	3	0.12 \pm 0.01 (0.10-0.13)	0.02, 0.02 ^m (<LOQ-0.02)	n.d.	0.25 \pm 0.03 (0.20-0.28)	0.13 \pm 0.01 (0.11-0.15)	10.6 \pm 1.03 (9.62-12.00)	0.03 \pm 0.00 (0.02-0.03)
Wappa	3	0.20 \pm 0.01 (0.18-0.22)	0.02 \pm 0.00 (0.02-0.03)	n.d.	0.25 \pm 0.01 (0.24-0.25)	0.20 \pm 0.01 (0.19-0.22)	11.7 \pm 0.74 (11.2-12.8)	0.28 \pm 0.01 (0.27-0.30)

Additional information on analyte detection: a) CBN <LOQ; b) CBN detected in n = 3 (100%), once < LOQ; c) CBD detected in n = 8 (100%), once <LOQ; d) CBN detected in n = 8 (100%), once <LOQ; e) THCV detected in n = 5 (63%), 4 times <LOQ; f) CBD detected in n = 3 (100%), once <LOQ; g) CBD detected in n = 0 (0%), CBDA detected in n = 3 (100%), twice <LOQ; h) CBG detected in n = 3 (100%), all >LOQ, CBGA detected in n = 3 (100%), twice <LOQ; i) CBN detected in n = 3 (100%), once <LOQ; j) THCV detected in n = 0 (0%), THCVA detected in n = 3 (100%), twice <LOQ; k) CBDV detected <LOQ; l) CBN detected in n = 3 (100%), once < LOQ; m) CBD detected in n = 0 (0%), CBDA detected in n = 3 (100%), once <LOQ. If not noted otherwise, acid forms were detected >LOQ in all samples.

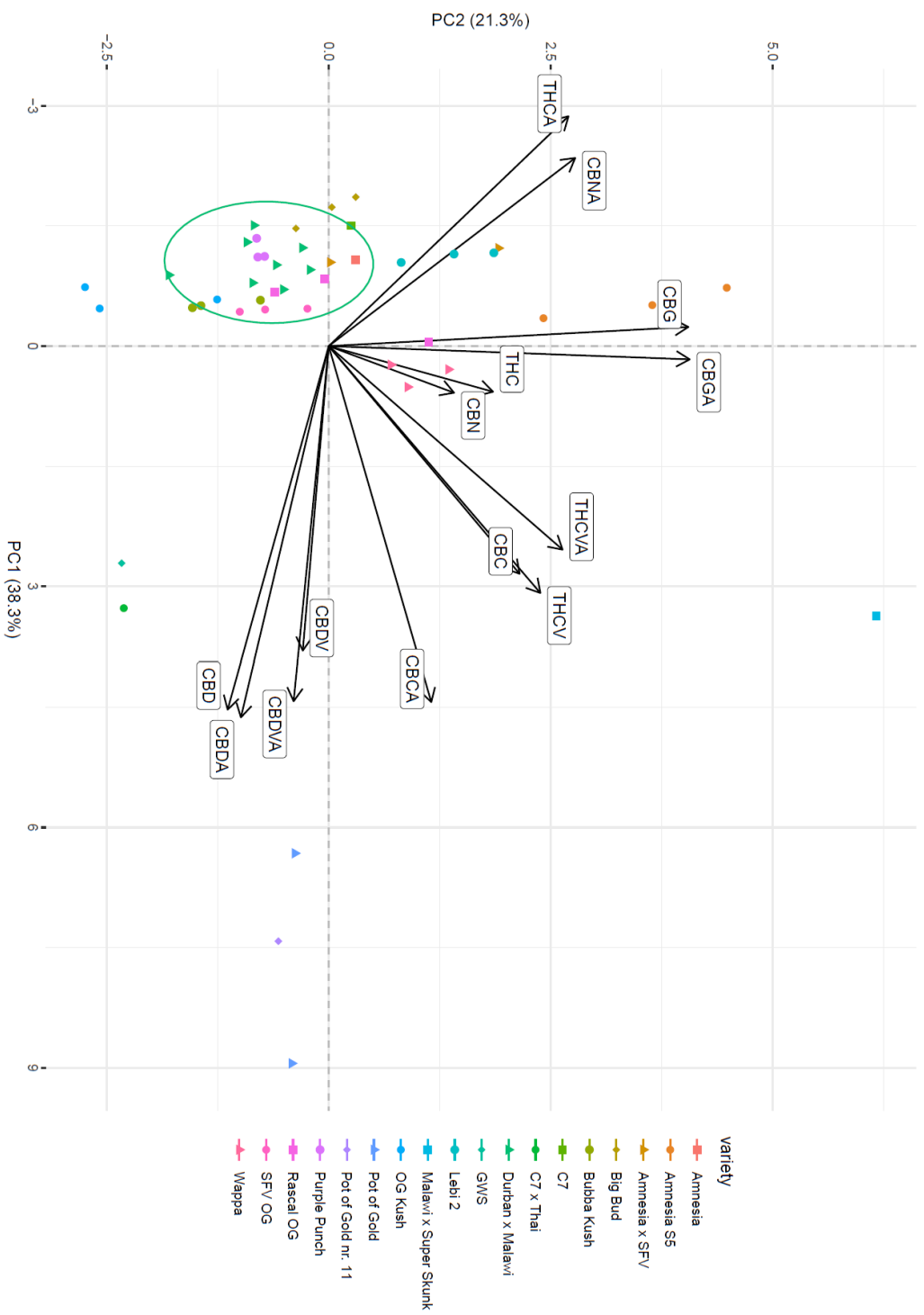


Figure S6 PCA loading plot of the targeted analysis. The 95% confidence interval (95%-CI) is indicated for the variety Durban x Malawi as green ellipse. Due to the limited number of plants per variety ($n \leq 3$), the 95%-CI could only be calculated for this variety ($n = 8$)

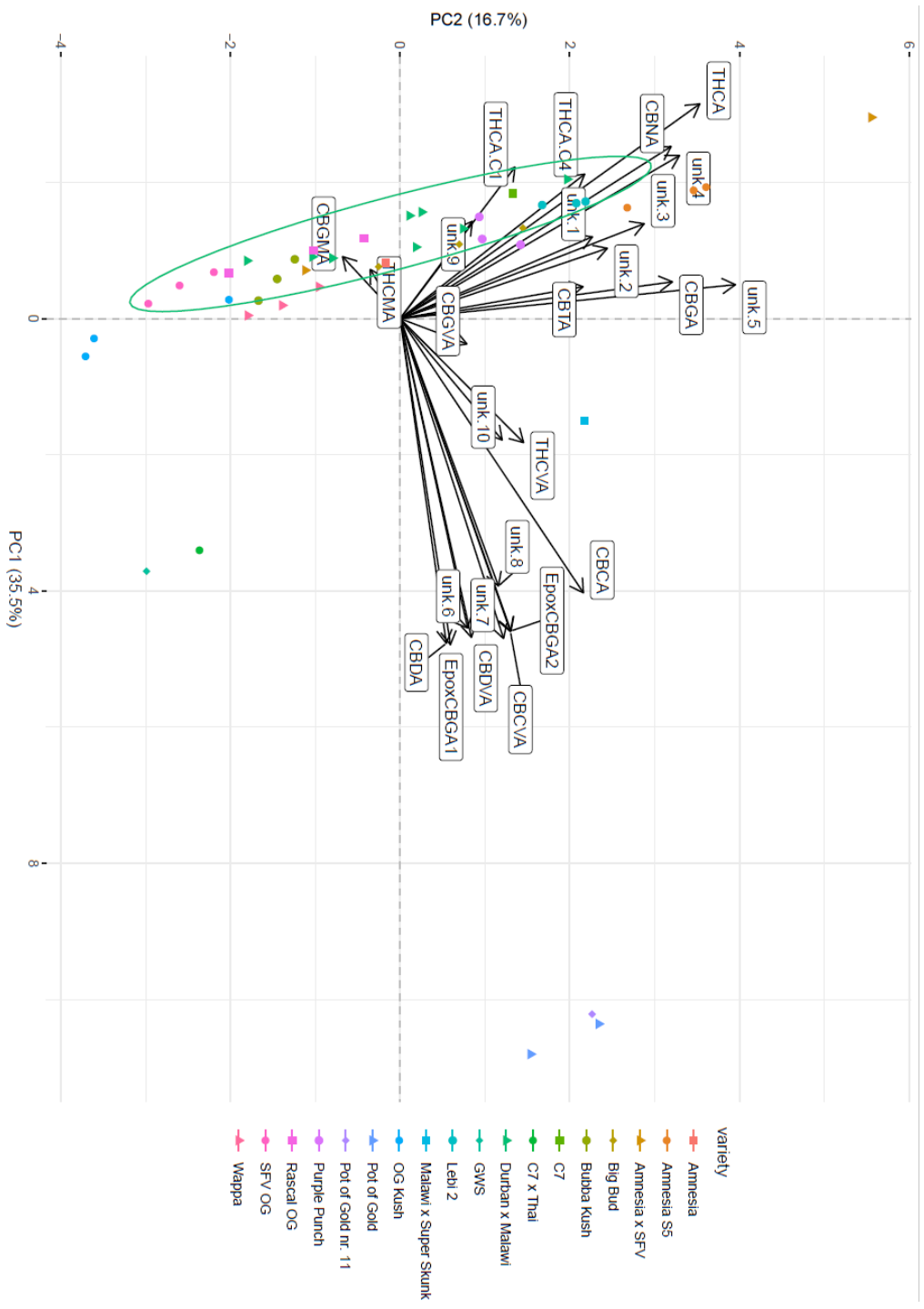


Figure S7 PCA loading plot of the untargeted analysis. The 95% confidence interval (95%-CI) is indicated for the variety Durban x Malawi as green ellipse. Due to the limited number of plants per variety ($n \leq 3$), the 95%-CI could only be calculated for this variety ($n = 8$)

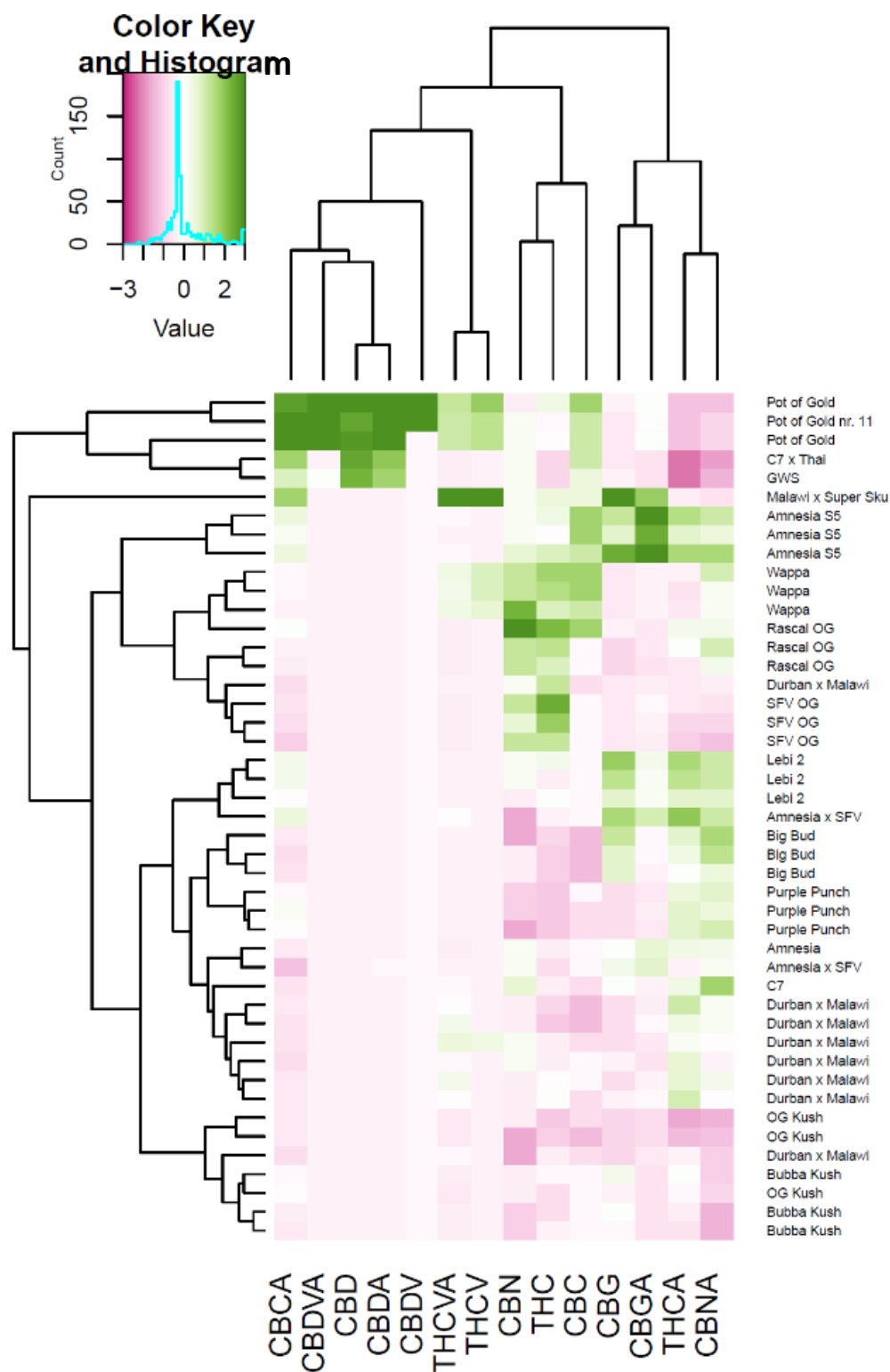


Figure S8 Heatmap applying hierarchical clustering of the targeted data (contents). Green indicates varieties with expressing above-average levels and red indicates where analytes are expressed in below-average levels. Compounds and varieties are sorted in a hierarchical manner, meaning that varieties are sorted based on similar chemical fingerprints, whilst analytes that are typically detected simultaneously are presented side by side. The clustering of the varieties Pot of Gold, Pot of Gold nr. 11, C7 x Thai, and GWS is largely explained by CBCA, CBDVA, CBD, CBDA, and CBDV. Malawi x Super Skunk presents elevated THCV and THCVA levels. Durban x Malawi (grown from seeds) presented six plants that hierarchically clustered close together, while two individual plants are more similar to other plant varieties (e.g., Bubba Kush, and OG Kush for one plant, and SVG OG, Rascal OG for the other). CBGA and CBG are expressed at highest levels for Malawi x Super Skunk and Amnesia S5.

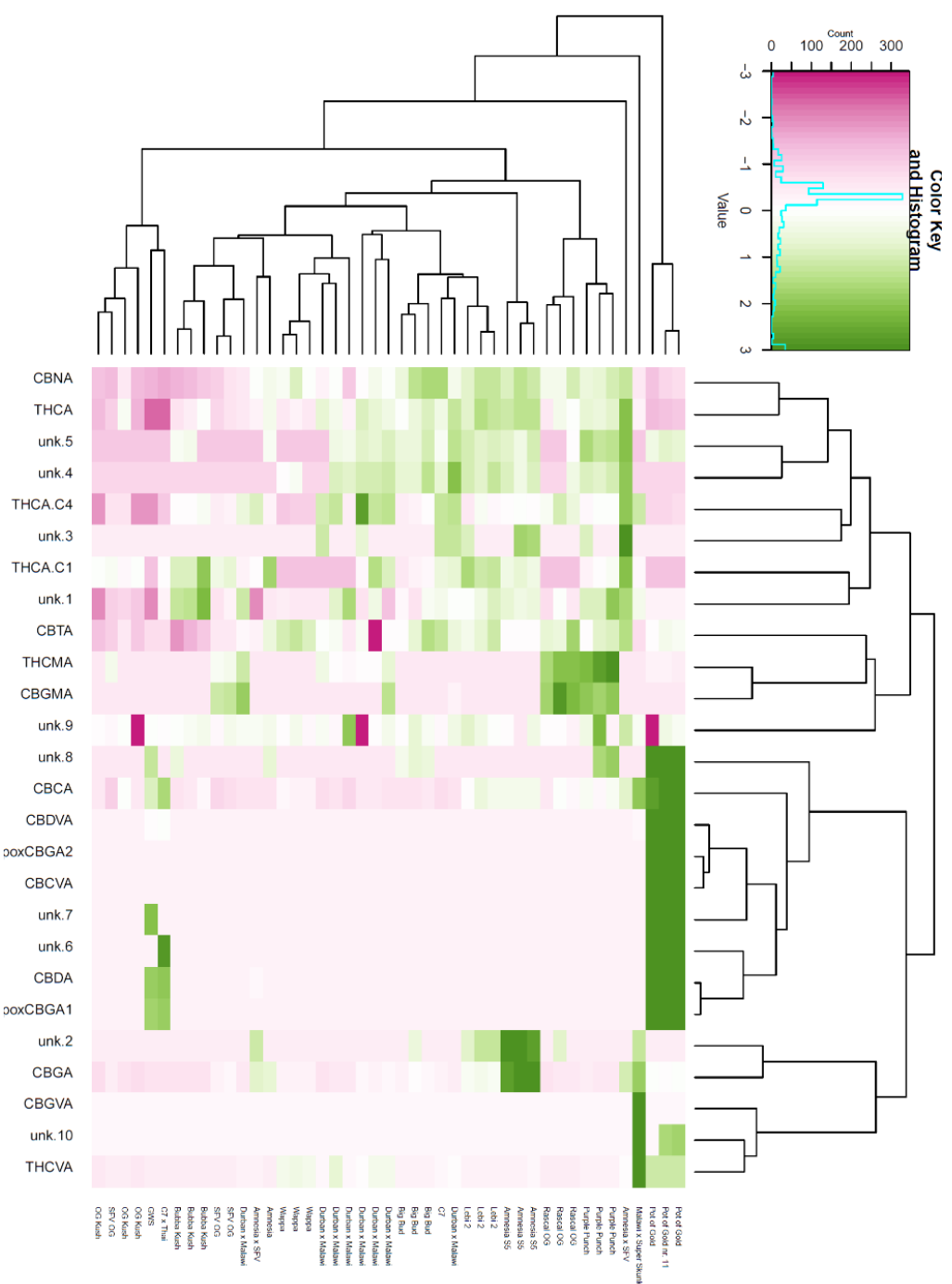


Figure S9 Heatmap applying hierarchical clustering of the untargeted data (weight normalized areas). Green indicates varieties with expressing above-overage levels and red indicates where analytes are expressed in below-average levels. Compounds and varieties are sorted in a hierarchical manner, meaning that varieties are sorted based on similar chemical fingerprints, whilst analytes that are typically detected simultaneously are presented side by side. The clustering of the varieties Pot of Gold, Pot of Gold nr. 11, CT x Thai, and GWS is largely explained by CBDA, CBCA, CBDVA, 6,7-Epoxy-CGA isomers 1 and 2, CBCVA, unknown 6, unknown 7, and unknown 8. Malawi x Super Skunk is characterized by elevated THC and THCV levels. THCMa and CBDMA are highly indicative for the varieties Purple Punch and Rascal OG. Malawi x Super Skunk presents a unique chemical fingerprint largely attributable to the presence of CBGVA, unknown 10, and THCVA.

5 Discussion

5.1 *In vitro* metabolism studies in forensic toxicology

One major challenge surrounding SCs is that, even over a decade since their first appearance as constituents of “Spice”, new SCs are readily entering the recreational drug market. The emergence of new SCs that are aimed to circumvent regulatory frameworks has resulted in an ongoing cat-and-mouse game, in which forensic institutions and lawmakers are considered always one step behind. The constant monitoring and detection of SCs is of great importance, especially considering the morbidity and mortality associated with this compounds class.^{78, 109} The detection of SCs, which is the basis for toxicologic investigations, requires forensic institutions to constantly adapt their analytical methods to keep up with the ever-changing SC market.⁷⁸ The detection of SCs in toxicologic case work, however, remains challenging. For instance, the high potency of many SCs results in low dosages, requiring sensitive analytical methods. As many SCs have been shown to be extensively metabolized, it is necessary to include metabolites into respective screening methods.^{108, 109} *In vitro* metabolism studies are used to gain information on the metabolic fate of a compound and additionally allow the definition of suitable screening targets.¹⁰⁸ The use of HRMS is considered highly advantageous in this regard, resulting in improved productivity and quality of results.¹⁰⁹ Exact mass results give enhanced information on the chemical formula, facilitating structure elucidation. Additionally, *in silico* assisted data mining platforms are of increasing popularity, as they allow for more straight forward data analysis.^{17, 109} These aforementioned advantages are also demonstrated by the presented study (*study I*), elaborating on the metabolism of two SCs. Besides the gained knowledge on the metabolism of CUMYL-THPINACA and ADAMANTYL-THPINACA, *study I* encompassed the development of a protocol and analytical workflow, which can readily be adapted for newly emerging SCs. This work is therefore considered to be one piece of the puzzle to ensure the reliable detection of SCs.

5.2 Unraveling a novel trend surrounding synthetic cannabinoids

In 2020, the emergence of cannabis products adulterated with SCs was observed in Switzerland. Initially, adulterated products comprised mainly adulterated cannabis flowers, which upon chemical analysis were found to be low-THC cannabis products. Dried cannabis flowers, containing <1% THC, can be legally produced and sold in Switzerland. Therefore, these adulterated cannabis products were first believed to be regionally limited to Switzerland. However, starting in autumn 2020, other European

countries also detected adulterated cannabis products. The adulterated cannabis flowers, and adulterated hashish products appearing shortly after, can neither visually nor olfactorily be distinguished from regular cannabis preparations, leaving the drug user unaware of the presence of SCs.¹²¹ The drug user's unawareness, coupled with the often-seen increased potency and toxicity of many SCs, resulted in serious public health concerns.⁵³ In direct response to these findings, various media releases were issued in order to inform the public.^{122, 123}

Study II comprises a comprehensive study investigating various aspects of these adulterated cannabis products, including SC prevalence, investigation of the applied carrier material, and pharmacologic outcomes. Tentatively issued hypotheses stating a connection between the broad availability of low-THC cannabis flowers and their use as carrier material for adulterated cannabis products were substantiated, as all analyzed cannabis flowers presented THC levels below Swiss threshold. Regarding Swiss law, hashish is illegal regardless of its THC content. Many hashish samples contained below-average to very low THC levels (median: 0.8%), thus implying that these products also originated from low-THC cannabis flowers. It remains unknown whether these low-THC cannabis flowers, which were either directly adulterated or further processed into hashish, were legally obtained from registered CBD retailers. The EMCDDA hypothesized that shortages of (high-THC) cannabis, e.g. due to the pandemic, and the wide availability of low-THC cannabis products might have resulted in criminal groups exploiting the possibility to adulterate low-THC cannabis products.⁵³ The typically low THC contents of adulterated cannabis posed challenges to police investigations and forensic case work due to the inherent risk of falsely classifying seized products (e.g., adulterated low-THC cannabis flowers) as legal low-THC cannabis products. Routinely applied methodologies for the quantification of THC generally do not allow for the detection of SCs. Neither are SCs detected by the rapid reagent tests sometimes applied by the Swiss police to distinguish low-THC from high-THC cannabis material. An unknown number of undetected cases of adulterated cannabis products must therefore be assumed. Based on the gained knowledge through *study II*, law enforcement and police were educated on the presence of adulterated cannabis products and corresponding analytical consequences. This ultimately led to the investigation and detection of various cases of adulterated low-THC cannabis and hashish materials issued for chemical characterization in the context of forensic case work.

For the presented study, collaboration with three drug checking services enabled to gain valuable information on the adverse effects and allowed the direct comparison between the effects associated with SCs compared to regular high-THC cannabis products. Increased likelihoods for adverse effects, particularly psychologic and cardiologic adverse effects, were noted for products containing SCs, thus confirming previously issued health concerns. Drug checking services enable the direct association of product and reported effect, thereby overcoming the common issue arising from the

lack of analytical confirmation, e.g., seen in data collected at poisons information centers.^{78, 124} The data on adverse effects of SCs presented here will help to better understand toxicologic aspects and potential health risks associated with SCs and these adulterated products, while complementing data obtained from more established routes, such as drug surveys, poisons information centers, case reports, and case series.⁷⁸

5.2.1 What can we learn for the rapid detection and monitoring of emerging NPS?

With over 800 compounds being monitored by the EMCDDA, NPS comprise a vast diversity of compounds spanning different substance classes, e.g., SCs, cathinones, phenethylamines, opioids, and benzodiazepines.⁵³ NPS are considered public health threats, as pharmacologic and toxicologic data are typically scarce.⁹⁶ Ultimately, this renders the monitoring of NPS an important task.⁵³ Although the presented study focused on a new phenomenon surrounding SCs, the gained knowledge will in the following be discussed in the broader context of NPS. Current approaches, the unique strengths of drug checking services in detecting new trends surrounding NPS, and the inherent value of collaborations between instances are highlighted.

NPS are often either sold under their own name, as with designer benzodiazepines, or as an adulterant, for instance in the cases of SCs and synthetic opioids that have been used to adulterate cannabis and heroin, respectively.^{36, 125} Regarding the former, even if a product states to contain a certain NPS, the mislabeling of NPS containing products is regularly reported.^{78, 96} Common sources to gain knowledge on the effects of NPS are drug surveys, online drug forums, and data collected at poisons information centers.^{53, 124, 126-128} Data on poisonings obtained from emergency departments and intensive care units can serve as further tools to investigate harms related to NPS, as demonstrated by a recent study by Helander *et al.*¹²⁹ Reports on drug seizures are used to investigate market developments surrounding drugs of abuse, including NPS.^{36, 53} Finally, toxicological case reports and case series are important sources on the toxicological aspects of NPS.^{84, 96, 130}

The presented work demonstrates the potential of drug checking services in the detection and monitoring of newly emerging trends surrounding NPS. Drug checking services have various strengths arising from their unique set-up. The possibility to monitor the market at consumer level, while additionally receiving information on the drug's effects, overcomes one of the largest limitations associated with data obtained from drug surveys and online forums, i.e., the lack of analytical confirmation. Besides giving valuable information on adverse effects associated with newly emerging NPS, user self-reports additionally play an important role for the detection of NPS, especially in cases where NPS are used as an adulterant or substitute. The detection of newly emerging preparations containing NPS is facilitated, as well seen with the example of

adulterated low-THC cannabis products: Such products were handed in at various drug checking services, along with self-reports stating adverse effects. As low-THC cannabis products themselves are considered non-intoxicating, the analysts were instantly suspicious about the presence of further pharmacologically relevant compounds, such as NPS. Finally, drug checking services offer drug consumers the possibility to have a drug analyzed without legal consequences. They serve as a unique platform for concerned drug users experiencing serious side effects after the consumption of an illicit drug. This will again facilitate the detection of new and potentially dangerous trends, which otherwise would remain underreported due to the user's fear of juridical consequences. Drug checking services, serve as valuable market monitoring tools, including aspects of pharmacovigilance.¹³¹ The Swiss Federal Office of Public Health (Bundesamt für Gesundheit; BAG) recognized the inherent possibilities arising from collaborations of health care institutions, drug checking services, and forensic institutions, as national substance monitoring is currently under review by means of a feasibility study.¹³²

There is not one all-encompassing solution to face the multidimensional challenges surrounding NPS. As demonstrated above, the monitoring of NPS requires the attention and work spanning various institutions, from public health instances, drug checking services, health professionals to clinical and forensic laboratories. Transnational public health and drug monitoring offices, such as EMCDDA and UNODC, play a key role in collecting data surrounding drugs of abuse and enable the rapid exchange of knowledge between the relevant parties by means of comprehensive reports (e.g., world drug report) and early warning systems.^{36, 37, 53, 133, 134} Future emphasis should lie within strengthening collaboration between these aforementioned institutions. In this work, the rather unconventional collaboration of a forensic institution and drug checking services was of great value in the monitoring a newly emerging trend surrounding SCs, highlighting its potential future role in facing novel challenges surrounding NPS.

5.2.2 Future role of high-resolution mass spectrometry

Reliable detection and confirmation of NPS rises and falls with the applied chemical analysis. HRMS techniques are particularly well suited for screening procedures, even more so whenever a high degree of flexibility regarding the integration of new analytes is required.⁹ The possibility to retrospectively evaluate HRMS data to screen for further compounds is especially valuable for the detection of newly emerging NPS.² Yet the thereby obtained results are only indicative and require verification using reference material.¹ Further advantages of HRMS arise from the higher selectivity when compared to low-resolution instruments, thereby limiting false positive results due to matrix interferences. The use of HRMS is therefore advantageous for bioanalytical analyses that are characterized by a diversity of complex matrices. An additional strength of HRMS techniques, especially when compared to targeted methods, lies within the number of

analytes that can be simultaneously assessed. HRMS, by applying full scan acquisition modes, offers the possibility to screen for thousands of compounds per run. Untargeted screening methods applying HRMS largely differ from common targeted methods for which the number of analytes is technically limited.⁹ The increasing availability of online spectra databases, e.g., mzCloud,¹³⁵⁻¹³⁷ as well as analytical data provided from forensic laboratories, e.g., accessible for forensic scientists via the GTFCh drug forum and EMCDDA early warning system, are facilitating the identification of unknown compounds.^{135, 136}

In the presented work, the use of HRMS enabled the comprehensive screening for SCs while providing a high degree of flexibility to rapidly integrate new SCs into the method as they emerged on the market. Despite the rather complex matrix containing a diversity of major and minor phytocannabinoids, good selectivity resulted in no matrix interferences for the detection of SCs. Online databases have been integrated in the workflow in cases where an unknown signal, potentially belonging to a new SC, was detected. The presented method shows that HRMS is particularly valuable in facing challenges associated with NPS. Attributed to its increasing affordability, versatility, adaptability, and unmatched selectivity, HRMS is increasingly becoming the gold-standard in forensic chemistry and toxicology.¹³⁸

5.3 Advances in phytocannabinoid characterization

The increasing spread of cannabis and cannabis based products for medical and recreational purposes raises questions about the pharmacologic relevance of minor cannabinoids and other compound classes (e.g., terpenoids) produced by *C. sativa*.^{51, 139, 140} Breeding and selection of *C. sativa* has resulted in over 700 varieties known today.¹⁴¹ Whilst a few licensed cannabis varieties exist (e.g., Bedrocan®), it remains largely unknown to what extent cannabis varieties differ in their chemical composition, which is then suspected to result in differing effects *in vivo*.^{141, 142} Overall, improved plant and product characterization and standardization beyond THC and CBD is necessary to understand cannabis's clinical effects.^{47, 142} This poses the need for comprehensive analytical techniques.^{143, 144} Capriotti *et al.*¹⁴³ reviewed approaches using mass spectrometry for the characterization cannabis and cannabis based products. The authors noted a trend away from more traditional methodologies (e.g., employing FID and ultraviolet detectors) towards the increasing use of MS, including targeted low-resolution MS and HRMS. Whilst targeted methodologies remain important to reliably quantify a small number of selected cannabinoids, the introduction of HRMS has opened many new possibilities for phytocannabinoid characterization. Untargeted methodologies employing HRMS analysis, bioinformatics, and chemometrics enable the comprehensive characterization and comparison of cannabis varieties and cannabis based products.¹⁴³ In recent years, various approaches applying comprehensive

analytical techniques combined with multivariate statistics, such as PCA, were used to investigate differences between cannabis varieties^{141, 143, 145, 146} and cannabis based products.^{40, 143, 144} Metabolomics studies with focus on phytocannabinoids are increasingly termed (*phyto*)*cannabinomics*.^{140, 147} *Study III* presented the development of a comprehensive analytical technique employing HPLC-HRMS for the analysis of cannabis inflorescences. A targeted method, validated for the quantification of 15 cannabinoids, was complemented with an untargeted analysis that enabled the detection of additional plant ingredients. The presented study highlights how technical advances in mass spectrometry are changing cannabis research. In accordance with other studies,^{141, 145, 146, 148} the results obtained herein surrounding the minor cannabinoid fingerprint of cannabis varieties revealed chemical subgroups that complement traditionally used classifications based on THC and CBD contents alone.

5.3.1 Minor cannabinoids in the forensic field – where do we go from here?

The growing scientific interest in minor cannabinoids was shared by the forensic field, albeit with adapted motives and applications. In forensic toxicology, minor cannabinoids have been widely investigated with the aim to improve bioanalytical data interpretation in the context of recreational and medical cannabis intake.^{64, 65, 71, 74} Scheunemann *et al.*⁴⁰ recently compared seized cannabis material to licensed herbal preparations in Germany, with the aim to identify distinguishing markers between products. This aforementioned study had several overlaps with the presented study (*study III*) as it comprises a largely identical set of targeted analytes. Both studies offer valuable insights into minor cannabinoid fingerprints because they inform on the general abundancies of minor cannabinoids in herbal cannabis preparations. The aforementioned authors focused on cannabinoid fingerprints of “authentic” samples, in the sense that these products are encountered on both the illicit and medicinal German cannabis market.⁴⁰ In contrast, *study III* examined 18 different cannabis varieties that were grown and stored under identical conditions, diminishing factors resulting from varying storage periods and conditions, enabling the assessment of intra- and inter-variety variability. The untargeted metabolomics approach applied herein resulted in the detection of 19 additional compounds, of which 9 were assigned to cannabinoids described in literature.

Ultimately, comprehensive studies on product level are required in order to proceed to the next step, which is minor cannabinoid analysis of human specimens. Minor cannabinoid implementation in forensic toxicology is still in its infancy arising from i) limited data on general minor cannabinoid contents at product level, including inter- and intra-variety and inter- and intra-product variability, and ii) the largely unknown pharmacokinetics of minor cannabinoids (e.g., bioavailability and metabolism). Further

challenges in minor cannabinoid bioanalysis arise from the low concentrations in which they are already contained at product level, resulting in extremely low concentrations in human specimens such as blood and urine samples. This is believed to result in short detection windows due to sensitivity issues. Furthermore, due to their lipophilic nature and as seen with the major representative THC, minor cannabinoids are expected to be extensively metabolized, hampering their detection in human specimens. The detection of corresponding metabolites could potentially improve their detectability, e.g., by extending the detection window. For this, knowledge on the metabolic fate of a substance is, however, required. Comprehensive pharmacokinetic data for CBD have been recently published.^{69, 149} Similar studies focusing on the pharmacokinetics of minor cannabinoids contained in different preparations and applied using different routes of administration (e.g., smoking, vaporizing, oral) are currently missing. This information is urgently needed to enable the interpretation of minor cannabinoid levels in human. Despite the described challenges, selected studies employing minor cannabinoid bioanalysis showed promising results.^{64, 65, 71} Although minor cannabinoids are just gaining attention and require further research, they are expected to play an important role in the future of forensic toxicology.

6 Conclusion

Forensic chemists and toxicologists are facing multidimensional challenges resulting from the ever-changing market surrounding SCs,^{53, 78} as well as the increasing legalization and medicalization of cannabis and cannabis based products.⁶⁴ Current issues and research topics were outlined in this work. Furthermore, three projects encompassing comprehensive analytical methods applying HRMS were implemented to face ongoing challenges the forensic field.

SCs remain important players in the world of NPS, thereby keeping forensic scientists busy throughout the world. This is largely attributed to i) the emergence of new SCs for which *in vitro* metabolism studies are required in order to effectively detect them,¹⁰⁸ and ii) the fact that new trends surrounding SCs are constantly developing, as seen with the phenomenon of adulterated cannabis products.¹²¹ Powerful means for the detection and monitoring of emerging trends surrounding SCs were presented, including *in vitro* metabolite generation resulting in recommended screening targets, and a comprehensive study elaborating on the phenomenon of adulterated cannabis products via collaboration with drug checking services. The inherent value of drug checking services and their unique strength in the detection and monitoring of novel trends surrounding NPS were highlighted. Collaborations with drug checking services, by allowing the direct connection between product and reported effects, are overcoming common issues of more established routes, making them a highly valuable source on effects of newly emerging NPS.

A comprehensive method for phytocannabinoid characterization of cannabis inflorescences was presented. Analytical methods targeting cannabinoids beyond THC and CBD are required for a better understanding of minor cannabinoid fingerprints. Knowledge at product level is the basis for future applications *in vivo*, e.g., enhanced bioanalytical data interpretation in the medico-legal context.

Lastly, throughout this work the application of HRMS was invaluable, as it enabled comprehensive and sensitive analyses whilst providing means for metabolomics and advanced screening procedures. The versatility of HRMS and its unmatched value in the context of NPS and phytocannabinoid analysis was demonstrated.

7 Curriculum Vitae

MANUELA CARLA MONTI

DATE OF BIRTH: 02-May-1993
MAIL: m.monti@gmx.ch
ORCID: 0000-0002-9959-398X

EDUCATION AND WORK EXPERIENCE

Feb 2019 – Apr 2022

Institute of Forensic Medicine,
Department of Biomedical Engineering, University of Basel
Doctoral studies

Aug 2018 – Jan 2019

Lonza Drug Product Services, Forensic Chemistry Group
Internship

EDUCATION

Feb 2019 – Apr 2022

Institute of Forensic Medicine,
Department of Biomedical Engineering, University of Basel
Doctoral studies

2016 – 2018

Department of Pharmaceutical Sciences, University of Basel
MSc in Drug Sciences
Master Thesis: University Hospital Basel, Clinical Chemistry Department

2013 – 2016

Department of Pharmaceutical Sciences, University of Basel
BSc in Pharmaceutical Sciences

8 Presentations and Posters

ORAL PRESENTATIONS

2021

“Low-THC cannabis adulterated with synthetic cannabinoids - information gained through drug checking services”

MC Monti, J Zeugin, K Koch, N Milenkovic, E Scheurer, K Mercer-Chalmers-Bender
SGRM Sommertagung, September 3, 2021, Arlesheim, Switzerland

“Phase I in vitro metabolics profiling of the synthetic cannabinoid receptor agonists CUMYL-THPINACA and ADAMANTYL-THPINACA using high-resolution mass spectrometry”

MC Monti, E Scheurer, K Mercer-Chalmers-Bender
XXII. Symposium der GTFCh, April 16, 2021, online

2020

“Drug Checking – Möglichkeit für Trend- und Marktbeobachtungen auf Konsumentenebene?”

MC Monti, J Zeugin, E Scheurer, K Mercer-Chalmers-Bender
99. Jahrestagung der Deutschen Gesellschaft für Rechtsmedizin (DGRM), September 3, 2020, Lucerne, Switzerland

POSTERS

2021

“Beyond THC and CBD – the potential of minor cannabinoid fingerprinting”

MC Monti, P Frei, S Weber, E Scheurer, K Mercer-Chalmers-Bender
7th DBE (Department of Biomedical Engineering) Research Day, September 7, 2021, Basel, Switzerland

❖ Awarded 2nd place by the poster committee

2020

“In vitro metabolic profiling of the synthetic cannabinoid receptor agonist CUMYL-THPINACA”

MC Monti, E Scheurer, K Mercer-Chalmers-Bender
6th DBE Research Day, September 8, 2020, Basel, Switzerland

2019

“Outlook: Study on the metabolism and pharmacodynamics of newly emerging synthetic cannabinoids”

MC Monti, E Scheurer, K Mercer-Chalmers-Bender
5th DBE Research Day, August 28, 2019, Basel, Switzerland

9 References

1. Remane, D.; Wissenbach, D. K.; Peters, F. T., Recent advances of liquid chromatography–(tandem) mass spectrometry in clinical and forensic toxicology — An update. *Clin Biochem* **2016**, *49* (13), 1051-1071.
2. Bell, S., Forensic Chemistry. *Annu Rev Anal Chem* **2009**, *2* (1), 297-319.
3. Eliuk, S.; Makarov, A., Evolution of Orbitrap Mass Spectrometry Instrumentation. *Annu Rev Anal Chem* **2015**, *8* (1), 61-80.
4. Aceña, J.; Stampachiachiere, S.; Pérez, S.; Barceló, D., Advances in liquid chromatography-high-resolution mass spectrometry for quantitative and qualitative environmental analysis. *Anal Bioanal Chem* **2015**, *407* (21), 6289-99.
5. Hernández, F.; Sancho, J. V.; Ibáñez, M.; Abad, E.; Portolés, T.; Mattioli, L., Current use of high-resolution mass spectrometry in the environmental sciences. *Anal Bioanal Chem* **2012**, *403* (5), 1251-64.
6. Cacciola, F.; Donato, P.; Sciarrone, D.; Dugo, P.; Mondello, L., Comprehensive Liquid Chromatography and Other Liquid-Based Comprehensive Techniques Coupled to Mass Spectrometry in Food Analysis. *Anal Chem* **2017**, *89* (1), 414-429.
7. Yoshimura, Y.; Zaima, N., Application of Mass Spectrometry Imaging for Visualizing Food Components. *Foods (Basel, Switzerland)* **2020**, *9* (5), 575.
8. Beccaria, M.; Cabooter, D., Current developments in LC-MS for pharmaceutical analysis. *Analyst* **2020**, *145* (4), 1129-1157.
9. Meyer, M. R.; Helfer, A. G.; Maurer, H. H., Current position of high-resolution MS for drug quantification in clinical & forensic toxicology. *Bioanalysis* **2014**, *6* (17), 2275-2284.
10. Maurer, H. H., What is the future of (ultra) high performance liquid chromatography coupled to low and high resolution mass spectrometry for toxicological drug screening? *J Chromatogr A* **2013**, *1292*, 19-24.
11. Smith, M. L.; Vorce, S. P.; Holler, J. M.; Shimomura, E.; Magluilo, J.; Jacobs, A. J.; Huestis, M. A., Modern instrumental methods in forensic toxicology. *J Anal Toxicol* **2007**, *31* (5), 237-53, 8a-9a.
12. Aslam, B.; Basit, M.; Nisar, M. A.; Khurshid, M.; Rasool, M. H., Proteomics: Technologies and Their Applications. *J Chromatogr Sci* **2017**, *55* (2), 182-196.
13. Züllig, T.; Köfeler, H. C., High Resolution Mass Spectrometry in Lipidomics. *Mass Spectrom Rev* **2021**, *40* (3), 162-176.
14. Herrero, M.; Simó, C.; García-Cañas, V.; Ibáñez, E.; Cifuentes, A., Foodomics: MS-based strategies in modern food science and nutrition. *Mass Spectrom Rev* **2012**, *31* (1), 49-69.
15. Zhang, T.; Chen, C.; Xie, K.; Wang, J.; Pan, Z., Current State of Metabolomics Research in Meat Quality Analysis and Authentication. *Foods (Basel, Switzerland)* **2021**, *10* (10).
16. Perez de Souza, L.; Alseekh, S.; Scossa, F.; Fernie, A. R., Ultra-high-performance liquid chromatography high-resolution mass spectrometry variants for metabolomics research. *Nat Methods* **2021**, *18* (7), 733-746.
17. Patti, G. J.; Yanes, O.; Siuzdak, G., Metabolomics: the apogee of the omics trilogy. *Nat Rev Mol Cell Biol* **2012**, *13* (4), 263-269.
18. Brockbals, L.; Kraemer, T.; Steuer, A. E., Analytical considerations for postmortem metabolomics using GC-high-resolution MS. *Anal Bioanal Chem* **2020**, *412* (24), 6241-6255.
19. Steuer, A. E.; Brockbals, L.; Kraemer, T., Metabolomic Strategies in Biomarker Research—New Approach for Indirect Identification of Drug Consumption and Sample Manipulation in Clinical and Forensic Toxicology? *Front Chem* **2019**, *7*.

20. Steuer, A. E.; Kamber, D.; Kraemer, T., Evaluation of endogenous urinary biomarkers for indirect detection of urine adulteration attempts by five different chemical adulterants in mass spectrometry methods. *Drug Test Anal* **2018**.
21. Castaneto, M. S.; Wohlfarth, A.; Pang, S.; Zhu, M.; Scheidweiler, K. B.; Kronstrand, R.; Huestis, M. A., Identification of AB-FUBINACA metabolites in human hepatocytes and urine using high-resolution mass spectrometry. *Forensic Toxicol* **2015**, *33* (2), 295-310.
22. Carlier, J.; Diao, X.; Huestis, M. A., Synthetic cannabinoid BB-22 (QUCHIC): Human hepatocytes metabolism with liquid chromatography-high resolution mass spectrometry detection. *J Pharm Biomed Anal* **2018**, *157*, 27-35.
23. Diao, X.; Wohlfarth, A.; Pang, S.; Scheidweiler, K. B.; Huestis, M. A., High-Resolution Mass Spectrometry for Characterizing the Metabolism of Synthetic Cannabinoid THJ-018 and Its 5-Fluoro Analog THJ-2201 after Incubation in Human Hepatocytes. *Clin Chem* **2016**, *62* (1), 157-69.
24. Swortwood, M. J.; Carlier, J.; Ellefsen, K. N.; Wohlfarth, A.; Diao, X.; Concheiro-Guisan, M.; Kronstrand, R.; Huestis, M. A., In vitro, in vivo and in silico metabolic profiling of α -pyrrolidinopentiothiophenone, a novel thiophene stimulant. *Bioanalysis* **2016**, *8* (1), 65-82.
25. Lu, H. C.; Mackie, K., An Introduction to the Endogenous Cannabinoid System. *Biol Psychiatry* **2016**, *79* (7), 516-25.
26. Silver, R. J., The Endocannabinoid System of Animals. *Animals (Basel)* **2019**, *9* (9), 686.
27. Mackie, K., Cannabinoid receptors as therapeutic targets. *Annu Rev Pharmacol Toxicol* **2006**, *46*, 101-22.
28. Gonçalves, E. D.; Dutra, R. C., Cannabinoid receptors as therapeutic targets for autoimmune diseases: where do we stand? *Drug Discov Today* **2019**, *24* (9), 1845-1853.
29. Engeli, S., Central and Peripheral Cannabinoid Receptors as Therapeutic Targets in the Control of Food Intake and Body Weight. In *Appetite Control*, Joost, H.-G., Ed. Springer Berlin Heidelberg: Berlin, Heidelberg, 2012; pp 357-381.
30. Gülck, T.; Møller, B. L., Phytocannabinoids: Origins and Biosynthesis. *Trends Plant Sci* **2020**, *25* (10), 985-1004.
31. Woodhams, S. G.; Chapman, V.; Finn, D. P.; Hohmann, A. G.; Neugebauer, V., The cannabinoid system and pain. *Neuropharmacology* **2017**, *124*, 105-120.
32. Russo, E. B., Cannabis Therapeutics and the Future of Neurology. *Front Integr Neurosci* **2018**, *12* (51).
33. Sampson, P. B., Phytocannabinoid Pharmacology: Medicinal Properties of Cannabis sativa Constituents Aside from the "Big Two". *J Nat Prod* **2021**, *84* (1), 142-160.
34. ElSohly, M. A.; Radwan, M. M.; Gul, W.; Chandra, S.; Galal, A., Phytochemistry of Cannabis sativa L. In *Phytocannabinoids: Unraveling the Complex Chemistry and Pharmacology of Cannabis sativa*, Kinghorn, A. D.; Falk, H.; Gibbons, S.; Kobayashi, J. i., Eds. Springer International Publishing: Cham, 2017; pp 1-36.
35. Mechoulam, R.; Gaoni, Y., The absolute configuration of delta-1-tetrahydrocannabinol, the major active constituent of hashish. *Tetrahedron Lett* **1967**, *12*, 1109-11.
36. United Nations Office on Drugs and Crime World Drug Report 2021. Booklet 3 - Drug market trends: Opioids, Cannabis. https://www.unodc.org/res/wdr2021/field/WDR21_Booklet_3.pdf (accessed January 3).
37. Manthey, J.; Freeman, T. P.; Kilian, C.; López-Pelayo, H.; Rehm, J., Public health monitoring of cannabis use in Europe: prevalence of use, cannabis potency, and treatment rates. *Lancet Reg Health Eur* **2021**, *10*, 100227.

38. Federal Office of Public Health (Bundesamt für Gesundheit; BAG) Pilot trials with cannabis. <https://www.bag.admin.ch/bag/en/home/gesund-leben/sucht-und-gesundheit/cannabis/pilotprojekte.html> (accessed January 7).
39. Freeman, T. P.; Hindocha, C.; Green, S. F.; Bloomfield, M. A. P., Medicinal use of cannabis based products and cannabinoids. *BMJ* **2019**, *365*, l1141-l1141.
40. Scheunemann, A.; Elsner, K.; Germerott, T.; Hess, C.; Zörntlein, S.; Röhrich, J., Extensive phytocannabinoid profiles of seized cannabis and cannabis-based medicines – Identification of potential distinguishing markers. *Forensic Sci Int* **2021**, *322*, 110773.
41. ElSohly, M. A.; Mehmedic, Z.; Foster, S.; Gon, C.; Chandra, S.; Church, J. C., Changes in Cannabis Potency Over the Last 2 Decades (1995-2014): Analysis of Current Data in the United States. *Biol Psychiatry* **2016**, *79* (7), 613-619.
42. Cooper, Z. D.; Williams, A. R., Cannabis and Cannabinoid Intoxication and Toxicity. In *Cannabis Use Disorders*, Montoya, I. D.; Weiss, S. R. B., Eds. Springer International Publishing: Cham, 2019; pp 103-111.
43. Matheson, J.; Le Foll, B., Cannabis Legalization and Acute Harm From High Potency Cannabis Products: A Narrative Review and Recommendations for Public Health. *Front Psychiatry* **2020**, *11*, 591979.
44. European Monitoring Centre for Drugs and Drug Addiction Low-THC cannabis products in Europe. <https://www.emcdda.europa.eu/system/files/publications/13471/TD0320749ENN01.pdf> (accessed February 1).
45. McGregor, I. S.; Cairns, E. A.; Abelev, S.; Cohen, R.; Henderson, M.; Couch, D.; Arnold, J. C.; Gauld, N., Access to cannabidiol without a prescription: A cross-country comparison and analysis. *Int J Drug Policy* **2020**, *85*, 102935.
46. Arnold, J. C., A primer on medicinal cannabis safety and potential adverse effects. *Aust J Gen Pract* **2021**, *50* (6), 345-350.
47. Ladha, K. S.; Ajrawat, P.; Yang, Y.; Clarke, H., Understanding the Medical Chemistry of the Cannabis Plant is Critical to Guiding Real World Clinical Evidence. *Molecules* **2020**, *25* (18), 4042.
48. de Hoop, B.; Heerdink, E. R.; Hazekamp, A., Medicinal Cannabis on Prescription in The Netherlands: Statistics for 2003-2016. *Cannabis Cannabinoid Res* **2018**, *3* (1), 54-55.
49. Hanuš, L. O.; Meyer, S. M.; Muñoz, E.; Tagliabatella-Scafati, O.; Appendino, G., Phytocannabinoids: A unified critical inventory. *Nat Prod Rep* **2016**, *33* (12), 1357-1392.
50. Walsh, K. B.; McKinney, A. E.; Holmes, A. E., Minor Cannabinoids: Biosynthesis, Molecular Pharmacology and Potential Therapeutic Uses. *Front Pharmacol* **2021**, *12* (3366).
51. Russo, E. B., Taming THC: potential cannabis synergy and phytocannabinoid-terpenoid entourage effects. *Br J Pharmacol* **2011**, *163* (7), 1344-1364.
52. Freeman, A. M.; Petrilli, K.; Lees, R.; Hindocha, C.; Mokrysz, C.; Curran, H. V.; Saunders, R.; Freeman, T. P., How does cannabidiol (CBD) influence the acute effects of delta-9-tetrahydrocannabinol (THC) in humans? A systematic review. *Neurosci Biobehav Rev* **2019**, *107*, 696-712.
53. European Monitoring Centre for Drugs and Drug Addiction European Drug Report 2021: Trends and Developments. https://www.emcdda.europa.eu/publications/edr/trends-developments/2021_en (accessed September 13).
54. Brighenti, V.; Protti, M.; Anceschi, L.; Zanardi, C.; Mercolini, L.; Pellati, F., Emerging challenges in the extraction, analysis and bioanalysis of cannabidiol and related compounds. *J Pharm Biomed Anal* **2021**, *192*, 113633.
55. Hartman, R. L.; Huestis, M. A., Cannabis effects on driving skills. *Clin Chem* **2013**, *59* (3), 478-492.

56. Karschner, E. L.; Schwoppe, D. M.; Schwilke, E. W.; Goodwin, R. S.; Kelly, D. L.; Gorelick, D. A.; Huestis, M. A., Predictive model accuracy in estimating last $\Delta 9$ -tetrahydrocannabinol (THC) intake from plasma and whole blood cannabinoid concentrations in chronic, daily cannabis smokers administered subchronic oral THC. *Drug Alcohol Depend* **2012**, *125* (3), 313-319.
57. Arkell, T. R.; Vinckenbosch, F.; Kevin, R. C.; Theunissen, E. L.; McGregor, I. S.; Ramaekers, J. G., Effect of Cannabidiol and $\Delta 9$ -Tetrahydrocannabinol on Driving Performance: A Randomized Clinical Trial. *Jama* **2020**, *324* (21), 2177-2186.
58. McCartney, D.; Arkell, T. R.; Irwin, C.; McGregor, I. S., Determining the magnitude and duration of acute $\Delta 9$ -tetrahydrocannabinol ($\Delta 9$ -THC)-induced driving and cognitive impairment: A systematic and meta-analytic review. *Neurosci Biobehav Rev* **2021**, *126*, 175-193.
59. Asbridge, M.; Hayden, J. A.; Cartwright, J. L., Acute cannabis consumption and motor vehicle collision risk: systematic review of observational studies and meta-analysis. *BMJ* **2012**, *344*, e536.
60. Huestis, M. A., Pharmacokinetics and Metabolism of the Plant Cannabinoids, $\Delta 9$ -Tetrahydrocannabinol, Cannabidiol and Cannabinol. In *Cannabinoids*, Pertwee, R. G., Ed. Springer Berlin Heidelberg: Berlin, Heidelberg, 2005; pp 657-690.
61. Johansson, E.; Agurell, S.; Hollister, L. E.; Halldin, M. M., Prolonged apparent half-life of delta 1-tetrahydrocannabinol in plasma of chronic marijuana users. *J Pharm Pharmacol* **1988**, *40* (5), 374-5.
62. Huestis, M. A.; Cone, E. J., Differentiating new marijuana use from residual drug excretion in occasional marijuana users. *J Anal Toxicol* **1998**, *22* (6), 445-54.
63. Watson, T. M.; Mann, R. E., International approaches to driving under the influence of cannabis: A review of evidence on impact. *Drug Alcohol Depend* **2016**, *169*, 148-155.
64. Karschner, E. L.; Swortwood-Gates, M. J.; Huestis, M. A., Identifying and Quantifying Cannabinoids in Biological Matrices in the Medical and Legal Cannabis Era. *Clin Chem* **2020**, *66* (7), 888-914.
65. Kraemer, M.; Madea, B.; Hess, C., Detectability of various cannabinoids in plasma samples of cannabis users: Indicators of recent cannabis use? *Drug Test Anal* **2019**, *11* (10), 1498-1506.
66. Huestis, M. A.; Smith, M. L., Cannabinoid Markers in Biological Fluids and Tissues: Revealing Intake. *Trends Mol Med* **2018**, *24* (2), 156-172.
67. Newmeyer, M. N.; Swortwood, M. J.; Barnes, A. J.; Abulseoud, O. A.; Scheidweiler, K. B.; Huestis, M. A., Free and Glucuronide Whole Blood Cannabinoids' Pharmacokinetics after Controlled Smoked, Vaporized, and Oral Cannabis Administration in Frequent and Occasional Cannabis Users: Identification of Recent Cannabis Intake. *Clin Chem* **2016**, *62* (12), 1579-1592.
68. Gasse, A.; Pfeiffer, H.; Köhler, H.; Schürenkamp, J., 8β -OH-THC and $8\beta,11$ -diOH-THC-minor metabolites with major informative value? *Int J Legal Med* **2018**, *132* (1), 157-164.
69. Pichini, S.; Malaca, S.; Gottardi, M.; Pérez-Acevedo, A. P.; Papaseit, E.; Perez-Maña, C.; Farré, M.; Pacifici, R.; Tagliabracci, A.; Mannonchi, G.; Busardò, F. P., UHPLC-MS/MS analysis of cannabidiol metabolites in serum and urine samples. Application to an individual treated with medical cannabis. *Talanta* **2021**, *223*, 121772.
70. Pichini, S.; Mannonchi, G.; Berretta, P.; Zaami, S.; Pirani, F.; Pacifici, R.; Busardò, F. P., $\Delta 9$ -Tetrahydrocannabinol and Cannabidiol Time Courses in the Sera of "Light Cannabis" Smokers: Discriminating Light Cannabis Use from Illegal and Medical Cannabis Use. *Ther Drug Monit* **2020**, *42* (1).
71. Scheunemann, A.; Elsner, K.; Germerott, T.; Groppa, S.; Hess, C.; Miederer, I.; Poplawski, A.; Röhrich, J., Identification of Potential Distinguishing Markers for the Use of Cannabis-Based Medicines or Street Cannabis in Serum Samples. *Metabolites* **2021**, *11* (5), 316.

72. Levin, F. R.; Mariani, J. J.; Brooks, D. J.; Xie, S.; Murray, K. A., Δ^9 -Tetrahydrocannabinol testing may not have the sensitivity to detect marijuana use among individuals ingesting dronabinol. *Drug Alcohol Depend* **2010**, *106* (1), 65-68.
73. Scheidweiler, K. B.; Barnes, A. J., Quantification of Eight Cannabinoids Including Cannabidiol in Human Urine Via Liquid Chromatography Tandem Mass Spectrometry. In *LC-MS in Drug Analysis: Methods and Protocols*, Langman, L. J.; Snozek, C. L. H., Eds. Springer New York: New York, NY, 2019; pp 11-22.
74. Hubbard, J. A.; Hoffman, M. A.; Ellis, S. E.; Sobolesky, P. M.; Smith, B. E.; Suhandynata, R. T.; Sones, E. G.; Sanford, S. K.; Umlauf, A.; Huestis, M. A.; Grelotti, D. J.; Grant, I.; Marcotte, T. D.; Fitzgerald, R. L., Biomarkers of Recent Cannabis Use in Blood, Oral Fluid and Breath. *J Anal Toxicol* **2021**, *45* (8), 820-828.
75. Drummer, O. H.; Gerostamoulos, D.; Woodford, N. W., Cannabis as a cause of death: A review. *Forensic Sci Int* **2019**, *298*, 298-306.
76. Cliburn, K. D.; Huestis, M. A.; Wagner, J. R.; Kemp, P. M., Identification and quantification of cannabinoids in postmortem fluids and tissues by liquid chromatography-tandem mass spectrometry. *J Chromatogr A* **2021**, *1652*, 462345.
77. Auwärter, V.; Dresen, S.; Weinmann, W.; Müller, M.; Pütz, M.; Ferreirós, N., 'Spice' and other herbal blends: harmless incense or cannabinoid designer drugs? *J Mass Spectrom* **2009**, *44* (5), 832-837.
78. European Monitoring Centre for Drugs and Drug Addiction Synthetic cannabinoids in Europe – a review. <https://www.emcdda.europa.eu/system/files/publications/14035/Synthetic-cannabinoids-in-Europe-EMCDDA-technical-report.pdf> (accessed September 16).
79. Pike, E.; Grafinger, K. E.; Caninaert, A.; Ametovski, A.; Luo, J. L.; Sparkes, E.; Cairns, E. A.; Ellison, R.; Gerona, R.; Stove, C. P.; Auwärter, V.; Banister, S. D., Systematic evaluation of a panel of 30 synthetic cannabinoid receptor agonists structurally related to MMB-4en-PICA, MDMB-4en-PINACA, ADB-4en-PINACA, and MMB-4CN-BUTINACA using a combination of binding and different CB(1) receptor activation assays: Part I-Synthesis, analytical characterization, and binding affinity for human CB(1) receptors. *Drug Test Anal* **2021**.
80. Norman, C.; Walker, G.; McKirdy, B.; McDonald, C.; Fletcher, D.; Antonides, L. H.; Sutcliffe, O. B.; Nic Daéid, N.; McKenzie, C., Detection and quantitation of synthetic cannabinoid receptor agonists in infused papers from prisons in a constantly evolving illicit market. *Drug Test Anal* **2020**, *12* (4), 538-554.
81. Norman, C.; Halter, S.; Haschimi, B.; Acreman, D.; Smith, J.; Krotulski, A. J.; Mohr, A. L. A.; Logan, B. K.; NicDaéid, N.; Auwärter, V.; McKenzie, C., A transnational perspective on the evolution of the synthetic cannabinoid receptor agonists market: Comparing prison and general populations. *Drug Test Anal* **2021**, *13* (4), 841-852.
82. Moosmann, B.; Angerer, V.; Auwärter, V., Inhomogeneities in herbal mixtures: a serious risk for consumers. *Forensic Toxicol* **2015**, *33* (1), 54-60.
83. Halter, S.; Mogler, L.; Auwärter, V., Quantification of Herbal Mixtures Containing Cumyl-PEGACLONE—Is Inhomogeneity Still an Issue? *J Anal Toxicol* **2019**, *44* (1), 81-85.
84. Kraemer, M.; Boehmer, A.; Madea, B.; Maas, A., Death cases involving certain new psychoactive substances: A review of the literature. *Forensic Sci Int* **2019**, *298*, 186-267.
85. Caninaert, A.; Sparkes, E.; Pike, E.; Luo, J. L.; Fang, A.; Kevin, R. C.; Ellison, R.; Gerona, R.; Banister, S. D.; Stove, C. P., Synthesis and in Vitro Cannabinoid Receptor 1 Activity of Recently Detected Synthetic Cannabinoids 4F-MDMB-BICA, 5F-MPP-PICA, MMB-4en-PICA, CUMYL-CBMICA, ADB-BINACA, APP-BINACA, 4F-MDMB-BINACA, MDMB-4en-PINACA, A-CHMINACA, 5F-AB-P7AICA, 5F-MDMB-P7AICA, and 5F-AP7AICA. *ACS Chem Neurosci* **2020**, *11* (24), 4434-4446.

86. Antonides, L. H.; Cannaert, A.; Norman, C.; NicDáeid, N.; Sutcliffe, O. B.; Stove, C. P.; McKenzie, C., Shape matters: The application of activity-based in vitro bioassays and chiral profiling to the pharmacological evaluation of synthetic cannabinoid receptor agonists in drug-infused papers seized in prisons. *Drug Test Anal* **2021**, *13* (3), 628-643.
87. Fabregat-Safont, D.; Mardal, M.; Noble, C.; Cannaert, A.; Stove, C. P.; Sancho, J. V.; Linnet, K.; Hernández, F.; Ibáñez, M., Comprehensive investigation on synthetic cannabinoids: Metabolic behavior and potency testing, using 5F-APP-PICA and AMB-FUBINACA as model compounds. *Drug Test Anal* **2019**.
88. Noble, C.; Cannaert, A.; Linnet, K.; Stove, C. P., Application of an activity-based receptor bioassay to investigate the in vitro activity of selected indole- and indazole-3-carboxamide-based synthetic cannabinoids at CB1 and CB2 receptors. *Drug Test Anal* **2019**, *11* (3), 501-511.
89. Hess, C.; Schoeder, C. T.; Pillaiyar, T.; Madea, B.; Müller, C. E., Pharmacological evaluation of synthetic cannabinoids identified as constituents of spice. *Forensic Toxicol* **2016**, *34*, 329-343.
90. Radaelli, D.; Manfredi, A.; Zanon, M.; Fattorini, P.; Scopetti, M.; Neri, M.; Frisoni, P.; D'Errico, S., Synthetic cannabinoids and cathinones cardiotoxicity: evidences actualities and perspectives. *Curr Neuropharmacol* **2021**.
91. Castaneto, M. S.; Gorelick, D. A.; Desrosiers, N. A.; Hartman, R. L.; Pirard, S.; Huestis, M. A., Synthetic cannabinoids: Epidemiology, pharmacodynamics, and clinical implications. *Drug Alcohol Depend* **2014**, *144*, 12-41.
92. Zaurova, M.; Hoffman, R. S.; Vlahov, D.; Manini, A. F., Clinical Effects of Synthetic Cannabinoid Receptor Agonists Compared with Marijuana in Emergency Department Patients with Acute Drug Overdose. *J Med Toxicol* **2016**, *12* (4), 335-340.
93. Seely, K. A.; Lapoint, J.; Moran, J. H.; Fattore, L., Spice drugs are more than harmless herbal blends: A review of the pharmacology and toxicology of synthetic cannabinoids. *Prog Neuropsychopharmacol Biol Psychiatry* **2012**, *39* (2), 234-243.
94. Adamowicz, P.; Gieroń, J.; Gil, D.; Lechowicz, W.; Skulska, A.; Tokarczyk, B., The effects of synthetic cannabinoid UR-144 on the human body—A review of 39 cases. *Forensic Sci Int* **2017**, *273*, e18-e21.
95. Krotulski, A. J.; Cannaert, A.; Stove, C.; Logan, B. K., The next generation of synthetic cannabinoids: Detection, activity, and potential toxicity of pent-4en and but-3en analogues including MDMB-4en-PINACA. *Drug Test Anal* **2021**, *13* (2), 427-438.
96. Luethi, D.; Liechti, M. E., Designer drugs: mechanism of action and adverse effects. *Arch Toxicol* **2020**, *94* (4), 1085-1133.
97. Angerer, V.; Jacobi, S.; Franz, F.; Auwärter, V.; Pietsch, J., Three fatalities associated with the synthetic cannabinoids 5F-ADB, 5F-PB-22, and AB-CHMINACA. *Forensic Sci Int* **2017**, *281*, e9-e15.
98. Barceló, B.; Pichini, S.; López-Corominas, V.; Gomila, I.; Yates, C.; Busardò, F. P.; Pellegrini, M., Acute intoxication caused by synthetic cannabinoids 5F-ADB and MMB-2201: A case series. *Forensic Sci Int* **2017**, *273*, e10-e14.
99. Gaunitz, F.; Andresen-Streichert, H., Analytical findings in a non-fatal intoxication with the synthetic cannabinoid 5F-ADB (5F-MDMB-PINACA): a case report. *Int J Legal Med* **2021**.
100. Harris, C. R.; Brown, A., Synthetic Cannabinoid Intoxication: A Case Series and Review. *J Emerg Med* **2013**, *44* (2), 360-366.
101. Patton, A. L.; Chimalakonda, K. C.; Moran, C. L.; McCain, K. R.; Radomska-Pandya, A.; James, L. P.; Kokes, C.; Moran, J. H., K2 toxicity: fatal case of psychiatric complications following AM2201 exposure. *J Forensic Sci* **2013**, *58* (6), 1676-80.

102. Labay, L. M.; Caruso, J. L.; Gilson, T. P.; Phipps, R. J.; Knight, L. D.; Lemos, N. P.; McIntyre, I. M.; Stoppacher, R.; Tormos, L. M.; Wiens, A. L.; Williams, E.; Logan, B. K., Synthetic cannabinoid drug use as a cause or contributory cause of death. *Forensic Sci Int* **2016**, *260*, 31-39.
103. Deng, H.; Verrico, C. D.; Kosten, T. R.; Nielsen, D. A., Psychosis and synthetic cannabinoids. *Psychiatry Res* **2018**, *268*, 400-412.
104. Brents, L. K.; Gallus-Zawada, A.; Radomska-Pandya, A.; Vasiljevik, T.; Prisinzano, T. E.; Fantegrossi, W. E.; Moran, J. H.; Prather, P. L., Monohydroxylated metabolites of the K2 synthetic cannabinoid JWH-073 retain intermediate to high cannabinoid 1 receptor (CB1R) affinity and exhibit neutral antagonist to partial agonist activity. *Biochem Pharmacol* **2012**, *83* (7), 952-961.
105. Rajasekaran, M.; Brents, L. K.; Franks, L. N.; Moran, J. H.; Prather, P. L., Human metabolites of synthetic cannabinoids JWH-018 and JWH-073 bind with high affinity and act as potent agonists at cannabinoid type-2 receptors. *Toxicol Appl Pharmacol* **2013**, *269* (2), 100-108.
106. Cannaert, A.; Storme, J.; Franz, F.; Auwärter, V.; Stove, C. P., Detection and Activity Profiling of Synthetic Cannabinoids and Their Metabolites with a Newly Developed Bioassay. *Anal Chem* **2016**, *88* (23), 11476-11485.
107. Wouters, E.; Mogler, L.; Cannaert, A.; Auwärter, V.; Stove, C., Functional evaluation of carboxy metabolites of synthetic cannabinoid receptor agonists featuring scaffolds based on L-valine or L-tert-leucine. *Drug Test Anal* **2019**, *11* (8), 1183-1191.
108. Diao, X.; Huestis, M. A., New Synthetic Cannabinoids Metabolism and Strategies to Best Identify Optimal Marker Metabolites. *Front Chem* **2019**, *7*, 109-109.
109. Diao, X.; Huestis, M. A., Approaches, Challenges, and Advances in Metabolism of New Synthetic Cannabinoids and Identification of Optimal Urinary Marker Metabolites. *Clin Pharmacol Ther* **2017**, *101* (2), 239-253.
110. Mogler, L.; Halter, S.; Wilde, M.; Franz, F.; Auwärter, V., Human phase I metabolism of the novel synthetic cannabinoid 5F-CUMYL-PEGACLONE. *Forensic Toxicol* **2019**, *37* (1), 154-163.
111. Mogler, L.; Wilde, M.; Huppertz, L. M.; Weinfurtner, G.; Franz, F.; Auwärter, V., Phase I metabolism of the recently emerged synthetic cannabinoid CUMYL-PEGACLONE and detection in human urine samples. *Drug Test Anal* **2018**, *10* (5), 886-891.
112. Giorgetti, A.; Mogler, L.; Haschimi, B.; Halter, S.; Franz, F.; Westphal, F.; Fischmann, S.; Riedel, J.; Pütz, M.; Auwärter, V., Detection and phase I metabolism of the 7-azaindole-derived synthetic cannabinoid 5F-AB-P7AICA including a preliminary pharmacokinetic evaluation. *Drug Test Anal* **2020**, *12* (1), 78-91.
113. Franz, F.; Angerer, V.; Brandt, S. D.; McLaughlin, G.; Kavanagh, P. V.; Moosmann, B.; Auwärter, V., In vitro metabolism of the synthetic cannabinoid 3,5-AB-CHMFUPPYCA and its 5,3-regioisomer and investigation of their thermal stability. *Drug Test Anal* **2017**, *9* (2), 311-316.
114. Gaunitz, F.; Thomas, A.; Fietzke, M.; Franz, F.; Auwärter, V.; Thevis, M.; Mercer-Chalmers-Bender, K., Phase I metabolic profiling of the synthetic cannabinoids THJ-018 and THJ-2201 in human urine in comparison to human liver microsome and cytochrome P450 isoenzyme incubation. *Int J Legal Med* **2019**, *133* (4), 1049-1064.
115. Nielsen, L. M.; Holm, N. B.; Olsen, L.; Linnet, K., Cytochrome P450-mediated metabolism of the synthetic cannabinoids UR-144 and XLR-11. *Drug Test Anal* **2016**, *8* (8), 792-800.
116. Jeremy Carlier, X. D., Ariane Sohlfarth, Karl Schweidweiler, Marylin A. Huestis, *In Vitro Metabolite Profiling of ADB-FUBINACA, A New Synthetic Cannabinoid*. *Curr Neuropharmacol* **2017**, *15* (15), 682-691.

117. Richter, M. J.; Wagmann, L.; Gampfer, T. M.; Brandt, S. D.; Meyer, M. R., In Vitro Metabolic Fate of the Synthetic Cannabinoid Receptor Agonists QMPSB and QMPCB (SGT-11) Including Isozyme Mapping and Esterase Activity. *Metabolites* **2021**, *11* (8), 509.
118. Kronstrand, R.; Norman, C.; Vikingsson, S.; Biemans, A.; Valencia Crespo, B.; Edwards, D.; Fletcher, D.; Gilbert, N.; Persson, M.; Reid, R.; Semenova, O.; Al Teneiji, F.; Wu, X.; Dahlén, J.; NicDaéid, N.; Tarbah, F.; Sutcliffe, O. B.; McKenzie, C.; Gréen, H., The metabolism of the synthetic cannabinoids ADB-BUTINACA and ADB-4en-PINACA and their detection in forensic toxicology casework and infused papers seized in prisons. *Drug Test Anal* **2021**.
119. Franz, F.; Jechle, H.; Wilde, M.; Angerer, V.; Huppertz, L. M.; Longworth, M.; Kassiou, M.; Jung, M.; Auwärter, V., Structure-metabolism relationships of valine and tert-leucine-derived synthetic cannabinoid receptor agonists: a systematic comparison of the in vitro phase I metabolism using pooled human liver microsomes and high-resolution mass spectrometry. *Forensic Toxicol* **2019**, *37* (2), 316-329.
120. Gaunitz, F.; Kieliba, T.; Thevis, M.; Mercer-Chalmers-Bender, K., Solid-phase extraction–liquid chromatography–tandem mass spectrometry method for the qualitative analysis of 61 synthetic cannabinoid metabolites in urine. *Drug Test Anal* **2019**, *12* (1), 27– 40.
121. Oomen, P. E.; Schori, D.; Tögel-Lins, K.; Acreman, D.; Chenorhokian, S.; Luf, A.; Karden, A.; Paulos, C.; Fornero, E.; Gerace, E.; Koning, R. P. J.; Galindo, L.; Smit-Rigter, L. A.; Measham, F.; Ventura, M., Cannabis adulterated with the synthetic cannabinoid receptor agonist MDMB-4en-PINACA and the role of European drug checking services. *Int J Drug Policy* **2022**, *100*, 103493.
122. Abteilung Sucht Gesundheitsdepartement des Kantons Basel-Stadt Factsheet Mai 2020 - Synthetische Cannabinoide und ihre Risiken. https://www.sucht.bs.ch/dam/jcr:eae1f8c4-7947-4171-bd53-080cfe5fdf62/Abt_Sucht_Syn_Cannabinoide.pdf.
123. Die Stellen für Suchtprävention Kanton Zürich Factsheet April 2020 - Synthetische Cannabinoide und ihre Risiken. https://www.suchtfachstelle.zuerich/images/PDFs/Factsheet_Cannabinoide_Suchtpraevention.pdf (accessed September 13).
124. Wood, D. M.; Hill, S. L.; Thomas, S. H.; Dargan, P. I., Using poisons information service data to assess the acute harms associated with novel psychoactive substances. *Drug Test Anal* **2014**, *6* (7-8), 850-60.
125. Zawilska, J. B.; Wojcieszak, J., An expanding world of new psychoactive substances—designer benzodiazepines. *NeuroToxicology* **2019**, *73*, 8-16.
126. Winstock, A. R.; Barratt, M. J., Synthetic cannabis: A comparison of patterns of use and effect profile with natural cannabis in a large global sample. *Drug Alcohol Depend* **2013**, *131* (1), 106-111.
127. Beharry, S.; Gibbons, S., An overview of emerging and new psychoactive substances in the United Kingdom. *Forensic Sci Int* **2016**, *267*, 25-34.
128. Rhumorbarbe, D.; Morelato, M.; Staehli, L.; Roux, C.; Jaquet-Chiffelle, D. O.; Rossy, Q.; Esseiva, P., Monitoring new psychoactive substances: Exploring the contribution of an online discussion forum. *Int J Drug Policy* **2019**, *73*, 273-280.
129. Helander, A.; Bäckberg, M.; Beck, O., Drug trends and harm related to new psychoactive substances (NPS) in Sweden from 2010 to 2016: Experiences from the STRIDA project. *PLoS One* **2020**, *15* (4), e0232038.
130. Kronstrand, R.; Guerrieri, D.; Vikingsson, S.; Wohlfarth, A.; Gréen, H., Fatal Poisonings Associated with New Psychoactive Substances. In *New Psychoactive Substances : Pharmacology*,

Clinical, Forensic and Analytical Toxicology, Maurer, H. H.; Brandt, S. D., Eds. Springer International Publishing: Cham, 2018; pp 495-541.

131. European Monitoring Centre for Drugs and Drug Addiction Drug checking as a harm reduction tool for recreational drug users: opportunities and challenges. https://www.emcdda.europa.eu/system/files/attachments/6339/EuropeanResponsesGuide2017_BackgroundPaper-Drug-checking-harm-reduction_0.pdf (accessed May 10).
132. Schweizerische Eidgenossenschaft ARAMIS Machbarkeitsstudie "Nationales Substanzmonitoring". <https://www.aramis.admin.ch/Texte/?ProjectID=40778&Sprache=en-US> (accessed January 30).
133. European Monitoring Centre for Drugs and Drug Addiction New psychoactive substances: health and social responses. https://www.emcdda.europa.eu/printpdf/publications/mini-guides/new-psychoactive-substances-health-and-social-responses_en.
134. European Monitoring Centre for Drugs and Drug Addiction EMCDDA initial report on the new psychoactive substance methyl 3,3-dimethyl-2-(1-(pent-4-en-1-yl)-1H-indazole-3-carboxamido)butanoate (MDMB-4en-PINACA). <https://www.emcdda.europa.eu/system/files/publications/13363/emcdda-initial-report-MDMB-4en-PINACA.pdf> (accessed February 1).
135. Kostyukevich, Y.; Zhrebker, A.; Orlov, A.; Kovaleva, O.; Burykina, T.; Isotov, B.; Nikolaev, E. N., Hydrogen/Deuterium and 16O/18O-Exchange Mass Spectrometry Boosting the Reliability of Compound Identification. *Anal Chem* **2020**, *92* (10), 6877-6885.
136. Zhu, C.; Lai, G.; Jin, Y.; Xu, D.; Chen, J.; Jiang, X.; Wang, S.; Liu, G.; Xu, N.; Shen, R.; Wang, L.; Zhu, M.; Wu, C., Suspect screening and untargeted analysis of veterinary drugs in food by LC-HRMS: Application of background exclusion-dependent acquisition for retrospective analysis of unknown xenobiotics. *J Pharm Biomed Anal* **2022**, *210*, 114583.
137. Ng, B.; Quinete, N.; Gardinali, P. R., Assessing accuracy, precision and selectivity using quality controls for non-targeted analysis. *Sci Total Environ* **2020**, *713*, 136568.
138. Maurer, H. H., Perspectives of liquid chromatography coupled to low- and high-resolution mass spectrometry for screening, identification, and quantification of drugs in clinical and forensic toxicology. *Ther Drug Monit* **2010**, *32* (3), 324-7.
139. Radwan, M. M.; ElSohly, M. A.; El-Alfy, A. T.; Ahmed, S. A.; Slade, D.; Husni, A. S.; Manly, S. P.; Wilson, L.; Seale, S.; Cutler, S. J.; Ross, S. A., Isolation and Pharmacological Evaluation of Minor Cannabinoids from High-Potency Cannabis sativa. *J Nat Prod* **2015**, *78* (6), 1271-1276.
140. Aliferis, K. A.; Bernard-Perron, D., Cannabinomics: Application of Metabolomics in Cannabis (Cannabis sativa L.) Research and Development. *Front Plant Sci* **2020**, *11* (554).
141. Hazekamp, A.; Fishedick, J. T., Cannabis - from cultivar to chemovar. *Drug Test Anal* **2012**, *4* (7-8), 660-667.
142. Berman, P.; Sulimani, L.; Gelfand, A.; Amsalem, K.; Lewitus, G. M.; Meiri, D., Cannabinoidomics – An analytical approach to understand the effect of medical Cannabis treatment on the endocannabinoid metabolome. *Talanta* **2020**, *219*, 121336.
143. Capriotti, A. L.; Cannazza, G.; Catani, M.; Cavaliere, C.; Cavazzini, A.; Cerrato, A.; Citti, C.; Felletti, S.; Montone, C. M.; Piovesana, S.; Laganà, A., Recent applications of mass spectrometry for the characterization of cannabis and hemp phytocannabinoids: From targeted to untargeted analysis. *J Chromatogr A* **2021**, *1655*, 462492.
144. Berman, P.; Futoran, K.; Lewitus, G. M.; Mukha, D.; Benami, M.; Shlomi, T.; Meiri, D., A new ESI-LC/MS approach for comprehensive metabolic profiling of phytocannabinoids in Cannabis. *Sci Rep* **2018**, *8* (1), 14280.

145. Hazekamp, A.; Tejkalová, K.; Papadimitriou, S., Cannabis: From Cultivar to Chemovar II—A Metabolomics Approach to Cannabis Classification. *Cannabis Cannabinoid Res* **2016**, *1* (1), 202-215.
146. Vásquez-Ocmín, P. G.; Marti, G.; Bonhomme, M.; Mathis, F.; Fournier, S.; Bertani, S.; Maciuk, A., Cannabinoids vs. whole metabolome: Relevance of cannabinomics in analyzing Cannabis varieties. *Anal Chim Acta* **2021**, *1184*, 339020.
147. Cerrato, A.; Citti, C.; Cannazza, G.; Capriotti, A. L.; Cavaliere, C.; Grassi, G.; Marini, F.; Montone, C. M.; Paris, R.; Piovesana, S.; Laganà, A., Phytocannabinomics: Untargeted metabolomics as a tool for cannabis chemovar differentiation. *Talanta* **2021**, *230*, 122313.
148. Fishedick, J. T.; Hazekamp, A.; Erkelens, T.; Choi, Y. H.; Verpoorte, R., Metabolic fingerprinting of *Cannabis sativa* L., cannabinoids and terpenoids for chemotaxonomic and drug standardization purposes. *Phytochemistry* **2010**, *71* (17), 2058-2073.
149. Pérez-Acevedo, A. P.; Busardò, F. P.; Pacifici, R.; Mannonchi, G.; Gottardi, M.; Poyatos, L.; Papaseit, E.; Pérez-Mañá, C.; Martin, S.; Di Trana, A.; Pichini, S.; Farré, M., Disposition of Cannabidiol Metabolites in Serum and Urine from Healthy Individuals Treated with Pharmaceutical Preparations of Medical Cannabis. *Pharmaceuticals (Basel, Switzerland)* **2020**, *13* (12).